CATHEPSIN B REGULATES PROGRAMMED CELL DEATH IN *ARABIDOPSIS THALIANA* AND EXHIBITS CASPASE-LIKE ACTIVITIES

A thesis submitted to The University of Manchester for the degree of PhD in the Faculty of Life Science

2010

Yuan Ge

Faculty of Life Science

DECLARATION

No portion of the work referred to in the thesis has been submitted in support of an application for another degree or qualification of this or any other university or other institute of learning.

COPYRIGHT STATEMENT

ABSTRACT

Thesis Title: Cathepsin B regulates programmed cell death in *Arabidopsis thaliana* and exhibits caspase-like activities

Candidate's Name: Yuan Ge

Degree Title: Degree of Doctor of Philosophy in Faculty of Life Science, the University of Manchester

Date: 29/09/2010

Programmed cell death (PCD) is a physiological cell death under the control of genetic mechanisms. In animals, apoptosis has been thoroughly elucidated at the molecular level. Cysteine aspartic acid specific proteases termed 'caspases' are central to the apoptotic initiation and execution in animals. However, although caspase-like enzymatic activities are required for plant PCD execution, there is no caspase homologue with caspase activity known in plants. Thus the search for caspase functional analogues is an important approach to improve the understanding of the regulatory mechanisms underlying plant PCD. The protease cathepsin B (AtCathB) was identified in fractions of partially purified caspase-3-like activities extracted from *Arabidopsis* seedlings after UV-C induction. In addition, an elevated cathepsin B-like enzymatic activity coinciding with the elevated caspase-3-like enzymatic activity was detected in *Arabidopsis* in response to oxidative stresses. Consequently, *AtCathB* double knockout and triple knockout transgenic lines were generated using T-DNA insertion as well as artificial microRNAs mediated gene silencing. *AtCathB* loss-of-function lines showed an abolished PCD triggered by oxidative stresses and a significant reduced cathepsin B-like activity and caspase-3-like activity.

Three *AtCathB* genes are present in the *Arabidopsis* genome and recombinant AtCathB-2 and AtCathB-3 were produced using *E.coli* and insect cell expression systems. Results from proteolytic activity assay and kinetic measurement confirmed the enzymatic similarity between human caspase-3 and *Arabidopsis* cathepsin B. Preliminary experiments aimed at identifying cathepsin B *in vivo* substrates have identified the enzyme RuBisCO as a strong candidate. At the subcellular level, AtCathB-2 was found to be localised in the vacuole and AtCathB-3 mainly in the apoplast.

In summary, *Arabidopsis* cathepsin B has caspase-3-like activity and regulates oxidative stress-induced PCD. The possible conservation through evolution from plants to animals of an ancestral cathepsins-mediated apoptosis/PCD regulatory pathway is discussed.

TABLE OF CONTENTS

Word count: 50,556 words

FIGURE LIST

TABLE LIST

ABBREVIATION

AAN	Ala-Ala-Asn
AIF	apoptosis-inducing factor
Apaf-1	apoptotic protease activating factor 1
BAX	BCL-2-assiciated protein X
BCL-2	B cell lymphoma 2
BID	BH3 interacting domain death agonist
BH	BCL-2 homology domain
bp	base pair
BSA	bovine serum albumim
caspase	cysteine dependent apartate specific protease
CARD	caspase activation and recruitment domain
CED	cell death defective
CPP32	32kDa cysteine protease
dad	defender against apoptotic death
DD	death domain
DED	death effector domain
DEVD	Asp-Glu-Val-Asp
DTT	dithiothreitol
E.coli	Escherichia coli
EDTA	ethylenediamine tetraacetic acid
ER	endoplasmic reticulum

FADD Fas Associated Death Domain Protein

FDA fluorescein diacetate

FR Phe-Arg

GUS β-glucronidase

HR hypersensitive reaction

HRP horseradish peroxidase

IAP inhibitor of apoptosis

ICE interleukin-1β-converting enzyme

ICH ice and ced-3 homologue

IETD Ile-Glu-Thr-Asp

IPTG isopropylthio-β-D-galactoside

ORF open reading frame

PARP poly (ADP-ribose) polymerase

PAGE polyacrylamide gel electrophoresis

PCD programmed cell death

PCR polymerase chain reaction

PMSF phenylmethanesulfonylfluoride

ROS reactive oxygen species

RR Arg-Arg

RT reverse transcription

SDS sodium dodecyl sulfate

T-DNA transfer DNA

TEMED N,N,N’,N’-tetramethyl ethylene diamine

TMV	tobacco mosaic virus
TNF-α	tumour necrosis factor alpha
TUNEL	terminal deoxynucleotidyl transferase mediated dutp nick end labeling
UV	ultraviolet
VAD	Val-Ala-Asp
VEID	Val-Glu-Ile-Asp
VPE	vacuolar processing enzyme
RFP	red fluorescent protein
RISC	RNA-induced silencing complex
WT	wild type
YFP	yellow fluorescent protein
YVAD	Tyr-Val-Ala-Asp

ACKNOWLEDGEMENTS

At the end of my PhD study in the University of Manchester, I would like first to thank Dr. Patrick Gallois as a profound and responsible supervisor. Four years supervision and instruction from Dr. Gallois taught me how to be a researcher in biology and how to be a good person in life. He is not only an excellent biologist and supervisor but also an indeed life-long mentor.

I am grateful to my advisors, Prof. Simon Turner and Dr. Clifford Bray for their invaluable guidance and instruction. Many thanks to principle investigators in the Molecular Plant Science Laboratory: Dr. Anil Day, Dr. Caroline Bowsher, Dr. Giles Johnson, Dr. Jon Pittman, Dr. Thomas Nuhse and Dr. Kim Minsung for their help.

I would like to thank Prof. Boris Turk and Prof. Paul Birch for providing recombinant human cathepsin B and seeds of transgenic plants. I would like also to convey my thanks to Dr. Edwards McKenzie, Dr. Richard Kammerer and Dr. Mauro Esposti for their great help in my research.

I would like to thank my father and mother for their support and continuous encouragement. Away from them, I realise the love from them is indispensably. I would like to thank my grandmother. She passed away when I was ten thousand miles away from her at her age of ninety-three. I wish she rest in peace and be proud of me forever.

I would like to thank my colleagues in Dr. Patrick Gallois' lab: Dr. He Rui, Dr. Georgina Drury, Mr. Bennett Young, Mr. Cai Yaomin, Mr. Galebotse Mathengwane and Mr. Michal Gwizdala for their friendly support and help. Many thanks to my colleagues in plant science groups: Mr. Jin Ding, Mr. Huang Xun, Dr. Rachael Webster, Dr. Adam Moolna and Dr. Maslin Osathanunkul.

I would also convey my thanks to my friends: Dr. Ni He, Dr. Lou Xiaodong, Dr. Cheng Xusen and Miss Cui Zhen for their warm friendship and encouragement when I feel lonely and depression.

CHAPTER 1

INTRODUCTION

1.1 Apoptosis and programmed cell death

1.1.1 Apoptosis and necrosis in animals

It can be argued that cell death is one of the most important event for an organism. In animals, two forms of cell death, necrosis and apoptosis have been discovered and distinct morphological features separate them. Morphological characteristics in necrotic cells are frequently used to distinguish the two cell death forms. Necrotic cells swell initially with little alteration in chromatin. Subsequently, cellular structure and compartments become disorganized including mitochondria swelling and shrinkage of inner mitochondrial membrane. At later stages of necrosis, along with the disruption of cyto-architecture, chromatin loses its organisation while nucleases and proteases are released from the lysosome. Cell necrosis triggers an inflammatory response, a striking consequence of cytoplasma membrane rupture and cell contents release in the surrounding tissue. Necrotic cells are eventually disposed of by monocytes and macrophages recruited to the death site. Necrosis is therefore a pathological cell death caused by external death factors and is harmful to surrounding cells. Each individual cell in multicellular organisms must function harmoniously with its neighbouring cells, its specialized tissue and the whole organism. Inappropriate death or proliferation of cells leads to the loss of tissue homeostasis. This has driven the evolution of a physiological in-built suicide mechanism under the genetic control, programmed cell death, which is pivotal to tissue homeostasis and a prerequisite to organism survival.

A novel form of cell death exhibiting morphological difference from necrosis was firstly discovered in vertebrate ontogeny and named ‘cell degeneration’ (Glucksmann, 1951). Subsequently, the definition of ‘programmed cell death’ was given on descriptive work as well as experimental verification by Saunders & Fallon (1966). With a description from its morphological features, a nomenclative phrase ‘programmed cell death’ was coined to refer to this novel concept of cell death discovered in animal embryogenesis (Lockshin & Beaulaton, 1974). The term ‘apoptosis’ was given by Kerr *et al.* in 1972 to refer the novel form of cell death in a wide range of physiological progresses after physiological stimuli

in addition to development. Until today, apoptosis remains the major form of programmed cell death that has been described in animals.

When cells undergo apoptosis, sequential morphological changes occur in the cell structure that is distinct from necrosis. Initially, apoptotic cells separate from neighbouring cells and lose their specialised membrane structure, i.e. microvilli and desmosomes. After cell shrinkage, apoptotic cells start blebbing, which is a reversible extruding and resorbing movement formed by cytosol and membrane. Subsequently, rapid and irreversible condensation of chromatin and compaction of cell organelles occur. Endoplasmic reticulum (ER) swells and connects to the cell surface whilst mitochondria appear normal. The final destination of apoptotic cells is phagocytosis carried out by viable neighbouring cells or specialised phagocytes. Macro-autophagy is an alternative pathway towards cell elimination, and some scientists even divide programmed cell death into type I (apoptosis ending in phagocytosis) and type II (autophagic cell death). In autophagic cell death, double membrane vesicles containing portion of cytoplasma and cell organelles are formed as autophagosome and then fused with lysosome for turnover. The use of autophagy or phagocytosis is determined by cell type, stress type and maybe some other mechanisms. Compared to necrosis, the most striking feature of apoptosis is that apoptotic cells disappear rapidly without inflammatory response. Changes on apoptotic cell surface enable them to be recognized and eliminated before cytoplasm membrane rupture thus inflammatory response is avoided (Savill, 1997). In apoptosis, DNA cleavage is an evident nuclear feature in contrast to necrosis. Genomic DNA is degraded randomly into 50kbp and 300kbp fragments. Furthermore, DNA fragments at 180bp and 200bp are detected with further cleavage in apoptotic cells. The degradation of DNA in necrosis leads to a smear called ‘DNA laddering’ on agarose electrophoresis gel.

Apoptosis widely exists in animal developmental, physiological and immune processes throughout the organism life time. In development, inappropriate differentiated cells and structures no longer required are eliminated by apoptosis. The disappearance of *Xenopus* tadpole tail is a frequently cited example of apoptosis in embryogenesis. Detrimental cells can be also eliminated through apoptosis. An intrinsic apoptotic strategy to prevent virus proliferation *in vivo* has evolved in animals. Virus-induced apoptosis in infected and neighbouring host cells can prevent infection spreading as primitive defence. As can be expected, viruses have evolved viral encoded apoptosis inhibitors. Conversely, aberrant

apoptosis is disastrous to tissue homeostasis and can lead to disease i.e. Alzheimer's disease.

Several experimental approaches can be used to distinguish apoptosis from necrosis, based on their respective morphological and biochemical features. Apoptotic cell blebbing and chromatin condensation can be identified using a microscope and electron microscope. Terminal deoxynucleotidyl transferase dUTP nick end labelling (TUNEL) is a method to detect DNA fragmentation *in situ* by labelling the exposed –OH group on the 3' end of nuclear DNA fragments. DNA laddering, cytochrome *c* release and induction of caspase activity are also widely used as indicators of apoptosis.

1.1.2 Programmed cell death in plants

Programmed cell death in plants refers to an apoptotic-like cell death, which is equally under a strict genetic control. Typical apoptosis in animal cells must exhibit all of the following features: cell shrinkage, chromatin condensation, DNA fragmentation and DNA laddering, caspase activation, apoptotic bodies and phagocytosis or autophagy. Except the shedding of apoptotic bodies and phagocytosis, other apoptotic features can be detected in plant cells undergoing PCD. For instance, plant protoplast retraction and cytoplasm condensation are defined features of heat shock-induced PCD (Reape *et al.*, 2008). Based on the genetic and morphological similarity in plant PCD and animal apoptosis, several animal apoptosis hallmarks are applied to characterise plant PCD. For example, cell death in monocot aleurone layers and endosperm, senescence of petal, carpel tissue and leaves or cell death during anther development or induced by different stimuli are defined as PCD using DNA laddering as a criterion (Danon *et al.*, 2000). TUNEL, the most widely used apoptotic detection method in animals is used in plant PCD identification, although it cannot distinguish DNA laddering from DNA smearing. The induction of caspase-like activity in plant PCD is detected. Specific features of plant PCD which are in fact absent from animal apoptosis such as crescent-shaped nucleus are also reported (Danon *et al.*, 2000).

Plant PCD occurs in developmental processes as well as response to abiotic or biotic stresses i.e. innate immune response against pathogens, heat shock and starvation. Plant cells undergoing PCD at a developmental stage show swelling vacuoles initially and

sequential elimination of the ER and other cell organelles. After the breakdown of mitochondria and nucleus, rupture of vacuolar membrane and plasma membrane shrinkage are observed. In some cells i.e. suspensor cells, xylem and phloem fibres, cork cells etc, the cell wall is not affected by PCD and specialised differentiated tissue with empty cell wall such as vascular bundle is therefore formed. On the contrary, cell walls in aerenchyma, endosperm and senescent mesophyll disappear completely after PCD (van Doorn & Woltering, 2005). Autophagy, which is a process of intracellular components turnover by lysosome and autophagosome provides an alternative destination for disposal cell, distinct from phagocytosis in animal apoptosis. In plant PCD, phagocytosis is absent due to the presence of the cell wall. In most of plant cells, the degradation of cell organelles in plant PCD is described as an autophagy exerted by proteases in the vacuole. However, PCD of endosperms in cereal such as barley, wheat and rice has been reported as an exception with absence of vacuole mediated autophagy.

The hypersensitive response (HR) is an innate immune response in plants against pathogen attack. HR includes PCD in infected and neighbouring cells, local anti-pathogen chemical secretion and induction of host resistance (Mur *et al.*, 2008). HR triggered by fungal toxin, bacteria and virus can reduce susceptibility of host plants to pathogens and reduce further invading. HR-mediated PCD is triggered and processed faster than that in plant development (del Pozo & Lam, 1998). Initiation of HR mediated HR relies on the interaction of 'resistance gene' (*R* gene) products and pathogen encoded avirulence gene (*avr* gene) products (Lorrain *et al.*, 2003). At the same time, basal defence response also occurs to prevent infection propagation along with *R*-gene mediated PCD.

1.1.3 Programmed cell death is ubiquitous throughout evolution

Apoptosis is ubiquitous in multicellular animals throughout evolution. The apoptotic machinery is also remarkably conserved from invertebrate to vertebrate with homologous apoptotic factors and pathways. The most clearly understood animal apoptotic pathway is that in nematode *Caenorhabditis elegans*, in which the predetermined differentiation fate of every individual cell was precisely mapped (Hengartner & Horvitz, 1994). In the 131 cell deaths in its ontogenesis from zygotes to adult, several genes are involved in *C. elegans* apoptotic regulation. Homologues of these thirteen genes with highly functional and structural similarity were identified in vertebrates; hence the relative simple apoptotic

pathway in nematode is a blue print for more complicated mammalian apoptosis. For instance, the 15 anti-apoptotic genes from the *bcl-2* family are mammalian homologues of the *ced-9* gene which can suppress apoptosis in *C. elegans* (Shi, 2004).

Plant PCD identified in xylem development, pollen self-incompatibility, senescence or hypersensitive reaction exhibits morphological alteration that is presumed analogous. However, lacking the major animal apoptotic genetic componants such as the caspase cascade, the genetic apoptotic pathway in plant PCD is still undefined. Extrapolation and identification of animal apoptotic analogues in plants is coming to the fore and will eventually improve the understanding of the mechanism in plant PCD. Interestingly, a monocellular organism such as yeast can undergo apoptotic-like death after chemical stimuli i.e. H_2O_2, acetic acid or sugar. Such apoptotic-like cell death is also detected in yeast aging and sexual reproduction. A cluster of apoptotic gene orthologues were identified (Madeo *et al.*, 2004; Wissing *et al.*, 2004; He *et al.*, 2007). An apoptotic-like mechanism has been described in the primitive monocellular protist *Dictyostelium discoideum*. The stalk formation is induced by nutrient starvation. This formation includes a cell death process showing high similarity with animal apoptosis in morphological aspects. It is therefore suggested that PCD evolves from a primitive single cell organism and might be a result of a conflict between archaebacteria and protomitochondria in early symbiosis events (Blackstone & Kirkwood, 2003). Phagocytosis is absent in the final stage of PCD in *Dictyostelium*, yeast and plant, while autophagy is demonstrated to contribute to the dead cell disposal (Levine & Klionsky, 2004; Hofius *et al.*, 2009).

1.2 Insight into the molecular mechanism of PCD

1.2.1 Apoptotic pathway in animals and plants

Animal apoptosis is transient and regulated by an integration of external and internal anti-apoptotic and pro-apoptotic factors after exposure to stimuli. Apoptosis regulatory genes in *C. elegans* (*ced-1* to *-14,* cell death abnormality; *nus-1*, nuclease-deficient; *ces-1*, *-2*, cell death specification; *egl-1*, EGg Laying defective) were identified using loss-of-function or gain-of-function mutant nematodes for the cell death of three specific cell types. In *C.elegans* embryogenesis, cells are first specified into three types with the regulation of *ces* genes before apoptosis. The gene *ced-3* encodes a protease with a cysteine amino acid residue in its active site and cleaves substrates specifically after aspartic acid residue in a four amino acid motif (Shi, 2004). A cluster of CED-3 protease homologues are active in mammalian apoptotic regulation and are named caspase. Like the *ced-3* gene, the gene *ced-4* is essential to apoptosis initiation and encodes a CED-3 activating protein. The *ced-9* gene generally prevents the cell against apoptosis by encoding a protein suppressing CED-3 and CED-4 protease activity. The engulfment of dead cell corpse is mediate by the gene *ced-5*, *-6, -7*, and *-10* (see Fig 1.1) After dead cell engulfment, the degradation of cell debris is mediated by the gene *nuc-1*.

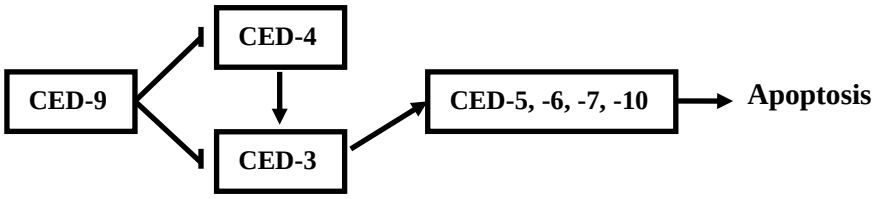

Fig 1.1 The major apoptotic pathway in *C.elegans*. Apoptosis is mediated by the *ced* genes as indicated. CED-3 is the main initiator and executioner in apoptosis which is activated by CED-4 and suppressed by CED-9. CED-5, -6, -7 and -10 are required for dead cell disposal.

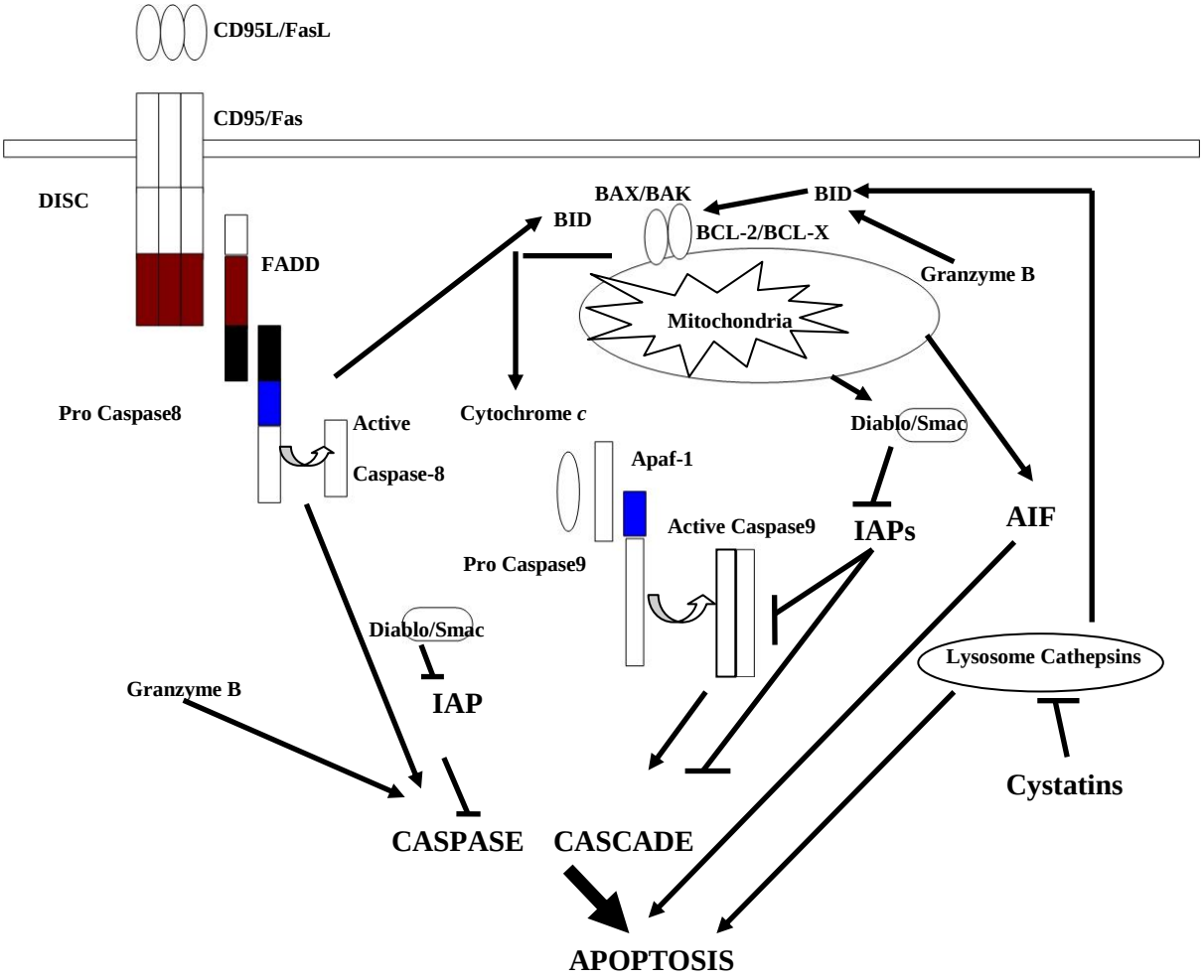

Fig 1.2 Three apoptotic pathways in mammalian cells: caspase-dependent and caspase-independent. In the extrinsic caspase-dependent pathway, CD95L binds to CD95 and activate DISC aggregation; caspase-8 is activated and triggers a caspase cascade. In the intrinsic caspase-dependent pathway, the mitochondrial outer membrance opens and release cytochrome *c*. Cytochrome *c* forms a complex (apoptosome) with Apaf-1 to activate caspase-9 and trigger a caspase cascade. The caspase-independent pathway triggers apoptosis by the release of cathepsins and cleavage of BID. IAPs are caspase inhibitors. BID operates as a linker among the three pathways.

In mammalian animals, three major apoptotic pathways are identified and at least two of them are caspase-dependent (see Fig 1.2 **)** Extrinsic apoptotic signalling is a coupling of apoptotic receptors with caspase members or regulators. Death signal-receptors i.e. CD95/Fas on the cell surface, are responsible for apoptotic signal recognition and transduction. Fas is a member of the tumour necrosis factor receptor (TNFR) family and binds to CD95L/FasL, members of the tumour necrosis factor (TNF) family. The binding between TNFR members and their specific ligands causes aggregation of the death-initiating signalling complex (DISC) and activates the receptors. The death domain on the C-terminus of CD95 binds to the homologous C-terminal domain of the adaptor protein

Fas associated death domain (FADD). Then FADD binds to another adaptor protein which is a caspase protease with a homologous N-terminal domain and the caspase cascade is thereby initiated (Bellamy *et al.*, 1995; Wyllie, 1997; Stoka *et al.*, 2001; Kroemer & Martin, 2005).

The intrinsic apoptotic pathway is mediated by mitochondria. The gene *bcl-2* is the first anti-apoptotic gene identified in mammalian cells and is a homologue of the nematode *ced-9*. Aberrant expression of *bcl-2* in cells leads to a higher survival capacity after stimuli and results in immune dysfunction. The *bcl-2* gene family encodes BCL-2 like proteins engaged in the downstream apoptotic regulation by altering cytochrome *c* release from mitochondria. They are either anti-apoptotic genes i.e. *bcl-2*, *bcl-x* or pro-apoptotic genes i.e. *bax*, *bak*, *bad* or *bik*. Four short BCL-2 homology domains (BH1-4) were discovered in these anti-apoptotic factors which bind to apoptotic effectors to suppress their lethal capacity. In addition, some anti-apoptotic factors bind to structurally related pro-apoptotic factors. In addition, the anti-apoptotic BCL-X can insert into intracellular membranes i.e. ER, mitochondria and nuclear envelop. Appropriate insertion of bcl2 members in membranes is essential for cell survival after particular injury. Proteins of this family can be detected in many cellular compartments, while mitochondria are where crucial protein interaction takes place (Green & Reed, 1998). Apaf-1, an apoptotic protease-activating factor, is homologue of CED-4 in *C.elegans*.

Some cytokines i.e. nerve growth factors (NFG), interleukin-3 (IL-3) and insulin-like growth factor 1 (IGF-1) are also central to apoptotic signalling and cell survival. They could suppress apoptotic stimuli and the withdrawal of such cytokines will trigger apoptosis. IAP (Inhibitors of apoptosis proteins) is another major negative regulatory protein family in apoptosis. The first identified IAPs are Cp-IAP and Op-IAP from baculovirus. They can inactivate specific caspase proteases and contribute to viral propagation in the host insect cell. Similarly, human X-linked IAP (XIAP) can suppress the apoptotic pathway by the inhibition of caspase-3, caspase-9 and caspase-7. However, the function of IAPs can be suppressed by Smac/Diablo proteins released from mitochondria after the apoptotic stimuli (Fig 1.2**)**.

Presumably, the genetic regulatory pathway in plant PCD shares some similarities albeit plant-specific cascades compared to animal apoptosis (Hoeberichts & Woltering, 2002). To establish a possible pathway in plant PCD, plant research groups looked for plant

homologues of animal apoptotic regulators. Some animal regulators, such as BAX, BCL-2 and BCL-XL exhibit similar regulatory function, induction or suppression of PCD, when overexpressed in plant cells (Danon *et.al* 2000; Chen & Dickman, 2004). AtBI-1, -2, -3 and OsBI1, which are homologues of human BAX inhibitor-1 (hBI-1) in *Arabidopsis* and rice, can suppress BAX-induced PCD in yeast (Sanchez *et al.*, 2000). Since BAX homologue is absent in plants, AtBI and OsBI may just bind to some other unknown regulators and suppress the PCD pathway in plants. However, without the discovery of BCL-2 plant homologues, these results are not sufficient to support the existence of a BCL-2 like regulatory pathway in plant PCD, since exogenous pro-apoptotic factors may merely alter plant mitochondrial permeability and cause cytochrome *c* release (Hoeberichts & Woltering, 2002). Two homologues of the animal *dad1* gene (defender against apoptotic death 1) have been identified in *Arabidopsis* (Danon *et al.*, 2000). First isolated from rodent animals, DAD1 modulates programmed cell death/apoptosis as a negative regulator conserved through the evolution. DAD1 interacts with various members in animal BCL-2 family (Danon *et al.*, 2000). However, the function of DAD1 homologues in plant PCD is still not clear since there are no plant *bcl-2* genes. The caspase cascade is also absent in plants, although plant metacaspases are considered orthologues of caspases because of sequence similarity but their enzymatic profile is quite different (reviewed later) (Vercammen *et al.*, 2007).

As reviewed in 1.1.2, HR is an immediate but sophisticated defence mechanism developed in plants. A variety of gene products involved in localized cell death provides a good experimental model to decipher the signalling pathway of plant PCD without autophagy (Mur *et al.*, 2008). Plant resistance genes (*R* gene) encode CARD (caspase recruitment domain) containing proteins. It is therefore postulated that an apoptosome-like complex exists in HR mediated PCD (van der Biezen & Jones, 1998). *R* gene products also contain several leucine-rich repeats (LRR), a nucleotide-binding site (NB) and an amino signalling domain (TIR, homologue of IL-1 receptor or CC, coil-coil motif) to form TIR-NB-LRR proteins or CC-NB-LRR proteins (Moffett *et al.*, 2002). These proteins provide platforms to interact with avirulence (*avr*) gene products and pathogen target proteins in cell. *R* gene products mediate pathogen-host proteins interaction and activate the PCD signalling pathway. The *Avr* gene products are pathogen effectors, which trigger host resistance with specific ligands binding to *R* gene products. Recent studies show that the *Avr* gene products enhance pathogen virulence and suppress HR when the corresponding *R* gene

products are absent (Belkhadir *et al.*, 2004; Fujikawa *et al.*, 2006). 149 *R* genes have been identified in *Arabidopsis* and their proteins are assembled into functional signalling complexes with pathogen targeting proteins to elicit a series of downstream events including ion leakage, accumulation of oxidatives and finally PCD (Simon *et al*., 2000). The molecular link between these signalling complexes and the execution of cell death remains ill-defined.

Abiotic stress-induced PCD has brought some additional insight into the initiation of PCD. PCD can be triggered by exposure to excessive levels of intra or extra-cellular reactive oxygen species (ROS). ROS are oxidative radicals and reagents including hydroxyl, alkoxyl, superoxide and hydrogen peroxide etc.(Simon *et al.*, 2000). Accumulation of ROS results in DNA and protein damage. In addition, ROS in plants act as signalling molecules in development and abiotic stress resistance by triggering PCD. ROS-responsive transcription factors, since a low ROS intracellular level is critical for survival. For example, additional exogenous H_2O_2 can activate the MAPK pathway and trigger PCD in *Arabidopsis* leaf cells (Kovtun *et al.*, 2000). In *Arabidopsis*, there are at least 289 genes encoding ROS-network related enzymes. In HR-mediated PCD, ROS intracellular concentration in infected cells is elevated swiftly to trigger PCD while the diffusion of ROS to neighbouring cells can induce the expression of antioxidant enzymes (Vranova *et al.*, 2002). Cytochrome *c* release from mitochondria induced by ROS has been reported in various plants PCD (Hoeberichts & Woltering, 2002).

In conclusion, despite the similarities confirmed between animal and plant PCD, the very defined pathways described in animal PCD are not replicated in plants at the molecular level. One obvious missing component in plants is the animal caspase cascade. Instead, other plant proteases have been reported to be involved in PCD regulation. The distinct protease cascade of PCD in animals and plants will be reviewed later.

1.2.2 Caspase family in animal apoptosis.

The gene *ced-3* (a caspase gene) plays a critical role in nematode apoptosis initiation and execution (Shi, 2004). Loss-of-function mutation in *ced-3* leads to the suppression of cell death in most of 131 cells, if not all, programmed to die during development (Yuan *et al.*, 1993). With the identification of a CED-3 homologue required for mammalian PCD, a

cysteine protease family that cleave substrates specifically after an aspartic acid residue, namely ‘cysteine aspartic acid specific protease’ (caspase) was unravelled. This mammalian homologue of CED-3 was named caspase-1. Till now, fourteen members in the caspase family have been identified and studied.

Proteases are generally divided into five subfamilies: cysteine proteases, aspartic protease (cathepsin D, E), serine proteases (granzyme, cathepsin G), metallo protease and threonine proteases based on their catalytic units in MEROPS. Cysteine proteases are further classified into papain like subfamily, caspase subfamily and calpain subfamily. Caspase catalytic dyad is His-Cys, an order which is unique in cysteine protease subfamilies. Although caspases-mediated cleavage requires a conserved aspartic acid residue on the substrate P1 position, P4 position is also pivotal to catalytic efficiency. Caspases members are divided into 3 groups based on their substrate specificity (Talanian *et al.*, 1997; Thornberry *et al.*, 1997). Group I caspases are inflammation mediators including caspase-1, -4, -5 and -14 the substrate prefered sequence is WEHD because hydrophobic residues are required at P4 position. In addition to its role in interleukin-1β precursor activation, caspase-1 (ICE) is also involved in various developmental stages and Fas mediated apoptosis pathway (Kamada *et al*., 1997). Caspase-4 and caspase-5 show high similarity with caspase-1 in sequence (Denault & Salvesen, 2002). Caspase-4 is involved in Fas mediated apoptosis and is able to mature procaspase-3 *in vitro*. It is also reported that caspase-4 may be localized on the ER membrane and involved in ER stress-induced apoptosis as well as Alzheimer's disease (Hitomi *et al.*, 2004). Overexpression of caspase-5 in mouse can induce apoptosis. Presumably, caspase-4 and -5 might be also cytokine mediators, because of their similar sequence and substrate preference as caspase-1. Caspases in group II are apoptotic effectors (‘downstream’ caspases) including caspase-2, -3 and -7. An aspartic acid residue is essential at P4 position in the substrates of group II caspases, thus DExD (DEHD or DEVD) is their substrate preferred motif. Most of their *in vivo* substrates are proteins pivotal to cell integrity. Caspase-3 can cleave poly (ADP-ribose) polymerase (PARP), which is important in DNA repair and cleave the DNase inhibitor (ICAD/DFF45) to trigger DNA fragmentation. Caspase-7 can cleave XIAP, an inhibitor of apoptosis. In addition to inactivating proteolysis, caspase-3 can also cleave prodomains off and activate other proteases i.e. ROCK I to induce membrane blebbing and apoptotic body shedding. Group III members are initiator caspases (‘upstream’ caspases) including caspase-6, -8, -9 and -10. They prefer substrates containing residues with

branched aliphatic side chains at the P4 position. Thus their substrate prefered motif is V/T/LExD. Caspase-6 cleaves lamin B1 and keratin 18 which are essential to nucleus and cytoskeleton integrity. Caspase-8, -9 and -10 transmit the apoptotic signal from stimuli to apoptotic executioners such as caspase-3 and caspase-7 and regulate this way the 'downstream' caspase cascade. Caspase-8 truncates BID to tBID and triggers the intrinsic PCD signalling pathway. Caspase-2 is expected to be an upstream caspase and caspase-6 is expected to be execution effectors based on their function identified in apoptosis (Roy & Cardone, 2002).

Caspases are expressed initially in the cytosol as zymogens, waiting for an activation signal. Caspase zymogens contain an N-terminal prodomain (Mw=2-25kDa), a large subunit (Mw=17-21kDa) and a small subunit (Mw=10-13kDa). In some procaspases, a short linker also exists between the large and small subunits. A pentapeptide QACxG (x represents R, Q or G) in which cysteine residue is encompassed is conserved in caspases. N-terminal prodomain of some caspases (caspase-1, -2, -4, -5, -9, -12 and -13) contain CARD, the caspase recruitment domain or DED, the death effector domain (caspase-8 and -10) which bind to death adaptors in the death-inducing signalling complex (DISC) or the caspase-activating complex (i.e. apoptosome) (Denault & Salvesen, 2002). Other caspases (caspase-3, -6 and -7) with short N-terminal peptide are regulated by the caspases containing long prodomain. The formation of DISC aggregates upstream caspases (caspase-2, -8, -10) and increases local concentration. The elevated local concentration of caspases leads to procaspases autoprocessing and activation since zymogenicity of single molecule of 'upstream' procaspases is low. Procaspase-8 possesses 1% activity compared to the catalytic form. In addition to autocatalysis, some other proteases such as granzyme B can also activate procaspase-8 and trigger apoptosis.

In some cases the formation of the apoptosome depends on the presence of cytochrome c in the cytoplasm. Cytochrome *c* released from mitochondria after a PCD stimulus, interacts with Apaf-1 and procaspase-9 in the presence of ATP. The apoptosome forms because CARD domains in procaspase-9 bind to Apaf-1 to create gathering points of procaspase-9 monomers. Dimerization of procaspase-9 will lead to activation without cleavage. Maturation of 'downstream' caspases relies on the removal of N-terminal peptides operated by 'upstream' caspases.

Finally, caspases can be activated without a DISC complex or an apoptosome. For example, procaspase-12 is activated in ER-stress induced apoptosis without cytochrome *c* release when unfolded and misfolded proteins accumulate in ER (Fan *et al.*, 2005). ER stress can be induced artificially by blocking N-glycosylation using tunicamycin. When tunicamycin induces ER stress in murine cell line C2C12, caspase-7 translocates from the cytosol to the ER membrane and cleaves the N-terminal peptide of procaspase-12. Caspase-12 cleaves procaspase-9 which then triggers 'downstream' caspases activation leading to apoptosis (Morishima *et al.*, 2002).

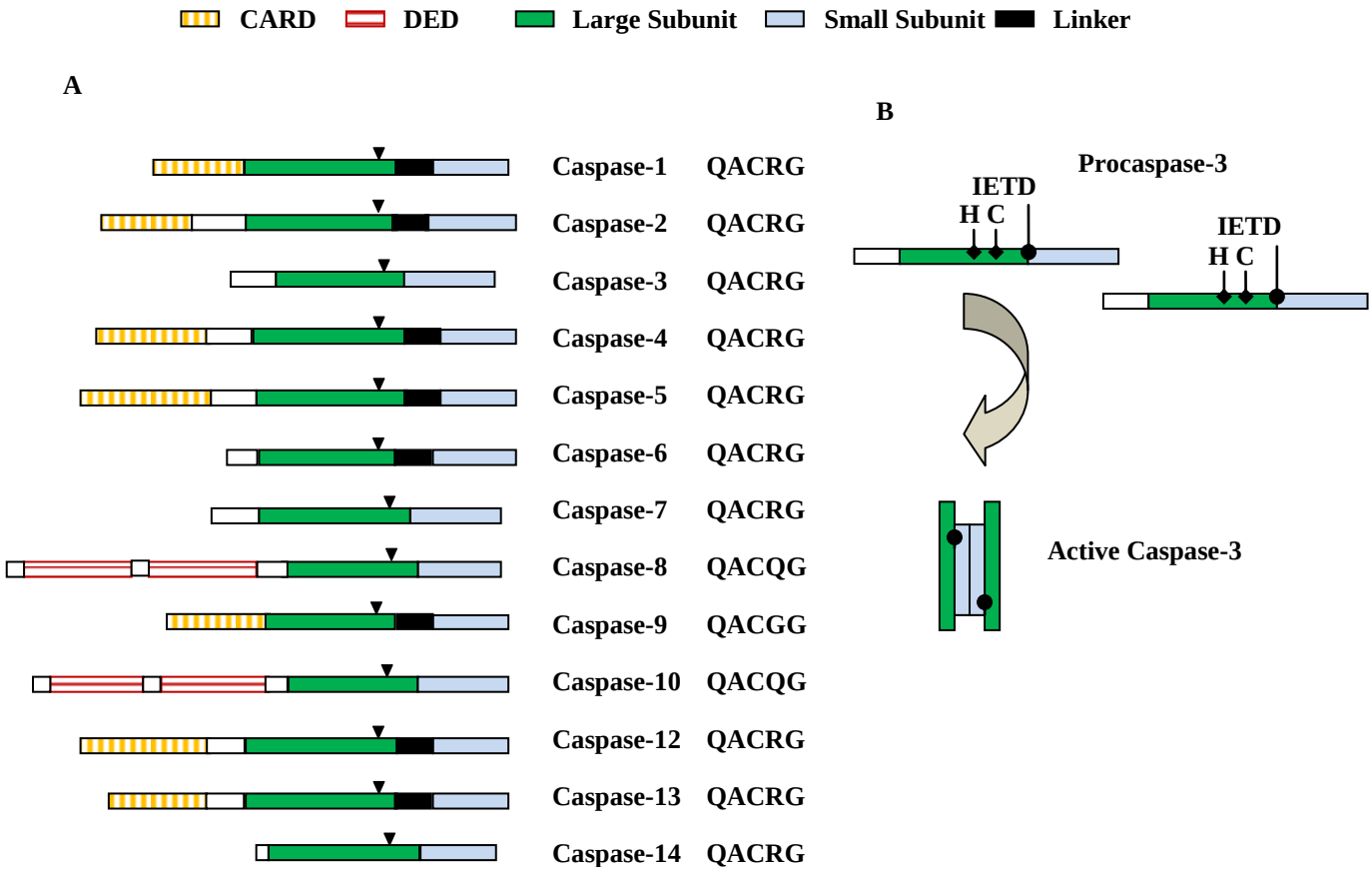

Fig 1.3 Schematic diagram of caspase zymogen structure and caspase-3 activation. (A) Caspases zymogens contain prodomain, large subunit and small subunit. Prodomain may contain DED, CARD or a short N-terminal peptide only. Sequences of the conserved pentapeptides are indicated by arrows and shown on the right. (B) Activation of procaspase-3. Procaspase-3 contains an IETD region which is cleaved by caspase-8 and a dimer is formed in activation.

Among the caspase family, caspase-3 is the most frequently activated. Caspase-3 is pivotal to survival in development: mice with caspase-3 loss-of-function die a few weeks after birth due to the failure of apoptosis in brain development. Caspase-3 contributes to some striking hallmarks in apoptosis i.e. chromatin condensation, DNA fragmentation and

membrane blebbing. Procaspase-3 contains a short N-terminal peptide as prodomain but lacks CARD or DED regions, which is important in signalling transduction. The maturation of procaspase-3 is executed by either caspase-8, -9, -10, CPP32 activating protease and granzyme B, through the removal of the N-terminal prodomain and the cleavage between large and small subunit. The motif IETD between the large and small subunit in the procaspase-3 sequence is the substrate preferred sequence by 'upstream' caspases and is likely to be the cleavage site for activation. The alternative splicing of caspase-3 transcripts leads to a truncated caspase-3, namely caspase-3S, lacking the catalytic motif QACRG. Caspase-3S competes with caspase-3 when overexpressed in human cells and suppresses apoptosis (Vegran *et al.*, 2006).

Caspase-3 substrates *in vivo* include other procaspases i.e. procaspase-6, procaspase-7, procaspase-9; nuclear related proteins i.e. DNA-protein kinase, PARP, ICAD and topoisomerase; cell morphology related proteins i.e. gelsolin and α-fodrin *etc.* However, most substrates of caspase-3 except α-fodrin and topoisomerase, are still cleaved in caspase-3 knockout mutants. It therefore implies that caspase-3 is not the only effectors for its specific stage of apoptosis. For example, PARP is still cleaved during TNF-α mediated apoptosis in caspase-3 loss-of-function MCF7 cells (Janicke *et al.*, 1998). Poly ADP ribose polymerase (PARP) is localised in the nucleus, contains a DNA binding domain and a catalytic domain and repairs damaged DNA (Ame *et al.*, 2004). PARP is inactivated by caspase-3, -6 and -7 clipping. Caspase-3 and caspase-7 both cleave PARP into two fragments in order to separate the DNA binding domain from the catalytic domain. The cleavage of PARP allows DNA fragmentation and eventually cell death (Wang *et al.*, 1997). On the contrary, α-fodrin, which is an actin binding protein, is not cleaved by other caspases and membrane blebbing is absent in caspase-3 knockout MCF7 cells (Janicke *et al.*, 1998).

1.2.3 Lysosome and caspase-independent pathways.

Several protease cascades distinct from the caspase-dependent pathway known in apoptosis have been identified and referred to caspase-independent pathway. These cascades include granzyme A, B, calpains, the proteasome and lysosomal cathepsins. These proteases may either provide alternative start points in caspase activation or operate apoptosis through alternative proteolysis.

Granzyme B is a serine protease produced by cytotoxic T lymphocyte (CTL) in endosomes. It possesses catalytic substrate specificity after an aspartic acid residue just like a caspase (Earnshaw *et al.*, 1999). Granzyme B can activate caspase-3 to trigger apoptosis directly or truncate BID to activate the intrinsic apoptotic pathway above mitochondria (Pinkoski *et al.*, 2001). Granzyme A also participates in CTL-induced apoptosis and may provide a backup to granzyme B. Regulation of granzyme B is integrated by the protease inhibitor 9(PI-9, an endogenous serpin/serine protease inhibitor) and cathepsin C which is essential for granzyme B processing.

Calpains are localised in the cytosol as zymogens and their activation relies on Ca^{2+} accumulation. Calpains either act as downstream and upstream regulators in caspase cascades or trigger an alternative apoptotic pathway without caspase. For example, vitamin D compounds can induce Ca^{2+}-calpain-dependent apoptosis in breast cancer cells without caspase activation detected (Mathiasen *et al.*, 2002).

The lysosome is a single layer membrane-bound vesicle arising from the golgi apparatus and containing more than fifty different hydrolytic proteases. A striking feature of the lysosome is the acidic pH value environment (pH4.8), which is quite different from the neutral or slightly alkaline cytosolic pH value. Initially, lysosome function was thought to be limited to non-specific degradation of macromolecules (i.e. intracellular proteins, extracellular matrix and pathogens) and cell compartments which are no longer required. The fusion of lysosome to endosome, phagosome and cell organelles makes it a dynamic microbody. Lysosomal proteolytic proteases, namely cathepsins, are an important group involved in caspase-independent apoptosis. Cathepsins were previously linked to autolysis and inflammation in necrosis but an involvement in apoptosis has become clearer in the last decade. Cathepsins include papain-like cysteine proteases (cathepsin B and L), aspartic protease (cathepsin D and E) and serine protease (cathepsin A and G). Cathepsins are synthesized in the ER as inactive zymogen, bind to mannose-6-phosphate receptors (MPRs) in the trans-golgi network and are then glycosylated. Eleven human cysteine cathepsin members have been identified till now: B, C, F, H, L, O, S, K, V, W and X. Most papain-like cysteine cathepsins prefer a hydrophobic residue in the P1 position. Cathepsin B, L, V, S, K, H are all endopeptidase while cathepsin B is also an exopeptidase (Turk *et al.*, 2002). Cathepsins cleave their substrates into small peptides because of a relatively low cleavage site specificity compared to caspase. Cathepsin D is a major

executioner in intracellular protein turnover and cathepsin G is involved in phagocytosis mediated by neutrophils.

Cathepsins are demonstrated to participate in several important physiological processes after translocation to the cytosol. For example, cathepsin B is verified to be involved in TNF-α-mediated hepatocyte apoptosis in rat (Guicciardi *et al*., 2000) and mice brain apoptosis. Lysosome permeabilization that leads to cathepsins leakage and translocation is a prerequisite of the lysosome mediated apoptosis pathway. A possible mechanism leading to lysosome permeabilization is ROS induction. Intralysosomal iron was found to catalyse oxidative processes contributing to lysosome leakage (Turk, 2002). However, numerous results suggest that the level of lysosomal proteases leakage is vital to the balance between necrosis and apoptosis: large scale destruction of lysosomes leads to necrosis, but small scale lysosome permeabilization leads to apoptosis.

Since cathepsins are initially synthesised as zymogens to avoid inappropriate proteolysis, activation is another prerequisite to their participation in apoptosis. A complicated mechanism is required for cathepsin activation including pH sensitivity and endogenous inhibitors. Generally, the acidic environment is vital to their activity: cathepsin are activated in acidic pH (lysosomal pH is 4.8) and inactive at neutral pH, the approximate pH of cytosol. Active cathepsins are therefore restricted to lysosome meanwhile cystatins, a group of endogenous cysteine protease inhibitors act as a double insurance of cathepsin. However, in case of neurodegradation and senescence, the accumulation of cathepsins in the cytosol has been reported. In addition, cathepsin B inhibitors suppress apoptosis without reducing cathepsin B release (Foghsgaard *et al.*, 2001). Cathepsin B also accumulates in the cytosol of mouse hepatocytes treated by TNF-α as well as actinomycin D (AcD), is the later being a transcription inhibitor to prevent additional cathepsin B synthesis (Guicciardi *et al.*, 2000). Surprisingly, cysteine cathepsins activity at neutral pH has been reported in non-pathological conditions. For example, cathepsin B is active at neutral pH for more than one hour and this enables its extralysosomal functions after translocation (Turk *et al.*, 1994). Some polysaccharides i.e. glycosaminoglycans (GAGs) and dextran sulphate may facilitate cathepsin activation in the cytosol (Caglic *et al.*, 2009).

How cathepsins trigger apoptosis is an attractive topic. Cathepsins process some caspase zymogens but not at typical activation sites. For example, cathepsin G cleaves procaspase-7 at distinct site with a low catalytic efficiency. However, *in vitro* results from Stoka *et al.*

(2001) suggest that purified cathepsins B, H, K, L, S, and X cannot activate recombinant or natural caspase zymogens. Faubion *et al.* (1999) reported that CrmA, a viral caspase-8 inhibitor, suppress glycochenodeoxycholate (GCDC)-induced cathepsin B activation as well as apoptosis in rat liver. It is therefore suggested that caspases might be required for cathepsin B activation and active cathepsin B might be involved in the caspase-dependent apoptotic pathway. *In vitro* studies show that synthetic caspase inhibitors (YVAD-CMK, YVAD-FMK, DEVD-CMK, DEVD-FMK and VAD-FMK) suppress cathepsins activity especially cathepsin B, suggesting that cathepsins may cleave caspase cleavage site *in vivo* (Turk *et al.*, 2002). Therefore collectively, cathepsins may be involved in apoptotic pathway through activating procaspases (Turk *et al*., 2001). Another possibility for cathepsins to regulate apoptosis is via cathepsin-mediated BID truncation. Lysosomal extracts cleave BID in *vitro* and mitochondria treated with the cleaved BID can release cytochrome *c* (Stoka *et al.*, 2001). Guicciardi *et al.* (2000) suggests that cathepsin B release is activated by caspase-8 and then cathepsin B induce cytochrome *c* release from mitochondria in cell free systems. Furthermore, cathepsin B loss-of-function mutant mouse cells show elevated survival capacity after TNF-α induction of PCD and TNF-α induced caspase activation and cytochrome *c* release are diminished. Such results collectively suggest that caspase-8 activates the release of cathepsin B in the cytosol then cathepsin B induce cytochrome *c* release and trigger caspase cascade. Alternative suggestion to role of cathepsin B in TNF-α-mediated apoptosis is provided by Salvesen (2001): cathepsin B is a promoter of TNF receptor 1 to promote apoptosis.

1.3 Identification of caspase homologues in plants

1.3.1 Caspase-like activities in plants and their roles

Given the pivotal role of caspases in apoptosis, the identification of plant caspase homologues or analogues is an important goal for a better understanding of plant PCD. Plant homologues may exists since Gingipain R, a bacterial cysteine protease from *Porphyromonas gingivalis,* was confirmed to have a tertiary structure similar to caspase strucutre suggesting an ancient origin of caspase family (Eichinger *et al.*, 1999). Alternatively, in support of the existence of caspase analogues, animal cells do have caspase analogues: calpain and granzyme B process procaspases and are considered to be functional analogues since they do not have any structural similarity. Although plant PCD shares some morphological features with animal apoptosis and although various caspase-like activity were detected in plants, the existence of caspase homologue in plants still needed to be demonstrated when I started my thesis (Bonneau *et al.*, 2008). The publication of entire genome sequence of *Arabidopsis* in 2000 and rice confirmed the absence of caspase orthologues in plants. The term 'caspase-like protease' was then used to either refer to proteases which have caspase-like enzymatic activity or to proteases with sequence and structural homology to caspase (van der Hoorn, 2008). Here, the first definition is used in this thesis.

The development of *in vitro* caspase substrates and inhibitors makes the detection of caspase-like activity and roles in plant PCD more convenient. As reviewed above, one *in vivo* substrate for caspase-3 is PARP and the sequence DEVD is identified as the substrate prefered motif of caspase-3 by mapping the cleavage site of PARP (Nicholson *et al.*, 1995). The same approach can be used for all caspases. Commercial synthetic caspase substrates are available as specific tetrapeptides modified with acetyl (Ac) at the N-terminus and conjugated at the C-terminus with fluorometric (i.e. 7-Amino-4-methylcoumarin, AMC; 7-amino-4-trifluoromethyl coumarin, AFC; rhodamine110) or colourimetric (i.e. p-nitroanilide, pNA) groups (Gurtu *et al.*, 1997). The same tetrapeptides conjugated with aldehydes (CHO) or methylketones (FMK, CMK) can suppress caspase reversibly or irreversibly. Methylketones coupled inhibitors are cell permeable and can be used in cell culture while aldehydes coupled inhibitors are widely used in cell free system or extracts. Commonly used synthetic substrates include ac-VAD-AMC (pan caspase), ac-

YVAD-AMC (caspase-1), ac-DEVD-AMC (caspase-3), ac-VEID-AMC (caspase-6), ac-IETD-AMC (caspase-8).

Table 1.1 Caspase-like activities detected in plants. (Reproduced from Bonneau *et al*., 2008)

Activity	Species and tissue	Reference
YVADase (Caspase-1)	Tobacco leaf tissue	del Pozo and Lam (1998)
	Barley embryonic suspension cells	Korthout *et al.* (2000)
	Arabidopsis thaliana seedlings	Danon *et al.* (2004)
	Germination of white spruce seeds	He and Kermode (2003)
	Tobacco (BY2) suspension cells	Mlejnek and Prochazka (2002)
	Pisum sativum seedlings	Belenghi *et al.* (2004)
	Fumonisin B-induced leaf lesion in *Arabidopsis*	Kuroyanagi *et al.* (2005)
DEVDase (Caspase-3)	Barley embryonic suspension cells	Korthout *et al.* (2000)
	Arabidopsis thaliana seedlings	Danon *et al.* (2004)
	Germination of white spruce (*Picea glauca*) seeds	He and Kermode (2003)
	Tobacco (BY2) suspension cells	Mlejnek and Prochazka (2002)
	Avena sativa leaves	Coffeen and Wolpert (2004)
	Tobacco (BY2) suspension cells	Tian *et al.* (2000)
	Embryogenic cell line of Norway spruce	Bozhkov *et al.* (2004); Suarez *et al.* (2004)
	Papaver pollen	Thomas and Franklin-Tong *et al.* (2004)
LEVDase (Caspase-4)	SI in *Papaver* pollen	Bosch and Franklin-Tong *et al.* (2007)
VEIDase (Caspase-6)	*Arabidopsis thaliana* seedlings	Rotari and Gallois, unpub
	Embryogenic cell line of Norway spruce	Bozhkov *et al.* (2004)
	Barley seeds	Boren *et al.* (2006)
	SI in *Papaver* pollen	Bosch and Franklin-Tong *et al.* (2007)
IETDase (Caspase-8)	*Arabidopsis thaliana* seedlings	Rotari and Gallois, unpub
	Avena sativa leaves	Coffeen and Wolpert (2004)
LEHDase (Caspase-9)	Leaf of *Nicotiana benthamiana*	Kim *et al.* (2003)
VKMDase (Saspase)	*Avena sativa* leaves	Coffeen and Wolpert (2004)
TATDase (Phytaspase)	Tobacco Xanthi leaves	Chichkova *et al.* (2004)
	Rice	Chichkova *et al.* (2010)

The first report of caspase-like activity involvement in plant PCD showed the abolishment of PCD in HR induced by pathogenic bacteria, using ac-YVAD-CMK and ac-DEVD-CHO (del Pozo & Lam, 1998). This was a very significant discovery in plant PCD research. Till now, there are at least eight caspase-like activities detected in plant PCD using synthetic substrates and inhibitors (table 1.1) (reproduced from Bonneau *et al.*, 2008). YVADase (caspase-1-like) and DEVDase (caspase-3-like) are widely detected in various plant PCD systems. As shown in table 1.2, PCD in plants can be suppressed by some of the synthetic capsase inhibitors. The combination of caspase-like activity detection in plant PCD together with the abolishment of PCD by the corresponding caspase inhibitor is an evidence of caspase-like activity involvement. For example, YVADase activity is detected in fumonisin B1-induced lesion formation in *Arabidopsis*, while biotin-YVAD-FMK suppresses lesion formation induced by fumonisin B1 (Kuroyanagi *et al.*, 2005). However, as shown in table 1.3, some caspase inhibitors are not efficient in plant PCD suppression. For example, ac-YVAD-CHO only has a slight effect on xylem formation in zinnia system (Fukuda, 1997) and pollen incompatibility in *papaver* (Thomas & Franklin-Tong, 2004). Interestingly, ac-DEVD-CHO does suppress HR induced by *P. syringae pv. tabaci* (Krzymowska *et al.*, 2007) but does not suppresses HR induced by TMV (Hatsugai *et al.*, 2004). Effects of DEVDase inhibitors on HR induced by *P. syringae pv. maculicola* and N gene-mediated HR in tobacco are also insignificant (Krzymowska *et al.*, 2007; Chichkova *et al.*, 2004). Therefore, different proteases might be implicated in HR-mediated PCD induced by varying pathogens in distinct plants.

However, the issue of substrate and inhibitor specificity is still a problem when using such synthetic tetrapeptides. The synthetic caspase substrates in animal are cleaved by several non-caspase proteases. Bonneau *et al.* (2008) suggested that even in animal cells synthetic caspase substrates lack specificity and therefore plant proteases involved in PCD may be blocked by synthetic caspase inhibitors without being proteases analogous to caspases. The search for *in vivo* substrates of caspase-like activities in plants has been very limited so far: only plant PARP has been shown as a substrate for plant caspase-like activities (Thomas & Franklin-Tong *et al.*, 2004).

Table 1.2 Synthetic caspase inhibitors suppress PCD in plants. (Reproduced from Bonneau *et al*., 2008)

Inhibitor	Experimental system	Reference
VAD-FMK	Nicotiana cv. Xanthi cell suspension PCD induced by xylanase	Elbaz *et al.* (2002)
	Embryogenic cell line of Norway spruce	Bozhkov *et al.* (2004)
	Isopentenyladenosine-induced PCD in tobacco BY2 cells	Mlejnek *et al.* (2002)
DEVD-CHO	Cell death in tobacco caused by P. syringae pv. phaseolicola	del Pozo and Lam (1998)
	Menadione-induced PCD in tobacco protoplasts	Sun *et al.* (1999)
	Camptothecin etc. induced PCD in tomato suspension	De Jong *et al.* (2000)
	UV-C-induced PCD in Arabidopsis protoplasts	Danon *et al.* (2004)
	Pollen incompatibility in Papaver	Thomas and Franklin-Tong (2004)
	Elimination of weaker shoots in Pisum sativum seedlings	Belenghi *et al.* (2004)
	Ce^{4+}-induced apoptosis of cultured Taxus cuspidata cells	Ge *et al*. (2005)
	Heat-shock-induced cell death in tobacco BY2	Vacca *et al.* (2006)
	Fusaric-acid-induced PCD on C. sativus root tips	Samadi *et al.* (2006)
	HR induced by P. syringae pv. tabaci	Krzymowska *et al.* (2007)
DEVD-CMK/FMK	Mega-gametophyte cells of white spruce seeds	He *et al.* (2003)
	Isopentenyladenosine-induced PCD in tobacco BY2 cells	Mlejnek *et al.* (2002)
TATD-CHO	N gene-mediated HR in tobacco	Chichkova *et al.* (2004)
VEID-FMK	Embryogenic cell line of Norway spruce	Bozhkov *et al.* (2004)
YVAD-CHO	UV-C-induced PCD in Arabidopsis thaliana protoplasts	Danon *et al.* (2004)
	HR induced using tobacco mosaic virus	Hatsugai *et al.* (2004)
	Fusaric acid-induced PCD on Crocus sativus root tips	Samadi *et al.* (2006)
YVAD-CMK/FMK	Tissue remodelling in lace plant	Gunawardena (2008)
	PCD in tobacco caused by P. syringae pv. phaseolicola	del Pozo and Lam (1998)
	Camptothecin etc. induced PCD in tomato suspension	De Jong *et al.* (2000)
	NO-induced PCD in Arabidopsis suspension cultures	Clarke *et al.* (2000)
	HR induced by P. syringae pv. tabaci	Krzymowska *et al.* (2007)
	Isopentenyladenosine-induced PCD in tobacco BY2 cells	Mlejnek *et al.* (2002)
	Fumonisin B1-induced lesion formation in Arabidopsis	Kuroyanagi *et al.* (2005)

Table 1.3 Synthetic caspase inhibitors cannot suppress plant PCD. (Reproduced from Bonneau *et al*., 2008)

Inhibitor	Experimental system	Reference
DEVD-CHO	HR induced using tobacco mosaic virus	Hatsugai *et al.* (2004)
	HR induced by P. syringae pv. maculicola	Krzymowska *et al.* (2007)
	N gene-mediated HR in tobacco	Chichkova *et al.* (2004)
LEHD-FMK	Embryogenic cell line of Norway spruce	Bozhkov *et al.* (2004)
YVAD-CHO	Xylem formation in Zinnia system	Fukuda (1997)
	Pollen incompatibility in Papaver	Thomas and Franklin-Tong (2004)
	HR induced by P. syringae pv. maculicola	Krzymowska *et al.* (2007)

1.3.2 Metacaspase: distant caspase orthologue without caspase-like activity

The search for distant caspase homologues in genome databases identified novel sequences showing significant similarity with caspases: initially a human EST (Expressed Sequence Tag), a slime fold *dictyostelium discoideum* EST and a nematode *C. elegans* ORF (Aravind *et al.*, 1999). Using the caspase-like domain of these sequences in further PSI-BLAST search, two families of caspase-like proteins were identified and designated paracaspase in animals and metacaspase in plants, fungi and protozoa. These proteins contain a conserved caspase-like catalytic dyad His-Cys, while their tertiary structures are also similar to caspase (Vercammen *et al.*, 2007). Based on their sequence similarity, plant metacapases were classified into a type I group containing a Pro or Gln rich N-terminal prodomain as well as a zinc finger motif and a type II group containing a linker between the large and small subunits (Uren *et al.*, 1999). Metacaspases were subsequently discovered in prokaryota, protozoa, fungi, chromista (only type I) and plants (both type I and type II) while paracaspase were discovered only in prokaryota and animals. As shown in table 1.4, there are nine metacaspases identified from *Arabidopsis* and divided into two groups: metacaspase I (AtMC1-3) and metacaspase II (AtMC4-9). Phylogenetic analysis revealed that caspase, paracaspase and metacaspase have similar distance in evolution (Vercammen *et al.*, 2007). There are nine metacaspase genes identified in *Arabidopsis*: *AtMC-1* to *-3* in type I and *AtMC-4* to *-9* in type II (Vercammen *et al.*, 2004).

AtMC-4, -8 and -9 were expressed in *E.coli* and their biochemical features were studied *in vitro* (Vercammen *et al.*, 2004; Watanabe & Lam, 2005; Vercammen *et al.*, 2007; He *et al.*,

2007). All of three are cysteine proteases that cleave synthetic substrate after a P1 Arg residue instead of the originally expected P1 Asp acid residue. However, metacaspase-9 can also cleave substrates after a P1 Lys residue with low efficiency. Interestingly, recombinant type II metacaspase can be autoprocessed while type I metacaspase cannot. It is therefore postulated that type I metacaspases are activated *via* aggregation, just like upstream caspases (Fuentes-Prior & Salvesen, 2004). Another similarity between caspases and metacaspases is S-nitrosylation. S-nitrosylation is the modification on Cys residues using nitrosothiol in proteases to mediate NO signalling.

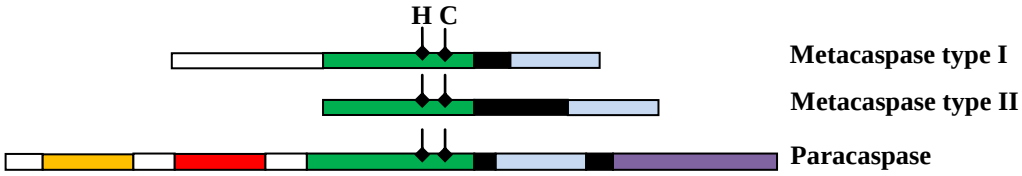

Fig 1.4 Schametic diagram of the structural properties of metacaspase and paracaspase. The catalytic domains contain a large subunit (green) and a small subunit (light blue). Cysteine and Histidine catalytic dyads are indicated. Type I metacaspases contain an N terminal prodomain while type II metacaspases contain an larger linker. Paracaspases possess N terminal prodomains containing a death domain (yellow) and one or two Ig domains (red) as well as an extended C-terminal domain shown in lilac. (Reproduced from illustration in Vercammen *et al.*, 2007)

One metacaspase gene, *YCA1* from yeast is widely used in metacaspase research. Higher sensitivity to aging and oxidative stress in *YCA1* overexpressing yeast strains suggests its involvement in PCD while *YCA1* gene loss-of-function mutants were less sensitive to exogenous stress (Madeo *et al.*, 2002). However, the role of this metacaspase in yeast PCD is still debatable since the report of a *YCA1*-independent cell death induced by Endonuclease G (Buttner *et al.*, 2007). Initially, extracts from H_2O_2 treated *YCA1* overexpressing yeast strain were shown to cleave the caspase substrates VEID-AMC and IETD-AMC (Madeo *et al.*, 2002), However, *YCA1*-independent caspase-like activity was reported (Hauptmann *et al.*, 2006). It was eventually verified that YCA1 has not caspase-like activity but cleaves substrates after Arg or Lys P1 residues just like plant metacaspases do (Watanabe & Lam, 2005).

The regulatory PCD pathway for the nine metacaspases genes identified from *Arabidopsis* is still unclear (He *et al.*, 2007). Overexpression of *AtMCP1b* (*AtMC2*) and *AtMCP2b* (*AtMC5*) in wild type yeast strain and *YCA1* gene disrupted strain demonstrated their

positive regulatory function in yeast PCD induced by oxidative stress and early aging process (Watanabe & Lam, 2005). Their proteolytic activity relies on the caspase-like processing by their catalytic dyad composed of His-Cys residues. What's more, the pan-caspase inhibitor, VAD-FMK suppresses the PCD in *AtMC2* and *AtMC5* overexpression yeast strain. It is speculated that some metacaspases could transduct the apoptotic signal just like initiator caspases do. They may be involved in the 'upstream' regulation of plant PCD by triggering apoptotic executioner protease cascades. For example, AtMC8 has been classified as a strong upstream mediator in PCD induced by UV-C, H_2O_2 as well as methyl viologen, three treatments that induce oxidative stress (He *et al.*, 2007). However, metacaspases in Norway spruce (*Picea abies*) have been shown to be involved in PCD activation and/or execution occurring during embryogenesis (Bozhkov *et al.*, 2004). A downstream VEIDase activity was shown to be involved in embryo suspensor cells differentiation and cell death. Finally, the expression level of *LeMCA1*, a type II metacaspase gene identified in tomato was increased in pathogen-induced cell death (Hoeberichts *et al.*, 2003).

In conclusion, metacaspases, the ancient and distant homologues of animal caspases are required for plant PCD regulation. It has been reported recently that McII-Pa, a type II metacaspase from Norway spruce is required for Tudor Staphylococcal Nuclease (TSN) proteolysis in PCD (Sundstrom *et al.*, 2009). TNS proteolysis in animal apoptosis is operated by caspase-3. It is therefore suggested that type II metacapase might share some similarity with the execution caspases (caspase-3, -6 or -7). Further research in metacaspases and *in vivo* substrates identification would benefit the undertanding of metacaspases function in plant PCD.

Table 1.4 Metacaspases in *Arabidopsis thaliana* (reproduced from Sanmartin *et al.*, 2005) Subcellular localisation is predicted.

Gene	Locus	Subcellular localisation	Expression
Type I			
AtMC1(AtMCP1a)	At5g64240	Mitochondrion	Ubiquitous
AtMC2(AtMCP1b)	At1g02170	Chloroplast	Leaves induced by Pst etc.
AtMC3(AtMCP1c)	At4g25110	Mitochondrion	Leaves induced by Pst, SA, $AgNO_3$ etc.
Type II			
AtMC4(AtMCP2a)	At1g79310	Cytosol	Wounded roots; Roots under salt, osmotic, genotoxic stress
AtMC5(AtMCP2b)	At1g79330	Cytosol	Seeds
AtMC6(AtMCP2c)	At1g79320	Cytosol	Roots
AtMC7(AtMCP2d)	At1g79340	Cytosol	Ubiquitous
AtMC8(AtMCP2e)	At1g16420	Cytosol	Leaves induced by Pst etc.
AtMC9(AtMCP2f)	At5g04200	Cell wall	Senescing cell cultures and flowers; Roots under osmotic stress

1.3.3 Saspase and phytaspase: subtilases with caspase-like activity

The serine protease family is the largest protease family in plants with more than two hundred members and shares a similar catalytic mechanism with cysteine protease (van der Hoorn, 2008). The subtilisin-like serine proteases or subtilases are serine proteases with a catalytic unit made of Asp, His and Ser residues. Most subtilases are non-specific endopeptidases which cleave several substrates with varying efficiency. The subtilase zymogen is processed at both termini during secretion and then activated. At least seventy subtilase genes are identified in *Arabidopsis*.

The victorin induces ribulose-1, 5-bisphosphate carboxylase/oxygenase (RuBisCO) proteolysis and ultimately PCD in oat (*Avena sativa*) (Navarre & Wolpert, 1999). The RuBisCO cleavage induced by victorin in oat is suppressed by several caspase inhibitors indicating that different types of caspase-like activities are involved (Coffeen & Wolpert, 2004). Isolation and characterization of these caspase-like proteases identified two proteases with a Ser residue rather than a Cys residue in their catalytic site. These proteases are homologous to subtilisin-like Ser proteases, thus named ‘serine protease active towards aspartate’, namely saspase (SAS1 and SAS2). Further biochemical characterization indicatesd that the saspase substrate specificity was strict for an Asp

residue on the P1 position, this being distinct from all other known serine proteases (Coffen & Wolpert, 2004). The activation of saspases was found to occur in the secretion pathway. However, the genes encoding saspases are still not cloned and this prevented their function in plant PCD to be further characterised.

Phytaspase (plant aspartate-specific protease) is another subtilisin-like protease with caspase-like activity shown to be involved in plant PCD. Phytaspase was identified recently from tobacco and rice (Chichkova *et al.,* 2004; Chichkova *et al.,* 2010) and the *Agrobacterium* VirD2 protein was found to be its substrate. VirD2 is a virulence protein which plays an important role in nuclear import and chromosomal integration during *Agrobacterium*-mediated DNA delivery (Bako *et al.*, 2003). The VirD2 protein in tobacco was found to be hydrolysed by proteases with caspase-like activity, resulting in the detachment of its C-terminal nuclear localisation signal (NLS). The cleavage of VirD2 by plant proteases with caspase-like activity is likely to be a defence mechanism against *Agrobacterium* infection (Reavy *et al.*, 2007). Phytaspase activity was first purified from tobacco and then rice and shown to cleave VirD2 after Asp400 residue in the TATD motif. Subsequently, after cloning the recombinant phytaspase was shown to cleave several synthetic caspase substrates including IETD-AFC, VEID-AFC, LEHD-AFC and YVAD-AFC. Phytaspase however has no DEVDase activity and is localized in both apoplast and cytosol RNAi studies showed that phytaspase is required for TMV-induced PCD during HR (Chichkova *et al.*, 2010).

1.3.4 Vacuole, vacuolar processing enzyme and caspase-1-like activity

Lysosome widely exists in all animal cells especially the disease defence cells such as leukocytes. Whether lysosome exists in plant cells is a long-time debating question. However, as a lytic compartment in plant cells, vacuole contains many homologous enzymes found in animal lysosome (Matile *et al.,* 1978; Wink, 1993) and acts as the lysosome. The vacuole is a remarkably important cellular compartment in plant PCD and performs dramatic alteration in the autolysis of dead cell corpses (Jones, 2001). The coincidence between vacuole collapse and the start of autolysis was observed, indicating a possible hydrolytic function in vacuole. However, distinct from lysosome rupture in animal apoptosis and necrosis, the collapse of plant vacuole is only discovered in the cells undergoing PCD in cell terminal differentiation, senescence and HR (Kuriyama & Fukuda,

2002). PCD specific proteases and nucleases are released into cytosol after the collapse of vacuole in the cells undergoing PCD and start to mediate cellular compartments breakdown i.e. the degradation of DNA and chlorophyll in nuclei and chloroplasts with an unknown mechanism (Kuriyama & Fukuda, 2002). However, some hydrolytic enzymes in vacuole appreciate an acidic catalytic environment but functions in a neutral pH environment in cytosol (Ye, 2002). It is reported that after the collapse of vacuole in *Arabidopsis* cells in PCD, pH value in cytosol was acidified immediately (Gallois & Young, submitted). Similar acidification of cytosol resulting from vacuole collapse has been reported in tracheary elements (TE) mediated PCD in zinnia cell culture (Obara e*t al.*, 2001). Thus hydrolytic enzymes can be completely activated after translocation. As reviewed previously, the involvement of animal lysosome in caspase-dependent cascade is verified. The counterparts of lysosome in plants, vacuole might mediate a similar PCD signalling pathway (Kuriyama & Fukuda, 2002).

Legumains are Asparaginyl-specific cysteine endopeptidases first isolated from plants and *Schistosoma*, which are responsible for specific protein maturation through a series of limited proteolysis (Chen *et al.*, 1998). Legumains are localised in the lysosome of mammalian cells and activate procathepsin B, H and L. The 'vacuolar processing enzyme' (VPE) is a plant legumain resident in the vacuole (Muntz & Shutov, 2002).

In addition to their role in protein precursor maturation and activation, VPEs were identified as a plant caspase that regulate vacuole-mediated PCD induced by pathogen in *Arabidopsis* and tobacco (Hara-Nishimura *et al.*, 2005; Bosch *et al.*, 2010). VPEs share several structural and functional similarities with animal caspase-1 and cleave at the aspartic acid residue in the caspase-1 substrate YVAD sequence (Hatsugai *et al.*, 2004). The pentapeptide of the active site in VPEs, E (A/G)CES, is homologous to the QACRG pentapeptide in animal caspase-1. There are four *VPE* genes discovered in *Arabidopsis* which are separated into vegetative type (*αVPE*, *ϒVPE*) and seed type (*βVPE*, *δVPE)* (Nakaune *et al.*, 2005). Vegetative VPE genes are involved in leaf senescence, lateral root formation and fungal toxin-induced PCD in *Arabidopsis* while *Arabidopsis δVPE* is implicated in the PCD of a cell layer of seed teguments. Similarly, *NbVPE* gene is involved in TMV-induced PCD.

The caspase-1-like activity of plant VPEs was confirmed by recombinant expression of NbVPE in insect cell system and *Papaver* VPE1 (PrVPE1) in *E.coli* system (Hara-

Nishimura *et al.*, 2005; Bosch *et al.*, 2010). In addition to caspase-1-like activity, PrVPE1 also possesses caspase-3-like activity.

1.3.5 The ubiquitin-proteasome system and caspase-3-like activity

The proteasome in mammalian cells is responsible for protein turnover and was found to have chymotrysin-like sites, trypsin-like sites and caspase-like sites (Kisselev *et al.*, 2003). The same is true for the plant proteasome.

The 20S proteasome has been reported recently to be involved in plant autonomous immunity (Hatsugai *et al.*, 2009). In plants, autonomous immunity is triggered by bacterial pathogens, and a proteasome-mediated fusion of the vacuolar membrane and the plasmamembrane occurs. This fusion discharges vacuolar antibacterial proteins into the apoplast. Cell death is the final stage of this process. Interestingly, in proteasome loss-of-function mutants, a reduced caspase-3-like activity was observed (Hatsugai *et al.*, 2009) suggesting that the proteasome is at the origin of the caspase-3 like activity detected in plants. Further research using various inhibitors of the proteasome established the link between the proteasome subunit PBA1 and caspase-3-like activity in plants is therefore established (Hatsugai *et al.*, 2009).

1.4 Cathepsin B in programmed cell death

1.4.1 Role of cathepsin B in animal apoptosis

As reviewed previously, cathepsins are defined as 'lysosomal proteolytic proteases' and are involved in various physiological processes in animal cells. Cathepsin B belongs to the papain-like cysteine protease family and has been shown to regulate animal apoptosis (Chwieralski *et al.*, 2006). Cathepsin B is synthesised as a preproenzyme with a signal peptide and prodomains. The signal peptide is removed co-translationally during the ER import. N-glycosylation of cathepsin B occurs during secretion through the ER and golgi apparatus. Two Arg-linked and phosphorylated-mannose-containing oligosaccharides are attached to procathepsin B. Cathepsin B is eventually transported to the lysosome by mannose-6-phosphate receptors in the trans-golgi network. In the acidic environment of lysosome, cathepsin B is processed by cathepsin D, elastase, cathepsin G and legumain *etc.* into its mature form. Autocatalysis is also reported to cause cathepsin B activation (Rowan *et al.*, 1992). In some conditions, various partially-activated cathepsin B forms exist in the lysosome which is likely to be fully activated after stimuli (Turk *et al*., 2009).

Alternative spliced mRNA variants of cathepsin B are produced in specific cases. For example, exon3 and exon7 are missing from cathepsin B mRNAs in human melanoma cells and human breast cancer cells. In some other human tumour cells, exon2 is absent from cathepsin B mRNAs. In addition, an increased level of mRNA transcripts is detected in many human tumours where the elevation of cathepsin B activity is mainly due to an increased expression level (Mort & Buttle, 1997).

Generally, cathepsin B is involved in protein turnover as an endopeptidase and as an exopeptidase. In cell free system, cathepsin B triggers chromatin condensation, which is a striking morphological feature of apoptosis (Vancompernolle *et al.*, 1998). In addition, human cathepsin B is involved in the apoptosis of hepatocytes, neuronal cells as well as immune cells. The putative pathway of cathepsin B mediated apoptosis is still under discussion (Stoka *et al.*, 2001). BID is cleaved by cathepsin B *in vitro* and so is considered a putative substrate to cathepsin B in an apoptotic pathway. Furthermore, cathepsin B as well as cathepsin L, S *in vitro* activates AIF a promoter of apoptosis (Yuste *et al.*, 2005). However, *in vivo* evidence supporting that cathepsin B can cleave BID or AIF is still absent.

TNF-α-induced apoptosis is suppressed when cathepsin B is inhibited (Liu *et al.*, 2003). In bile salt-induced apoptosis of mouse hepatocyte, cathepsin B is required for the caspase-8 apoptotic pathway (Roberts *et al.*, 1997; Jones *et al.*, 1998; Faubion & Gores, 1999). In WEHI-S fibrosarcoma cells, the cathepsin B inhibitor cystatin A and antisense-mediated cathepsin B depletion both suppress apoptosis induced by TNF. It is therefore speculated that cathepsin B acts as a dominant execution protease in TNF-induced apoptosis (Foghsgaarda *et al.*, 2001). In addition to a role in TNF-α-induced apoptosis in hepatocytes, cathepsin B is also implicated in neuronal cell apoptosis. Indeed, cathepsin B and cathepsin L double knockout mice die around postnatal day 12 from neurodegeneration because of the reduced apoptosis in the brain (Felbor *et al.*, 2002). Interestingly, cathepsin B extracted from mouse brain exhibits caspase-3 like activity at acidic pH (Yakovlev *et al.*, 2008). Mouse brain extract possesses caspase-3-like activity and such activity is located in lysosomes. Furthermore, a protease from mouse brain extract with caspase-3-like activity was purified and eventually identified as cathepsin B by MALDI-TOF mass spectrometry. It is therefore postulated that in some cases such as hypoxia, cathepsin B participates in the proteolysis of caspase-3 substrate in brain cells. However, direct evidence supporting that cathepsin B can cleave caspase-3 substrate *in vivo* is still absent.

1.4.2 Cathepsin B in plant PCD regulation

Cathepsin B is encoded by one single gene in mammals while a multi-gene family of cathepsin B paralogues exists in the nematode genome. Multi-gene families of cathepsin B-like proteases are also identified in parasite and in some plants genomes. Although various plant cathepsin B genes have been cloned, the research in their function and especially in their role in PCD is still limited.

Gilroy *et al* (2007) reported on the function of *Nicotiana benthamiana* Cathepsin B (*NbCathB*) in HR-mediated PCD induced by non-host pathogens by *NbCathB* mRNA transcripts expression level were induced in HR; HR induced by non-host pathogens is suppressed in *NbCathB* silenced tobacco. However, the pathogen *Cladosporium fulvum* AVR4 induced a PCD that was independent of *NbCathB*. *NbCathB* was found to be secreted and localised in the apoplast. *NbCathB* was found to be activated during secretion.

From this it is concluded that *NbCathB* is involved in HR regulation but not in all plant-pathogen systems.

Three cathepsin B-like genes have been identified in *Arabidopsis thaliana*: *AtCathB-1,-2* and *-3*. McLellan *et al.* (2009) reported that the three *AtCathB* genes are involved in pathogen-inducible PCD. The phenotype of reduced HR is only visible in the triple gene knockout mutant as single KO lines have no phenotypes In addition, *AtCathB* is reported to be involved in senescence as a positive regulator without being an absolute requirement for the process (McLellan *et al.*, 2009).

1.4.3 Is *Arabidopsis* cathepsin B a functional analogue of caspase-3?

The search for caspase functional analogues in plants is a hot area of plant PCD research. Saspase, VPE have been identified as plant analogue to caspase-6 and caspase-1. PBA1, a subunit of the 20S proteasome, is reported to be responsible for caspase-3-like activity in HR-mediated PCD.

So far it has been reported that cathepsin B purified from mouse brain presents a caspase-3-like activity *in vitro*, which is the only report connecting cathepsin B with caspase-3 like activity published till now. However, *Arabidopsis* cathepsin B is also a protease responsible for caspase-3 like activity in UV-C induced PCD (Gallois *et al.* unpublished). UV-C irradiation can induce PCD in *Arabidopsis* seedlings and induce caspase-3 like activity (Danon *et al.* 2004). In addition, cysteine proteases were purified from UV-C induced *Arabidopsis* seedlings using a bacitracin-sepharose column followed by CM sepharose chromatography. The purified fraction was labelled using biotin-DEVD-FMK to block caspase-3 like proteases and then purified again using streptavidin chromatography. One main protein band was visualised in the streptavidin fraction using SDS-PAGE and silver staining. This band was identified using LC-mass spectrometry as the product of the *Arabidopsis* gene *At4g01610*, namely *AtCathB-3*. This constitutes the initial evidence supporting the hypothesis that *Arabidopsis* cathepsin B is responsible for caspase-3-like activity in plants. Further research into the association between *Arabidopsis* cathepsin B and caspase-3-like activity in plant PCD was the proposed aim of this thesis.

1.5 Project introduction

Although the role of cathepsin B in animal apoptosis has been reported in numerous research papers, the role of plant cathepsin B has been only studied during senescence and HR mediated PCD. On another note, Dr. Gallois' laboratory established a preliminary link between *Arabidopsis* cathepsin B and caspase-3 like activity in oxidative stress-induced. This led to the question of my thesis: Is *Arabidopsis* cathepsin B really responsible for the caspase-3 like activity detected during PCD? The answer to this question would be useful to improve the understanding of the plant PCD regulatory pathway and it may bring evidence that a conserved and common PCD regulatory pathway using cathepsin B has been conserved through evolution, from plants to animals.

1.5.1 Project aims

To analyse the function of *Arabidopsis* cathepsin B in oxidative stress-induced PCD using loss-of-function mutant plants and establish a reliable link between *Arabidopsis* cathepsin B and caspase-3 like activity detected in plants *in vivo* and *in vitro*.

1.5.2 Project objectives

1.5.2.1 Confirm in plant extracts that cathepsin B has caspase-3 activity.

The purification of caspase-3 like proteases from *Arabidopsis extracts* using bacitracin affinity chromatography is established in the lab. The evidence that *Arabidopsis* cathepsin B has caspase-3-like activity needs confirmation using selective cathepsin B inhibitors and plant protease fractions.

1.5.2.2 Investigate the involvement of *Arabidopsis* cathepsin B in oxidative stress-induced PCD.

AtCathB double knockout transgenic plants and triple knockout transgenic plants will be generated and used in a functional analysis aimed at finding a reduced cell death phenotype after oxidative stress induction. To strengthen a possible link with PCD, *Arabidopsis* cathepsin B gene expression, protein concentration level and proteolytic activities in response to oxidative stress will be analysed.

1.5.2.3 Investigate the subcellular localization of *Arabidopsis* cathepsin B

Because animal cathepsin B changes subcellular localisation during PCD, *Arabidopsis* cathepsin B will be fused to a fluorescent protein tag and introduced into plants to discover its sub cellular localization before and during cell death.

1.5.2.4 Characterise possible *in vivo* substrates of *Arabidopsis* cathepsin B

To provide direct and reliable evidence that *Arabidopsis* cathepsin B possesses caspase-3-like proteolytic activity, the recombinant *Arabidopsis* cathepsin B will be produced and analysed for its enzymatic activity *in vitro*. In addition, a preliminary characterisation of *in vivo* protein substrates will be attempted using a proteomic approach.

CHAPTER 2

MATERIALS AND METHODS

2.1 Plant materials and growth conditions

2.1.1 Plant materials

Arabidopsis thaliana Columbia-0 ecotype (Col0) was used as wild type plants. Seeds of *Arabidopsis* cathepsin B single knockout lines SALK_49118, SALK_89030 and SALK_19630 were purchased from European Arabidopsis Stock Centre, Nottingham, UK.

2.1.2 Growth on compost

Seeds were sown on the compost in pots and placed in 4 ℃ for 64h for stratification before being transferred to the growth chamber. The growth condition was 16h light 22 ℃ and 8h dark 15 ℃ cycles (Percival AR-66l Arabidopsis Chamber, Emersacker, Germany).

2.1.3 Growth on MS culture medium

Materials

Seedling germination medium	pH 5.7
Murashige and Skoog salts	4.4g/l
Glucose	20g/l
Phytagel	4g/l
MES	0.5g/l

Method

Seeds were surface sterilized with 70% (v/v) ethanol in rotation for 10 min before being plated on the germination medium. Sown seeds were then placed in 4 ℃ for 64h for stratification before being transferred to the growth chamber. Seedlings were grown in 12 h light, 12h dark cycle at 23 ℃ in growth chamber (SANYO MLR-350 Versatile

Environmental Test Chamber, SANYO Electric Co. Ltd., Japan) until 2-4 weeks old depending on the experimental requirement.

2.2 Plasmids construction

2.2.1 Construction of plasmids pSCherry-AtCB2 and pSCherry-AtCB3

The gene sequence of protease AtCathB-2 with 27 N-terminal amino acid residues deletion and protease AtCathB-3 with 25 N-terminal amino acid residues deletion were amplified respectively from the plasmid pU12892 (*AtCathB-2* cDNA) or the plasmid pU17098 (*AtCathB-3* cDNA) in PCR reactions using VELOCITY DNA polymerase (Bioline Ltd., UK). Primers were designed with a *BamH* I restriction site in forward and an *EcoR* I restriction site in reverse. The PCR products and pSCherry2 expression vector (Delphi Genetics SA., Belgium) were digested in successive reactions with *BamH* I and *EcoR* I restriction enzymes (Roche Applied Science, Germany). Following a PCR clean up with NucleoSpin Extract II kit (Macherey-Nagel, Germany), the purified PCR products were ligated into digested pSCherry2 vector using T4 DNA ligase (Roche Molecular Biochemicals, Germany). The gene sequences of *AtCathB-2* and *AtCathB-3* with deletion were therefore introduced into pSCherry2 expression vector under the control of a T7 RNA promoter (Fig. 2.1) and fused to a Cherry-tag and a 6×His-tag. Plasmids were transformed into *E.coli* strain CYS21 cells for cloning and selected on 100 μg/ml ampicillin LB agar culture medium. The DNA sequences of constructs were verified by DNA sequencing. Correctly constructed plasmids were transformed into SE1 *E.coli* strain for protein expression.

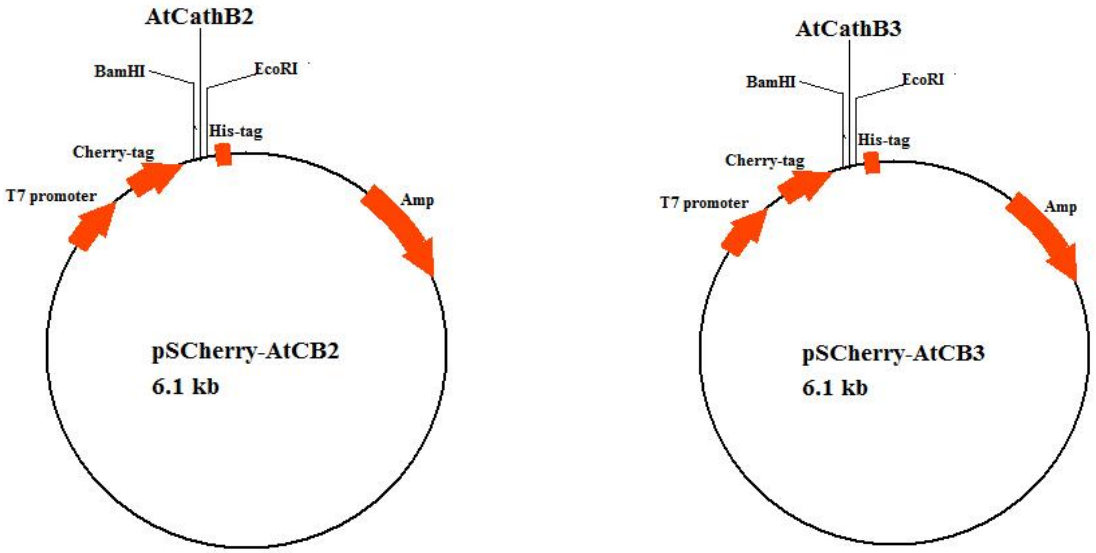

Fig 2.1 Maps of pSCherry-AtCB2 and pSCherry-AtCB3 plasmids. The cDNA sequence of gene *AtCathB-2* and *AtCathB-3* with 5' end deletion were cloned from pU12892 and pU17098 and introduced into pSCherry2 expression vectors in which the a Cherry-tag and a 6×His-tag were incorporated for a better expression and purification of recombinant protein. Maps of plasmids were produced by BVTech plasmid software.

Table 2.1 Primers used in pSCherry-AtCB2 and pSCherry-AtCB3 plasmids construction

Gene	Primer	Primer Sequence 5'-3'
AtCathB-2	AtCB2Cherry-F	CGGGATCCTTGCAGGGTATTGCAGCTG
AtCathB-2	AtCB2Cherry-R	GGAATTCAAAAATGAGGAAACAAGAAG
AtCathB-3	AtCB3Cherry-F	CGGGATCCTTGAAGGGTATAGAAGCAG
AtCathB-3	AtCB3Cherry-R	GGAATTCAAAACCGATGCAACCGGAAG

2.2.2 Construction of plasmids pAcGP-AtCB2Cherry, pAcGP-AtCB3Cherry, pAcGP-AtCB3tPro and pAcGP-AtCB3m

The gene sequences of the protease AtCathB-2 with the N-terminal 27 amino acid residues deletion (AtCB2Cherry), protease AtCathB-3 with the N-terminal 25 amino acid residues deletion (AtCB3Cherry), protease AtCathB-3 with the N-terminal 45 amino acid residues deletion (AtCB3tPro) and protease AtCathB-3 with the N-terminal 102 amino acid residues deletion (AtCB3m) were amplified from the plasmid pSCherry-AtCB2 and

pSCherry-AtCB3 respectively in PCR reactions using VELOCITY DNA polymerase (Bioline Co. Ltd., UK). Primers for pAcGP-AtCB2Cherry and pAcGP-AtCB3Cherry plasmid construction were designed with an *Xba* I restriction site in forward and a *Pst* I restriction site reverse primers. Forward primer for pAcGP-AtCB3tPro plasmid construction contained an *Xba* I resctriction site and 6×His-tag DNA sequence while reverse primer contained a 6×His-tag DNA sequence and a *Pst* I restriction site. Forward primer for pAcGP-AtCB3m plasmid construction contained an *Xba* I resctriction site and 6×His-tag DNA sequence while reverse primer contained a *Pst* I restriction site. The PCR products and pAcGP67A baculovirus transfer vector (BD Bioscience, US) were digested using *Xba* I and *Pst* I restriction enzymes (Roche Applied Science, Germany). The digested PCR products were cleaned up using NucleoSpin Extract II kit (Macherey-Nagel, Germany) and ligated into linarized pAcGP67A transfer vector using T4 DNA ligase (Roche Molecular Biochemicals, Germany). The gene sequences of *AtCathB-2* and *AtCathB-3* with different deletion were cloned into pAcGP67A transfer vector under the control of a polyhedrin promoter to be recombinated into the linarized baculovirus genome DNA for protein expression (Fig. 2.2). Plasmids were transformed into *E.coli* strain XL1-blue competent cells and selected on 100 µg/ml ampicillin LB agar culture medium. DNA sequencing were carried out on several selected independently colonies.

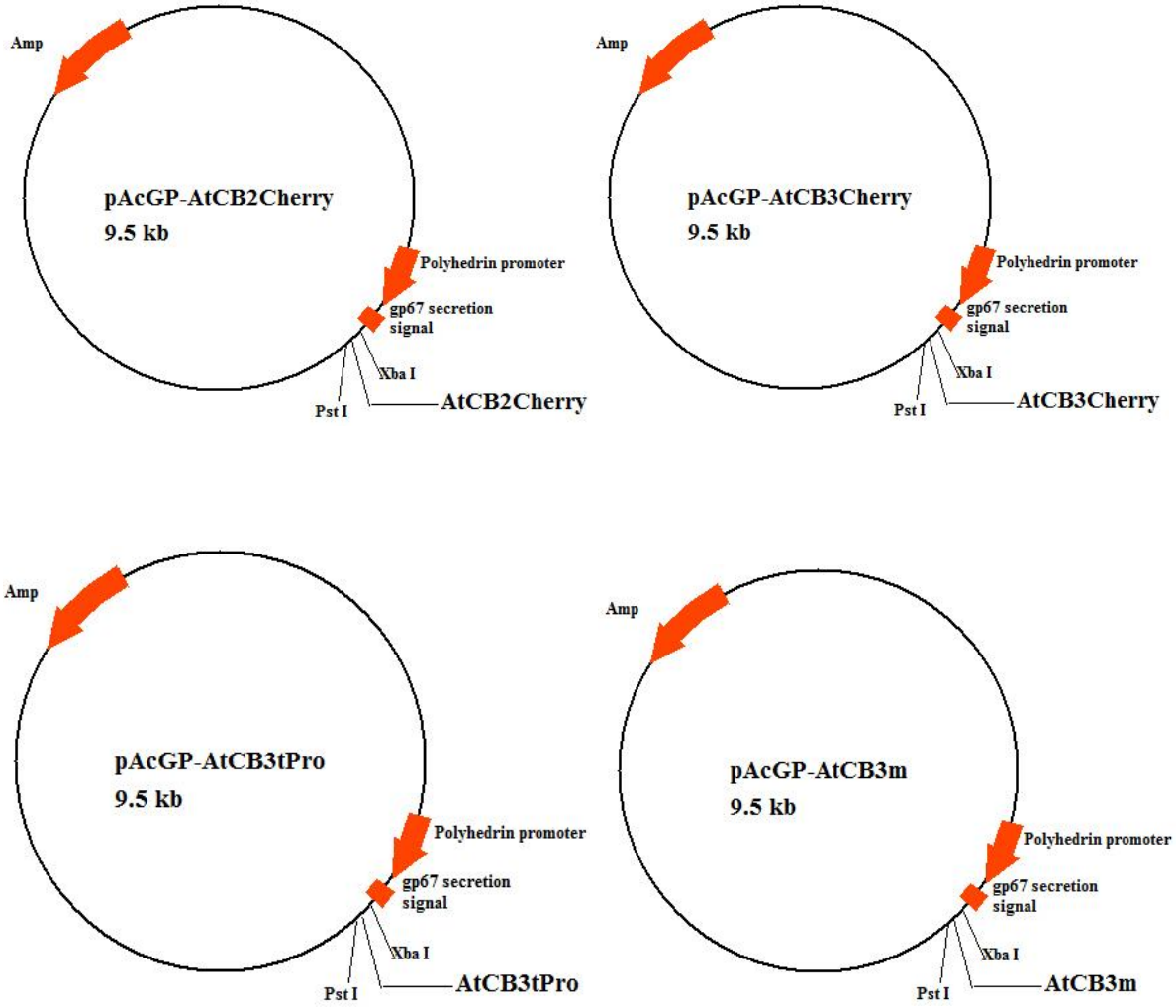

Fig 2.2 Maps of pAcGP-AtCB2Cherry, pAcGP-AtCB3Cherry, pAcGP-AtCB3tPro and pAcGP-AtCB3m plasmid. The cDNA sequences of the gene *AtCathB-2* and *AtCathB-3* with 5' end deletion were cloned from pSCherry-AtCB2 and pSCherry-AtCB3 respectively and introduced into pAcGP67A baculovirus transfer vector in which a 6×His-tag was incorporated for purification of recombinant protein. Maps of plasmids were produced by BVTech plasmid software.

Table 2.2 Primers used in pAcGP-AtCB2Cherry, pAcGP-AtCB3Cherry, pAcGP-AtCB3tPro and pAcGP-AtCB3m plasmids construction

Gene	Primer	Primer Sequence 5'-3'
AtCathB-2	CB2CherryF	GCTCTAGAAATGGCAGAACAAAGCGACAAGG
AtCathB-2	CB2CherryR	AACTGCAGTCAGTGGTGGTGGTGGTGGTG
AtCathB-3	CB3CherryF	GCTCTAGAAATGGCAGAACAAAGCGACAAG
AtCathB-3	CB3CherryR	AACTGCAGTCAGTGGTGGTGGTGGTGG
AtCathB-3	CB3tProF	GCTCTAGAACATCATCACCACCATCACGGTTCCGGTCAGGATGAG ATTGTGAAGAAA
AtCathB-3	CB3tProR	AACTGCAGTTAGTGATGGTGGTGATGATGACCGCTGCCTCTGGGC ACCAAGCTTGAAGGCAAACCAGCTAC
AtCathB-3	CB3mF	GCTCTAGAACATCATCACCACCATCACGGTTCCGGTTTGGTGCCCA GAGGCAGCCTACCTAAAGCTTTTGATGC
AtCathB-3	CB3mR	AACTGCAGTTAGCTTGAAGGCAAACCAGCTAC

2.2.3 Construction of plasmid pH2GW-2300i and plasmid pH2GW-2305i

Sequences of artificial microRNAs to silence *AtCathB-1* and *AtCathB-2* were designed by WMD3 web microRNAs designer (wmd3.weigelworld.org) and named amiRNA2300 and amiRNA2305. Precursors of amiRNA2300 and amiRNA2305 were produced by a two steps PCR using VELOCITY DNA polymerase (Bioline Ltd., UK) and primers designed by WMD3 web oligo designer. PCR step 1 was composed of the amplification of three short nucleotides using pRS300 (miR319a) as a template. The three short nucleotides were used as templates in PCR step 2 to amplify the amiRNA precursors. The PCR products of amiRNA2300i precursor and amiRNA2305i precursor and the pENTR1A entry vector (Invitrogen Co. Ltd., US) were digested using *EcoR* I restriction enzymes (Roche Applied Science, Germany). The digested PCR products were cleaned up using NucleoSpin Extract II kit (Macherey-Nagel, Germany) and ligated into the pENTR1A entry vector using T4 DNA ligase (Roche Molecular Biochemicals, Germany) and named pENTR1A-2300i and pENTR1A-2305i respectively. Thus the DNA sequences of amiRNA2300i and amiRNA2305i precursors were introduced into an entry vector between attL1 and attL2 sequences. The DNA sequences of amiRNA2300i and amiRNA2305i precursors in pENTR1A vectors were subsequently transferred into the Gateway vector pH2GW7 for *Agrobacterium*-mediated plant transformation mediated by LR clonase^{TM} II enzyme

(Invitrogen Co. Ltd., US). Plasmids were transformed into *E.coli* strain XL1-blue competent cells and selected on 100 µg/ml ampicillin LB agar culture medium (Fig 2.3 and Fig 2.4). The DNA sequences were verified by DNA sequencing.

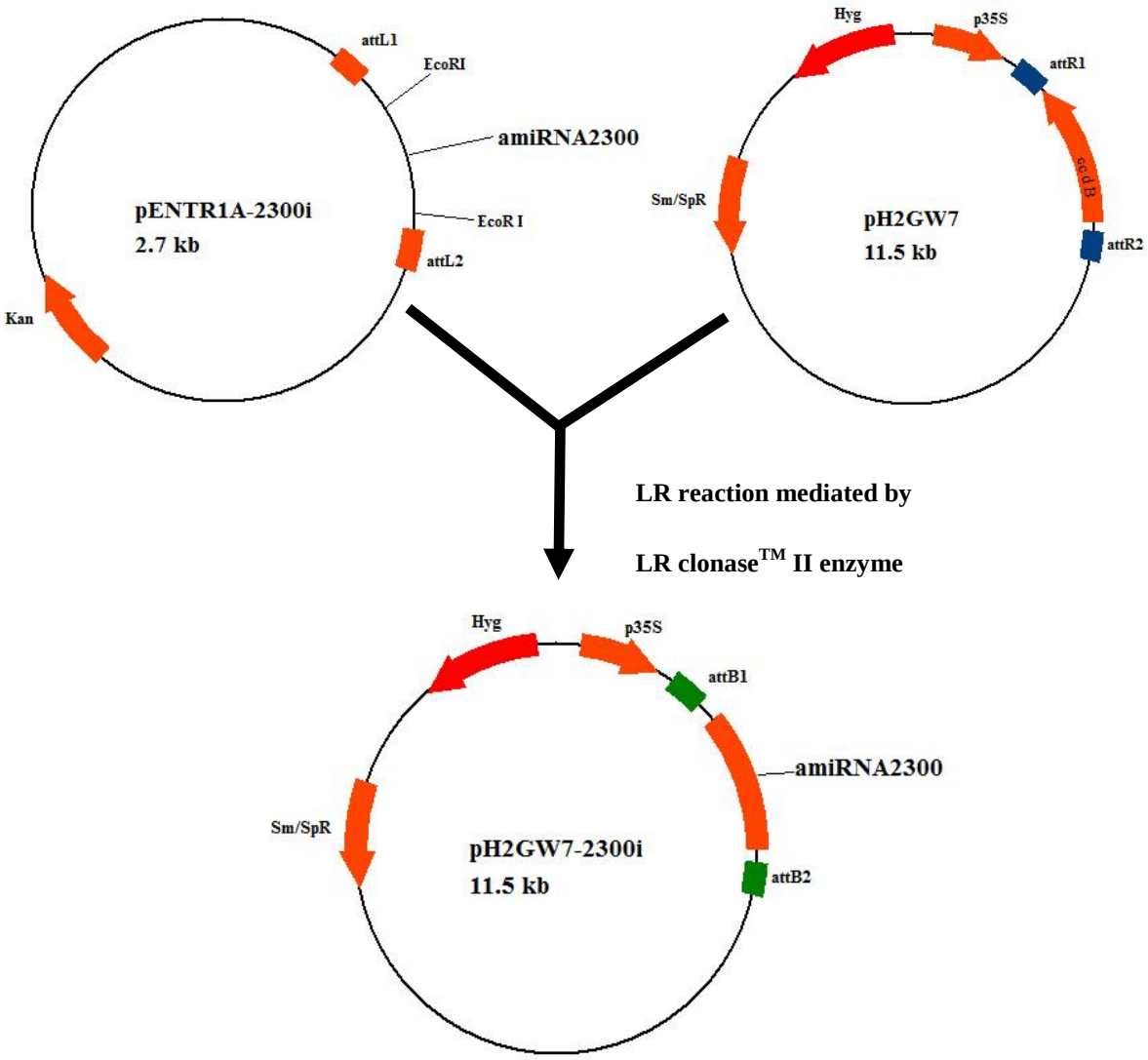

Fig 2.3 Maps of pENTR1A-2300i and pH2GW7-2300i plasmid. The gene sequence of amiRNA2300i precursor were engineered, cloned into pENTR1A vector and then introduced into pH2GW7 *Agrobacterium*-mediated plant transformation vector using LR clonase™ II enzyme.Maps of plasmids were produced by BVTech plasmid software.

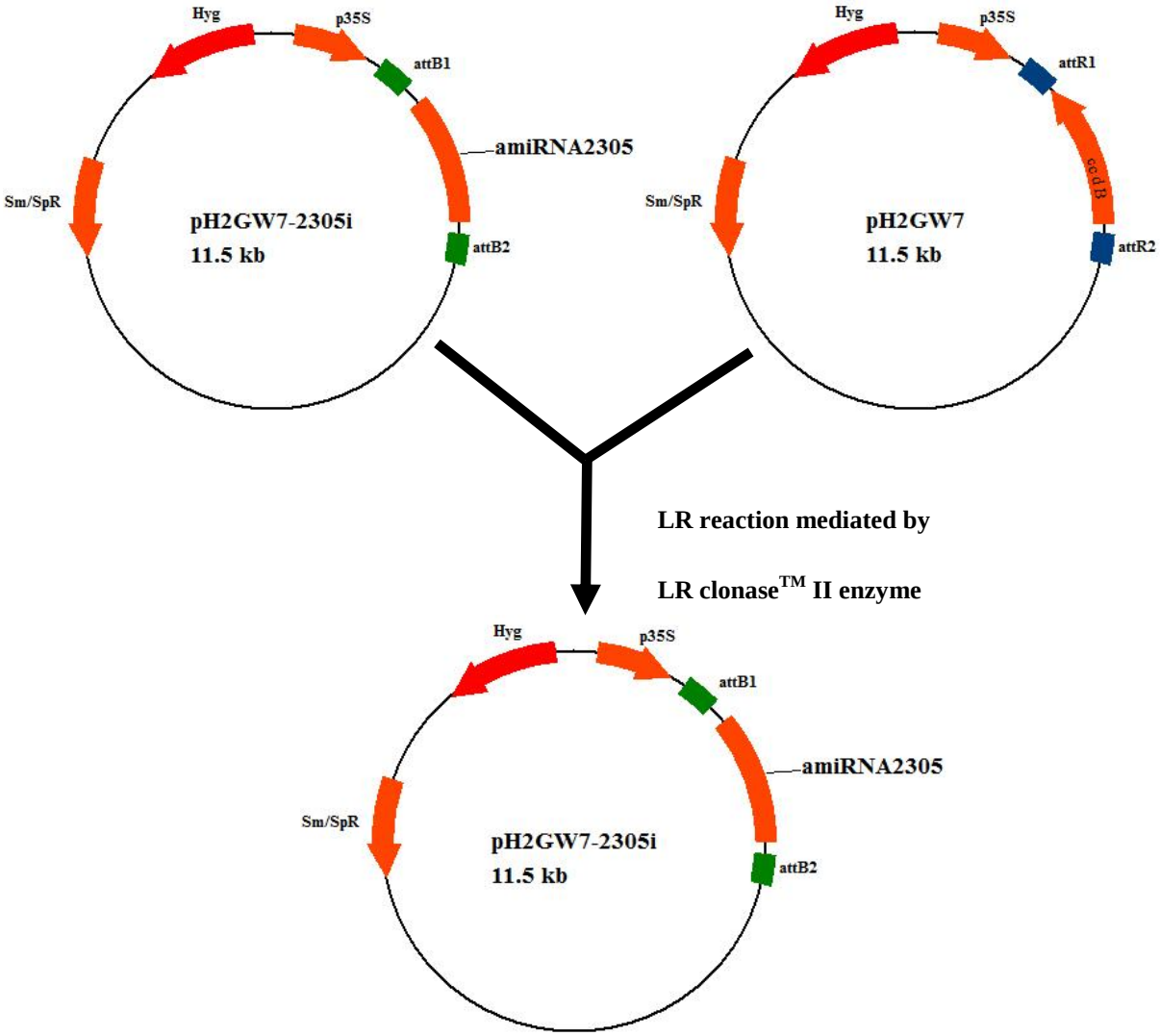

Fig 2.4 Maps of pENTR1A-2305i and pH2GW7-2305i plasmid. The gene sequence of amiRNA2305i precursor were engineered, cloned into pENTR1A vector and then introduced into pH2GW7 *Agrobacterium*-mediated plant transformation vector using LR clonase™ II enzyme. Maps of plasmids were produced by BVTech plasmid software.

Table 2.3 Primers used in pENTR1A2300i and pENTR1A2305i plasmids construction

Gene	Primer	Primer Sequence 5'-3'
amiRNA2300	300A	CTGCAAGGCGATTAAGTTGGGTAAC
amiRNA2300	300*a	GAAGTACACGTA AGTATGCCTCCTCTACATATATATTCCT
amiRNA2300	300*s	GAGGAGGCATACTTACGTGTACTTCACAGGTCGTGATATG
amiRNA2300	300a	GAGGCGGCATACTTAGGTGTACATCAAAGAGAATCA ATGA
amiRNA2300	300s	GATGTACACCTAAGTATGCCGCCTCTCTCTTTTGTATTCC
amiRNA2300	300B	GCGGATAACAATTTCACACAGGAAACAG
amiRNA2305	305A	CTGCAAGGCGATTAAGTTGGGTAAC
amiRNA2305	305*a	GAACTGATA AATTATCGGCTACTCTACATATATATTCCT
amiRNA2305	305*s	GAGTAGCCGATAATTCTATCAGTTCACAGGTCGTGATATG
amiRNA2305	305a	GAGTGGCCGATAATTGTATCAGATCAAAGAGAATCAATGA
amiRNA2305	305s	GATCTGATACAATTATCGGCCACTCTCTCTTTTGTATTCC
amiRNA2305	305B	GCGGATAACAATTTCACACAGGAAACAG

2.2.4 Construction of plasmids pH7RWE-AtCB2 and pMDC83Y-AtCB3

The sequences of *AtCathB-2* and *AtCathB-3* ORF with 3' end stop codon deletion were amplified from the plasmid pU12892 and pU17098 in PCR reactions using VELOCITY DNA polymerase (Bioline Co. Ltd., UK) and primers designed with *EcoR* I and *Xho* I restriction sites. The PCR products and the pENTR1A entry vector (Invitrogen Co. Ltd., US) were digested using *EcoR* I and *Xho* I restriction enzymes (Roche Applied Science, Germany). The digested PCR products were cleaned up using NucleoSpin Extract II kit (Macherey-Nagel, Germany) and ligated into the pENTR1A entry vector using T4 DNA ligase (Roche Molecular Biochemicals, Germany) and named as pENTR1A-AtCB2nostop and pENTR1A-AtCB3nostop respectively. The DNA sequences of *AtCathB-2* ORF with 3' end stop codon deletion were subsequently transferred into the Gateway vector pH7RWE containing red fluorescent protein DNA sequence for *Agrobacterium*-mediated plant transformation mediated by LR clonase^{TM} II enzyme (Invitrogen Co. Ltd., US) (Fig 2.5). The DNA sequences of *AtCathB-3* ORF with 3' end stop codon deletion were

subsequently transferred into the Gateway vector pMDC83Y containing yellow fluorescent protein DNA sequence for *Agrobacterium*-mediated plant transformation mediated by LR clonase^{TM} II enzyme (Invitrogen Co. Ltd., US) (Fig 2.6). Plasmids were transformed into *E.coli* strain XL1- blue competent cells and selected on 50 µg/ml kanamycin LB agar culture medium. The DNA sequence was verified by DNA sequencing.

Table 2.4 Primers used in pENTR1A-AtCB2nostop and pENTR1A-AtCB3nostop construction

Gene	Primer	Primer Sequence 5'-3'
AtCathB-2	AtCB2-ATGF	GGAATTCCCATGGCTGATAATTGTATCAGAC
AtCathB-2	AtCB2-nostopR	GGGTCTCGAGGTAAATGAGGAAACAAGAAGATC
AtCathB-2	AtCB3-ATGF	GGAATTCCCATGGCTGTTTACAATACCAAAC
AtCathB-2	AtCB3-nostopR	GGGTCTCGAGGTAACCGATGCAACCGGAAGATC
YFP	YFP 45R	ACAAGAATTGGGACAACTCC
RFP	RFP-RW	CCGGAATTCGGCGCCGGTGGAGTGGCGGC

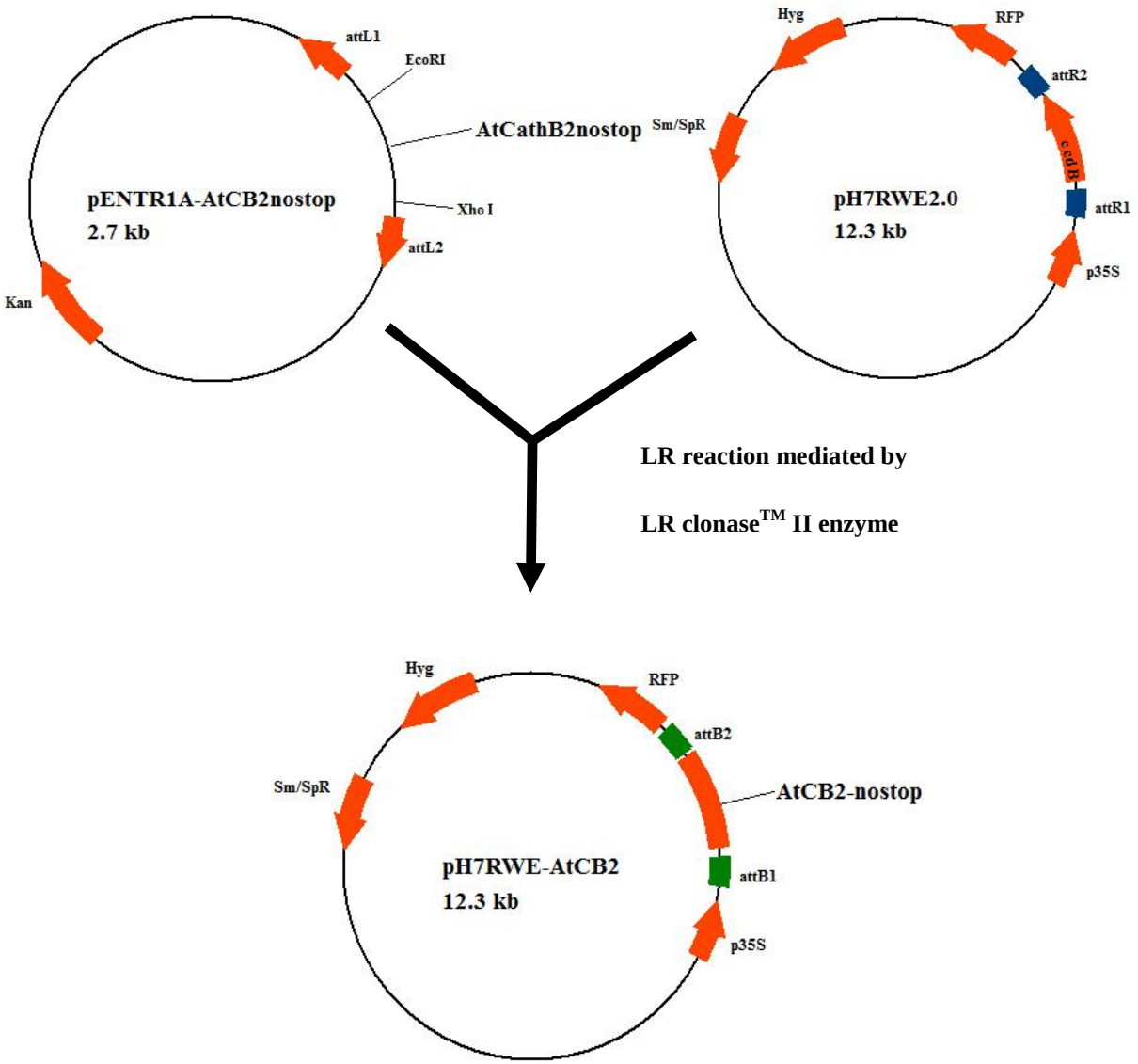

Fig 2.5 Maps of pENTR1A-AtCB2nostop and pH7RWE-AtCB2 plasmid. The gene sequence of *AtCathB-2* ORF with 3' end stop codon deletion were cloned into pENTR1A vector and therefore introduced into pH7RWE Agrobacterium-mediated plant transformation vector using LR clonase™ II enzyme. Maps of plasmid were produced by BVTech plasmid software.

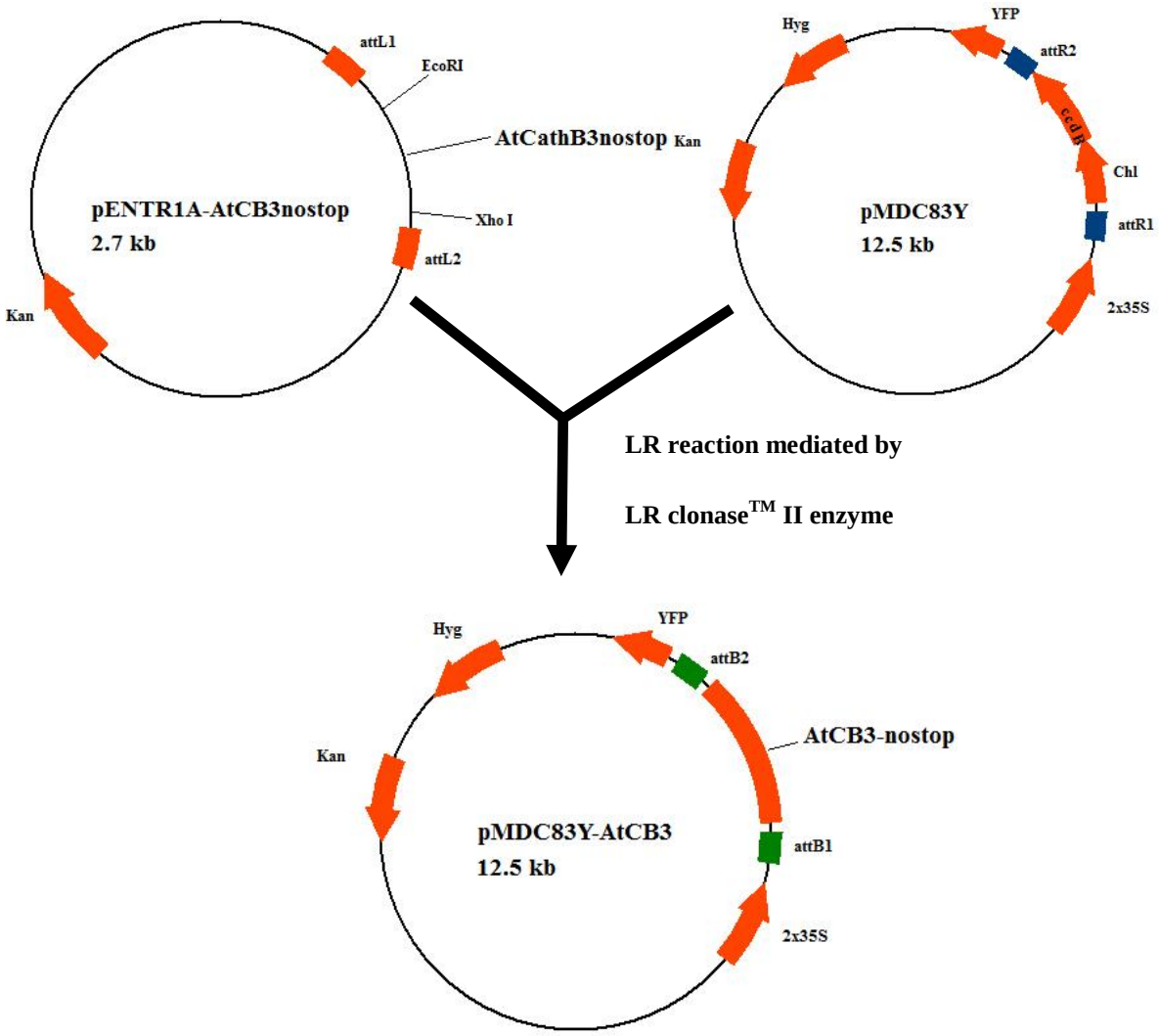

Fig 2.6 Maps of pENTR1A-AtCB3nostop and pMDC83Y-AtCB3 plasmid. The gene sequence of *AtCathB-3* ORF with 3' end stop codon deletion were cloned into pENTR1A vector and therefore introduced into pMDC83Y *Agrobacterium*-mediated plant transformation vector using LR clonase™ II enzyme. Maps of plasmid were produced by BVTech plasmid software.

2.2.5 Construction of plasmid pENTR1A-AtCB1

Total mRNA was extracted from *Arabidopsis* cathepsin B double knockout plants (dbKO2×3 lines) using RNeasy mini kit (QIAGEN Co. Ltd., Germany) with or without heat shock induction. The synthesis of cDNA was carried out using M-MLV transcriptase kit (Promega Corporation, US). The ORFs of *AtCathB-1* were amplified in two steps nested PCR using VELOCITY polymerase and primers with *EcoR* I and *Xho* I restriction sites.

The PCR products were cleaned up using NucleoSpin Extract II kit (Macherey-Nagel, Germany). Reclaimed PCR products and the pENTR1A entry vector (Invitrogen Co. Ltd, US) were both digested in successive reactions with *EcoR* I and *Xho* I restriction enzymes (Roche Applied Science, Germany). Following a PCR clean up with NucleoSpin Extract II kit (Macherey-Nagel, Germany), the purified PCR products were ligated into the pENTR1A vector using T4 DNA ligase (Roche Molecular Biochemicals, Germany) (Fig 2.7). The gene sequences of *AtCathB-1* were therefore analyzed by DNA sequencing. Plasmids were transformed into *E.coli* strain XL1-blue competent cells and selected on 100 µg/ml kanamycin LB agar culture medium.

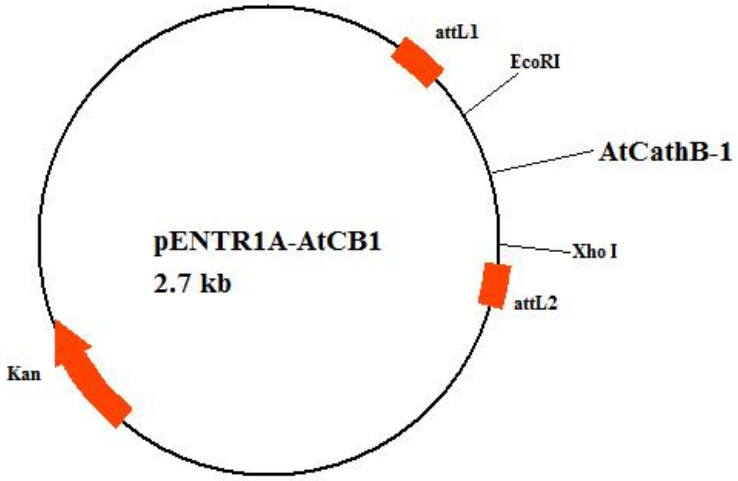

Fig 2.7 Maps of pENTR1A-AtCB1 plasmid. The ORF of AtCathB-1 was amplified using nested PCR and cloned into pENTR1A vector for DNA sequencing analysis. Maps of plasmid were produced by BVTech plasmid software.

Table 2.5 Primers used in nested PCR for *AtCathB-1* cloning

Gene	Primer	Primer Sequence 5'-3'
AtCathB-1	-5F	GTACAAGGGAGATTCATCATG
AtCathB-1	-5R	ACACAAGTAGGGACACATCG
AtCathB-1	ATG-F	GAATTCCATGGCTGATAGTTGTTGTATCAGAC
AtCathB-1	STOP-R	GGTCTCGAGGTTTAGACTGAGGAAACCAGAAG

2.2.6 Restriction endonuclease digestion and ligation

Materials

Restriction endonuclease digestion

10×restriction endonuclease buffer H	10μl
Restriction endonuclease (20U)	1μl
MilliQ H_2O	to 50μl final

Ligation

T4 ligase (20U)	1μl
10×T4 ligase reaction buffer	1μl
MilliQ H_2O	to 10μl final

Methods

100ng of DNA or 500ng of plasmid was incubated with 10μl 10×restriction endonuclease buffer H and 1μl restriction endonuclease (20U) in a 50μl reaction system at 37℃ for 2h. The digestion was stopped by additional incubation at 60℃ for 10min. 50ng of insert and 500ng of vector was incubated with 1μl T4 ligase and 1μl 10×T4 ligase reaction buffer in a 10μl reaction system at room temperature overnight.

2.2.7 Gateway LR reactions

Materials

Entry vector	150ng
Destination Vector	100ng
TE buffer, pH 8.0	to 9μl final
LR clonase^{TM} II enzyme	1μl
Proteinase K solution	1μl

Methods

150ng of entry vector and 100ng of destination vector was mixed with TE buffer, pH8.0 to final volume of 9μl. 1μl of LR clonase^{TM} II enzyme was added into the reaction system and incubated at 25℃ for 16h. 1μl proteinase K solution was added and the mixture was incubated at 37℃ for 10min to stop the reaction.

2.2.8 PCR products clean-up

Materials

NucleoSpin Extract II Kit (Macherey-Nagel, Germany)

Methods

The clean-up of PCR products was carried out according to the kit manual. PCR products were mixed with two times volume of buffer NT and bound to NucleoSpin Extract II column. After twice wash using buffer NT3, PCR products were eluted in 50μl buffer NE.

2.2.9 Transformation of plasmid into *E.coli*

Materials

LB Agar culture medium

Antibiotics:

Kanamycin, Sepctinomycin	50mg/ml
Ampicillin, Hygromycin,	100mg/ml

S.O.C culture medium

E.coli strains: XL1-blue competent cells, CYS21 cloning cells and SE1 expression cells

Methods

1μl of plasmid of interest was mixed with 50μl of competent cells *E.coli* suspension and incubated on ice for 30min. After the incubation at 42℃ for 5sec, 250μl S.O.C culture

medium was added and the mixture was incubated in a shaking bed at 37℃ for 1h. 300μl mixture was plated on the LB agar culture medium selection plate supplemented with corresponding antibiotics. The colonies that grew up were then selected and cultured on LB agar culture medium containing specific antibiotics as a master plate.

2.2.10 Plasmid mini preparation

Materials

NucleoSpin plasmid kit

LB broth medium or TERRIFIC broth medium

Antibiotics

Methods

LB broth medium was used for the cultivation of *E.coli* harbouring high-copy plasmids while TERRIFIC broth medium was used for the low-copy plasmids cultivation (pH2GW7 vector and pH7RWE vector). 5ml of LB broth medium or 15ml of TERRIFIC broth medium were used for cell culture in constant shaking bed at 37℃, 220rpm for 12-16h. Plasmid preparation was carried out according to the kit manual. Briefly, culture pellets were spun down in a centrifugation at 2,000g and lysed using buffer A1, A2 and A3. The lysate was then bound to the silica column. After twice wash of the column using buffer AW and A4, plasmid was eluted in 50μl AE buffer.

2.3 DNA-based experiments

2.3.1 Genomic DNA mini preparation

Materials

Genomic DNA extraction buffer

Tris pH8.0	50mM
EDTA	10mM, pH8.0

NaCl	100mM
SDS	1.0% (w/v)
NH_4Ac	5M

TE buffer

Tris-HCl	10mM, pH 8.0
EDTA	1mM

Method

Arabidopsis leaves sized about 0.5-1cm were homogenized using genomic DNA extraction buffer and incubated at 65℃ for 10min. 5M NH_4Ac was added to the extracts to a final concentration of 1M and then kept on ice for 10min. After centrifugation at 11,000g, 4℃ for 10min, supernatant was mixed with the same volume of isopropanol and centrifugated at 11,000g, 4℃ for 20min. The DNA pellets at the bottom of the tube were washed with 70% ethanol (v/v) using centrifugation at 11,000g, 4℃ for 10min. The DNA pellets were then resuspended in 50μl TE buffer and stored in a -20°C freezer.

2.3.2 DNA sequencing

Materials

NaOAc, pH 5.2	3M
Ethanol	100% (v/v)
Ethanol	70% (v/v)

ABI DNA sequencing kit (AB Life Technologies Co. Ltd.)

Methods

2μl sequencing terminator, 4μl 5×SBS buffer and 1μl primer were mixed with 500ng plasmid and MilliQ water to a final volume of 20μl. Sequencing programme was carried out using the PCR cycler (MJ Research Co. Ltd., USA). After the amplification, PCR products were transferred to a 1.5ml Eppendorf tube and 20μl MilliQ water was added. After adding 1μl blue glycol, 4μl NaOAc and 80μl 100% ethanol (v/v), the mixture was

precipitated at room temperature for 10min. The precipitated DNA was spun down in centrifugation at 11,000g at room temperature for 30min. After washing using 70% ethanol (v/v), DNA sequencing was carried out in the DNA Sequencing Facility, University of Manchester using Applied Biosystems 3730 DNA Analyzer. The sequencing results were analysed using the software Vector NTI Advanced 11, Invitrogen Co. Ltd., USA.

2.4 RNA-based experiments

2.4.1 Total RNA isolation

Materials

QIAGEN RNeasy Mini Kit (QIAGEN Co. Ltd., Germany)

β-mercaptoethanol

Ethanol 100% (v/v)

Methods

Total RNA isolation from *Arabidopsis* seedlings was carried out using QIAGEN RNeasy mini kit as described in kit manual. Briefly, two-week-old *Arabidopsis* seedlings grown in vitro were harvested and frozen in liquid nitrogen immediately. Frozen seedlings were then homogenized in lysis buffer RLT supplemented with β-ME. The supernatant was separated using QIAshredder columns, mixed with 0.5×volumes of 100% ethanol (v/v) and bound to RNeasy spun columns. After washing using buffer RW1 and buffer RPE, total RNA was eluted in 50µl RNase-free water.

2.4.2 cDNA synthesis and RT-PCR

3µg total RNA extracted from *Arabidopsis* seedlings was mixed with 1µl DNase RQ1 10×buffer and 3µl DNase RQ 1 (Promega) and incubated at 37℃ for 30min. 1µl DNase RQ1 stop buffer was added and the mixture was incubated at 65℃ for 30min to inactivate the DNase. The cDNA synthesis was carried out using the M-MLV transcriptase kit (Promega Co. Ltd., USA). 5µl of the DNase treated RNA was mixed with 1µl oligo-dT

(5'-TTTTTTTTTTTTTTTTT-3') and distilled water to the final volume of 13 µl. The mixture was incubated at 70 ℃ for 5min to remove the secondary structure. After that, 4 µl 5 ×first strand synthesis buffer, 1 µl M-MLV reverse transcriptase, 1 µl DTT at 100mM, 2 µl dNTP mixture (5mM stock) were added to the reaction mixture. Mixture was incubated at 42 ℃ for 60min and then inactivated at 75 ℃ for 10min. The synthesised cDNA was diluted to 200 µl using distilled water for further analysis. *Actin 2* or *DAD1* gene were used as internal reference.

Table 2.6 Primers used in RT-PCR for internal reference

Gene	Primer	Primer Sequence 5'-3'
Actin 2	Actin 2-F	GTTAGCAACTGGGATGATATGG
Actin 2	Actin 2-R	CAGCACCCAATCGTGATGACTTGCCC
DAD1	DAD1-TOT5	GGATGCTCAGGATCTATTTCG
DAD1	DAD1-CT23	GTGAAACCTCTATCCGAGGAAGTTG

2.5 Polymerase chain reaction (PCR)

2.5.1 PCR using Taq DNA polymerase

Materials and reaction set up

2 x Reddy PCR reaction Master Mixture (Biolabs Co. Ltd., UK)	4 µl
10 µM forward primer	1 µl
10 µM reverse primer	1 µl
DNA template	1 µl
Distilled water	2 µl

Methods

Denaturation	95 ℃	5min	1 cycle

Denaturation	95 ℃	1min	
Annealing (TM according to the primers)		1. 2min	30 cycles
Elongation	72 ℃	2min	
Elongation	72 ℃	10min	1 cycle

2.5.2 PCR using high fidelity DNA polymerase

Materials and reaction set up

10 × PCR buffer	5 µl
50mM $MgCl_2$	1.5 µl
5mM dNTPs	10 µl
VELOCITY DNA polymerase (Bioline Co. Ltd., UK)	0.5 µl
DNA template	2 µl
Distilled water	25 µl

Methods

Denaturation	98 ℃	2min	1 cycle
Denaturation	98 ℃	30sec	
Annealing	60 ℃	30sec	24 cycles
Elongation	72 ℃	15sec per kb	
Elongation	72 ℃	4min	1 cycle

2.5.3 Real time quantitative PCR (qRT-PCR)

Materials and reaction set up

MESA Blue qPCR MasterMix Plus for SYBR Assay (Eurogentec, Belgium)	12.5 µl
cDNA template	2 µl

Primers		1.5µl	
Distilled water		9µl	

Methods

Initial step	50 ℃	2min	1 cycle
Polymerase activation	95 ℃	10min	1 cycle
Amplication	95℃	15sec	40 cycles
	60 ℃	1min	
Hold	50 ℃		

1.5µl of the synthesised cDNA was amplified in a 25µl qRT-PCR reaction system using a set up programme as stated above with ABI Prism 7000 sequence detection system (Applied Biosystems, USA). *DAD1* gene or *18s* gene was used as internal reference. Results were given as the percentage of copy numbers of gene of interest against internal reference gene in the same sample.

Table 2.7 Primers used in qRT-PCR (*AtCathB* primers were designed in McLellan *et al.*, 2009)

Gene	Primer	Primer Sequence 5'-3'
AtCathB-1	TMCathB1-F	CCACGGTGTAGTAACCCAAGA
AtCathB-1	TMCathB1-R	GTATGCGCCGACACCATAG
AtCathB-2	TMCathB2-F	GTGTTAGCGGAAACCAGCTT
AtCathB-2	TMCathB2-R	CAGTGAAGGCAACCTCAACA
AtCathB-3	TMCathB3-F	GAAATGCGTTAGCGACAACA
AtCathB-3	TMCathB3-R	CTGCCATGATATCTTGTGGATT
18S	18S-F	GGTCTGTGATGCCCTTAGATGTT
18S	18S-R	GGCAAGGTGTGAACTCGTTGA

2.5.4 Agarose gel electrophoresis

Materials

Agarose (Melford)	
Ethidium Bromide (SERVA)	1% (w/v)

0.5 ×TBE buffer

Tris base	89mM
Boric acid	89mM
EDTA	2mM

Method

0.8%-2% agarose (w/v) gel was prepared for the electrophoresis using the electrophoresis apparatus (Bio-Rad Co. Ltd., USA). The electrophoresis was run at 135V for 15min. Visualisation and imaging was carried out on a UV transilluminator (Uvtec BTS20. M, Uvtec Ltd, UK).

2.6 General analysis of protein

2.6.1 Protein extraction from *Arabidopsis* seedlings

Materials

Protein Extraction Buffer

NaCl	200mM
NaOAc	50mM
Adjust pH to 5 with acetic acid	
DTT	3mM

Methods

Arabidopsis seedlings were harvested and homogenized with pre-chilled extraction buffer on ice. Generally, 1ml extraction buffer was added and homogenized with each 150mg

Arabidopsis tissue. The lysate was vortexed vigorously at 4℃ for 15min and centrifuged at 4℃, 13,000g for 10min. The supernatant was collected as total protein extracts.

2.6.2 Protein concentration measurement

The protein concentration was measured in triplicate and then an average was taken. 200µl Bradford dye (Bio-Rad), 790µl sterile water and 10µl protein extracts were mixed in a cuvette. One cuvette without protein extraction was measured as blank. After incubation at room temperature for 10min, the protein concentration was measured using the Bradford programme in Eppendorf Biophotometer (Eppendorf, Germany).

2.6.3 SDS polyacrylamide gel electrophoresis and coomassie brilliant blue staining

Materials

1×SDS-PAGE running buffer

Tris-HCl	25mM, pH8.3
Glycine	190mM
SDS	1g/l
Adjust pH to 8.3	

1×SDS-PAGE loading buffer

Tris-HCl	50mM, pH6.8
SDS	2% (w/v)
Glycerol	10% (w/v)
DTT	100mM
Bromophenol blue	0.1% (w/v)

Coomassie brilliant blue staining

Coomassie brilliant blue G250	0.5% (w/v)

SDS PAGE gel solution

	15% resolving gel (ml)	5% stacking gel (ml)
Sterile H_2O	2.3	1.4
30% acrylamide mix	5.0	0.33
1.5M Tris (pH8.8)	2.5	0.25
10% SDS (w/v)	0.1	0.02
10% ammonium persulfate (w/v)	0.1	0.02
TEMED	0.004	0.002
Total Volume	10	2

Methods

The same volume of SDS-PAGE loading buffer was added into protein sample and boiled to denature at 90℃ for 5min. 15μl boiled protein samples in SDS-PAGE loading buffer was loaded into SDS polyacrylamide gel and separated at 100V for 30min and then 150V for 1h. The SDS polyacrylamide gel was rinsed briefly with distilled water after electrophoresis and stained with coomassie brilliant blue staining buffer on shaking bed at room temperature overnight. Destaining was carried out after the staining with plenty of distilled water on shaking bed at room temperature.

2.6.4 Diagonal SDS-PAGE and silver staining

Materials

Diagonal SDS-PAGE

Same as materials in 2.6.3

Fixation buffer

Ethanol	40% (v/v)
Acetic acid	10% (v/v)

Silver staining for mass spectrometry

Thermo scientific pierce silver stain for mass spectrometry kit:

Silver stain sensitizer	
Silver stain buffer	
Silver stain enhancer	
Silver stain developer	
Silver destain reagent A	
Silver destain reagent B	
Ethanol solution	10% (v/v)
Acetic acid	5% (v/v)

Methods

The diagonal SDS-PAGE was carried out as described in Shao *et al*., 2007. Briefly, total protein extracts from *Arabidopsis* seedlings were separated on the first dimension SDS-PAGE as described in 2.6.3. Two lanes from the first dimension gel were excised and submerged in fixation buffer for 10min, then washed in 30% ethanol (v/v) for 10min and subsequently washed in MilliQ water for 10min twice. The lanes were then dried at room temperature and incubated in enzymatic activity assay buffer (pH5.5) with or without 2mg of the recombinant AtCathB-2 (AtCB2Cherry produced in insect cell) at 30 ℃ overnight. After proteolysis, the lanes were washed in MilliQ water twice and boiled in SDS-loading buffer at 95 ℃ for 10min. The lanes were then placed flat on top of the second dimension gels. After electrophoresis, the second dimension gels were fixed using fixation and visualised using a silver staining kit as described in the kit manual. Briefly, the second gel was washed twice using 10% ethanol (v/v) and incubated in 1/500 diluted silver stain sensitizer for 1min. After 1min wash with MilliQ water twice, the gel was incubated in 1/100 silver stain enhancer for 5min followed by a MilliQ water wash for 10min. The gels were developed using enhancer and developer mixture (1:100) for 3min. The staining was stopped with 10% acetic acid (v/v) incubation for 10min. Visualised protein spots under the diagonal line were identified using LC-MS/Mass Spectrometry in Biomolecular Analysis Facility, the University of Manchester.

2.6.5 Western blot

Materials

1 × Transfer buffer pH 8.4

Tris-HCl	25mM
Glycine	192mM
Methanol	20% (v/v)

Phosphate buffered saline (PBS), pH7.5

Na_2HPO_4	0.08M
NaH_2PO_4	0.025M
NaCl	0.1M

Phosphate buffered saline-Tween (PBS-T)

PBS, pH7.5

Tween 20	0.1% (v/v)

Membrane blocking buffer

Bovine serum albumin (BSA)	3% (w/v)

PBS-T

Supersignal west femto maximum sensitivity substrate kit (Thermo Scientific, USA)

Supersignal west pico maximum sensitivity substrate kit (Thermo Scientific, USA)

Methods

After electrophoresis, proteins were transferred to a Hybond-P membrane (Amersham Biosciences) at 100V for 1h in transfer buffer. The membrane was then blocked with membrane blocking buffer at 4℃ overnight. After the blocking using BSA, the membrane was washed three times using washing buffer and incubated with primary antibodies at room temperature for 1h in gently agitation. The membrane was then washed three times

with PBS-T buffer and incubated with secondary antibodies at room temperature for 1h. After three times wash in agitation, the membrane was treated with a mixture of supersignal west femto maximum sensitivity substrate (1×vol) and west pico maximum sensitivity substrate (5×vols) for 1min and laid down for up to 1h with Kodak scientific imaging film and developed with a Compact 2 processor.

2.6.6 N-terminal protein sequencing

Materials

1×transfer buffer for N-terminal protein sequencing, pH 11

3-cyclohexylamino-1-propane sulphonic acid (CAPS)	10mM
Methanol	10% (v/v)

N-terminal protein sequencing staining buffer

Coomassie brilliant blue	0.5% (w/v)
Methanol	40% (v/v)
Acetic acid	10% (v/v)

N-terminal protein sequencing destaining buffer

Methanol	30% (v/v)
Acetic acid	10% (v/v)

Methods

Protein samples were separated using 15% SDS-PAGE and transferred onto a Hybond-P membrane at 50mA for 1.5h. The membrane was stained using N-terminal protein sequencing staining buffer in agitation for 10min and then destained until background was transparent and protein bands were visible. Protein bands were excised and N-terminal protein sequence was analysed in the Protein Sequencing Facility, the University of Leeds using a Procise 494 high-throughput gas-phase/liquid-pulse sequencer (Edman degradation method).

2.6.7 LC-mass spectrometry and MALDI-TOF-mass spectrometry

Mass spectrometry in this project was carried out in the Biomolecular Analysis Facility, the University of Manchester. Protein bands of interest were excised from the gel, reduced with 10mM dithiothreitol and alkylated with 55mM iodoacetamide. Samples were digested with trypsin overnight at 37°C and analysed by LC-MS/MS using a NanoAcquity LC (Waters, Manchester, UK) coupled to a 4000 Q-TRAP (Applied Biosystems, Framingham, MA). Peptides were selected for fragmentation automatically by data dependant analysis. Data produced were searched using Mascot (Matrix Science UK), against the Uniprot database with taxonomy of *Arabadopsis* selected. MALDI-TOF-MS was carried out in the Biomolecular Analysis Facility, the University of Manchester using an Applied Biosystems 4800 MALDI instrument.

2.7 Partial purification of caspase-3-like proteases from *Arabidopsis* seedlings

Materials

CNBr-activated sepharose 4B

Bacitracin from *Bacillus licheniformis* (Sigma Co. Ltd, Germany)

Bovine serum albumin (BSA) 2% (w/v)

Loading/wash buffer, pH5

NaCl 0.2M

NaOAc 50mM

DTT 3mM

Elution buffer

MilliQ water

DTT 3mM

High salt wash buffer, pH 5

NaCl 0.2M

NaOAc 50mM

Methods

A bacitracin affinity column was prepared using CNBr-activated sepharose 4B and pre-equilibrated using 2% BSA (w/v). Total proteins extracted from two-weeks-old *Arabidopsis* seedlings grown *in vitro* after a 50kJ/m^2 UV-C irradiation and loaded onto the bacitracin-sepharose column that has been pre-equilibrated using protein extraction buffer. Bacitracin is a weak and broad specificity protease inhibitor, which could bind to various cysteine proteases as a ligand. Hence, cysteine proteases in the extracts would bind to the bacitracin-sepharose in the loading process. Other proteases and proteins would be collected in the flow through. The bacitracin sepharose column was connected to a protein station (Bio-Rad Laboratories, USA) with a pump at a flow rate of approx. 1ml/min, a UV lamp to monitor protein concentration by measuring absorbance at 280nm, a conductivity meter to measure salt concentration and a chart recorder. After washing with plenty of wash buffer, the bacitracin-bound cysteine proteases were eluted in water and each 4ml fractions were collected. In the elution, the salt concentration decreased while the protein absorbance increased. It is proposed that only cysteine proteases were blocked in the column. Since the inhibitory efficiency of bacitracin is low, water was used to elute cysteine proteases to avoid further dialysis or desalting.

2.8 Purification of recombinant protein

2.8.1 Protein purification using Ni-NTA and TALON cobalt resins and refolding

Materials

Formate 1M

Porcine pepsin (Sigma Co. Ltd, Germany)

Lysis buffer

Sodium phosphate buffer 50mM

(pH 8.0 for Ni-NTA resins, pH7.0 for TALON cobalt resins)

NaCl 300mM

Lysozyme (Sigma Co. Ltd, Germany) 10mg/ml

Wash buffer for protein purification under native condition

Sodium phosphate buffer 50mM

(pH 8.0For Ni-NTA resins, pH7.0 for TALON cobalt resins)

NaCl 300mM

Elution buffer for protein purification under native condition

Sodium phosphate buffer 50mM

(pH 8.0For Ni-NTA resins, pH7.0 for TALON cobalt resins)

NaCl 300mM

Imidazole 150mM

Denaturing buffer/ Wash buffer for protein purification under denaturing condition

Sodium phosphate buffer, pH 7.0 50mM

NaCl 300mM

Urea 8M

Elution buffer for protein purification under denaturing condition

Sodium phosphate buffer, pH 7.0 50mM

NaCl 300mM

Imidazole 150mM

Urea 6M

Denaturing dilute buffer

Tris-HCl 100mM

EDTA 5mM

Urea 6M

Dialysis tubing preparation buffer

Na_2CO_3	2% (w/v)
EDTA	1mM

Dialysis buffer I

Sodium phosphate buffer, pH 7.0	100mM
EDTA	5mM
Cysteine	5mM

Dialysis buffer II

Sodium phosphate buffer, pH 7.0	100mM
EDTA	5mM

Ni-NTA resins (Promega Co. Ltd, USA)

TALON cobalt resins (Clontech Co. Ltd, USA)

Methods

Auto-induced *E.coli* producing recombinant protein was spun down and lysed using lysozyme treatment and sonication. After a centrifugation at 4℃, 11,000g for 30min, supernatant was collected for native purification and pellets were used in denaturing purification. Supernatant was mixed with pre-equilibrated Ni-NTA resins or TALON cobalt resins respectively and rotated at 4℃ for 1h (20μl 50% slurry resins was used in each 1ml supernatant). Resins were therefore loaded onto a 5ml column and washed for four times. Recombinant protein was eluted in 1ml elution buffer after wash. Dialysis tubing was boiled in dialysis tubing preparation buffer at 70℃ for 10min and then washed. After another boiling at 70℃ for 10min in 1mM EDTA buffer, dialysis tubing was kept in freezer. Pellets obtained from lysed *E.coli* were resuspended in denaturing buffer and mixed with pre-equilibrated TALON resins. After rotation at 4℃ for 1h, resins were loaded onto a 5ml column and washed for four times. Recombinant protein was eluted in 1ml denaturing elution buffer and diluted to the concentration of 10μg/ml. After dilution, denatured protein eluate was loaded into prepared dialysis tubing and dialysed in

100×volume dialysis buffer I at 4℃ for 15h. Another dialysis was subsequently carried out in 100×volume dialysis buffer II at 4℃ for 4h to remove additional cysteines. Recombinant protein after dialysis was acidified to pH 3.5 and activated using pepsin at the molar ratio of 1:100. After activation, pH was increased to 7.0 with 1M sodium phosphate pH8.0 to inactivate the pepsin.

For the purification of recombinant protein produced in insect cell, TALON cobalt resins were applied. Transfected insect cell was cultured in 5ml flask in a 28℃ CO_2 incubator for 48h and spun down in a centrifugation at 300g for 10min. Supernatant was mixed with TALON cobalt resins and rotated at 4℃ for 1h. Resins were therefore loaded onto a 20ml column connected with a Bio-Rad protein station with a pump at a flow rate of approx. 1ml/min. After plenty of washing, recombinant protein was eluted.

2.8.2 Protein purification using cation exchange chromatography

Materials

HiTrap SP FF (GE Healthcare)	1ml

Start buffer, pH 4.5

NaOAc	50mM

Elution buffer, pH 4.5

NaCl	0.1M-1M
NaOAc	50mM

Methods

Recombinant protein was acidified to pH 4.5 and loaded onto a 1ml HiTrap SP FF cation exchanger pre-equilibrated using 5ml start buffer at a flow rate of 1ml/min. After binding, the column was washed with 2ml start buffer and eluted using elution buffer containing varying NaCl concentrations from 0.1M to 1M.

2.9 Fluorimetric assay of enzymatic activity

Materials

Synthetic fluorescent substrates (Bachem Ltd.)	10mM
Inhibitors except CA-074	100 μM
CA-074	1mM

2 ×enzymatic assay buffer, pH 5

NaCl	200mM
NaOAc	50mM
Adjust pH to 5 with acetic acid	
DTT	3mM
1 ×Roche complete inhibitor cocktail	

2 ×enzymatic assay buffer, pH7 *(For lactone and ac-PnLD-CHO inhibitory efficiency analysis)*

HEPES	100mM
KCl	50mM
NaCl	20mM
$MgCl_2$	2mM

Methods

Enzymatic activities of protein samples were measured using synthetic fluorescent substrates and a Fluoroskan Ascent microplate fluorometer (Labsystems, DYNEX Technologies, USA). For substrates conjugated with 7-amino-4-methylcoumarin (AMC), excitation wavelength was set at 355nm and emission wavelength was set at 460nm. For ac-DEVD-rhodamine110, excitation wavelength was set at 485nm and emission wavelength was set at 538nm. The first five readings (10min) were eliminated and slopes were expressed as fluorescent unit/min/mg protein. For inhibitory efficiency analysis, protein samples were incubated with inhibitors at the final concentration 100 μM or 1mM at 30 ℃ for 30min before the enzymatic activity assay. For the inhibitory efficiency

analysis in proteasome inhibitors lactone and ac-PnLD-CHO, pH7 enzymatic assay buffer was used.

2.10 *Agrobacterium*-mediated in-planta transformation

Materials

Sucrose	5% (w/v)
Silwet L-77 (OSi)	

YEP medium

Yeast extracts	10g/l
Peptone	10g/l
NaCl	5g/l

Methods

10µg DNA plasmid was added into 50µl competent cells *Agrobacterium tumefaciens* suspension, kept on ice for 5min and then transferred to liquid nitrogen for 5min. The mixture was incubated 37℃ for 5min, and then 1ml LB broth was added. The mixture was recovered on a rocking table at room temperature for 4h and then spread on LB agar culture medium supplemented with appropriate antibiotics for both T-DNA vector and plasmid of interest selecting. Transformed *Agrobacterium* from single colony was cultured in 3ml YEP at 30℃ overnight. The culture medium with transformed *Agrobacterium* was then inoculated into 200ml YEP and cultured at 30℃ overnight in agitation. Cells were spun down and then resuspended using 5% sucrose (w/v) with Silwet L-70 in magenta. *Arabidopsis* seedlings were inverted into the vacuum basin. Plant flowers and stem were submerged into infiltration solution and 10^4 Pa of vacuum pressure was applied for 30sec.

2.11 Transgenic plants screening

Isolation of double knockout homozygous plants

Arabidopsis seeds from F1 progeny of double knockout lines were grown on composts. Genomic DNA was extracted from leaves harvested from each plant. Genotyping PCR was carried out using primers designed for *AtCathB* genomic gene sequence and primer for T-DNA insertion (LBb1). Genotypes of homozygous double knockout plants were confirmed by RT-PCR.

Table 2.8 Primers used in genotyping PCR

Gene	Primer	Primer Sequence 5'-3'	Annealing TM (℃)
AtCathB-1	118LP	GCCAATGAGCTTAACTGCATG	60
AtCathB-1	118RP	AGAGTTTAAGCGACTCCTCGG	60
AtCathB-2	030LP	CGTTGGTCACACATAGTGCAG	60
AtCathB-2	030RP	GACAATACTGGTTGCTCGCAC	60
AtCathB-3	629LP	TAGGGACATTGTGGTTCTTGC	60
AtCathB-3	629RP	TCCACATTCATTAGTTCCTCTCC	60
T-DNA insert	LBb1	GCGTGGACCGCTTGCTGCAACT	60

Table 2.9 Primers used in confirmatory RT-PCR

Gene	Primer	Primer Sequence 5'-3'	Annealing TM (℃)
AtCathB-1	S-4F	GGCCATGGCTGATAGTTGTTG	60
AtCathB-1	S-4R	GACTCGAGACTGAGGAAACCAG	60
AtCathB-2	714F	TAGTGCGTACAAGGTCAG	55
AtCathB-2	1050R	ACCTTTAACTACGTTCCTG	55
AtCathB-2	775F	CCTGTTGAGGTTGCCTTCAC	61
AtCathB-2	1080R	CTTCTTTTTGGGTTGAAAGTCG	61
AtCathB-3	687F	GAGCGAGTCGAAGCATTAC	58
AtCathB-3	1023R	AGGCAAACCAGCTACTGG	58

Isolation of triple knockout homozygous plants produced by amiRNAs-mediated gene silencing

Arabidopsis seeds from T1 generation were grown *in vitro* on MS medium supplemented with 100 µg/ml hygromycin. *Arabidopsis* seedlings resistant to hygromycin were transferred to composts for further growth in a short day light chamber. Total RNA was then extracted from each plant. The expression of *AtCathB-1* gene was detected using RT-PCR with *AtCathB-1*-S-4F primer and *AtCathB-1*-S-4R primer.

2.12 Analysis of oxidative stress-induced PCD

UV-C irradiation of Arabidopsis seedlings

Two-week-old *Arabidopsis* seedlings grown *in vitro* or protoplasts were irradiated using a UV-C Stratalinker with 8 watt, 254nm UV-C light bulbs. 50kJ/m^2 UV-C was delivered to *Arabidopsis* seedlings to induce proteolytic activity and *AtCathB* gene expression. 30 KJ/m2 UV-C was delivered to *Arabidopsis* leaf discs for ion leakage conductivity measurement. 10KJ/m2 UV-C was delivered to protoplasts isolated from Two-week-old *Arabidopsis* seedlings grown *in vitro* for cell death detection. After UV-C irradiation, incubation in light was applied on samples before further experiments.

Methyl viologen treatment of Arabidopsis

For germination and cotyledon bleaching analysis, various concentrations of methyl viologen from 0.25 µM to 10 µM were supplemented into MS culture medium without glucose. For proteolytic activity and *AtCathB* gene expression induction using methyl viologen, two weeks old *Arabidopsis* seedlings grown on MS culture medium were transferred onto MS culture medium supplemented with 25 µM methyl viologen and an additional 5h growth in light was followed.

H_2O_2 treatment of Arabidopsis

For ion leakage measurement, 30mM H_2O_2 was applied to induce PCD in Arabidopsis leaf discs. For proteolytic activity and *AtCathB* gene expression induction using H_2O_2, two weeks old *Arabidopsis* seedlings grown on MS culture medium were transferred onto MS

culture medium supplemented with 30mM H_2O_2 and an additional 5 h growth in light chamber was followed.

2.13 Isolation of protoplasts from *Arabidopsis* seedlings and cell death detection

Materials

Leaf digestion medium

1 ×Murashige & Skoog medium (Sigma)

Sucrose	0.4M
Cellulase R-10 Onozuka (Yakult Honsha Co. Ltd)	0.96% (w/v)
Macerozyme (Yakult Honsha Co. Ltd)	0.64% (w/v)

W5 medium, pH 5.6-5.8

NaCl	154mM
KCl	5mM
Glucose	5mM
$CaCl_2$	125mM

Protoplast culture medium, pH5.8

1 ×Murashige & Skoog medium (Sigma)

Sucrose	0.4M
D-mannitol (Sigma)	0.4M
MES	0.5g/l

0.5% Evans' Blue stock solution

Methods

The following procedure was carried out on the flow bench. The leaves cut from *Arabidopsis* seedlings were laid in 10ml digestion medium in a 90mm diameter sterile plastic petri dish. The petri dish was sealed with parafilm and incubated at 20℃ in dark for 16h without shaking. The liquid was pipetted up and down gently for several times to free the protoplasts. A sterile 100μM sieve were fixed on top of a 38μM sieve and put on a 50ml glass beaker. 10ml protoplast suspension were poured over the sieve mesh into one 14ml sterile plastic screw cap centrifuge tube and sealed with parafilm. The suspension was spun down at 200 g, room temperature for 10min. Protoplasts were in the floating band on top of the liquid after the centrifugation. Protoplasts were transferred to a new tube and mixed with 10ml W5 medium. The mixture was centrifuged at 200g, room temperature for 5min as washing. The protoplasts in pellets after the centrifugation were resuspended with another 10ml W5 medium. The washing step was repeated twice. Protoplasts were observed using a microscope and the number of living cells in every 100 cells was calculated as the density. Protoplasts were suspended and diluted to 10^6/ml using the culture medium. 1ml protoplast suspension was added to one well and three replicates were detected for each sample. A 10kJ/m^2 UV-C irradiation was used to induce PCD. The protoplasts were then incubated in continuous light for 4h. 50μl protoplast suspension in each well was pipetted into an Eppendorf tube and 1μl Evans' blue stock solution was added into the tube. After incubation at room temperature for 5min, the stained suspension was loaded on a slide and observed under the microscope (Leica, Germany). The percentage of number of Evans' blue stained protoplasts over the total protoplast number was calculated as the cell death percentage.

2.14 Ion leakage conductivity measurement

Materials

Horiba ion conductivity meter (Horiba Ltd., Kyoto, Japan)

Calibration Buffer (as the conductivity of 1.41mS/cm)

KCl	0.01M

Methods

Arabidopsis grown on compost was watered 1d before the ion leakage conductivity measurement. Leaf discs were cut out from the mesophyll using a 3mm metal borer and the mid-rid were avoided. Three discs were immersed into 1100µl MilliQ water per one well. A 30 kJ/m^2 UV-C irradiation was used to induce PCD. 1h after the immersion, a measurement was taken using 100µl as a blank. The petri dishes were then incubated in continuous light and ion leakage conductivity was measured after 18h. The conductivity was calculated by subtracting the pre-reading and the 3 replicates were averaged.

2.15 Biolistic particle bonbardment

Materials

Gold particles (Invitrogen Co. Ltd., USA)

$CaCl_2$	1M
Spermine (Sigma)	0.1M

Biolistic PDS-1000/HE Particle Delivery System (BIO-RAD Laboratories, USA)

Methods

5µg of DNA plasmid, 250µl 1M $CaCl_2$ and 20µl 0.1M spermine were mixed with 60µl gold particle suspension. Plasmids were bound to particles in 5min vigorously vortexing. After washing using 100% ethanol (v/v), DNA coated gold particles were resuspended in 40µl 100% ethanol (v/v) and deposited on the macroprojectiles. Bombardment of plasmids into onion epidermal cells was carried out using biolistic PDS-1000/HE particle delivery system connected with a vacuum. Fired onion epidermis was observed after 2 d incubation in dark using a Leica DM5500 microscope fitted with a Photometrics cascade II 512B EMCCD camera (Photometrics UK).

CHAPTER 3

IDENTIFICATION OF *ARABIDOPSIS* CATHEPSIN B AMONG PARTIALLY PURIFIED CASPASE-3-LIKE PROTEASES

3.1 Introduction

Although caspase-3 plays a crucial role in animal apoptotic cascade, the existence of caspase-3 homologue in plants is still not clear. However, at least one caspase-3-like protease is required in plant PCD regulation because caspase-3-like activity is detected in plant PCD using synthetic tetrapeptide substrates and PCD is suppressed by caspase-3 inhibitors (Bonneau *et al.*, 2008). Thus the identification of a caspase-3 functional analogue is central to the understanding of plant PCD mechanism. As distant homologues of caspases in plants, metacaspases are considered as ancient caspases and proposed to be involved in PCD regulation. However, recombinant metacaspases don't cleave caspase substrates *in vitro*. The 20S proteasome was reported recently by Hara-Nishimura and her colleagues to be responsible for caspase-3-like activity both in animals and plants (Hatsugai *et al.*, 2009). Although a caspase pathway seems to be absent in plants PCD, our hypothesis is that a caspase-independent pathway has been conserved through evolution. In support of this, cathepsin B, an important lysosomal protease involved in animal and plant programmed cell death, might be responsible for part of the caspase-3-like activity detected in *Arabidopsis thaliana* (Gallois *et al.*, unpublished).

UV-C overexposure-induced cell death in *Arabidopsis* was classified as plant PCD using several apoptotic cellular and molecular hallmarks of animal apoptotis (Danon *et al.*, 2004). Interestingly, UV-C induced PCD is light dependent. After UV-C irradiation and at least 30min light incubation, caspase-3-like activity and caspase-1-like activity were induced and apoptotic alterations occurred (Danon *et al.*, 2004; He *et al.*, 2007). Bacitracin is an antibiotic which inhibits all classes of proteases. It has a better binding affinity to cysteine proteases and is consequently used in cysteine proteases isolation (Irvine *et al.*, 1993; Faisal *et al.*, 1999). As a caspase inhibitor, bacitracin has been widely used in caspase functional analysis (Janicke *et al.*, 1998; Matsui *et al.*, 2003).

In this chapter, we used bacitracin-sepharose affinity chromatography to partially purify all cysteine proteases including caspases-like proteases, papain and legumain from

Arabidopsis thaliana after a UV-C 50kJ/m^2 irradiation. The purified fraction was then labelled using biotinylated caspase-3 inhibitors to reveal caspase-3-like proteases. Various protease inhibitors were subsequently applied to the partially purified caspase-3-like proteases to sort out which protease was responsible for the caspase-3-like activity in *Arabidopsis* after UV-C irradiation.

3.2 Results

3.2.1 Investigaion of the correlation between *Arabidopsis* cathepsin B and caspase-3-like activity in response to UV-C irradiation

As reviewed previously, inducible caspase-3-like activity has been detected in different types of plant PCD. Resembling the function of caspase-3 in animal apoptosis, plant caspase-3-like activity is also essential for DNA fragmentation and other nuclear events in PCD. It was reported that UV-C irradiation can trigger PCD in *Arabidopsis* at the lethal dose of 50kJ/ m^2 (Danon *et al.*, 2004). In addition, the PCD induced by UV-C irradiation is light-dependent *via* an unknown mechanism (He *et al.*, 2007). Since *Arabidopsis* cathepsin B has been identified as a possible caspase-3-like protease in UV-C irradiated *Arabidopsis* seedlings (Gallois *et al.*, unpublished), the correlation of cathepsin B and caspase-3 like activity was investigated further. Two kinds of caspase-3 substrates, ac-DEVD-rhodamine110 and ac-DEVD-AMC were used to assay for enzymatic activity variation with time after 50 kJ/m^2 UV-C irradiation. An optimal synthetic substrate for human cathepsin B, z-RR-AMC was also used. In addition, the transcript levels of the *AtCathB-1, -2,-3* genes in response to UV-C irradiation were analyzed using qRT-PCR.

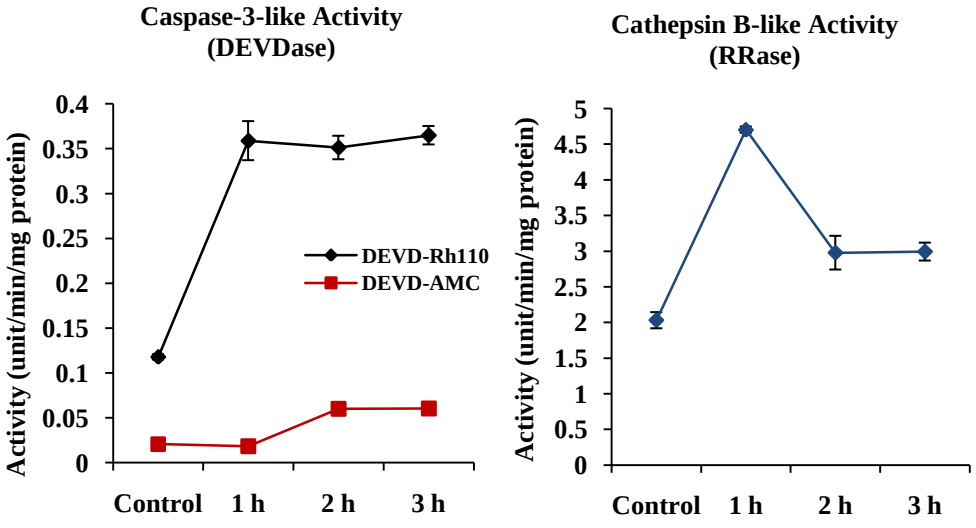

Fig 3.1 Caspase-3-like activity (DEVDase) and cathepsin B-like activity (RRase) over time after 50kJ/m^2 UV-C irradiation in *Arabidopsis*. Two-week-old *Arabidopsis* seedlings grown *in vitro* were irradiated with 50kJ/m^2 UV-C and then incubated in continuous light. Samples were taken at different time points and total proteins were extracted as described in chapter 2. Enzymatic activity was assayed as described in chapter 2 using ac-DEVD-rhodamine110, ac-DEVD-AMC and z-RR-AMC as substrates. Enzymatic activity is given as fluorescent unit/min/mg protein. Error bars indicate ±S.D. value for triplicates.

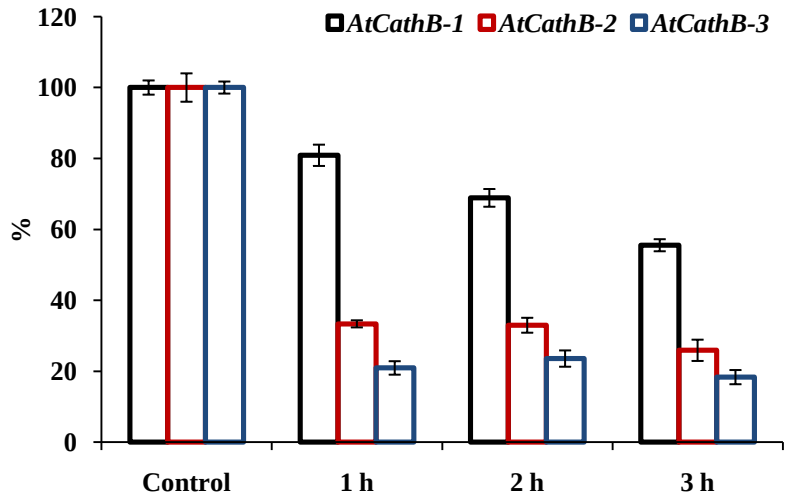

Fig 3.2 Transcript levels of *AtCathB-1*, *-2* and *-3* over time after 50kJ/m^2 UV-C irradiation in *Arabidopsis*. Two-week-old *Arabidopsis* seedlings grown *in vitro* were irradiated with 50kJ/m^2 UV-C and then incubated in continuous light. Samples were taken at different time points. Total RNA extraction, cDNA synthesis and qRT-PCR were carried out as described in chapter 2. Primers for qRT-PCR were designed as in McLellan *et al.* (2009). The *DAD-1* gene was used as an internal reference. Transcript levels are calculated as relative *AtCathB/DAD-1* ratio and then the value is given as a relative percentage of the control set as 100%. Error bars indicate ±S.D. value for triplicates.

The results in Fig 3.1 showed a small of increase of both caspase-3-like and cathepsin B-like activity after 50kJ/m^2 UV-C irradiation. After 1h light incubation, caspase-3-like activity against ac-DEVD-rhodamine110 increased by three fold while the enzymatic activity against ac-DEVD-AMC remained the same. In the second hour, a peak of DEVD-AMC cleavage activity developed with an increase of approx. three fold. The peak of ac-DEVD-rhodamine110 cleavage activity is higher than the peak of ac-DEVD-AMC cleavage activity by six fold. This suggests that there may be two different caspase-3-like proteases responsible for the cleavage of DEVD-AMC and DEVD-rhodamine110 respectively. In addition, cathepsin B-like activity increased by 2.5-fold after 1h incubation but decreased in the following 2h. However, the transcript levels of *AtCathB-1*, *-2* and *-3* were all reduced during the incubation after UV-C (Fig 3.2).

3.2.2 Partial purification of caspase-3-like proteases from *Arabidopsis thaliana* using bacitracin affinity chromatography

Since caspase-3 can be inhibited by bacitracin *in vitro*, a bacitracin-sepharose column was prepared for the partial purification of caspase-3-like proteases in *Arabidopsis*. After a 50 kJ/m^2 UV-C irradiation and 1 h light incubation, total proteins were extracted from two-week-old *Arabidopsis* seedlings and loaded to a pre-equilibrated bacitracin-sepharose column at a flow rate of 1ml/min at 4℃. Forty elution fractions (NO.1 to NO. 40) of 2 ml each were collected. A peak of 280nm absorbance (proteins) came between NO.15 to NO. 17. The flow through was also collected for analysis. It is suggested that approx. 60% to 80% of total caspase-3-like activity binds to the bacitracin-sepharose and then elute off while the rest of the caspase-3-like activity stayed in the flow through without binding (data not shown).

Caspase-3-like activity in NO.11 to NO. 22 purified fractions were assayed using both ac-DEVD-rhodamine110 and ac-DEVD-AMC (Fig 3.3). Interestingly, ac-DEVD-rhodamine110 cleavage activity peak came earlier than ac-DEVD-AMC cleavage activity. Compared with the six-fold higher activity shown in Fig 3.1, ac-DEVD-rhodamine110 cleavage activity is only higher than ac-DEVD-AMC cleavage activity by approx. 2.3 folds after bacitracin chromatography. As shown in Fig 3.4, both caspase-3-like and human cathepsin B-like activity increased after purification. Caspase-3-like activity increased by ten to forty fold against Ac-DEVD-AMC while cathepsin B-like activity increased by approx. twenty fold. This result suggests the existence of endogenous inhibitors which may suppress those activities in *Arabidopsis* extract and are lost during purification. A possible candidate would be the serine protease inhibitor encoded by the gene *At2g35580*. It is predicted to interact with AtCathB-2 in Arabidopsis Interactions Viewer of the database BAR (Popescu *et al.*, 2007; Popescu *et al.*, 2009).

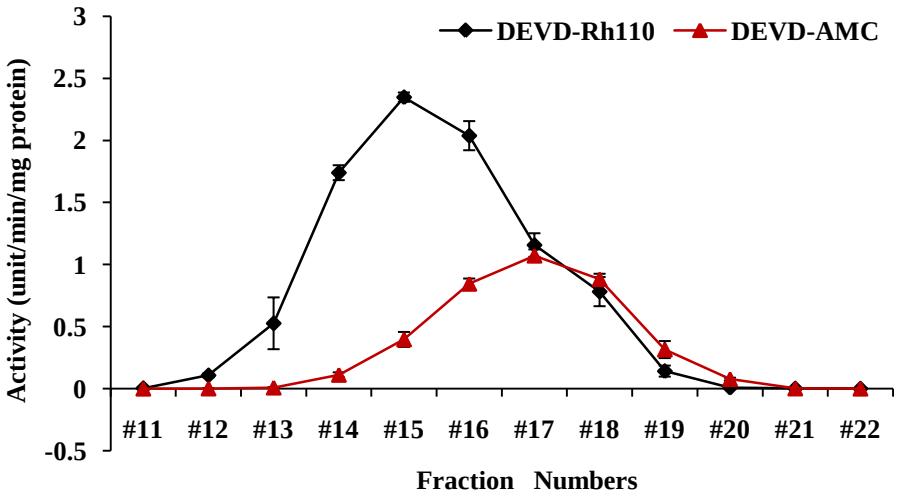

Fig 3.3 Caspase-3-like activity in fractions purified using bacitracin-sepharose chromatography purified. Two-week-old *Arabidopsis* seedlings grown *in vitro* were irradiated with 50kJ/m^2 UV-C. After 1h incubation in continuous light, total proteins in *Arabidopsis* seedlings were extracted as described in chapter 2 and loaded into a bacitracin-sepharose column with a flow rate of 1ml/min. Forty eluate fractions of 2ml each were collected after washing. Protein concentration was monitored by measuring absorbance at 280nm, salt concentration was measured using a conductivity meter. Enzymatic activity was assayed as described in chapter 2 using ac-DEVD-rhodamine110 and ac-DEVD-AMC as substrates. Activity is given as fluorescent unit/min/mg protein. Error bars indicate ±S.D. value for triplicates.

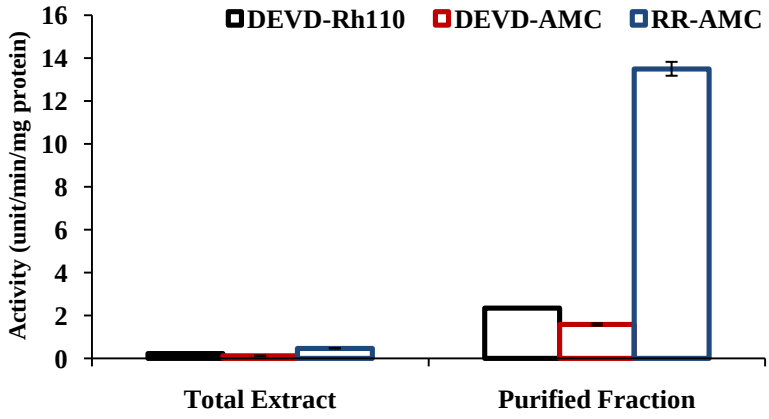

Fig 3.4 Caspase-3-like activity and cathepsin B-like activity in *Arabidopsis* before and after bacintracin chromatography purification. Two-week-old *Arabidopsis* seedlings grown *in vitro* were irradiated with 50KJ/m^2 UV-C. After 1h incubation in continuous light, total proteins in *Arabidopsis* seedlings were extracted and purified using a bacitracin-sepharose column as described in chapter 2. Enzymatic activity was assayed as described in chapter 2 using ac-DEVD-rhodamine110, ac-DEVD-AMC and z-RR-AMC as substrates. Activity is given as fluorescent unit/min/mg protein. Error bars indicate ±S.D. value for triplicates.

In addition to the substrates ac-DEVD-AMC, ac-DEVD-rhodamine110 and z-RR-AMC, proteolytic activity of the purified fraction against several other synthetic substrates was also detectable as shown in Fig 3.5. It is shown in Fig 3.5(A) that RRase, FRase, GRRase and AANase activities are detectable in the purified fraction. Z-FR-AMC is a substrate for papain. It can also be cleaved by cathepsin B. GRR-AMC is widely used in metacaspase research as an optimal substrate for metacaspase-4, -8 and -9 in *Arabidopsis* (Vercammen *et al.*, 2007; He *et al.*, 2007). AAN-AMC is a substrate for legumain, the cysteine protease called VPE in plants. Moreover, the results in Fig 3.5 (B) confirmed the detection of other caspase-like activities in UV-C induced seedlings, in which the caspase-3-like activity is the main caspase-like activity.

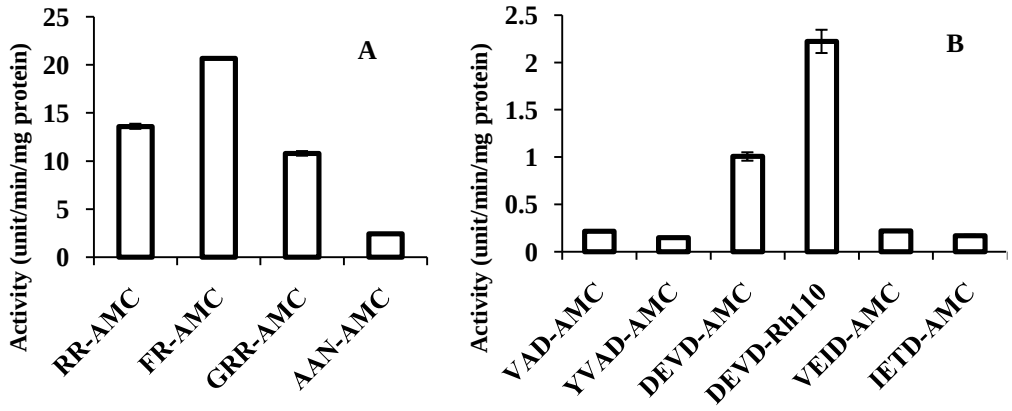

Fig 3.5 Proteolytic activities in the purified fraction obtained from bacitracin chromatography. Two-week-old *Arabidopsis* seedlings grown *in vitro* were irradiated with 50kJ/m^2 UV-C. After 1h incubation in continuous light, total proteins in *Arabidopsis* seedlings were extracted and purified using a bacitracin-sepharose column as described in chapter 2. Enzymatic activity was assayed as described in chapter 2 using various synthetic substrates. Activity is given as fluorescent unit/min/mg protein. Error bars indicate ±S.D. value for triplicates. (A) Cathepsin B (RR), papain (FR), *Arabidopsis* metacaspase-9(GRR) and legumain like (AAN) activity detected in purified fraction obtained from bacitracin chromatography. (B) Pan-caspase (VAD), caspase-1 (YVAD), caspase-3 (DEVD), caspase-6 (VEID), caspase-8 (IETD) like activity detected in purified fraction obtained from bacitracin chromatography.

3.2.3 Effect of inhibitors and cations on caspase-3-like activity in *Arabidopsis*

To optimize pre-incubation conditions for *in vitro* inhibition studies, the loss of caspase-3-like activity at various incubation temperatures and duration was assayed. The results (Fig 3.6) suggested that caspase-3-like activity in *Arabidopsis* decreased sharply during a 37℃

incubation. Only 6% caspase-3-like activity remained after 60min incubation at 37℃. After 15min and 30min incubation at 30℃, the remaining activity was 97% and 90% respectively. Caspase-3-like activity loss at 30℃ was 30% after 60min. Therefore for pre-incubation of proteases and inhibitors, a 30 ℃ pre-incubation for 30min was used in further experiments.

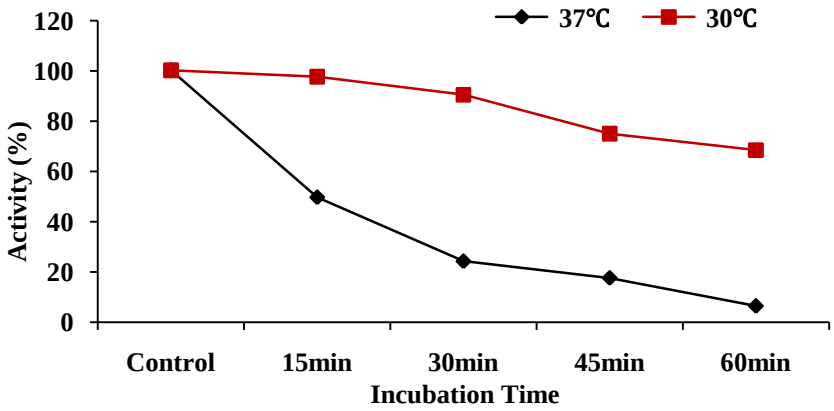

Fig 3.6 Caspase-3-like activity loss during pre-incubation. Two-week-old *Arabidopsis* seedlings grown *in vitro* were irradiated with 50kJ/m^2 UV-C. After 1h incubation in continuous light, total proteins in *Arabidopsis* seedlings were extracted as described in chapter 2. Pre-incubation was carried out at 30℃ and 37℃ with different time courses. DTT was added to a final concentration of 6mM. Enzymatic activity was assayed as described in chapter 2 using ac-DEVD-rhodamine110 as the substrate. Caspase-3-like activity detected in the purified fraction before incubation (2.6unit/min/mg protein) was set as 100%. The remaining activity is given as a percentage of the control. Error bars indicate ±S.D. value for triplicates.

Inhibitors are widely used in protease functional analysis and for caspase-like activity identification in plant PCD. To investigate the contribution of different proteases to caspase-3-like activity in UV-C induced PCD, the inhibitory effects of several inhibitors were assayed. The caspase-3 reversible inhibitor, ac-DEVD-CHO, could suppress nearly 95% caspase-3-like activity against ac-DEVD-rhodamine110. PMSF is a general serine protease inhibitor which suppressed 30% caspase-3-like activity in the purified fraction (Fig 3.7).

As an irreversible cathepsin B inhibitor, z-FA-FMK inhibits cysteine proteases potently including ‘downstream’ animal caspases (caspase-3, -6 and -7) *in vitro.* In the purified fraction, approx. 40% caspase-3-like activity was suppressed by FA-FMK. Two human cathepsin B selective inhibitors, z-LVK-CHO and CA-074 were also used. Z-LVK-CHO is derived from leupeptin which is a serine protease/cysteine protease inhibitor with higher inhibitory efficiency. Surprisingly, both of z-LVK-CHO and leupeptin could inhibit no

more than 10% of the total caspase-3-like activity in the purified fraction. CA-074 is a potent human cathepsin B irreversible inhibitor derived from the inhibitor E64. In animal cell free system, CA-074 inhibits cathepsin B but not cathepsin L/S. The results (Fig 3.5) showed that CA-074 could attenuate caspase-3-like activity by 30% and suggested that cathepsin B homologues only contribute partially to caspase-3-like activity in UV-C induced PCD in *Arabidopsis*.

Clasto-lactacystin β-lactone is a specific selective inhibitor to the 20S proteasome and ac-PnLD-CHO is an inhibitor of PBA1, a subunit in the 20S proteasome. PBA1 was recently reported to contribute to caspase-3-like activity in HR-mediated PCD in tobacco (Hatsugai *et al.*, 2009). In the purified fraction, clasto-lactacystin β-lactone could inhibit 60% caspase-3-like activity while ac-PnLD-CHO could only suppress less than 30% of the activity.

In animal apoptosis, the caspase-1 inhibitor, ac-YVAD-CHO is not tightly specific since it inhibits other caspases i.e. caspase-4 reversibly. This may explain why in our result ac-YVAD-CHO could inhibit caspase-3-like activity efficiently. In addition, the inhibitors of caspase-6 and -8, ac-VEID-CHO and ac-IETD-CHO could inhibit approx. 60% of the caspase-3-like activity in the purified fraction. It is not surprising that caspase-6 inhibitor could compete with the ac-DEVD-rhodamine110 substrate in enzymatic assay since caspase-6 is homologous to caspase-3 in function and structure in animals.

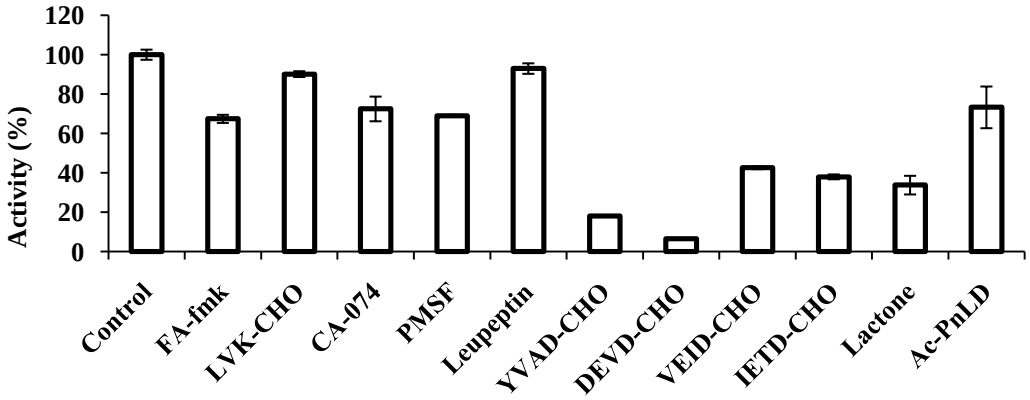

Fig 3.7 Inhibition of caspase-3-like activity in the purified fraction using bacitracin chromatography. Two-week-old *Arabidopsis* seedlings grown *in vitro* were irradiated with 50kJ/m^2 UV-C and then incubated in continuous light for 1h. Total proteins were then extracted and purified using a bacitracin-sepharose column as described in chapter 2. The purified fraction was pre-incubated with various inhibitors at 100 μM (except CA-074 concentration of 1mM) for 30min at 30 ℃. A purified fraction pre-incubated without inhibitor in the exact same conditions was used as a control. DTT was added to a final concentration of 6mM. Enzymatic activity assays were carried out as described in chapter 2 using ac-DEVD-rhodamine110 as the substrate. Caspase-3-like activity detected in the purified fraction before inhibitor incubation (2.6unit/min/mg protein) was set as 100%. The remaining activity is given as a percentage of the control. Error bars indicate ±S.D. value for triplicates.

PCD in plants is accompanied by cation efflux and influx from cells and conductivity measurement of ion leakage is an important method to quantifying PCD. Demidchik *et al.* (2010) have shown that ROS increase induces Ca^{2+} influx as well as K^{+} efflux in plant PCD. In addition, the author found that a K^{+}-efflux channel (GORK) was essential for HR-induced activation of caspase-like activity in *Arabidopsis*. In animal apoptosis, Zn^{2+} has been proved as a potent inhibitor to caspase-3 (Perry *et al.*, 1997). To investigate the effect of cations on caspase-3-like activity in UV-C induced PCD, K^{+}, Ca^{2+}, Mg^{2+} and Zn^{2+} were preincubated with total protein extracts at varying concentration. The results as shown in Fig 3.8 confirmed only a slight effect of K^{+} on caspase-3-like activity. Ca^{2+} and Mg^{2+} had similar inhibitory efficiency while additional Zn^{2+} could suppress caspase-3-like activity in *Arabidopsis* completely.

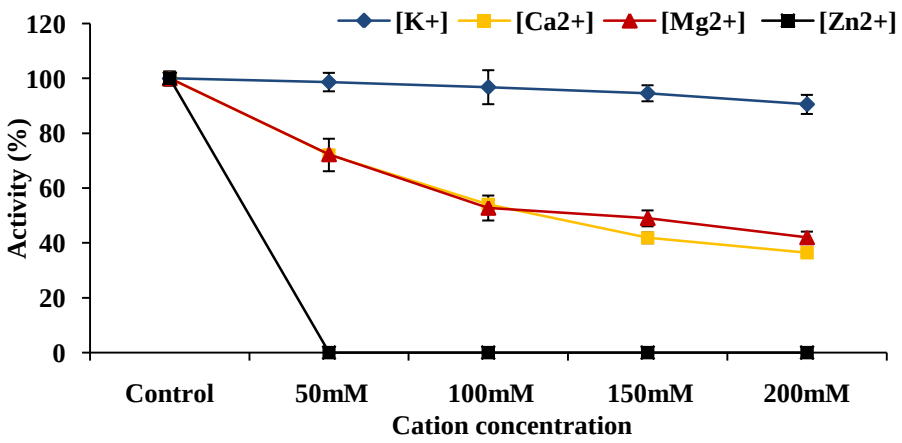

Fig 3.8 Effect of cations on UV-C induced caspase-3-like activity. Two-week-old *Arabidopsis* seedlings grown *in vitro* were irradiated with 50kJ/m^2 UV-C and then incubated in continuous light for 1h. Total proteins were then extracted as described in chapter 2. The lysate was pre-incubated with various cations at varying concentration for 30min at 30 ℃. The lysate pre-incubated without cation in the same conditions was used as control. DTT was added to a final concentration of 6mM. Enzymatic activity assays were carried out as described in chapter 2 using ac-DEVD-rhodamine110 as the substrate. Caspase-3-like activity detected in the extracts without additional cation (0.5unit/min/mg) was used as 100%. The remaining activity is given as a percentage of control. Error bars indicate ±S.D. value for triplicates.

3.2.4 Labelling of *Arabidopsis* cathepsin B using biotinylated caspase-3 inhibitor

The total protein extracts from *Arabidopsis* after UV-C overexposure was incubated with an irreversible biotinylated caspase-3 inhibitor, biotin-DEVD-FMK, which labelled caspase-3-like proteases and allowed their detection on protein blots using streptavidin-

HRP (Fig 3.9). Several bands are detectable in total extracts at 50kDa, 30 to 37kDa and 25kDa. The bacitracin affinity chromatography enables partial purification of caspase-3-like protease from total protein extracts and reduces the complexity of the proteases present. After labelling, the purified fraction showed three strong bands and one smaller slight band. According to their size, the top three bands between 25kDa and 37kDa are likely to be *Arabidopsis* cathepsin B while the lower band might be PBA1, a subunit of the 20S proteasome (Hatsugai *et al.*, 2009).

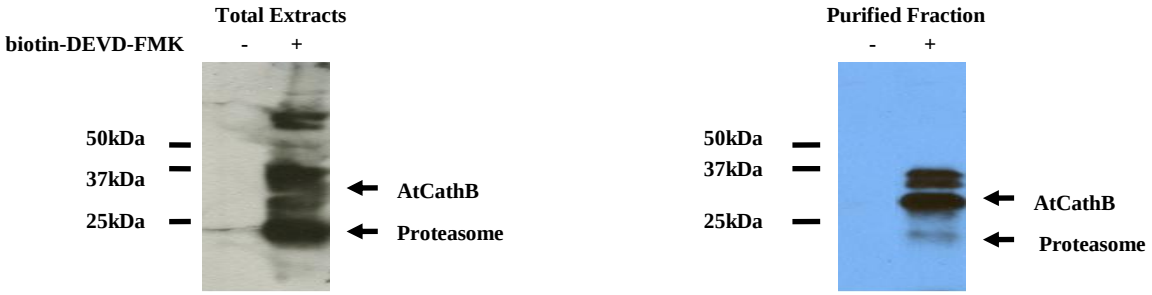

Fig 3.9 Biotinylation of caspase-3-like proteases in total protein extracts and the purified fraction using bacitracin chromatography in *Arabidopsis*. Two-week-old *Arabidopsis* seedlings grown *in vitro* were irradiated with 50kJ/m^2 UV-C and then incubated in continuous light for 1h. Total proteins were then extracted and purified using a bacitracin-sepharose column as described in chapter 2. Total extracts and the purified fraction were labelled with 10µM biotin-DEVD-FMK at 30℃ for 1h. DTT was added to a final concentration of 6mM. After labelling, 15µl protein solution from every sample were separated on 15% SDS-PAGE and transferred to a membrane. After incubation with streptavidin-HRP, the biotinylated proteins were detected using a mixture of supersignal west pico chemiluminescent substrate (4/5 vol) and west femto chemiluminescent substrate (1/5 vol).

In order to verify the labelling of *Arabidopsis* cathepsin B, the purified fraction was inhibited with 1mM CA-074 or 100µM LVK-CHO before biotinylation. The results in Fig 3.10 indicated that CA-074, LVK-CHO could attenuate the labelling significantly. Biotinylation of band II and band III was nearly abolished in CA-074 and LVK-CHO treated samples. From this results, we conclude preliminarily that *Arabidopsis* cathepsin B is labelled by the biotinylated caspase-3 inhibitor, which is indirect evidence supporting our speculation: cathepsin B is responsible for the caspase-3-like activity detected in *Arabidopsis* after UV-C irradiation.

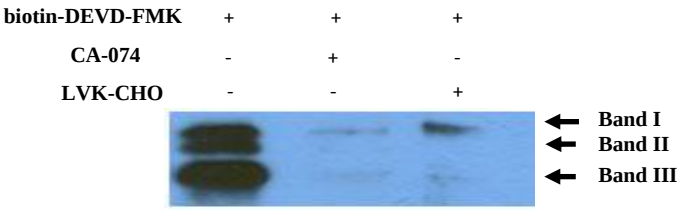

Fig 3.10 Inhibition of caspase-3-like proteases labelling using caspase-3 and cathepsin B inhibitors. Two-week-old *Arabidopsis* seedlings grown *in vitro* were irradiated with 50kJ/m^2 UV-C and then incubated in continuous light for 1 h. Total proteins were then extracted and purified using a bacitracin-sepharose column as described in chapter 2. A purified fraction was pre-incubated with 100 µM LVK-CHO or 1mM CA-074 at 30 ℃ for 30min before labelling with 10 µM biotin-DEVD-FMK for 1h at 30 ℃. DTT was added to a final concentration of 6mM. Following labelling, 15 µl protein solution from every sample were separated on 15% SDS-PAGE and transferred to a membrane. After incubation with streptavidin-HRP, the biotinylated proteins were detected using a mixture of supersignal west pico chemiluminescent substrate (4/5 vol) and west femto chemiluminescent substrate (1/5 vol).

3.3 Discussion

In this chapter, we confirmed the induction of caspase-3-like activity and cathepsin B-like activity as well as a reduction of *AtCathB* transcript levels in response to UV-C stress. By contrast, the elevated cathepsin B-like activity observed in human apoptosis is mainly ascribed to an increase of transcript level (Turk *et al.*, 2002), indicating different cell death mechanisms between animals and plants. It should be noted that the induction of *Arabidopsis* cathepsin B activity may be distinct from the total RRase activity detected over time since the z-RR-AMC substrate may be hydrolyzed by other proteases in the extract of *Arabidopsis* i.e. metacaspase-8 in addition to cathepsin B (He *et al.*, 2007).

In UV-C induced PCD in *Arabidopsis*, distinct caspase-3-like activity profiles are achieved when using ac-DEVD-rhodamine110 or ac-DEVD-AMC as substrates. We found ac-DEVD-rhodamine110 to possess a striking advantage compared to ac-DEVD-AMC by producing less background as it is completely silent before hydrolysis. What's more, ac-DEVD-rhodamine110 is stable in a wider pH range (pH 3-9) than ac-DEVD-AMC with an optimal pH at 7.5. However, the hydrolysis against ac-DEVD-rhodamine110 requires two steps because of its distinct molecular structure (Fig 3.11) and is more complicated than ac-DEVD-AMC hydrolysis. This report is the first time that proteolytic activities against ac-DEVD-rhodamine110 and ac-DEVD-AMC have been measured. The different activity profiles obtained suggests that at least two different proteases are required for caspase-3-like activity in *Arabidopsis*. It would be important for the future to determine if only one activity or both activities are linked to plant PCD induction.

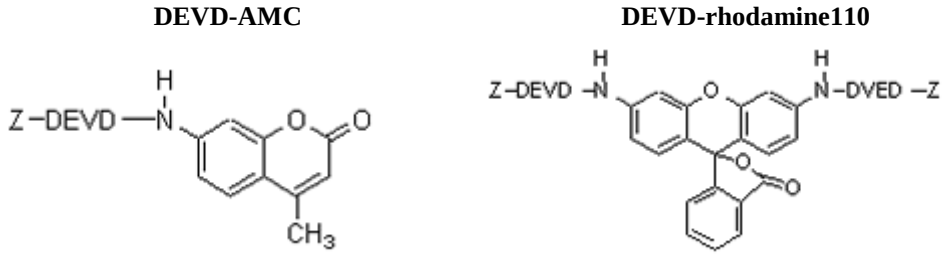

Fig 3.11 Molecular formula of DEVD-AMC and DEVD-rhodamine110. DEVD-AMC contains only one tetrapeptide conjugated with 7-amino-4-methylcoumarin; DEVD-rhodamine110 contains two tetrapeptides conjugated to distinct $–NH_2$ group in the same rhodamine110. (Reproduced from the Bachem catalogue

The caspase-3-like activity in *Arabidopsis* in response to UV-C irradiation is suppressed by the caspase competitive inhibitors (YVAD-CHO, DEVD-CHO, IETD-CHO and VEID-CHO) with various efficiency. In addition, serine protease inhibitor (PMSF), 20S proteasome inhibitors (lactone and ac-PnLD-CHO) and cathepsin B inhibitors (FA-FMK, LVK-CHO, CA-074) are effective, suggesting the possible contribution to caspase-3-like activity of cathepsin B, proteasome and serine protease. However, caution should be used in the interpretation, as the lack of inhibition specificity of these inhibitors must be taken into consideration. For example, lactone and ac-PnLD-CHO inhibits not only the 20S proteasome but also recombinant *Arabidopsis* cathepsin B *in vitro* (Gallois *et al.*, unpublished).

With the results of biotin-DEVD-FMK labelling and inhibition of labelling provided by this chapter, a link between *Arabidopsis* cathepsin B and the caspase-3-like activity detected after UV-C irradiation in seedlings can be established. Since our hypothesis is that *Arabidopsis* cathepsin B is responsible for the caspase-3-like activity required in plant PCD regulation, these results justify further research to be carried out on cathepsin B functions and enzymatic properties.

CHAPTER 4

FUNCTIONAL ANALYSIS OF *ARABIDOPSIS* CATHEPSIN B IN OXIDATIVE STRESS-INDUCED PCD USING TRANSGENIC PLANTS

4.1 Introduction

AtCathB-1(*At1g02300*), *AtCathB-2*(*At1g02305*) and *AtCathB-3*(*At4g01610*) are annotated as cathepsin B homologues in the genome of *Arabidopsis thaliana* and are sharing 36.6%, 41.3% and 38.1% similarity with human cathepsin B at the protein sequence level respectively. Cathepsin B is a versatile protease localised in the lysosome and translocated into the cytosol after some apoptotic stimuli (Chwieralski *et al.*, 2006). Human cathepsin B can enhance *cytochrome c* release by truncating the protein BID (BH3 interacting domain death agonist) which interacts with the mitochondria and cause cytochrome *c* leakage (Guicciardi *et al.*, 2000). *Nicotiana benthamiana* cathepsin B (*NtCathB*) and *Arabidopsis* cathepsin B (*AtCathB*) have been published to be essential for HR-mediated PCD triggered by bacterial pathogen (Gilroy *et al.*, 2007; McLellan *et al.*, 2009). In addition, a positive regulatory function of *Arabidopsis* cathepsin B has been reported in dark induced senescence (McLellan *et al.*, 2009).

Since we have identified that *Arabidopsis* cathepsin B displays caspase-3-like activity and caspase-3-like activity is required for plant PCD, we hypothesized a conserved cathepsin B pathway with caspase specificity in plant PCD regulation. Several lines of evidences in chapter 3 supported the suggestion that cathepsin B had caspase-3-like activity. In this chapter, a functional analysis of the three *Arabidopsis* cathepsin B genes during PCD is carried out using various *AtCathB* transgenic plants.

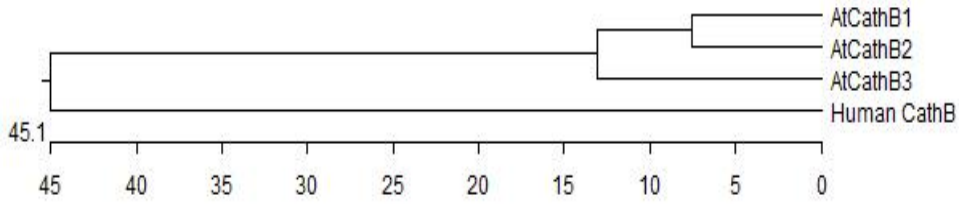

Fig 4.1 Phylogenetic tree of the human cathepsin B and *Arabidopsis* Cathepsin B. The phylogenetic tree was constructed using MegAlign (DNAStar) CLUSTAL W method; the branch length represents the evolutionary distance. Protein sequence of human cathepsin B (AAC37547) is obtained from the GenBank database. Protein sequences of *Arabidopsis* Cathepsin B are obtained from NASC database (*AtCathB-1=At1g02300*, *AtCathB-2=At1g02305*, *AtCathB-3=At4g01610*).

Gene knockout is a frequently used genetic technique in comprehensive analysis of gene function in important model organisms. With the gene of interest disrupted, particular phenotypes can be very informative about its normal function (Reski, 1998). In diploid organisms, both allele genes are required to be mutated. The T-DNA segment from *Agrobacterium tumefaciens* which is able to insert into the *Arabidopsis* genome randomly, can be transformed into *Arabidopsis thaliana* to disrupt genes by insertional mutagenesis (Feldmann, 1991). With 25 bp repeats borders on both ends, the T-DNA integrates into plant genomic DNA from left border to right border. Numerous gene knockout *Arabidopsis thaliana* lines produced by T-DNA mutagenesis are available in the two stock centres: Arabidopsis biological resource centre (ABRC) and Nottingham Arabidopsis stock centre (NASC). In this project, *AtCathB-1, AtCathB-2* and *AtCathB-3* single knockout lines produced by SALK institute, USA were purchased from NASC.

In addition to T-DNA mutagenesis, small interfering RNAs (siRNAs) and artificial microRNAs (amiRNAs) can be used to generate gene silencing. *In vivo*, natural miRNAs are encoded by endogenous *MIR* genes while siRNAs are originated from exogenous genes, RNA virus or transposons. Natural miRNAs are synthesised and folded as hairpin shaped precursors with double strand stem loop structure. As endoribonuclease, Dicer or Dicer-like protein (DLC) cleave pre-miRNAs into 20-25 nucleotides miRNAs with two overhang bases on 3' end (Ossowski *et al.*, 2008). In *Arabidopsis*, there are four types of DLCs identified and DLC-1 is responsible for the pre-miRNA processing. Mature miRNAs are employed in RNA-induced silencing complex (RISC) with protein factors and bind to target mRNAs. Artificial microRNAs (amiRNAs) can be generated based on the structure and properties of natural miRNAs and used to introduce post-transcriptional silencing into target genes. In this chapter, two amiRNAs were designed against *AtCathB-1* and *AtCathB-2* using web microRNAs designer (Schwab *et al.*, 2006).

As demonstrated in chapter 3, UV-C irradiation with at least 1h continuous light incubation can induce caspase-3-like activity in *Arabidopsis thaliana*. In addition to UV-C, methyl viologen and H_2O_2 were used as stimuli to induce PCD in both wild type plants and transgenic plants in this chapter. Methyl viologen generates superoxide radicals in the chloroplast that react with lipid membrane (Fujibe *et al.* 2004). In plants, H_2O_2 is generated in response to specific biotic and abiotic stresses. H_2O_2-induced PCD is

essential in various developmental progresses as well as environmental stresses (Bais *et al.*, 2003; Apel & Hirt, 2004).

After transcription, pre-mRNA must be matured for translation through RNA splicing. RNA splicing is a process to excise introns (intervening sequences) and ligate exons together. Most of the time, an intron contains a clear splicing signal. In pre-mRNA sequences, three sites are essential to localise splicing signals: splice donor, splice acceptor and branch site (Wu & Krainer, 1999). In addition, some other cis-acting elements exist *in vivo* and provide splicing sites preferential to specific tissue. Regulation from trans-acting elements can also result in alternative splicing. Mutated splicing site or splicing-related sequences will lead to the aberrant splicing or reading frame skipping (Cogan *et al.*, 1997). In humans, elevated cathepsin B expression level is linked to malignant tumours (Mehtani *et al.*, 1998). Human cathepsin B from alternative splicing lacks exon 2 and exon 3 and translates into a mature catalytic unit (Berardi *et al.*, 2001). Aberrant RNA splicing of tumour suppressor genes is common in tumour cells whereas mutation in splicing sites is absent (Kaufmann *et al.*, 2002; Venables 2004). The aberrant splicing in tumour cells without gene mutation is probably caused by environmental factors i.e.low pH, higher temperature or additional splicing machinery (Kaufmann *et al.*, 2002). In this chapter, ORF of *AtCathB-1* was isolated from *Arabidopsis* cathepsin B double knockout transgenic plants and amplified using a nested PCR in order to investigate its mutated catalytic unit and aberrant splicing.

4.2 Results

4.2.1 Isolation and characterisation of *AtCathB* transgenic lines

4.2.1.1 Isolation and characterisation of *AtCathB* double knockout lines

AtCathB single knock out lines, SALK_49118, SALK_89030 and SALK_19630 were produced by T-DNA mutagenesis using Columbia-0 ecotype (Col-0). Localisation of the T-DNA insertion is annotated in Fig 4.2. The T-DNA insertions into *AtCathB* genes can be predicted to generate truncated proteases that will not fold properly and will be inactive. This prediction is reinforced by our finding in chapter 5 showing that the C-terminal prodomain was a necessary chaperon for cathepsin B folding. All the *AtCathB* single knockout lines develop normally. Unfortunately, there was no phenotype obtained in PCD induced by UV-C, methyl viologen or H_2O_2 in *AtCathB* single knockout plants compared to wild type (WT) plants (data not shown). This can be explained by the redundancy of *AtCathB*: the function of the disrupted cathepsin B gene is possibly compensated by other cathepsins in this gene family (Stoka *et al.*, 2001).

Fig 4.2 Localisation of the T-DNA insertion in *Arabidopsis* cathepsin B single knockout lines. Insertion positions of T-DNA in *AtCathB* genes are annotated with 10-11 exons (Ex). (A) *AtCathB-1* gene: T-DNA (367 bp) is inserted into exon5. (B) *AtCathB-2* gene: T-DNA (402 bp) is inserted into exon9. (C) *AtCathB-3* gene: T-DNA (316 bp) is inserted into exon8.

For the generation of double knockout lines, SALK_19630 was used as female parent while SALK_49188 and SALK_89030 were used as male parents respectively in crossing. Genotype analysis in F2 progeny was carried out using genotyping PCR with *AtCathB-1,-2 or-3* forward primers and reverse primers and a T-DNA left border primer. According to the law of Mendelian segregation, the segregation of two independent genes results in the following genotypes: wild type (WT): heterozygote (HT): homozygote (HZ) is 1:14:1 in F2 progeny. As shown in Fig 4.3, a 1050bp (*AtCathB-2*) or 1180bp (*AtCathB-3*) band amplified from wild type plants represented intact *AtCathB-2* (Fig 4.3 A) or intact *AtCathB-1* (Fig 4.3 B) respectively. In homozygous double knockout plants, only one 402bp (*AtCathB-2*) or 316bp (*AtCathB-3*) band detecting the T-DNA insertion was amplified. Thus two bands were amplified in heterozygous knockout plants since only one allele is disrupted by T-DNA insertion. After identification of homozygous double knockout plants, RT-PCR was subsequently carried out for confirmation of double gene knockout (Fig 4.4).The transcript of *AtCathB* gene was not amplified in the corresponding knockout plants. *Actin 2* gene was used as an internal reference.

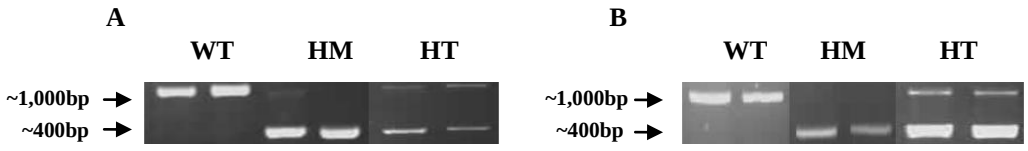

Fig 4.3 Genotypes analysis in F2 progeny of dbKO1×3 line and dbKO2×3 line using genotyping PCR. Genomic DNA was extracted as described in chapter 2. (A) Genotyping PCR results of dbKOCathB1×3 line F2 progeny with a mixture of primers: AtCathB-3 629LP, AtCathB-3 629RP and T-DNA LBb1. (B) Genotyping PCR results of dbKOCathB2×3 line F2 progeny with a mixture of primers: AtCathB-2 030LP, AtCathB-2 030RP and T-DNA LBb1. For each genotype two independent progeny are shown.

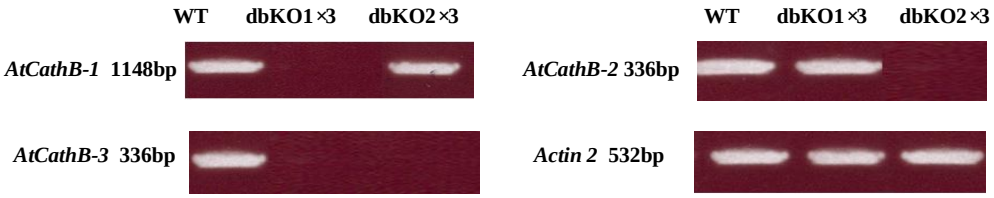

Fig 4.4 Confirmation of dbKO1×3 and dbKO2×3 homozygotes using RT-PCR. Total RNA was extracted from WT, dbKO1×3 and dbKO2×3 seedlings and cDNAs were synthesised as described in chapter 2. RT-PCRs with specific primers (*AtCathB-1*: S-4F, S4R; *AtCathB-2*: 714F, 1050R; *AtCathB-3*: 687F, 1023R) were carried out. *Actin 2* gene was used as internal reference.

4.2.1.2 Isolation and characterisation of *AtCathB* triple knockout lines

Arabidopsis cathepsin B triple knockout lines could not be generated from the crossing of T-DNA single knockout and double knockout lines since *AtCathB-1* and *AtCathB-2* are located in tandem on the same chromosome. Thus, two oligonucleotides were designed to generate artificial microRNAs in order to silence *AtCathB-1* and *AtCathB-2* in corresponding double knockout lines. In addition, one *Arabidopsis* cathepsin B triple knockout line generated using siRNA-mediated gene silencing was kindly provided by Prof. Paul Birch from the Scottish Crop Research Institute, UK.

Generation of AtCathB triple knockout line (tplKOmi) using artificial-microRNAs-mediated gene silencing

Two oligonucleotides for *AtCathB-1* or *AtCathB-2* silencing, namely amiRNA2300 and amiRNA2305, are designed using WMD3 web microRNA designer (Schwab *et al.*, 2006; Ossowski *et al.*, 2008) as highlighted in yellow in Fig 4.5. As shown in Fig 4.5 D, overlapping PCR was used to generate amiRNA precursors step by step using primers designed by the web designer and the template plasmid pRS300. In the overlapping PCR, amiRNAs (amiRNA2300 and amiRNA2305) and their complementary sequences (amiRNA2300* and amiRNA2305*) were amplified and ligated together with a loop sequence as intron. All PCR were carried out using high fidelity polymerase VELOCITY (Bioline, UK).

The amiRNA precursors were cloned into the pENTR1A vector and eventually transferred into the pK2GW7 vector for expression under the control of a 35S promoter. The two vectors, pK2GW-2300i and pK2GW-2305i were sequenced to verify the accuracy of the sequences and clones with no sequence errors were introduced into the complementary *Arabidopsis* cathepsin B double knockout lines using *Argobacterium*-mediated in-planta transformation. The hairpin structure of the oligonucleotides is expected to fold *in vivo* as annotated in Fig 4.5C. Subsequently, amiRNA2300 and amiRNA2305 are expected to be released by Dicer-like nuclease cleavage and targeted to either *AtCathB-1* or *AtCathB-2* mRNA respectively. However, only pK2GW2300i was transformed into the *AtCathB* dbKO2 ×3 transgenic lines to generate a triple knockout line named as tplKOmi.

A

miR300a

Primer A → **EcoR I** ↓ **amiRNA2300***

CTGCAGGCGATTAAGTTGGGTAACGCC….GAATTC….TATATATGTAGAGGAGGCATACTTACGTGTACTTC

miR300b

amiRNA2300* **Loop sequence** **amiRNA2300**

GAGGAGGCATACTTACGTGTACTTC….aattagcttccgactcat….GATGTACACCTAAGTATGCCGCCTC

miR300c

amiRNA2300

GATGTACACCTAAGTATGCCGCCTCT….GCGGCCGC….GGTCATAGCTGTTTCCTGTGTGAAATTGTTATCCGC

Not I ↑ **Primer B** ←

amiRNA2300 precusor

CTGCAGGCGATTAAGTTGGGTAACGCCAGGGTTTTCCCAGTCACGACGTTGTAAAACGACGGCCAGTG
AATTGTAATACGACTCACTATAGGGCGAATTGGGTACCGGGCCCCCCCTCGAGGTCGACGGTATCGAT
AAGCTTGATATGAATTCCTGCAGCCCcaaacacacgctcggacgcatattacacatgttcatacacttaatactcgctgttttgaattgatgtttA
GGAATATATATGTAGAGGAGGCATACTTACGTGTACTTCacaggtcgtgatatgattaattagcttccgactcattcatccaaatacc
gagtcgccaaaattcaaactagactcgttaaatgaatgaatgatgcggtagacaaattggaTCATTGATTCTCTTTGATGTACACCTAAGTA
TGCCGCCTCTCTCTTTTGTATTCCaattttcttgattaatctttcctgcacaaaaacatgcttgatccactaagtgacatatatgctgccttcgtatatatag
ttctggtaaaattaacattttgggtttatctttatttaaggcatcgccatgGGGGGATCCCTAGTTCTAGAGCGGCCGCCACCGCGGTGG
AGCTCCAGCTTTTGTTCCCTTTAGTGAGGGTTAATTCCGAGCTTGGCGTAATCATGGTCATAGCTGTTT

B

miR305a

Primer A → **EcoR I** ↓ **amiRNA2305***

CTGCAGGCGATTAAGTTGGGTAACGCC….GAATTC….TATATATGTAGAGTAGCCGATAATTCTATCAGTTC

miR305b

amiRNA2305* **Loop sequence** **amiRNA2305**

GAGTAGCCGATAATTCTATCAGTTC ….aattagcttccgactcat….GATCTGATACAATTATCGGCCACTC

miR305c

amiRNA2305

GATCTGATACAATTATCGGCCACTCT….GCGGCCGC….GGTCATAGCTGTTTCCTGTGTGAAATTGTTATCCGC

Not I ↑ **Primer B** ←

amiRNA2305 precusor

CTGCAGGCGATTAAGTTGGGTAACGCCAGGGTTTTCCCAGTCACGACGTTGTAAAACGACGGCCAGTG
AATTGTAATACGACTCACTATAGGGCGAATTGGGTACCGGGCCCCCCCTCGAGGTCGACGGTATCGAT
AAGCTTGATATGAATTCCTGCAGCCCcaaacacacgctcggacgcatattacacatgttcatacacttaatactcgctgttttgaattgatgtttA
GGAATATATATGTAGAGTAGCCGATAATTCTATCAGTTCacaggtcgtgatatgattaattagcttccgactcattcatccaaataccg
agtcgccaaaattcaaactagactcgttaaatgaatgaatgatgcggtagacaaattggaTCATTGATTCTCTTTTCTGATACAATTATCGG
CCACTCTCTTTTGTATTCCaattttcttgattaatctttcctgcacaaaaacatgcttgatccactaagtgacatatatgctgccttcgtatatatagttctggtaa
aattaacattttgggtttatctttatttaaggcatcgccatgGGGGGATCCCTAGTTCTAGAGCGGCCGCCACCGCGGTGGAGCTC
CAGCTTTTGTTCCCTTTAGTGAGGGTTAATTCCGAGCTTGGCGTAATCATGGTCATAGCTGTTTCCTGT
GTGAAATTGTTATCCGC

C Hairpin structure of amiRNA precursors *in vivo*

amiRNA2300 **5'-TGTACACCTAAGTATGCCGCC-3'** amiRNA2305 **5'-TCTGATACAATTATCGGCCAC-3'**
amiRNA2300* **3'-TCATGTGCATTCATACGGAGG-5'** amiRNA2305* **3'-TGACTATCTTAATAGCCGATG-5'**

D Overlapping PCR

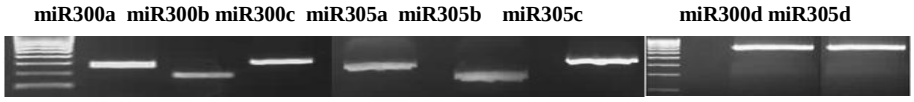

Fig 4.5 Engineering of amiRNA2300 and amiRNA2305. Oligonucleotides to generate amiRNA2300 and amiRNA2305 were designed using WMD3 web microRNA designer. The WMD designer delivered 4 short nucleotides miRa, miRb, miRc and miRd. Short nucleotides miRa,miRb and miRc were constructed using plasmid pRS300 as template. Oligonucleotide miRd was generated using miRa, miRb and miRc as template. (A)DNA sequence of miR300a, miR300b, miR300c and miR300d; (B) DNA sequence of miR305a, miR305b, miR305c and miR305d; (C) Expected map of amiRNA2300 precursor (oligonucleotide miR300d) and amiRNA2305 precursor (oligonucleotide miR305d) in *Arabidopsis*. (D) Overlapping PCR in oligonucleotide engineering. Overlapping PCR using HF VELOCITY polymerase was carried out as described in chapter 2.

Seeds harvested from transformed plants were grown on MS selection culture medium containing 100μg/ml hygromycin. As shown in Fig 4.6, RT-PCR using *AtCathB-1* specific primers was applied to screen for *AtCathB-1* gene silenced plants in T1 seedlings. Out of 19 plants tested, plants NO.18 and NO.19 are confirmed as successful *Arabidopsis* cathepsin B triple knockout mutants.

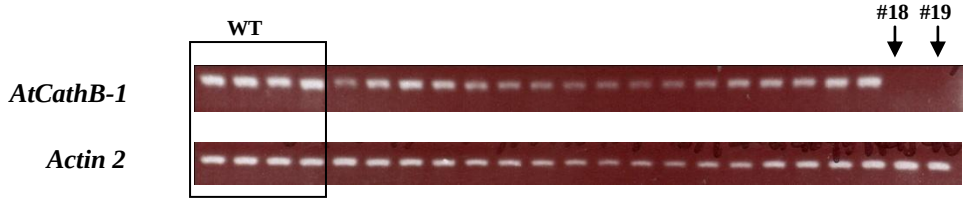

Fig 4.6 Screening for triple knockout mutants produced using amiRNA2300. Total RNA of *Arabidopsis* seedlings resistant to 100μg/ml hygromycin were extracted and cDNAs were synthesised as described in chapter 2. RT-PCR with *AtCathB-1* specific primers (S-4F, S-4R) was carried out. Total RNA extracted from wild type plants was used as control and the *Actin 2* gene was used as internal reference. The plants in which *AtCathB-1* transcript is not detectable are indicated by arrows.

Characterisation of AtCathB triple knockout line (tplKOsi) generated from RNAi

Another *Arabidopsis* cathepsin B triple knockout lines generated using siRNA-mediated *AtCathB-2* gene silencing was provided by Prof. Paul Birch. An RNAi hairpin construct as shown in Fig 4. 7 was produced using the highlighted sequence from the *AtCathB-2* ORF. The highlighted sequence was cloned into the pGreen0229 vector for expression under the control of the 35S promoter with a *GUS* gene inserted to separate the two parts of the hairpin. A 95% reduction in *AtCathB-2* mRNA transcript quantified by qTR-PCR analysis is reported in specific lines (McLellan *et al.*, 2009).

CATTGGAGGTCATGCTGTTAAACTTATTGGCTGGGGAACTTCTGATGACGGTGAAGA
TTATTGGTTGCTTGCAAATCAATGGAACCGAAGCTGGGGTGATGATGGGTACTTCAA
GATCAGGAGAGGAACAAACGAATGTGGCATTGAACATGGTGTTGTAGCTGGTTTACC
TTCAGACAGGAACGTAGTTAAAGGTATTACTACTTCAGATGATCTTCTTGTTTCCTC

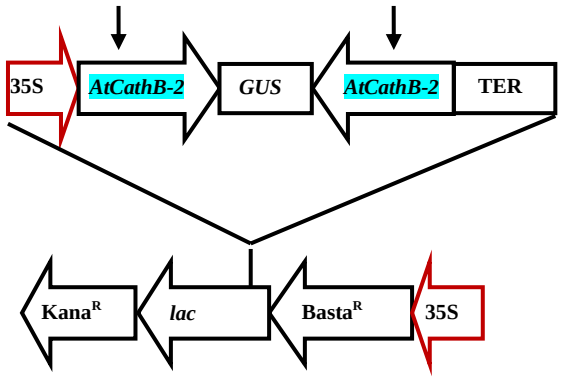

Fig 4.7 Schematic diagram of the RNAi hairpin construct used to silence *AtCathB-2*. The highlighted sequence from *AtCathB-2* is cloned into pGreen0229 for expression under the control of the 35S promoter. A *GUS* gene was inserted to separate the two parts of the hairpin.

4.2.2 Reduction of proteolytic activity in *AtCathB* knockout plants

In chapter 3, the elevated caspase-3-like activity (against DEVD-AMC and DEVD-rhodamine110) and cathepsin B-like activity (against RR-AMC) after UV-C irradiation followed by continuous light incubation has been established in wild type *Arabidopsis*. Since we postulated *Arabidopsis* cathepsin B to have caspase-3-like activity which is required for plant PCD, the analysis of proteolytic activities in *AtCathB* knockout plants in response to UV-C irradiation is of importance in this project.

Protein extracts from wild type and knockout plants after UV-C overexposure were partially purified using a bacitracin-sepharose column. As shown in Fig 4.8, a remarkable

reduction occurred in both caspase-3-like activity and cathepsin B-like activity in *AtCathB* knockout plants, indicating the three *AtCathB* genes are responsible for approx. 60% caspase-3-like activity in *Arabidopsis* purified fractions. Caspase-3-like activity against DEVD-AMC reduced by 20.9% in dbKO1×3 line, 37.8% in dbKO2×3 line and 62.8% in tplKOsi line compared to the wild type plants. Meanwhile caspase-3-like activity against DEVD-rhodamine110 reduced by 36.9%, 55.2% and 62.9% respectively in dbKO1×3 line, dbKO2×3 line and tplKOsi line. In contrast to the dbKO1×3 plants, plants from dbKO2×3 line exhibited even lower caspase-3-like and cathepsin B-like proteolytic activity. Thus the importance of *AtCathB-2* in caspase-3-like activity must be highlighted. In addition, this result suggests that some other proteases are able to hydrolyse the synthetic substrates for caspase-3 or cathepsin B.

It should be noted that CA-074, the selective cathepsin B inhibitor cold merely suppress caspase-3-like activity in the same condition by approx. 30% (Fig 3.5). The simplest explanation is that CA-074 at the concentration used is not efficient enough to block completely *Arabidopsis* cathepsin B activity. However, it cannot be excluded at this stage that some other possible proteases with caspase-3-like proteolytic activity are activated downstream of *Arabidopsis* cathepsin B. Thus in *AtCathB* knockout lines, these downstream proteases would be activated and this would contribute to the overall reduction observed in caspase-3-like activity. The 20S proteasome, which has been reported to display caspase-3-like activity in HR-mediated PCD in plants, is predicted to interact with AtCathB-2 and AtCathB-3 *in vivo* (Popescu *et al.*, 2007; Hatsugai *et al.*, 2009; Popescu *et al.*, 2009).

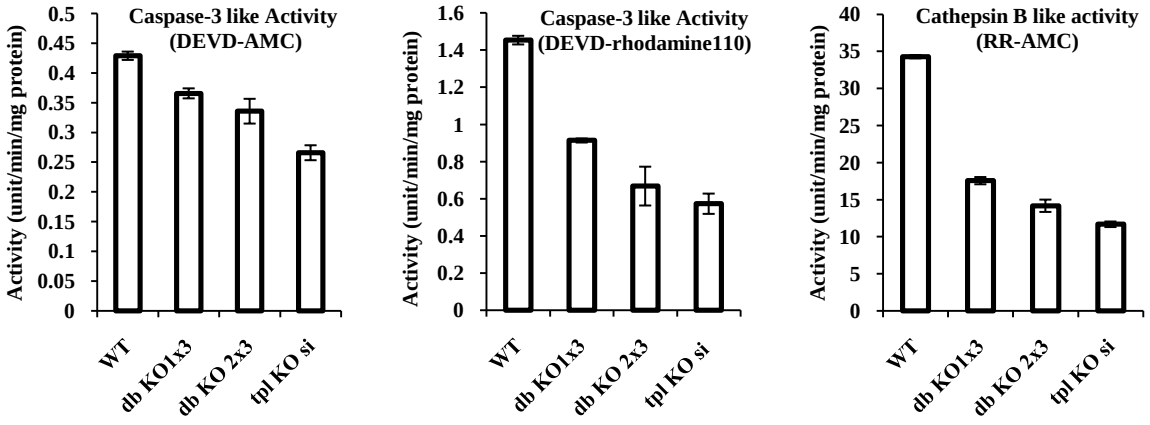

Fig 4.8 Proteolytic activity assays of the bacitracin chromatography purified fractions from *AtCathB* knockout lines. Two-week-old *Arabidopsis* seedlings from various *AtCathB* knockout lines grown *in vivo* were irradiated with 50kJ/m^2 UV-C and incubated in continuous light for 1h. Total proteins were extracted and purified using a bacitracin-sepharose column as described in chapter 2. Enzymatic activities were assayed using various synthetic substrates: DEVD-AMC, DEVD-rhodamine110 and RR-AMC. Activity is given in fluorescent unit/min/mg protein. Error bars indicate ±S.D. value for triplicates.

Consistent with the reduction in proteolytic activity, significant attenuation in biotin-DEVD-FMK labelling was shown in *AtCathB* double and triple knockout plants (Fig 4.9). After biotin-DEVD-FMK labelling, there were three bands detected between 25kDa and 37kDa in protein blot (Fig 3.7; Fig 4.9 WT lane). By contrast, in *AtCathB* triple knockout plants, the labelling of caspase-3-like proteases was abolished, suggesting a strong correlation between *Arabidopsis* cathepsin B and caspase-3-like activity.

In addition, the labelling using a biotinylated caspase-3 inhibitor in double knockout plants provided information regarding the activation status of AtCathB-1 and AtCathB-2 *in vivo* (Fig 4.9). Human cathepsin B is synthesised as pro-enzyme *in vivo* and truncated irreversibly into a smaller active form (Mort & Buttle, 1997). However, various partially truncated forms exist at the same time in the lysosome, a cellular compartment acting as a reservoir of proteolytic activity. Labelled bands probed in dbKO1×3 lane should be ascribed to AtCathB-2 (Fig 4.9). Combined with the predicted Mw of pro-AtCathB-2 (40kDa) and complete mature AtCathB-2 (26.7kDa), conclusion can be made that the majority of AtCathB-2 exists *in vivo* in its activated form. Thus the labelled bands in dbKO2×3 lane in Fig 4.9 may suggest the existence of a population of relatively inactive AtCathB-1 *in vivo* after UV-C irradiation. Therefore, an inactive cathepsin B reservoir may exist in *Arabidopsis* as described in animal cells.

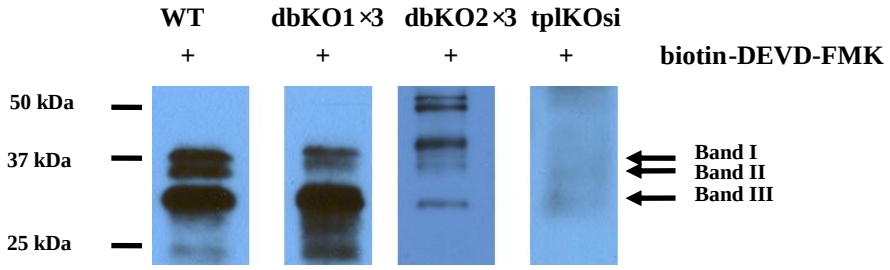

Fig 4.9 Labelling of caspase-3-like proteases in the bacitracin chromatography purified fractions from *AtCathB* knockout lines. Two-week-old *Arabidopsis* seedlings from various *AtCathB* knockout lines grown *in vivo* were irradiated with 50kJ/m^2 UV-C and incubated in continuous light for 1h. Total proteins were extracted and purified using a bacitracin-sepharose column as described in chapter 2. Purified fractions were labelled with 10μM biotin-DEVD-FMK at 30℃ for 1h. DTT was added to a final concentration of 6mM. Following labelling, same amount proteins (100μg) from every samples were separated on 15% SDS-PAGE and transferred to a membrane. After incubation with streptavidin-HRP, the biotinylated proteins were detected using a mixture of supersignal west pico chemiluminescent substrate (4/5 vol) and west femto chemiluminescent substrate (1/5 vol).

Although there was very little *Arabidopsis* cathepsin B labelled as caspase-3-like proteases in *AtCathB* triple knockout plants, caspase-3-like proteolytic activity was not completely abolished in enzymatic activity assay. It has been reported that PBA1, a subunit of the 20S proteasome, possessed caspase-3-like activity in *Arabidopsis* (Hatsugai *et al.*, 2009). In chapter 3, the presence and caspase-3-like activity of PBA1 in the bacitracin chromatography purified fraction from wild type *Arabidopsis* was proposed. We therefore postulate that PBA1 is responsible for the remaining caspase-3-like activity in *AtCathB* triple knockout plants. As shown in Fig 4.10, cathepsin B selective inhibitors, LVK-CHO and CA-074 had no effect in the purified fraction from *AtCathB* triple knockout plants, indicating cathepsin B is no longer present. By contrast, ac-PnLD-CHO, an inhibitor of PBA1 subunit activity and lactone the pan-proteasome activity inhibitor significantly suppressed the remaining caspase-3-like activity in *AtCathB* loss-of-function plants. However, the inhibitory effect of ac-PnLD and lactone are not tightly specific. We demonstrated the inhibitory effect of them at least on recombinant *Arabidopsis* cathepsin B in addition to the 20S proteasome. Whether some other proteases in *Arabidopsis* are responsible for the remaining caspase-3-like activity in *AtCathB* triple knockout plants requires further investigation.

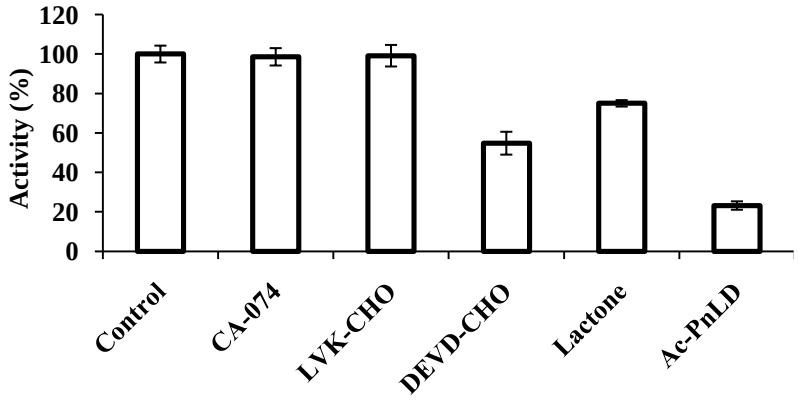

Fig 4.10 Effect of inhibitors on caspase-3-like activity in bacintracin chromatography purified fractions from *AtCathB* triple knockout lines. Two-week-old *Arabidopsis* seedlings from *AtCathB* triple knockout lines grown *in vivo* were irradiated with 50kJ/m^2 UV-C and incubated in continuous light for 1h. Total proteins were extracted and purified using a bacitracin-sepharose column as described in chapter 2. Purified fractions were pre-incubated with various inhibitors at the concentration of 100 μM (except CA-074 concentration was 1mM) for 30min at 30 ℃. Fractions pre-incubated without inhibitor in the exact same conditions was used as control. DTT was added to a final concentration of 6mM. Enzymatic activity assays were carried out as described in chapter 2 using ac-DEVD-rhodamine110 as substrate. Caspase-3-like activity detected in the fraction before inhibitor incubation (0.9unit/min/mg protein) was set as 100%. The remaining activity is given as a percentage of the control. Error bars indicate ±S.D. value for triplicates.

4.2.3 Reduced PCD in *AtCathB* knockout plants treated with methyl viologen, UV-C or H_2O_2

Human cathepsin B has been proposed to be a housekeeping gene because of its promoter structure and lethality has been reported in cathepsin B deficient transgenic mouse (Mort & Buttle, 1997; Turk *et al.*, 2002). However, *AtCathB* double and triple knockout plants do not exhibit obvious morphological phenotype in early developmental stages. The simplest explanation is that cathepsin B is not required during normal development in plants or compensated by other *Arabidopsis* cathepsins i.e. cathepsin L. The phenotype of *AtCathB* knockout plants and their wild type counterpart were analysed after several oxidative stresses including methyl viologen, UV-C and H_2O_2.

4.2.3.1 Effect of methyl viologen on germination and seedling bleaching in *AtCathB* knockout plants

Methyl viologen (N, N'-dimethyl-4, 4'-bipyridinium dichloride, MV) is a herbicide that is reduced to radical ions in the chloroplast and generates superoxide radical. The induction of PCD in plants by MV has been demonstrated with the formation of a DNA ladder

(Chen & Dickman, 2004; He *et al.*, 2007; Doyle *et al.*, 2010). Seeds from wild type and *AtCathB* knockout lines: dbKO 1×3 line, dbKO 2×3 line and tplKOsi were grown on MS medium containing varying MV concentration (0.25μM to 100μM). Depending on the MV concentration and genotypes, various phenotypes were observed and scored: germination suppression, cotyledon bleaching, growth cessations in seedlings at the first true leaf stage and postponed but normal development. In table 4.1, the germination percentage was obtained by simply counting the number of germinated and un-germinated seeds. The percentage of green cotyledon was calculated as the number of non-bleached cotyledon in all germinated cotyledon. Similarly, the data for green leaf referred to the percentage of non-bleached leaf in all seedlings (the seedlings stopped at cotyledon stage were excluded). As shown in Fig 4.1, a higher tolerance to MV was observed in seeds and seedlings of *AtCathB* knockout plants. The four *AtCathB* knockout plants germinated up to 5μM MV in medium while germination percentage in wild type plants was remarkably reduced. A slight higher tolerance is observed in dbKO2×3 compared to dbKO1×3, which is another evidence supporting the dominance of *AtCathB-2* in PCD. Fig 4.11 shows the cotyledon bleaching in wild type and green seedlings in the triple knockout background.

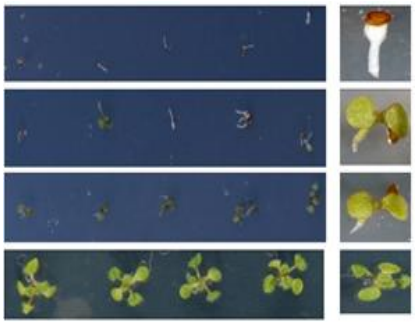

Fig 4.11 *AtCathB* knockout lines have a higher tolerance to methyl viologen. Sterile seeds were plated *in vitro* on solid MS media supplemented with 5μM methyl viologen and germinated in continuous light at 22℃. Photographs are illustrations of the phenotypes observed after 10d growth. The percentage of germination, green cotyledon and green seedlings are presented in Table 4.1

Table 4.1 Effect of MV on *Arabidopsis thaliana* germination and bleaching of cotyledon and leaf. (Various concentrations of methyl viologen ranging from 0.25 µM to 10 µM were supplemented into the MS culture medium.Sterile seeds were plated *in vitro* on solid MS culture medium supplemented with methyl viologen and germinated in continuous light at 22 ℃. The percentage of germination, green cotyledon and green seedlings were counted and calculated. ±S.D. value was calculated in triplicates.)

Lines	Control	0.25 µM	1 µM	2 µM	5 µM	10 µM (MV con.)
			Germination (%)			
WT	100	58.11 ±6.4	53.72 ±6.8	49.4 ±3.7	23.6 ±6.9	18.1 ±3.4
dbKO 1×3	100	100	100	100	100	89.8 ±2.1
dbKO 2×3	100	100	100	100	100	95.6 ±0.9
tplKO si	100	100	100	100	100	No Data
			Green Cotyledons (%)			
WT	100	57.6 ±7.2	53.7 ±6.9	40.2 ±1.3	20.2 ±3.1	0
dbKO1×3	100	97 ±0.2	94.5 ±1.8	90.6 ±2.3	31.6 ±2.1	11.7 ±3.3
dbKO 2×3	100	99.1 ±0.8	96.1 ±3.2	94.8 ±1.6	60.8 ±6.3	12.1 ±5.8
tplKO si	100	No Data	No Data	No Data	97.8 ±2.3	No Data
			Green Seedlings (%)			
WT	100	42.5 ±4.2	4.2 ±1.3	0	0	0
dbKO 1×3	100	97.6 ±2.1	88.6 ±1.4	68.1 ±2.9	38.7 ±3.1	No Data
dbKO 2×3	100	99.8 ±1.1	90.8 ±2.1	70.5 ±1.8	47.5 ±2.7	No Data
tplKO si	100	No Data	No Data	No Data	92.6 ±1.2	No Data

4.2.3.2 PCD in *AtCathB* knockout plants challenged by UV-C and H_2O_2

Leaf discs and protoplasts were prepared from wild type and *AtCathB* knockout transgenic plants and exposed to UV-C or H_2O_2 for PCD induction. As shown in Fig 4.12, ion leakage and protoplast death percentage are both induced in wild type plants after exposure to UV-C and H_2O_2, indicating the PCD was triggered in these stress conditions.

As expected, *AtCathB* double and triple knockout protoplasts showed a reduced PCD triggered by UV-C or H_2O_2 compared to wild type plants (Fig 4.12 A and B). Protoplast death percentages in *AtCathB* transgenic plants were reduced by up to 60%. In triple

knockout plants, all induced protoplast death was nearly abolished compared with wild type plants.

However, clear phenotype is not available using ion leakage conductivity as a marker in plant PCD measurement. Conductivity of ion leakage was induced by approx. 3.5-fold after UV-C or H_2O_2 treatment. However, conductivity in double knockout plants shows only a slight difference compared with wild type plants (Fig 4.12 C). The contrast between the ion leakage and protoplasts results may be explained by the removal of the cell wall in protoplasts. Protoplasts may lack cell wall components that compensate for the absence of cathepsin B. Alternatively, the ion leakage measured in leaf discs is upstream of the loss of cell permeability observed by Evans' blue in protoplasts. In other words, the absence of cathepsin B is only effective on cell permeability to Evans' blue but does not affect ion leakage. A similar result was obtained in *Arabidopsis* metacaspase-8 knockout plants (He *et al.*, 2007). It therefore suggests that ion leakage occurs in early stages of PCD while *Arabidopsis* cathepsin B and metacaspase-8 are involved in downstream regulation.

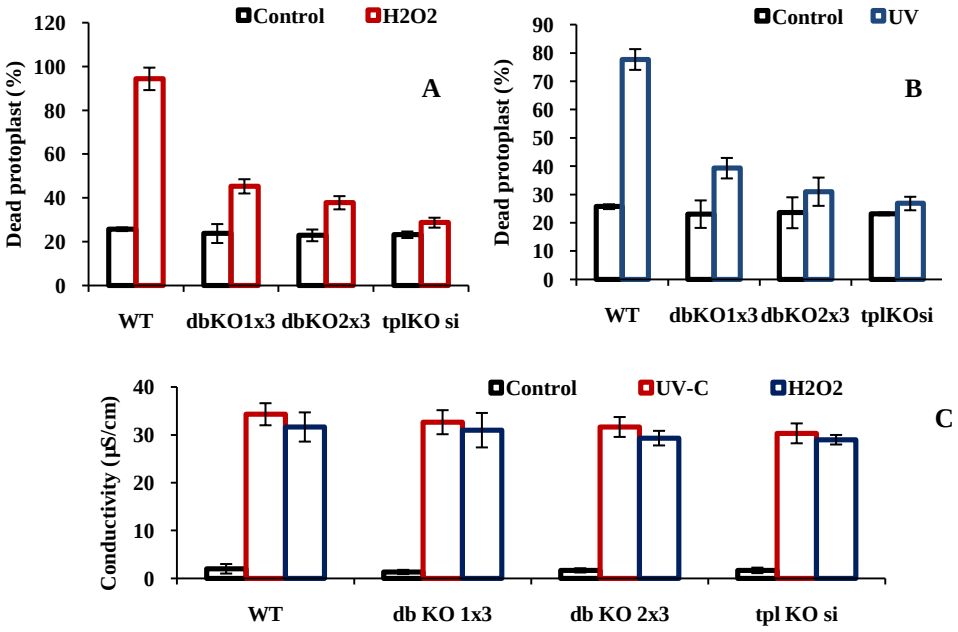

Fig 4.12 Protoplasts cell death and leaf discs ion leakage in wild type and *AtCathB* knockout lines exposed to UV-C or H_2O_2. (A) Protoplasts were isolated from seedlings of wild type and *AtCathB* knockout plants and treated with 10mM H_2O_2. Protoplasts were stained using Evans' blue after 4 h continuous light incubation. Results are given as the mean values of the percentage of cell death in the population. Error bars indicate ±S.D. value for triplicates. (B) Protoplasts were isolated from seedlings of wild type and *AtCathB* knockout plants and exposed to 10kJ/m^2 UV-C irradiation. Protoplasts were stained using Evans' blue after 4h continuous light incubation. Results are given as the mean values of the percentage of cell death in the population. Error bars indicate ±S.D. value for triplicates. (C) 3mm leaf discs were punched from four-week-old wild type and *AtCathB* knockout plants leaves and floated on distilled water. After 30mM H_2O_2 or 30kJ/m^2 UV-C exposure, leaf discs were incubated in continuous light for 16h. Ion leakage conductivity was measured before and after the treatment and calculated by the later reading minus the pre-reading. Mean values are given from triplicates. Error bars indicate ±S.D. value for triplicates.

4.2.4 Aberrant RNA splicing of *AtCathB-1*

In human cathepsin B, there are four active site residues required by its catalytic activity: Glu102, Cys110, His278 and Asn279. The same active site residues are conserved in other animal and plant cathepsin B. One exception is shown in Fig 4.13, where AtCathB-1 contains a unique insertion sequence (GYILNNVLLWSTITLWFWFL) whereby the Glu residue is replaced by a Leu residue at the conserved position. In the gene sequences of *AtCathB-2* and *-3*, an extra small exon (exon5) which is composed of five nucleotides (AT CAG) exists and encodes the active site residue Glu. This extra small exon is absent from *AtCathB-1* ORF prediction as shown in Fig 4.14. In the cDNA sequence of *AtCathB-1*, the nucleotide sequence of AG GGT present in *AtCathB-2* is mutated to TG GGT and therefore a Leu residue is introduced instead of the Glu residue. If this splicing prediction is correct, the protease AtCathB-1 is expected to be enzymatically inactive.

Expression level of *AtCathB-1* mRNA is low in physiological condition as reported by the AtGenExpress database (Winter *et al.*, 2007). However, AtGenExpress database indicates *AtCathB-1* expression is induced by heat shock (38 ℃ heating for 3h followed by a recovery at 28 ℃ for 4h). Total mRNA was isolated from both induced and un-induced dbKO2×3 line plants and nested PCR using high fidelity polymerase was subsequently carried out successfully. The benefit of using dbKO2×3 plants is that only the gene *AtCathB-1* is expressed. PCR products (Fig 4.15) were cloned into the pENTR1A vector and forty independent colonies were selected for DNA sequencing using forward and reverse primers from the pENTR1A vector as well as from *AtCathB-1*.

```
.
          AtCathB1   (98) DLSLKLPKEFDARTAWSHCTSIRRILVGYILNNVLLWSTITLWFWFLLGH
          AtCathB2  (101) DISLKLPKEFDARTAWSQCTSIGRILD--------------------QGH
          AtCathB3   (98) DPSLKLPKAFDARTAWPQCTSIGNILD--------------------QGH
        Glycine max  (96) PKTLKLPKNFDARTAWSQCSTIGRILD--------------------QGH
  Medicago truncatula  (95) PKSLKLPKDFDARTAWSQCSTIGRILD--------------------QGH
        Homo sapiens   (75) TEDLKLPASFDAREQWPQCPTIKEIRD--------------------QGS
       Xenopus laevis  (75) ADDLDLPDSFDSRAAWPNCPTIREIRD--------------------QGS
      Hordeum vulgare  (96) PKSADLPKEFDARTQWSSCSTIGNILD--------------------QGH
    Triticum aestivum  (93) P-EMDLPKEFDARTQWSSCSTIGNILD--------------------QGH
        Oryza sativa   (97) PRSLMLPKEFDARSAWSQCNTIGTILD--------------------QGH
Nicotiana benthamiana  (95) PKLLELPQEFDARVAWSNCSTIGRILD--------------------QGH
```

Fig 4.13 Alignment of part of various cathepsin B protein sequences containing the first active site residue. Protein sequences of various animal and plant cathepsin B were aligned using Align X programme in vector NTI advanced 11. Identical residues are highlighted in yellow. Active site residue Q is highlighted in red. Insertion sequence in AtCathB-1 is indicated in green. Protein sequences of animal and plant cathepsin B are obtained from protein database in NCBI. Protein sequences of AtCathB are obtained from NASC database.

***AtCathB-1*: predicted Exon4-Intron4-Exon5-Intron5-Exon6**

```
 V  A  E  F  K  R  L  L  G  V  I  Q  T  P  K  T  A  Y  L  G
GTTGCAGAGTTTAAGCGACTCCTCGGTGTTATACAAACACCAAAGACGGCATACTTAGGT

 V  P  I  V  R  H  D  L  S  L  K  L  P  K  E  F  D  A  R  T
GTACCTATTGTAAGACATGATTTATCGTTGAAGCTTCCTAAAGAATTTGATGCTAGAACC

 A  W  S  H  C  T  S  I  R  R  I  L  E
GCTTGGTCACATTGCACCAGTATTCGAAGGATCTTAGgtcggttttaatctcttagcttccactatctctgtcattaac

                                                      G  Y
ccaatgatttactgactcttcttatgtttgtttcaaattatctccctctttattgcactaaagatcaggtgaaacatcatttcatttgagTGGGTTAT

 I  L  N  N  V  L  L  W  S  T  I  T  L  W  F  W  F  L  L  G
ATATTGAACAATGTGTTACTCTGGTCGACGATAACTTTATGGTTTTGGTTTCTTTTGGGT

 H  C  G  S  C  W  A  F  G  A  V  E  S  L  S  D  R  F  C  I
CATTGTGGTTCTTGCTGGGCATTTGGTGCTGTTGAATCACTGTCCGACAGGTTCTGCATC

 K  Y  N  L
AAATATAACTTGgtaacacaactttctccatcaagccaagattgacgattgctacagctttttaatgtaattgctcttcttcccttgcag

 N  V  S  L  S  A  N  D  V  I  A  C  C  G  L  L  C  G  F  G
AATGTTTCCTTATCTGCCAATGATGTCATAGCATGTTGTGGATTACTTTGCGGTTTTGGT

 C  N  G  G  F  P  M  G  A  W  L  Y  F  K  Y  H  G  V  V  T
TGTAATGGTGGTTTCCCAATGGGTGCATGGTTGTACTTTAAGTACCACGGTGTAGTAACC

 Q  E
CAAGAG
```

***AtCathB-2*: predicted Exon4-Intron4-Exon 5-Intron5-Exon6**

```
 V  A  E  F  K  R  L  L  G  V  K  P  T  P  K  T  E  F  L  G
GTTGCAGAGTTTAAGCGCCTTCTTGGTGTTAAACCAACACCAAAGACGGAATTTTTGGGT

 V  P  I  V  S  H  D  I  S  L  K  L  P  K  E  F  D  A  R  T
GTGCCTATTGTAAGCCATGATATATCTTTGAAGCTTCCAAAAGAATTTGATGCTAGAACC

 A  W  S  Q  C  T  S  I  G  R  I  L  D
GCTTGGTCACAGTGCACCAGTATTGGAAGGATCTTAGggtcggttttaatcttttagatttccactatctctgtttttttc

                                        Q
tatccaatgatttactgactcttcttatgtttgtgttaaatcctctccataatcgtctcactaaagATCAGgtaacagatcatttacttgagtttatattgc

                                  G  H  C  G  S  C  W  A  F  G  A
ataatgggttctcagacagatataaacattttggttttggtttgtttagGGTCACTGTGGTTCTTGCTGGGCCTTTGGTGCT

 V  E  S  L  S  D  R  F  C  I  K  Y  N  M
GTTGAATCACTGTCTGACAGATTCTGCATCAAATATAACATG
```

Fig 4.14 Predicted exons and introns sequence in *AtCathB-1* and *AtCathB-2*. Sequences of exon4, intron4, exon5, intron5 and exon6 from *AtCathB-1* and *AtCathB2* are indicated. Exons are highlighted in yellow. Amino acid residues are indicated on top of corresponding codons.

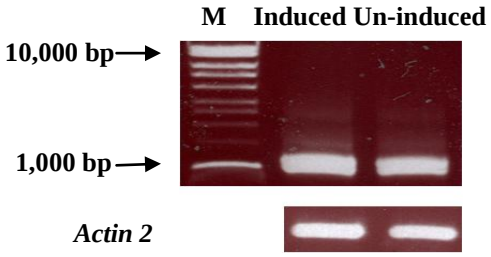

Fig 4.15 Nested PCR amplification of AtCathB-1 cDNA from induced and un-induced dbKO2×3 plants. Total mRNA isolation from induced and un-induced dbKO2×3 plants, cDNA synthesis and nested PCR were carried out as describe in chapter 2. Marker used here was hyperladder I (Bio-Rad, USA). *Actin 2* gene was used as internal reference. PCR products were separated on 1% agarose gel.

In all, three distinct isoforms of *AtCathB-1* were identified in the cDNA fragments amplified from mRNA isolated from induced and un-induced dbKO2×3 plants. In *AtCathB-1* isoform 1, similar excising of a small exon AT CAG as *AtCathB-2* occurred in the predicted intron5. Part of the predicted exon 5 was also excised. Thus a conserved Glu was therefore introduced as in AtCathB-2. Unfortunately, a stop codon TAA was introduced in the truncated exon5 because of a reading frame shift (Fig 4.16 A). Similar excising before AT CAG also occurred in *AtCathB-1* isoform 2, whereas, the predicted intron sequence after AT CAG was not spliced thus a stop codon TGA was introduced (Fig 4.16 B). In addition, a third *AtCathB-1* isoform was identified in only one colony. Isoform 3 contained part of the predicted intron4 and exon5. However, excision of intron4 did not start from AT CAG (Fig 4.16 C), which is different from isoform 1 and 2. A stop codon TGA occurred in exon5. Collectively, aberrant RNA splicing of *AtCathB-1* occurred in the double knockout background and only truncated AtCathB-1 proteins can be predicted from the three isoforms recovered.

A. *AtCathB-1* mRNA isoform 1

DNA Sequence

ATGGCTGATAGTTGTTGTATCAGACTTCACTTATTAGCCTCTGTTTTCTTGCTCTTATTTTCATCC
TTCAACTTGCAGGGTATTGCAGCGGAAAATCTTTCCAAGCAGAAACTGACCTCACTGATTCTTC
AGAATGAGATTGTAAAGGAAGTCAATGAGAATCCAAACGCTGGTTGGAAAGCTGCTTTCAATG
ATCGGTTTGCAAATGCCACCGTTGCAGAGTTTAAGCGACTCCTCGGTGTTATACAAACACCAAA
GACGGCATACTTAGGTGTACCTATTGTAAGACATGATTTATCGTTGAAGCTTCCTAAAGAATTT
GATGCTAGAACCGCTTGGTCACATTGCACCAGTATTCGAAGGATCTTAGatcagGTTCTGCATCAA
ATATAACTTGgtaacacaactttctccatcaagccaagattgacgattgctacagcttttaatgta

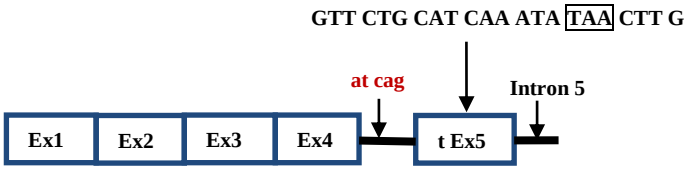

Predicted Protein Sequence Mw:18.39 kDa

MADSCCIRLHLLASVFLLLFSSFNLQGIAAENLSKQKLTSLILQNEIVKEVNENPNAGWKAAFNDRF
ANATVAEFKRLLGVIQTPKTAYLGVPIVRHDLSLKLPKEFDARTAWSHCTSIRRILGETSFHLSGLYI
EQCVTLVDDNFMVLVSFGSLWFLLGIWCC

B. *AtCathB-1* mRNA isoform 2

ATGGCTGATAGTTGTTGTATCAGACTTCACTTATTAGCCTCTGTTTTCTTGCTCTTATTTTCATCC
TTCAACTTGCAGGGTATTGCAGCGGAAAATCTTTCCAAGCAGAAACTGACCTCACTGATTCTTC
AGAATGAGATTGTAAAGGAAGTCAATGAGAATCCAAACGCTGGTTGGAAAGCTGCTTTCAATG
ATCGGTTTGCAAATGCCACCGTTGCAGAGTTTAAGCGACTCCTCGGTGTTATACAAACACCAAA
GACGGCATACTTAGGTGTACCTATTGTAAGACATGATTTATCGTTGAAGCTTCCTAAAGAATTT
GATGCTAGAACCGCTTGGTCACATTGCACCAGTATTCGAAGGATCTTAGatcaggtgaaacatcatttcatttga
gTGGGTTATATATTGAACAATGTGTTACTCTGGTCGACGATAACTTTATGGTTTTGGTTTCTTTT
GGGTCATTGTGGTTCTTGCTGGGCATTTGGTGCTGTTGAATCACTGTCCGACAGGTTCTGCATCA
AATATAACTTGgtaacacaactttctccatcaag

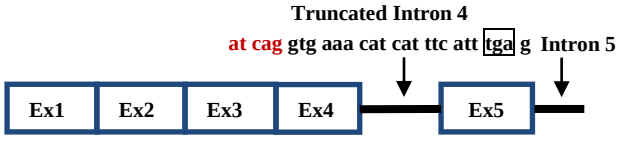

Predicted Protein Sequence Mw:14.61kDa

MADSCCIRLHLLASVFLLLFSSFNLQGIAAENLSKQKLTSLILQNEIVKEVNENPNAGWKAAFNDRF
ANATVAEFKRLLGVIQTPKTAYLGVPIVRHDLSLKLPKEFDARTAWSHCTSIRRILDQVLHQI

C. *AtCathB-1* mRNA isoform 3

ATGGCTGATAGTTGTTGTATCAGACTTCACTTATTAGCCTCTGTTTTCTTGCTCTTATTTTCATCC
TTCAACTTGCAGGGTATTGCAGCGGAAAATCTTTCCAAGCAGAAACTGACCTCACTGATTCTTC
AGAATGAGATTGTAAAGGAAGTCAATGAGAATCCAAACGCTGGTTGGAAAGCTGCTTTCAATG
ATCGGTTTGCAAATGCCACCGTTGCAGAGTTTAAGCGACTCCTCGGTGTTATACAAACACCAAA
GACGGCATACTTAGGTGTACCTATTGTAAGACATGATTTATCGTTGAAGCTTCCTAAAGAATTT
GATGCTAGAACCGCTTGGTCACATTGCACCAGTATTCGAAGGATCTTAGgtgaaacatcatttcatttgagTG
GGTTATATATTGAACAATGTGTTACTCTGGTCGACGATAACTTTATGGTTTTGGTTTCTTTTGGG
TCATTGTGGTTCTTGCTGGGCATTTGGTGCTGTTGAATCACTGTCCGACAGGTTCTGCATCAAAT
ATAACTTG

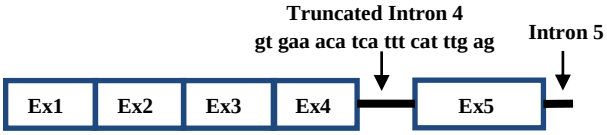

Predicted Protein Sequence Mw: 14.78kDa

MADSCCIRLHLLASVFLLLFSSFNLQGIAAENLSKQKLTSLILQNEIVKEVNENPNAGWKAAFNDRF
ANATVAEFKRLLGVIQTPKTAYLGVPIVRHDLSLKLPKEFDARTAWSHCTSIRRILDQVKHHFI

Fig 4.16 DNA sequences, annotation and predicted protein sequence from three different *AtCathB-1* mRNA isoforms isolated from dbKO2×3 line. Construction and DNA sequencing of pENTR1A-AtCathB1 plasmids were carried out as described in chapter 2. (A) *AtCathB-1* isoform 1 isolated from dbKO2×3 plants. (B) *AtCathB-1* isoform 2 isolated from dbKO2×3 plants. (C) *AtCathB*-1 isoform 1 isolated from dbKO2×3 plants. In (A), (B) and (C), DNA sequences of exons and introns are obtained from NASC database. Lower case sequences present predicted intron in NASC database. Protein translation and Mw calculation were obtained using the ExPASy proteomic server. The active site residue Q required for cathepsin B proteolytic activity is indicated in red.

4.3 Discussion

The function of animal cathepsin B is relatively well elucidated, however, reports of plant cathepsin B function are still limited. In chapter 3, a correlation between *Arabidopsis* cathepsin B and caspase-3-like activity in response to UV-C irradiation was suggested with preliminary data. The involvement of *Arabidopsis* cathepsin B in senescence and basal resistance to virulent bacterial pathogen has been published recently (McLellan *et al.*, 2009). In this chapter, several convincing genetic evidences supporting the hypothesis that *Arabidopsis* cathepsin B regulates PCD triggered by ROS are provided. Another important aspect in this project, the correlation between *Arabidopsis* cathepsin B and caspase-3-like activity is also demonstrated.

AtCathB double knockout lines were produced through crossing of single knockout lines. Triple knockout lines were obtained through amiRNAs-mediated gene silencing as well as RNAi. Oxidative stress: UV-C, methyl viologen or H_2O_2 were used as PCD inducer while protoplast death percentage, ion leakage conductivity and proteolytic activity were measured as indicators in PCD. A reduced death of *AtCathB* knockout plants in response to methyl viologen and UV-C irradiation suggests the involvement of AtCathB proteases in the chloroplast-mediated PCD pathway (Fujibe *et al.*, 2004; He *et al.*, 2007). *Arabidopsis* metacaspase-8 knockout plants have similar tolerance (He *et al.*, 2007), however, the link between metacaspases and cathepsin B in PCD pathway still remains to be established. To reinforce the functional analysis results, the generation of *AtCathB* overexpression lines is in progress.

Although *AtCathB* transcripts levels are reduced in response to UV-C stress, caspase-3-like activity and cathepsin B-like activity are both induced transiently after oxidative stress treatment. Posttranslational modifications and/or activation may be ascribed to this proteolytic activity increase. However, the elevated transcript level of *AtCathB-2* and *AtCathB-3* has been demonstrated after *Pst* DC3000 *Avr*B challenge (McLellan *et al.*, 2009). The author reported that *AtCathB* double knockout plants exhibited no phenotype compared to wild type plants when challenged by *Pst* DC3000 *Avr*B. By contrast, we showed that oxidative stress-induced PCD were obviously reduced in *AtCathB* double knockout plants. We therefore postulate that different PCD regulatory pathways may be implicated in plants while cathepsin B may act as a linker between these pathways.

In the bacitracin chromatography purified fraction from wild type plants, three bands (band I, II, III) between 25kDa and 37kDa were visualised on protein blot after biotin-DEVD-FMK labelling. In dbKO1×3 plants, the labelling of band I and II were attenuated while band III was not affected. Band III may therefore represent mainly AtCathB2. By contrast, the labelling of the three bands was attenuated in dbKO2×3 plants, representing the labelling of AtCathB-1. We can conclude collectively that the three bands obtained in wild type plants total protein extract labelling represent different activated statuses of the same AtCathB isoform.

The reduction of caspase-3-like activity in *AtCathB* knockout plants strongly suggest an association between cathepsin B and caspase-3-like activity detected in *Arabidopsis* seedlings undergoing PCD. However, there are relative differences in the contributions of three AtCathB proteases. AtCathB-2 shares 90% similarity at protein sequence level with AtCathB-1, but is speculated from enzymatic activity assay and DEVD-biotinylation to contribute most of the caspase-3 like activity. Microarray data displayed at the BAR website (University of Toronto) indicate a low expression level of the *AtCathB-1* transcript under normal physiological conditions. Analysis of the protein sequence deduced from the genome annotation shows that the conserved Glu residue which is essential to cathepsin B proteolytic activity is mutated in the AtCathB-1 protease. Cloning of *AtCathB-1* ORF from double knockout plants using nested PCR revealed three different mRNA isoforms. All the three isoforms are expected to produce truncated and non-functional proteases and different from the splicing prediction in NASC database. The source of variation in isoforms was always in the area of intron4-exon5-intron5. The rest of the introns / exons structure, the ATG and the stop were the same in all clones and very similar to AtCathB-2. This variable excision pattern may be partially explained by the excision sequences of intron5 in *AtCathB-1*. The 3'excision site of intron5 appears mutated to GT TG in *AtCathB-1* compared to the sequence GT AG in *AtCathB-2*. AG has been published as the consensus sequence for intron 3'splice site in *Arabidopsis* (Filichkin *et al.*, 2010). As predicted by the translation of the three mRNA isoforms, we expect several truncated AtCathB-1 forms in the double knockout background and very likely in wild type background. Similar truncated variants have also been reported in the caspase family. For instance, caspase-3S, the caspase-3 variant from an alternative mRNA splicing event, lacks the conserved sequence 'QZCXG' and is inhibitory to normal caspase-3 (Fan

et al., 2005). Since a function of *AtCathB-1* in plant PCD was confirmed, how can truncated AtCathB-1 forms regulate PCD requires further investigation.

Results from proteolytic activity assays suggested some other caspase-3-like protease may exist in *Arabidopsis* possibly downstream of cathepsin B. The 20S proteasome shares some functional similarity in protein turnover with cathepsin in animals (Kisselev *et al.*, 2003). Linking the two putative caspase-3-like proteases in *Arabidopsis*, proteasome and cathepsin B, in the PCD regulatory pathway requires further elucidation.

In summary, the regulatory function of *Arabidopsis* cathepsin B in oxidative stress-induced PCD is confirmed in this chapter. Furthermore, a functional association connecting *Arabidopsis* cathepsin B with caspase-3-like activity required for plant PCD is also established successfully. Cathepsin B is therefore postulated to be an ancestral modulator in a caspase-independent PCD pathway which is complementary to the caspase-dependent apoptotic pathway unravelled in animals. However, elucidation of a detailed PCD regulatory pathway containing cathepsin B requires further data. Recombinant expression, subcellular localisation and *in vivo* substrate analysis will be carried out in next chapters and will eventually benefit the plant PCD research.

CHAPTER 5

EXPRESSION OF RECOMBINANT *ARABIDOPSIS* CATHEPSIN B *IN VITRO* AND PRELIMINARY IDENTIFICATION OF POSSIBLE *IN VIVO* SUBSTRATES

5.1 Introduction

As published previously, caspase-3-like activity is detected in *Arabidopsis thaliana* and verified to be essential in UV-C induced PCD regulation (Danon *et al.*, 2004). Cathepsin B was identified as present in caspase-3 like proteases partially purified from *Arabidopsis* undergoing PCD using a bacitracin affinity chromatography. Results from chapter 4 confirmed the involvement of *Arabidopsis* cathepsin B in oxidative stress induced PCD. The reduction of caspase-3 like activity and cathepsin B like activity in *AtCathB* double knockout and triple knockout transgenic plants indicates a link between *Arabidopsis* cathepsin B and caspase-3. What's more, although recombinant human cathepsin B lacks caspase-3 like activity, cathepsin B purified from mouse brain is able to cleave synthetic caspase-3 substrate *in vitro* (Yakovlev *et al.*, 2008). However, direct evidence supporting *Arabidopsis* cathepsin B has caspase-3 like activity is still absent. In this chapter, recombinant AtCathB-2 and AtCathB-3 were produced in both prokaryotic expression system and eukaryotic expression system respectively. Their enzymatic properties were assayed and analyzed subsequently. A preliminary identification of possible *in vivo* substrates to *Arabidopsis* cathepsin B was also carried out for a further elucidation of its authentic function in plant PCD.

E.coli expression system is widely used in recombinant protein production. In this approach, a heterologous gene of interest is inserted into a plasmid vector downstream of a strong promoter and the resulting plasmid is introduced into *E.coli*. The protein of interest is then produced using host resource and accumulates in the cytoplasm or the periplasm. The T7 bacteriophage promoter is one of the most efficient promoters in *E.coli* expression system. It is recognized merely by the T7 RNA polymerase. The gene encoding the T7 RNA polymerase is recombined into the *E.coli* genome under the control of a lacUV5 promoter. Consequently, the gene of interest can be produced selectively by IPTG induction. What's more, T7 RNA polymerase is five times more efficient than *E.coli* RNA polymerase. However, although *E.coli* expression systems provide a rapid and inexpensive

approach, several problems in this system can make the production of protein of interest unavailable. Difference between the condon usage (bias/condon) preference in original organism of the interested protein and *E.coli* can severely depress protein synthesis (Terpe, 2006). The formation of inclusion bodies from misfolding protein is another serious disadvantage in *E.coli* expression systems. Protein of interests with disulfide bonds are easily to be misfolded in the reducing environment of the cytoplasm. Misfolded heterologous proteins ars insoluble and therefore aggregate in the cytoplasm as inclusion bodies (Hockney, 1994; Makrides, 1996). To circumvent this problem, the target protein can be fused to a leader peptide and designated to accumulate in the periplasm which provides a less reducing environment (Terpe, 2006). In some case, co-expression of specific chaperones can facilitate the correct folding of target protein in *E.coli* and eventually improve expression yield (Baneyx & Mujacic, 2004).

The baculovirus-insect cell expression system presents a useful platform for target protein expression and posttranslational modification research. It has several advantages compared to other expression systems (Ikonomou *et al.*, 2003; Muntener *et al.*, 2005). The base of this system is a baculovirus that can produce a large amount of occlusion bodies consisting of polyhedrin proteins in host insect cells since a highly efficient polyhedrin promoter exists in the viral genome (Blissard, 1996). In a baculovirus-insect cell protein expression system, a transfer vector containing the target gene ORF is co-transfected with linarized baculovirus (i.e. AcNPV) DNA into insect cells. Consequently, the target gene replace the polyhedrin gene through a homologous recombination event resulting in a recombinant viral genome that can be expressed in infected insect cell line such as Sf9 (from *Spodoptera frugiperda*) or High5 (from *Trichoplusia ni*) (Luckow & Summers 1988; Jarvis 1997). The newly synthesised recombinant protein is modified by the insect cell glycosylation pathway which may or may not be distinct from the authentic pathway followed by the target protein in the organism of origin (Jarvis & Finn, 1996; Jarvis, 1997). In this system, however, proteolysis of the target protein by baculovirus encoded proteases is a common problem (Ikonomou *et al.*, 2003).

Recombinant human, rat and mouse cathepsin B have been expressed in various systems including *E.coli*, yeast (*Saccharomyces cerevisiae* and *Pichia pastoris*), mammalian cell as well as insect cell (Steed *et al.*, 1998). Expression of the mouse preprocathepsin B in *E.coli* failed since the signal peptide was found to be cytotoxic (Mort *et al.*, 1988). Human procathepsin B expressed in *E.coli* aggregates in inclusion bodies and can be purified

under denaturing condition (Kuhelj *et al.*, 1995). Procathepsin B expressed in yeast and insect cell is converted into its mature form rapidly after synthesis (Mach *et al.*, 1994; Muntener *et al.*, 2005). It is reported that N-glycosylation has no effect on cathepsin B function or folding compentency *in vitro* (Hasnain *et al.*, 1992; Muntener *et al.*, 2005), indicating that heterogeneous post-translational modification in eukaryotic expression system will not affect the proteolytic function of recombinant cathepsin B. The prodomain of cathepsin B was found to act as a chaperone for correct folding, in addition to its inhibitory function of enzymatic activity (Muntener *et al.*, 2005).

Exertion of proteases function relies on proteolysis against specific substrates. Proteolysis of substrates can result in activiation or inactivation, secretion, localisation alteration and eventually control the entry into a specific event (Damme *et al.*, 2008). In caspase-dependent apoptotic pathway research, 2D-gel electrophoresis has been used for caspase substrates characterization (Denault & Salvesen, 2002). As reviewed previously, cathepsin B is a multifaceted protease responsible for protein turnover and zymogens activation *in vivo* (Turk *et al.*, 2001; van Acker *et al.*, 2002). The optimal synthetic substrate for human cathepsin B is RR-AMC. However, we have established a link between plant caspase-3-like activity and *Arabidopsis* cathepsin B. That is, cathepsin B is speculated to be responsible for the caspase-like activity detected in plants. As a protease, a survey of *in vivo* substrates for cathepsin B is essential to reveal its function *in vivo*. In this chapter, an initial analysis of possible substrate for *Arabidopsis* cathepsin B is carried out using recombinant *Arabidopsis* cathepsin B in a diagonal SDS-PAGE approach.

5.2 Results

5.2.1 Sequence analysis and prediction of AtCathB-2 and AtCathB-3 maturation

As reviewed in chapter 1.4, human cathepsin B are synthesised as preprocathepsin B firstly and then activated. Protein sequences of AtCathB-2 and AtCathB-3 were aligned with the human cathepsin B protein sequence using Align X programme in Vector NTI advance 11 (Fig 5.1). The signal peptides of AtCathB-2 and AtCathB-3 were predicted using SignalP 3.0. Possible signal peptide cleavage sites were predicted after Ala33 in AtCathB-2 and Ala32 in AtCathB-3 (Fig 5.1). Catalytic unit and prodomain clipping sites of AtCathB-2 and AtCathB-3 were also predicted manually using the alignment with human cathepsin B.

Human cathepsin B contains 14 cysteine residues and 12 of them: Cys93-Cys122, Cys105-Cys150, Cys141-Cys207, Cys142-Cys146, Cys179-Cys211 and Cys187-Cys198 (reviewed in UniProtKB P07858 CATB-HUMAN) form 6 disulfide bonds in its structure. As stated above, protein with disulfide bonds tend not to be folded properly in the reducing environment of *E.coli* cytoplasm. Thus, recombinant human cathepsin B expressed in *E.coli* is very likely to aggregate in inclusion bodies. The AtCathB protein sequence, which is homologous to human cathepsin B, is also rich in Cys residues. Possible disulfide bonds of AtCathB-2 and AtCathB-3 were predicted using the DiANNA 1.1 web server. The protein sequence of AtCathB-2 and AtCathB-3 were analyzed using PSI-BLAST and secondary structures (helix, strand and coil regions) were predicted using the PSIPRED protein structure prediction server V3.0. In this approach, disulfide oxidation state predictions were carried out and then disulfide bonds were predicted using a trained neural network (Ferre & Clote, 2005). Six disulfide bonds were predicted in the catalytic unit of AtCathB-2 (Cys131-Cys174, Cys148-Cys219, Cys165-Cys223, Cys166-Cys196, Cys170-Cys210, Cys205-Cys311) while five disulfide bonds were predicted in the catalytic unit of AtCathB-3 (Cys131-Cys328, Cys145-Cys216, Cys162-Cys220, Cys163-Cys193, Cys202-Cys207). From this result, it is therefore predicted that the recombinant expression of both AtCathB-2 and AtCathB-3 is likely to be misfolded in *E.coli*.

Glycosylation is the most significant post-translational modification. It adds glycans to specific sites of polypeptide chains (Steed *et al.*, 1998). N-glycosylation occurs at the Asn residue in Asn-X-Ser (X can be any amino acid residue except Pro) and is important for

protein functions i.e. proteolysis, folding, localisation and protein-protein recognition. Possible N-glycosylation sites in AtCathB2 and AtCathB-3 were predicted using NetNGlyc 1.0 Server (Fig 5.1). However, N-glycosylation sites depend not only of the protein sequence but also of the tissue and the species considered. In human cathepsin B, N-glycosylation has no affect on its folding or function (Hasnain *et al.*, 1992; Muntener *et al.*, 2005). Therefore, determining the real N-glycosylation sites of AtCathB and the effect of N-glycosylation in AtCathB *in vivo* would require further experimental evidence.

The cathepsin B structure contains an occluding loop that is a unique, absent in other cathepsins, which provides cathepsin B with an exopeptidase activity. A possible occluding loop was also predicted using protein sequence alignment with human cathespin B. Resembling the occluding loop sequences found in other plants, only one His residue exsits in AtCathB occluding loop (Fig 5.1).

```
    AtCathB2     (1) MADNCIRLLHSASVFFCLGLLISSFNLLQGIAAENLSKQKLTSWILQNEI
    AtCathB3     (1) -MAVYNTKLCLASVFLLLGLLLAFD--LKGIFAESLTKQKLDSKILQDEI
Human CathB      (1) --------MWQLWASLCCLLVLANAR--------S----RPSFHPLSDEL

    AtCathB2    (51) VKEVNENPNAGWKASFNDRFANATVAEFKRLLGVKPTPKTEFLGVPIVSH
    AtCathB3    (48) VKKVNENPNAGWKAAINDRFSNATVAEFKRLLGVKPTPKKHFLGVPIVSH
Human CathB     (31) VNYVNKR-NTTWQAGHN--FYNVDMSYLKRLCGTFLGGPKPPQ---RVMF

    AtCathB2   (101) DISLKLPKEFDARTAWSQCTSIGRILDQGHCGSCWAFGAVESLSDRFCIK
    AtCathB3    (98) DPSLKLPKAFDARTAWPQCTSIGNILDQGHCGSCWAFGAVESLSDRFCIQ
Human CathB     (75) TEDLKLPASFDAREQWPQCPTIKEIRDQGSCGSCWAFGAVEAISDRICIH

    AtCathB2   (151) YNMNVSLSVN--DLLACCGFLCGQGCNGGYPIAAWRYFKHHGVVT-----
    AtCathB3   (148) FGMNISLSVN--DLLACCGFRCGDGCDGGYPIAAWQYFSYSGVVT-----
Human CathB    (125) TNAHVSVEVSAEDLLTCCGSMCGDGCNGGYPAEAWNFWTRKGLVSGGLYE

    AtCathB2   (194) -------EECDPYFDNTGCSHPGCEPAYPTPKCARKCVSGNQ-LWRESKH
    AtCathB3   (191) -------EECDPYFDNTGCSHPGCEPAYPTPKCSRKCVSDNK-LWSESKH
Human CathB    (175) SHVGCRPYSIPPCEHHVNGSRPPCTGEGDTPKCSKICEPGYSPTYKQDKH

    AtCathB2   (236) YGVSAYKVRSHPDDIMAEVYKNGPVEVAFTVYEDFAHYKSGVYKHITGTN
    AtCathB3   (233) YSVSTYTVKSNPQDIMAEVYKNGPVEVSFTVYEDFAHYKSGVYKHITGSN
Human CathB    (225) YGYNSYSVSNSEKDIMAEIYKNGPVEGAFSVYSDFLLYKSGVYQHVTGEM

    AtCathB2   (286) IGGHAVKLIGWGTSDDGEDYWLLANQWNRSWGDDGYFKIRRGTNECGIEH
    AtCathB3   (283) IGGHAVKLIGWGTSSEGEDYWLMANQWNRGWGDDGYFMIRRGTNECGIED
Human CathB    (275) MGGHAIRILGWGVEN-GTPYWLVANSWNTDWGDNGFFKILRGQDHCGIES

    AtCathB2   (336) GVVAGLPSDRNVVKGITTSDDLLVSSF
    AtCathB3   (333) EPVAGLPSSKNVFRVDTGSNDLPVASV
Human CathB    (324) EVVAGIPRTDQYWEKI-----------
```

Fig 5.1 Prediction of signal peptide cleavage site, prodomain and catalytic unit in AtCathB-2 and AtCathB3. The protein sequences of AtCathB-2, -3 and human cathB were aligned using Align X programme in vector NTI advanced 11. Signal peptides in blue were predicted using signalP3.0. Prodomains in cyan were predicted from data on human cathB. Identical amino acid residues were highlighted in yellow. Occluding loops are highlighted in grey and essential His are indicated in red. N-glycosylation sites of AtCathB-2 and -3 predicted using NetNGlyc 1.0 Server are circled.

5.2.2 Expression of recombinant AtCathB-2 and AtCathB-3 in *E.coli*

To produce recombinant AtCathB-2 and AtCathB-3 in *E.coli*, AtCB2Cherry (AtCathB-2 with first 25 N-terminal amino acid residues deleted) and AtCB3Cherry (AtCathB-3 with first 27 N-terminal amino acid residues deleted) constructs were made and expressed using plasmid and reagent in a Cherry^{TM}codon kit (Eurogentec, Belgium). As shown in Fig 5.2, AtCB2Cherry and AtCB3Cherry contain full length of prodomain and catalytic unit fused with a cherry-tag on N-terminus as well as a 6×His-tag on C-terminus. The cherry-tag is a red short peptide (approx. 11 kDa) which is highly soluble. Fused with the cherry-tag, soluble AtCB2Cherry and AtCB3Cherry are also red when expressed properly. The fusion of a cherry-tag is suggested to possibly increase the solubility of recombinant protein.

```
AtCB2Cherry     (1) ADPGYLLGMAEQSDKDVKYYTLEEIQKHKDSKSTWVILHHKVYDLTKFLE
AtCB3Cherry     (1) ADPGYLLGMAEQSDKDVKYYTLEEIQKHKDSKSTWVILHHKVYDLTKFLE

AtCB2Cherry    (51) EHPGGEEVLGEQAGGDATENFEDVGHSTDARELSKTYIIGELHPDDRSKI
AtCB3Cherry    (51) EHPGGEEVLGEQAGGDATENFEDVGHSTDARELSKTYIIGELHPDDRSKI

AtCB2Cherry   (101) AKPSETLDDDDKHMGSLQGIAAENLSKQKLTSWILQNEIVKEVNENPNAG
AtCB3Cherry   (101) AKPSETLDDDDKHMGSLKGIEAESLTKQKLDSKILQDEIVKKVNENPNAG

AtCB2Cherry   (151) WKASFNDRFANATVAEFKRLLGVKPTPKTEFLGVPIVSHDISLKLPKEFD
AtCB3Cherry   (151) WKAAINDRFSNATVAEFKRLLGVKPTPKKHFLGVPIVSHDPSLKLPKAFD

AtCB2Cherry   (201) ARTAWSQCTSIGRILDQGHCGSCWAFGAVESLSDRFCIKYNMNVSLSVND
AtCB3Cherry   (201) ARTAWPQCTSIGNILDQGHCGSCWAFGAVESLSDRFCIQFGMNISLSVND

AtCB2Cherry   (251) LLACCGFLCGQGCNGGYPIAAWRYFKHHGVVTEECDPYFDNTGCSHPGCE
AtCB3Cherry   (251) LLACCGFRCGDGCDGGYPIAAWQYFSYSGVVTEECDPYFDNTGCSHPGCE

AtCB2Cherry   (301) PAYPTPKCARKCVSGNQLWRESKHYGVSAYKVRSHPDDIMAEVYKNGPVE
AtCB3Cherry   (301) PAYPTPKCSRKCVSDNKLWSESKHYSVSTYTVKSNPQDIMAEVYKNGPVE

AtCB2Cherry   (351) VAFTVYEDFAHYKSGVYKHITGTNIGGHAVKLIGWGTSDDGEDYWLLANQ
AtCB3Cherry   (351) VSFTVYEDFAHYKSGVYKHITGSNIGGHAVKLIGWGTSSEGEDYWLMANQ

AtCB2Cherry   (401) WNRSWGDDGYFKIRRGTNECGIEHGVVAGLPSDRNVVKGITTSDDLLVSS
AtCB3Cherry   (401) WNRGWGDDGYFMIRRGTNECGIEDEPVAGLPSSKNVFRVDTGSNDLPVAS

AtCB2Cherry   (451) FLNSSSVDKLAAALEHHHHHH
AtCB3Cherry   (451) VEFAR-------RLEHHHHHH
```

Fig 5.2 Protein sequences of AtCB2Cherry and AtCB3Cherry constructs. Protein sequences of AtCB2Cherry and AtCB3Cherry were aligned using Align X programme in vector NTI advanced 11. A sequence containing six amino acid residues of the signal peptide (blue background), complete prodomain (cyan background) and catalytic unit (yellow background) of AtCathB-2 and AtCathB-3 was fused to a N-terminal cherry-tag (red) and a C-terminal 6×His-tag (lilac). An enterokinase cleavage site (green background) is provided by pSCherry vector.

Corresponding DNA sequences were amplified from pU17098 (cDNA of *AtCathB-2*) and pU12892 (cDNA of *AtCathB-3*) and ligated using *BamHI* and *EcoRI* into pSCherry2 vector between the cherry-tag gene and 6×His-tag sequence respectively. In the pSCherry2 vector, the cherry tag-target protein fusion is downstream to a T7 promoter. The resulting constructs of pSAtCB2Cherry and pSAtCB3Cherry were transformed into cloning *E.coli* strain CYS21 lacking T7 RNA polymerase gene for screening. After selecting and sequencing plasmids prepared from three independent colonies, one selected plasmid was then transformed into the expression *E.coli* strain SE1 for recombinant expression.

5.2.2.1 Auto-inducible expression of AtCB2Cherry and AtCB3Cherry in *E.coli*

Staby^{TM}switch auto-inducible culture medium was selected for inducing protein expression in culture. As shown in Fig 5.3(C), the pellets of auto-induced *E.coli* expressing AtCB2Cherry and AtCB3Cherry were red while non-induced pellets were white. It is proved that a soluble recombinant AtCB2Cherry and AtCB3Cherry was produced successfully in auto-induced culture under the growth condition used.

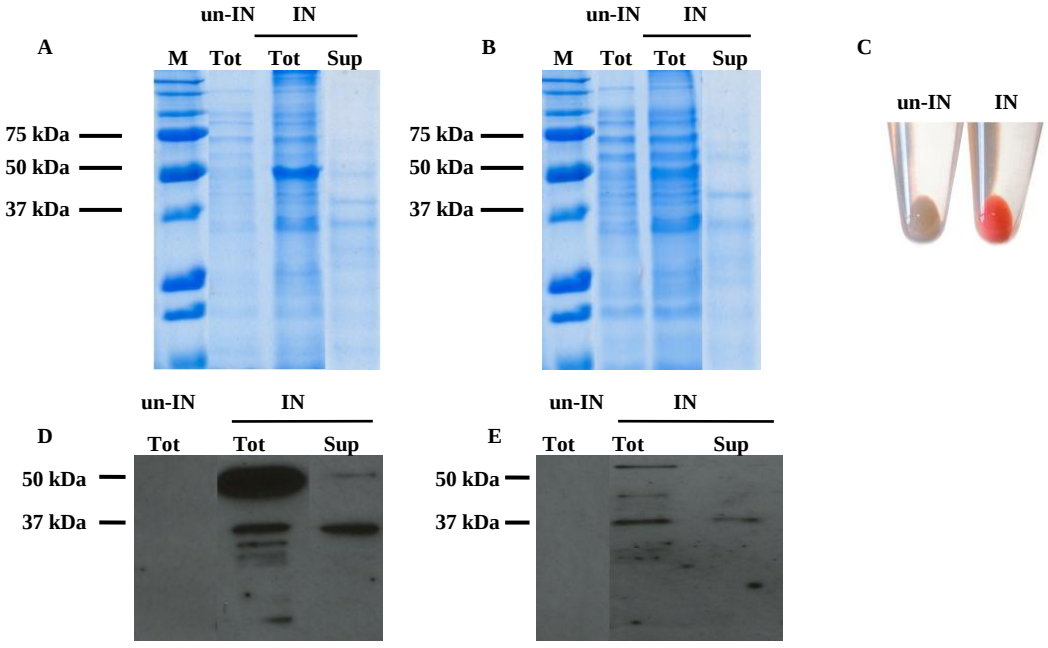

Fig 5.3 Auto-inducible AtCB2Cherry and AtCB3Cherry expression in SE1 strain *E.coli*. SE1 strain (protein expression strain) *E.coli* containing pSAtCB2Cherry or pSAtCB3Cherry plasmid was inoculated into 10ml Staby^{TM}Switch auto-inducible medium in 50ml conical tubes. Culture and lysis were carried out as described in chapter 2. (A) SDS-PAGE of total cell lysate from un-induced, total cell lysate and soluble proteins from induced *E.coli* expressing AtCB2Cherry; (B) SDS-PAGE of total cell lysate from un-induced, total cell lysate and soluble proteins from induced *E.coli* expressing AtCB3Cherry; (C) Un-induced cell pellet (white) and induced cell pellet (red); (D) Anti-His tag western blot of total cell lysate from un-induced, total cell lysate and soluble proteins from induced *E.coli* expressing AtCB2Cherry; (E) Anti-His tag western blot of total cell lysate from un-induced, total cell lysate and soluble proteins from induced *E.coli* expressing AtCB3Cherry.

After disruption of cell pellets using lysozyme and sonication, the supernatant was collected after centrifugation. The combined results of SDS-PAGE and anti-His tag western blot proved soluble recombinant AtCB2Cherry and AtCB3Cherry to be expressed in the soluble fraction with a size at approx. 37kDa, which is consistent with the predicted Mw of activated AtCathB. In total lysate, recombinant AtCB2Cherry and AtCB3Cherry are also detectable as an additional band with a size at approx. 50kDa, which is consistent with the predicted Mw of full length AtCathB-cherry. This suggested that part of the recombinant protein was soluble while another part was insoluble and aggregated in inclusion bodies. Furthermore, proteolytic activity against the substrates RR-AMC, DEVD-AMC and DEVD-rhodamine110 was also detected in auto-induced supernatant of AtCB2Cherry and AtCB3Cherry but was absent in non-induced supernatant (data not shown).

5.2.2.2 Purification of recombinant AtCB2Cherry and AtCB3Cherry from *E.coli*

Purification of soluble AtCB2Cherry and AtC3Cherry expressed in E.coli under native condition using Ni-NTA resins and TALON metal affinity resins

It is suggested from Fig 5.3 that both soluble and insoluble recombinant proteins fused a 6×His-tag were expressed in auto-induced culture. The 6×His-tag region has a specific binding affinity to Ni^{2+} or Co^{2+} cations, which can be immobilized on various resins. The binding ligand of Ni^{2+}/Co^{2+} cations to the 6×His-tag region can be disrupted at high imidazole concentrations. Thus Ni-NTA resins and TALON cobalt affinity resins can be used in rapid purification of 6×His-tag fused proteins by metal chelation chromatography. In order to obtain active and soluble recombinant proteins for enzymatic activity analysis, purifications were carried out under native conditions using auto-induced supernatant of AtCB2Cherry and AtCB3Cherry. Both Ni-NTA resins and TALON cobalt affinity resins were tested. In the native purification using Ni-NTA resins, imidazole concentrations in bind buffer/wash buffer, resins amount and purification temperature were optimized by many experiments (data not shown). Only a low imidazole concentration in the bind buffer (less than 0.2mM) was compatible with the caspase-3-like and human cathepsin B-like proteolytic activity being detectable in eluate and not in flow through. Unfortunately, many contaminating host proteins were co-eluted along with the recombinant proteins and this made the results of enzymatic activity assays unreliable. In the native purification using TALON cobalt resins, recombinant proteins failed to bind even in the absence of

imidazole in the bind buffer. We could conclude that the 6×His-tag region was partially hidden in the soluble forms of AtCB2Cherry and AtCB3Cherry (37kDa bands) because these two recombinant proteases expressed in *E.coli* had a lower binding affinity to Ni^{2+}/Co^{2+} resins than expected. This situation can be due to either the tertiary structure of the recombinant protein or a partial misfolding.

Purification of AtCB2Cherry expressed in E.coli under partial denaturing condition using Ni-NTA resins

Because the 6×His-tag in recombinant protein is partially hidden and not accessible under native condition, purification under partial denaturing condition was carried out using Ni-NTA resins. The rational is that the addition of low urea concentration (1M to 4M) to the cell lysate will partially denature the recombinant protein, some hydrogen bonds being broken, possibly exposing the 6×His-tag and enhancing the affinity of recombinant proteins to Ni-NTA resins. 10 mM of the antioxidant β-mercaptoethanol (β-ME) was also used in order to reduce the disulfide bonds in the recombinant proteins. The partial denatured and β –ME treated recombinant proteins were subsequently eluted from binding resins using a native elution buffer, in which spontaneous refolding/reoxidation of the recombinant protein may occur. Unfortunately, this approach did not improve the purification (Fig 5.4) while the proteolytic activities against the substrate of DEVD-AMC, DEVD-rhodamine110 and RR-AMC were no longer detectable in all the different elution fractions (E1 to E5).

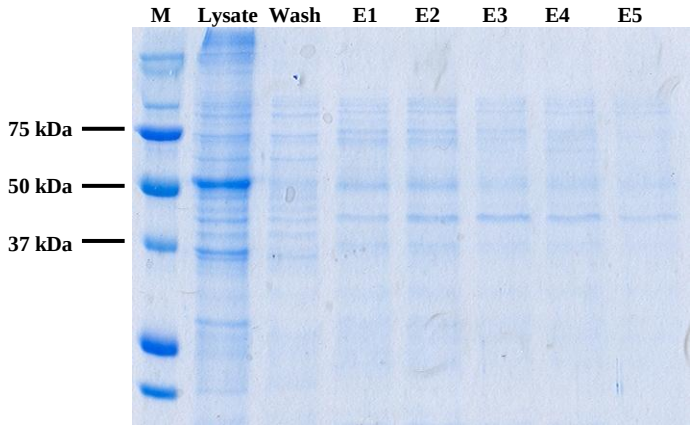

Fig 5.4 Purification of AtCB2Cherry under partial denaturing conditions using Ni-NTA resins. Various concentrations of denaturant urea (1M, 2M, 3M, 4M) and 10 mM antioxidant β-mercaptoethanol were added to the lysate of cultures expressing recombinant AtCB3Cherry. The lysate was then mixed with pre-equilibrated Ni-NTA resins and the purification was carried out as described in chapter 2. Partially denatured fractions were eluted in a native elution buffer. E1: eluate from lysate denatured by 1M urea; E2: eluate from lysate denatured by 2M urea; E3: eluate from lysate denatured by 3M urea; E4: eluate from lysate denatured by 4M urea; E5: eluate from lysate with additional β-ME only. 15μl Total lysate, wash off and elution fractions were separated using 15% SDS-PAGE and visualised using G250 coomassie brilliant blue staining.

Purification of AtCB2Cherry and AtCB3Cherry expressed in E.coli under denaturing conditions and refolding

It can be clearly observed in Fig 5.3 that recombinant AtCB2Cherry and AtCB3Cherry accumulate both in the cytoplasm (soluble form at 37kDa) and inclusion bodies (insoluble form at 50kDa). With the failure of the purification of the soluble recombinant protein under native condition, the insoluble recombinant proteins from inclusion bodies were collected from the pellet of cell lysate after centrifugation. Recombinant AtCB2Cherry and AtCB3Cherry aggregated in inclusion bodies were solubilised using mild denaturant 8M urea and 10mM dithiothreitol (DTT). 8M urea was used to denature the recombinant proteins and disentangle all disulfide bonds. This eventually destroys the protein structure. Thus we expect the 6×His-tag region to be fully released and therefore recognized by the metal cations in resins. Indeed highly purified recombinant AtCB2Cherry and AtCB3Cherry were obtained when the purification was carried out under denaturing condition (8M urea) using TALON cobalt resins (Fig 5.5 A).

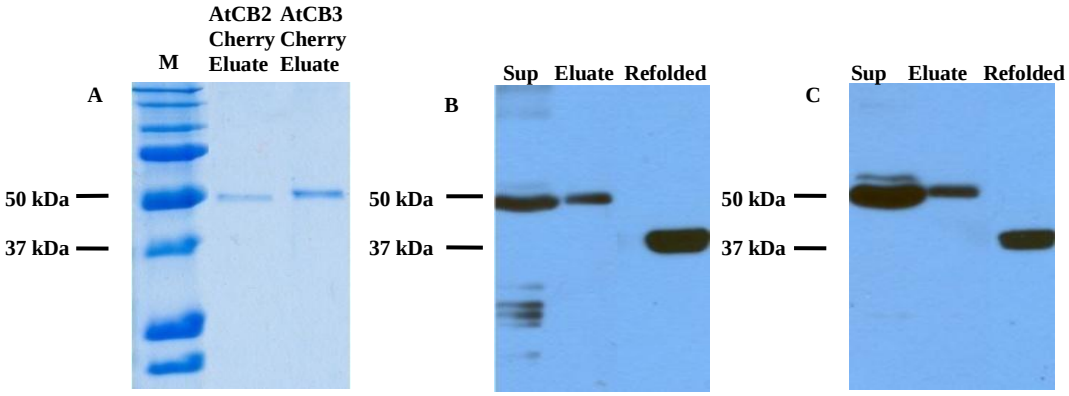

Fig 5.5 Purification of AtCB2Cherry and AtCB3Cherry expressed in *E.coli* under denaturing conditions and refolding. 8M denaturant urea was added into auto-induced cell culture lysate and the supernatant (sup) was collected using 12,000g centrifugation for 30min at room temperature. Denaturing purification was carried out as described in chapter 2 using TALON metal affinity resins. Refolding of the denatured recombinant protein was obtained using dialysis as described in chapter 2 and protease activation was carried out using pepsin treatment. (A) 15µl purified fractions of AtCB2Cherry and AtCB3Cherry were separated using 15% SDS-PAGE. (B) Anti-His tag western blot analysis of AtCB2Cherry pellet purified fraction and refolded protein. (C) Anti-His tag western blot analysis of AtCB3Cherry pellet purified fraction and refolded protein.

Generally, refolding is a process whereby denatured proteins regenerate correct disulfide bonds and eventually retrieve its natural structure as well as biological functions. This is

obtained by dialysing out the denaturant gradually. The effect of pH, temperature, redox status, protein concentration in refolding must be optimized. In our research, refolding of guanidine-HCl denatured AtCB3Cherry was optimized using a PIERCE Ltd. refolding kit but this failed: no cathepsin B-like activity or caspase-3-like activity was detected after refolding and pepsin activation (data not shown). For both AtCB2Cherry and AtCB3Cherry obtained from urea denaturing purification, refolding was carried out as described by Kuhelj *et al.* (1995). Denaturing purified AtCB2Cherry and AtCB3Cherry were diluted to a concentration of 10μg/ml and refolded in two dialysis steps at pH 7.0 at 4℃. Free cysteine was supplemented into the step I dialysis buffer to facilitate the formation of correct disulfide bonds which are essential to cathepsin B structure. The additional cysteine was finally removed in the second dialysis step. Porcine pepsin can activate procathepsin B by cleaving one Glu-Asp peptide bond in the recombinant protein that is closed to the prodomain cleavage site used *in vivo* (Kuhelj *et al.* 1995). It is reported that the refolded procathepsin B is degraded by procine pepsin in low pH if the refolding is incorrect. Although the refolded AtCB2Cherry and AtCB3Cherry could not be detected by SDS-PAGE and coomassie brilliant blue staining after pepsin treatment, they were detectable using anti-His tag western blot analysis at approx. 37kDa (Fig 5.5 B and C). This is therefore suggesting that the purification of recombinant AtCB2Cherry and AtCB3Cherry under denaturing condition as well as the refolding were successfully completed. Autocatalytic processing of refolded AtCB2Cherry and AtCB3Cherry at pH 5 and at either 4℃, 22℃ or 30℃ for 1h, 2h or 24h was tested to obtain procathepsin B activation using a pepsin treatment. It seemed that the autocatalytic processing could not occur in the tested conditions as no proteolytic activity increasing was detected after treatment (data not shown).

5.2.2.3 Proteolytic activity assay of AtCB2Cherry and AtCB3Cherry expressed in *E.coli*

The pepsin used to activate AtCB2Cherry and AtCB3Cherry was denatured irreversibly by an alkaline pH (8.0) treatment and removed from the activated samples by spinning down. The same concentration of pepsin solution and the same treatment was used in control samples in order to make sure that the added pepsin did not contribute in further proteolytic activity assay.

The optimal pH of refolded recombinant AtCB2Cherry and AtCB3Cherry expressed in *E.coli* was determined using DEVD-rhodamine110 as substrate. Both of proteases displayed a maximum catalyzing efficiency at pH 5.5 (Fig 5.6). The same pH optimum was achieved using refolded recombinant human cathepsin B provided by Prof. Boris Turk (Kuhelj *et al.*, 1995) against RR-AMC because human cathepsin B lacks caspase-3-like activity. Proteolytic activity of refolded recombinant AtCB2Cherry and AtCB3Cherry are therefore carried out using pH5.5 assay buffer.

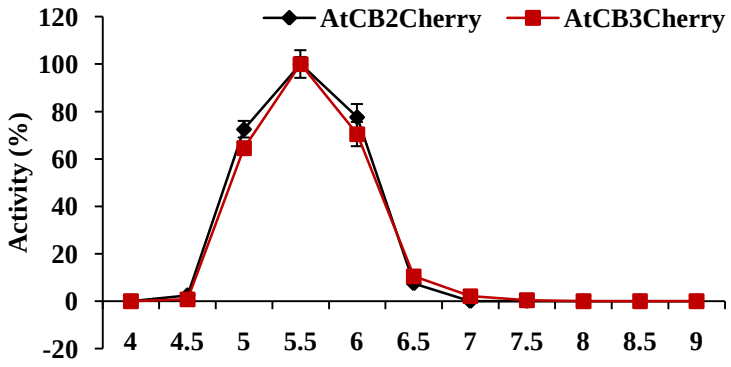

Fig 5.6 The optimal pH of refolded AtCB2Cherry and AtCB3Cherry expressed in *E.coli*. Denaturing purified and refolded recombinant AtCB2Cherry and AtCB3Cherry were produced and the proteolytic activity was assayed as described in chapter 2 using DEVD-rhodamine110 as substrate in different assay buffer at 50mM: sodium acetate buffer (pH 4-5), MES buffer (pH 5.5-6.5) and Tris-HCl buffer (pH 7-9). Highest caspase-3-like activity (197unit/min/mg protein) at pH5.5 was set at 100% and other activities are given as a percentage of the highest. Error bars indicate ±S.D. value for triplicates. N.D. means corresponding proteolytic activity was not detected.

Substrate affinity of the human cathepsin B and recombinant AtCathB are exhibited in Fig 5.7. Human cathepsin B-like activity was detected in both of the refolded proteases. Although the cathepsin B-like activity in AtCB2Cherry and AtCB3Cherry is low, we considered this as evidence supporting the success of refolding: the natural biological function is retained. In addition to cathepsin B-like activity, human cathepsin B displayed papain like activity (FRase), legumain like activity (AANase) and GRRase activity. But these activities were all absent in refolded AtCB2Cherry and AtCB3Cherry. However, proteolytic activity of AtCB2Cherry and AtCB3Cherry was highlighted by their caspase-like activity. As expected, caspase-3-like activity against DEVD-AMC and DEVD-rhodamine110 were both detected. Some caspase-1 like activity (YVADase) is also detected in both of AtCB2Cherry and AtCB3Cherry.

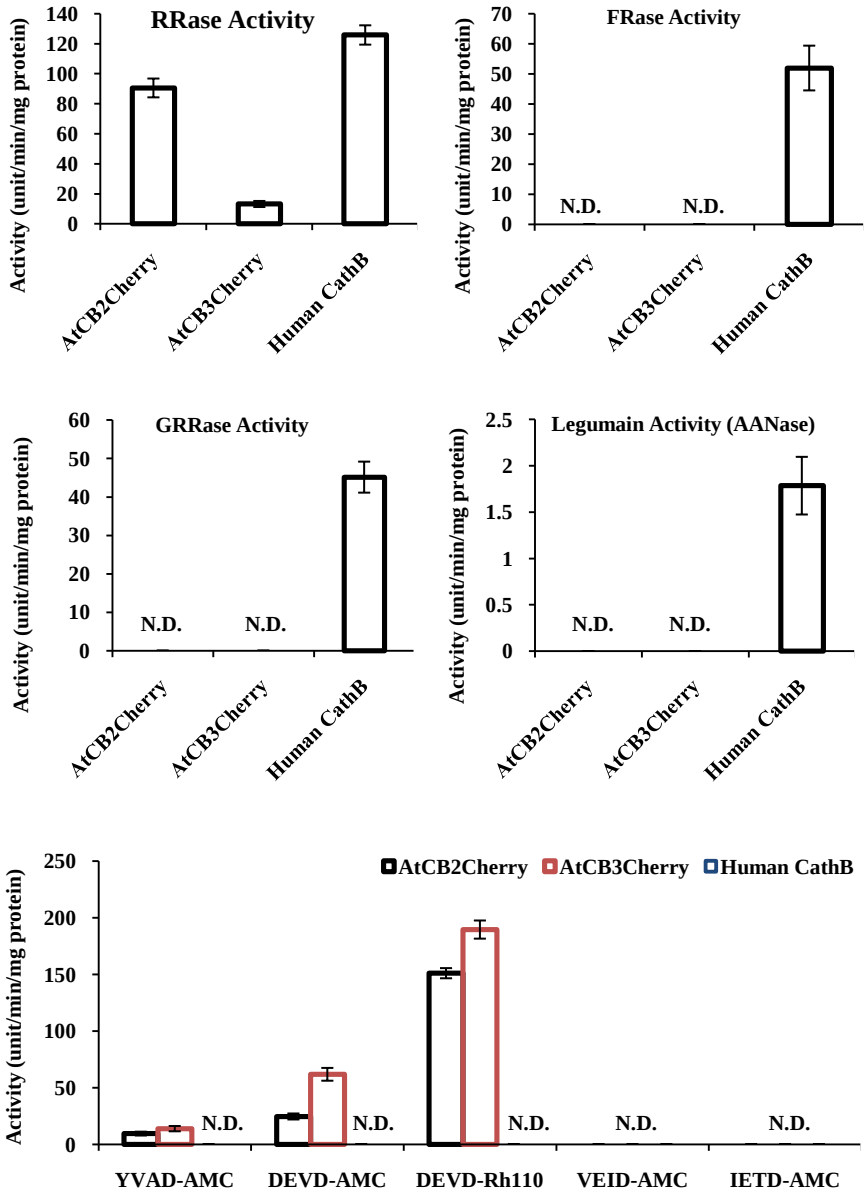

Fig 5.7 Proteolytic activity of AtCB2Cherry, AtCB3Cherry and human cathepsin B expressed in *E.coli*. Denatured, purified and refolded recombinant AtCB2Cherry and AtCB3Cherry were produced as described in chapter 2. Refolded recombinant human CathB was provided by Prof. B. Turk. Proteolytic activity was assayed as described in chapter 2 using RR-AMC (cathepsin B subsrate), FR-AMC (papain substrate), GRR-AMC, AAN-AMC (legumain substrate) and synthetic caspase substrates: YVAD-AMC, DEVD-AMC, DEVD-rhodamine110, VEID-AMC and IETD-AMC. Activity is given as fluorescence unit/min/mg protein. Error bars indicate ±S.D. value for triplicates. N.D. means corresponding proteolytic activity was not detected.

Inhibition studies of caspase-3-like activity of AtCB2Cherry and AtCB3Cherry as well as the cathepsin B-like activity (RRase) in human cathepsin B using various inhibitors are shown in Table 5.1. The most efficient inhibitor for both AtCB2Cherry and AtCB3Cherry

was CA-074, which is a selective inhibitor for human cathepsin B. Other human cathepsin B specific inhibitors, LVK-CHO and FA-FMK could also suppress the caspase-3-like activity of AtCB2Cherry and AtCB3Cherry by nearly 80% and 50% respectively. The caspase-3 specific inhibitor, DEVD-CHO inhibited caspase-3-like activity in AtCB2Cherry and AtCB3Cherry and was slightly more efficient than LVK-CHO. Surprisingly, although caspase-1-like and caspase-3-like activity is not detected in human cathepsin B, both YVAD-CHO and DEVD-CHO suppressed its cathepsin B-like activity (RRase) efficiently.

As stated previously in chapter 3, *Arabidopsis* cathepsin B partially purified from seedlings undergoing PCD can be labelled using biotin-DEVD-FMK. Similarly, AtCB2Cherry and AtCB3Cherry activated by pepsin were labelled and migrated at approx. 37kDa on protein blot (Fig 5.8). This result with recombinant AtCathB-2 and AtCathB-3 supports clearly that *Arabidopsis* cathepsin B correspond to the caspase-3-like proteases that are labelled by the biotinylated caspase-3 inhibitor in extracts.

Table 5.1 Effect of inhibitors on proteolytic activity of AtCB2Cherry, AtCB3Cherry and human cathB

Inhibitors	Concentration	Remained Activity (%)		
		AtCB2Cherry(DEVDase)	AtCB3Cherry(DEVDase)	human cathB (RRase)
Control	**N/A**	100 ±2.465	100 ±1	100 ±0.816
FA-FMK	**100µM**	47.901 ±2.184	39.894 ±3.381	0
LVK-CHO	**100µM**	19.68 ±2.511	17.891 ±1.584	0
CA-074	**1mM**	10.127 ±2.338	10.748 ±9.896	0
Leupeptin	**100µM**	36.624 ±3.562	51.685 ±2.018	1.354 ±0.193
Pepstatin	**100µM**	45.869 ±2.519	49.036 ±3.047	80.112 ±1.226
PMSF	**100µM**	97.732 ±3.972	97.926 ±2.034	73.392 ±5.712
YVAD-CHO	**100µM**	47.859 ±1.789	39.841 ±2.017	8.366 ±0.246
DEVD-CHO	**100µM**	18.548 ±1.943	17.736 ±1.831	18.667 ±1.699
VEID-CHO	**100µM**	64.318 ±3.266	65.003 ±2.012	67.675 ±5.421
IETD-CHO	**100µM**	65.595 ±2.872	52.414 ±2.116	75.623 ±1.255

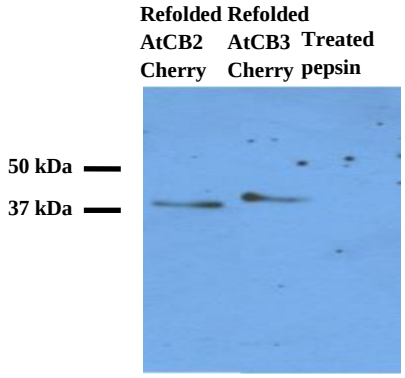

Fig 5.8 Labelling of refolded AtCB2Cherry and AtCB3Cherry expressed in *E.coli* using biotinylated caspase-3 inhibitor. Denatured, purified and refolded recombinant AtCB2Cherry and AtCB3Cherry were produced and labelled with 10 µM biotin-DEVD-FMK at 30 ℃ for 1h as described in chapter 2. DTT was added to a final concentration of 6mM. The same concentration of pepsin used to activate refolded recombinant AtCB2Cherry and AtCB3Cherry was also labelled as a control after same treatment. Following labelling, 15 µl proteins were separated on 15% SDS-PAGE and transferred to a membrane. After incubation with streptavidin-HRP, the biotinylated proteins were detected using a mixture of supersignal west pico chemiluminescent substrate (4/5 vol) and west femto chemiluminescent substrate (1/5 vol).

5.2.3 Expression of recombinant AtCathB-2 and AtCathB-3 in insect cell

5.2.3.1 Folding competence analysis of truncated AtCathB-3 variants expressed in insect cell using BacMagic baculovirus expression kit

Although expression of recombinant AtCathB-2 and AtCathB-3 in *E.coli* demonstrates their caspase-3-like activity, high yield and native purified recombinant AtCathB is essential for further research. It was therefore decided to produce AtCathB-2 and AtCathB-3 in a baculovirus-insect cell expression system.

In addition to its function in activity inhibition, the prodomain region in cathepsins and some other cysteine protease, i.e papain, acts as a chaperone to facilliate correct folding (Traut, 1994; Hasnain *et al.*, 1992; Muntener *et al.*, 2005). In human cathepsin B expression in insect cell, the first α-helix (Asp11-Arg20) has been demonstrated to be nesseccary for inhibition but not indispensible for its correct folding. The first β-sheet (Trp24-Ala26) is essential for correct folding since Trp24 interacts with Tyr183, Tyr188 and Phe180 to anchor prodomain on the enzyme surface (Turk *et al.* 1996; Muntener *et al.* 2005). Whereas, the possible auxiliary function of C terminal prodomain in correct folding has not been reported yet.

Secondary struture of AtCathB-2 and AtCathB-3 were predicted using PSI-PRED server v3.0 (Jones 1999). As shown in Fig 5.9, α-helix 1, 2 and β-sheet 1 found in the human cathepsin B secondary structure are conserved in AtCathB-2 and AtCathB-3. Another α-helix upstream to α-helix 1 was predicted in AtCathB and was named α-helix 0.

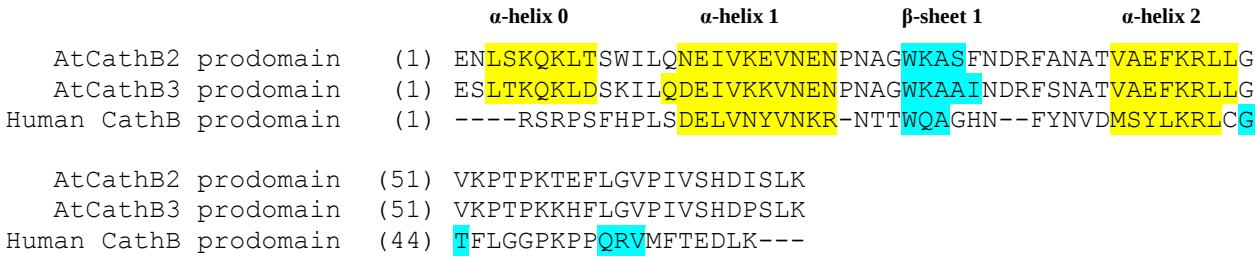

Fig 5.9 Prediction of secondary structure of prodomain in AtCathB-2 and AtCathB-3. Protein sequences of prodomain in AtCathB-2, AtCathB-3 and human CathB were aligned using Align X programme in vector NTI advanced 11. Secondary structures of prodomain in AtCathB2 and AtCathB3 were predicted using PSI-PRED v3.0 (Jones 1999): α-helices are highlighted in yellow and β-sheets are highlighted in cyan.

To investigate the function of prodomain in AtCathB in folding, two more constructs of AtCathB-3 with different truncation were produced and expressed in insect cell (Fig 5.10). AtCB3Cherry possesses same sequence as the construct used in recombinant eukaryotic expression. N-terminal prodomain of AtCB3tPro is truncated before α-helix 1 while whole C-terminal prodomain is clipped. AtCB3m contains the catalytic unit of AtCathB-3 only. The corresponding DNA fragments were amplified and cloned into the pAcGP67A transfer vector in order to produce plasmids pAcGPAtCB3Cherry, pAcGPAtCBtPro and pAcGPAtCB3m respectively. The transfer vectors containing the target genes were co-transfected into insect cell with linarized baculovirus DNA BacMagic-3. Recombinant baculovirus was selected and used to infect insect cell for expression.

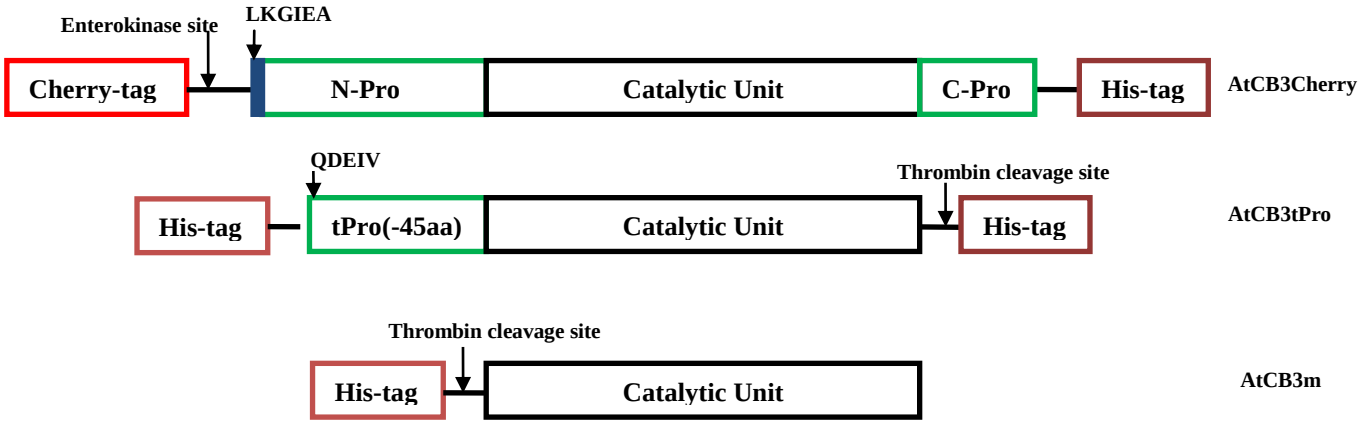

Fig 5.10 Schematic diagram of various truncated AtCathB2 and AtCathB3 forms expressed in insect cells. AtCB3Cherry contains a C terminal cherry tag, full prodomain, full catalytic unit and N terminal 6× His-tag. AtCB3tPro contains a truncated N-terminal prodomain with 45 amino acid residues deleted and no C terminal prodomain. AtCB3m contains the full catalytic unit only. Enterokinase site and thrombin cleavage site are also indicated.

The culture time after baculovirus infection (48h and 72h) and baculovirus MOIs (2 µl to 600 µl) were optimized to obtain the maximum recombinant protein yield with each of the three constructs (Fig 5.11, Fig 5.12, Fig 5.13, and some data not shown). A culture time of 48h and 100 µl baculovirus suspension from a high titre stock were proved to be the optimal expression conditions since longer propagation and higher titre of the baculovirus did impair the secretory pathway in the host cells.

Soluble AtCB3Cherry was demonstrated by mass spectrometry to be secreted into culture medium but the protein could not be detected using anti-His tag antibody and western blot analysis (Fig 5.11). The size of soluble AtCB3Cherry (approx. 37kDa) was smaller than the full length AtCathB-3 prediction (52.3kDa), suggesting that the C-terminal prodomain of AtCB3Cherry is processed by a virus encoding proteases or by autoproteolysis. AtCB3tPro (Fig 5.12) and AtCB3m (Fig 5.13) were expressed in the cell culture pellets only and were not detectable in culture medium, indicating they are unfolded or misfolded. Therefore it seemed that lacking the prodomain region as a folding chaperone caused misfolding of AtCB3tPro and AtCB3m which were retained in the ER and could not enter the secretory pathway.

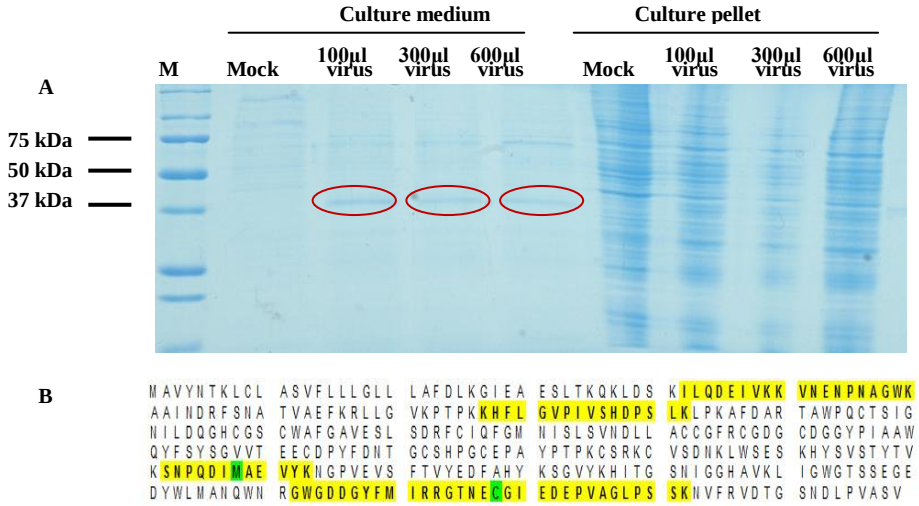

Fig 5.11 AtCB3Cherry expression test in Hi5 insect cells with varying baculovirus MOIs. Hi5 cells ($1.5x10^6$) were infected with varying volume (100µl, 300µl and 600µl) of recombinant virus encoding AtCB3Cherry for 48h in a 28℃ CO_2 incubator. Culture medium and pellet were separated by a 2,000g centrifugation at 4℃ for 10min. The pellet was lysed 10min at 90 ℃ boiling with SDS-loading buffer. (A) Culture medium and lysed pellet (15µl each) were separated using 15% SDS-PAGE and stained using G250 coomassie brilliant blue; (B) Circled bands were analysed using LC-MS/MS and identified as Arabidopsis cathepsin B, the peptides of AtCathB detected are highlighted in yellow background.

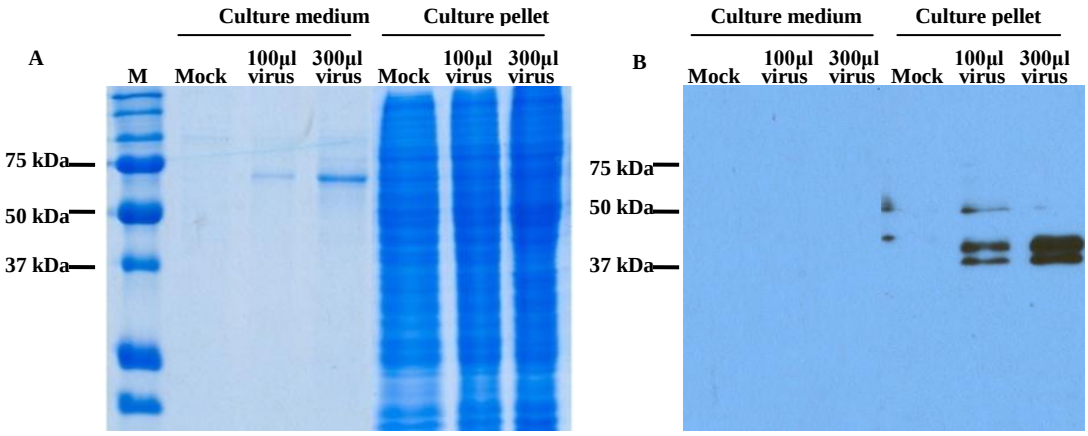

Fig 5.12 AtCB3tPro expression test in Hi5 insect cell with varying baculovirus MOIs. Hi5 cells ($1.5x10^6$) were infected with varying volume (100µl and 300 µl) of recombinant virus encoding AtCB3tPro 48h in a 28℃ CO_2 incubator. Culture medium and pellet were separated by a 2,000g centrifugation at 4℃ for 10min. The pellet was lysed 10min at 90 ℃ boiling with SDS-loading buffer. (A) Culture medium and lysed pellet (15µl each) were separated using 15% SDS-PAGE and stained using G250 coomassie brilliant blue; (B) Anti-His tag western blot of culture medium and lysed pellet was carried out as described in chapter 2.

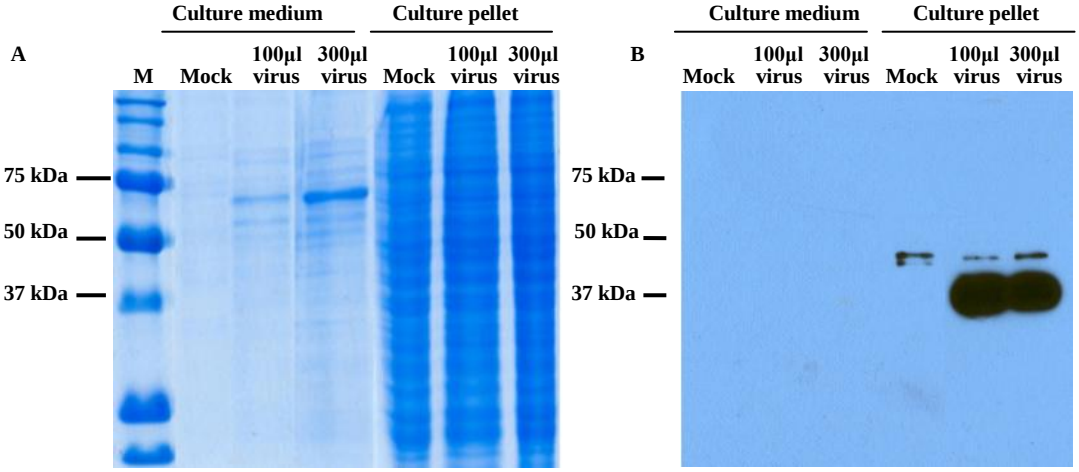

Fig 5.13 AtCB3m expression test in Hi5 insect cell with varying baculovirus MOIs. Hi5 cells ($1.5x10^6$) were infected with varying volume (100µl and 300 µl) of recombinant virus encoding AtCB3m 48h in a 28 ℃ CO_2 incubator. Culture medium and pellet were separated by a 2,000g centrifugation at 4 ℃ for 10min. The pellet was lysed 10min at 90 ℃ boiling with SDS-loading buffer. (A) Culture medium and lysed pellet (15 µl each) were separated using 15% SDS-PAGE and stained using G250 coomassie brilliant blue; (B) Anti-His tag western blot of culture medium and lysed pellet was carried out as described in chapter 2.

5.2.3.2 Expression of AtCB2Cherry and AtCB3Cherry in insect cell using OET baculovirus expression kit (viral genome with a cathepsins deletion)

Proteolysis of target protein by viral cathepsins is a common challenge in insect cell expression system. *In vivo*, human procathepsin B is matured by cathepsin D and L. Similar proteolysis may occur in AtCB3Cherry expression using BacMagic kit (Fig 5.11). We postulated the truncation observed in previous experiments was due to viral cathepsins. Consequently, recombinant AtCB2Cherry and AtCB3Cherry were expressed in insect cell using a new baculovirus strain: OET strain, in which cathepsins and chitinase are deleted from viral genome.

Optimization of the expression condition is also carried out with regards to culture time (48h and 72h),various virus MOIs (2µl to 100µl) and different insect cell lines (Sf9 and Hi5) for many times (Fig 5.14 and Fig 5.15, and some data not shown). As shown in Fig 5.14 and Fig 5.15, soluble recombinant AtCB2Cherry (predicted Mw=52.30kDa) and AtCB3Cherry (predicted Mw=51.54kDa) were produced and secreted into the culture medium. In contrast to AtCB3Cherry produced by the BacMagic baculovirus kit, the newly expressed AtCB2Cherry and AtCB3Cherry could be probed detected using anti-His tag antibody and western blot analysis at the correct predicted size. This result

demonstrated that AtCB3Cherry proteolysis in the insect cell expression system should be ascribed to the processing by viral cathepsins. Production of recombinant animal procathepsin B using eukaryotic expression system was reported to be challenging because of the autocatalytic processing. Cleavage site mutations had to be introduced in order to avoid maturation (Mach *et al.* 1994). Here we established a reliable approach for procathepsin B expression using the appropriate combination of insect cell and baculovirus.

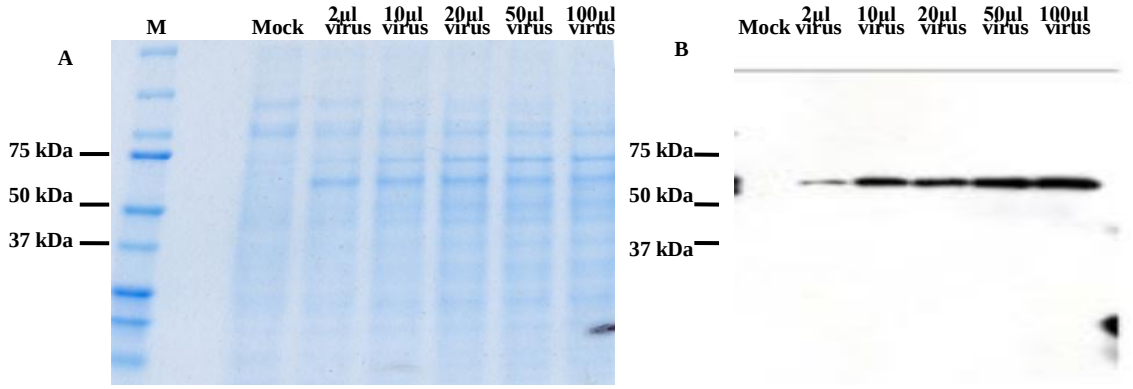

Fig 5.14 AtCB2Cherry expression test in Hi5 insect cell line with varying cathepsins deletion baculovirus MOIs. Hi5 cells ($1.5x10^6$) were infected with varying volume (2µl to 100µl) of recombinant cathepsins depletion virus encoding AtCB2Cherry for 48h in a 28℃ CO_2 incubator. Culture medium was collected by 2,000g centrifugation at 4℃ for 10min. (A) Culture medium (15µl each) were separated using 15% SDS-PAGE and stained using G250 coomassie brilliant blue; (B) Anti-His tag western blot of culture medium was carried out as described in chapter 2.

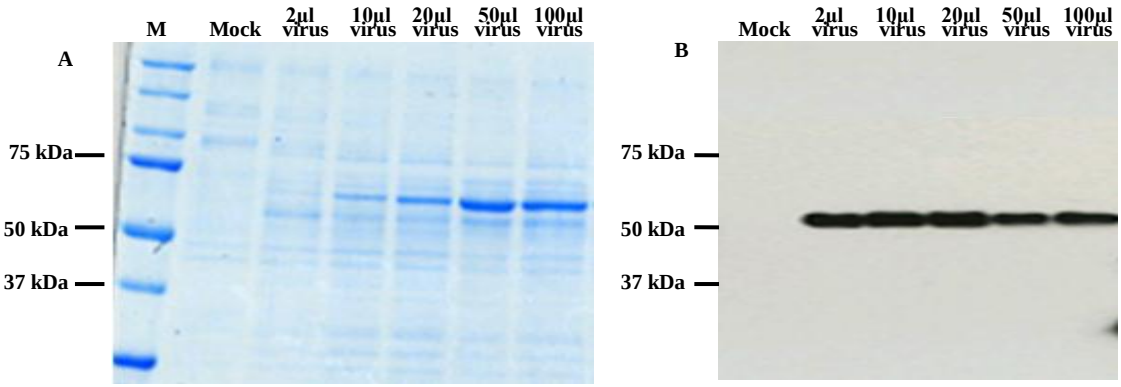

Fig 5.15 AtCB3Cherry expression test in Hi5 insect cell line with varying cathepsins deletion baculovirus MOIs. Hi5 cells ($1.5x10^6$) were infected with varying volume (2µl to 100µl) of recombinant cathepsins depletion virus encoding AtCB3Cherry for 48h in a 28℃ CO_2 incubator. Culture medium was collected by 2,000g centrifugation at 4℃ for 10min. (A) Culture medium (15µl each) were separated using 15% SDS-PAGE and stained using G250 coomassie brilliant blue; (B) Anti-His tag western blot of culture medium was carried out as described in chapter 2.

5.2.3.3 Purification of AtCB2Cherry and AtCB3Cherry expressed in insect cell

Purification of AtCB2Cherry expressed in insect cell using OET baculovirus expression kit

Since AtCB2Cherry contains a 6×His-tag, purification was carried out using TALON cobalt resins. Factors which are important for the purity such as resins amount, imidazole concentration in bind/wash buffer were all carefully optimized. As shown in Fig 5.16, intact AtCB2Cherry was purified and kept in a buffer at neutral pH to avoid autocatalytic processing.

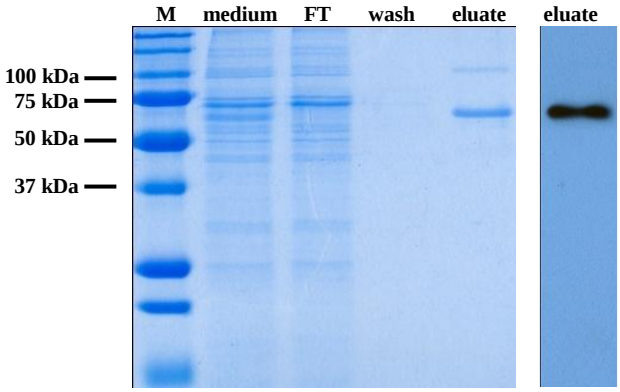

Fig 5.16 AtCB2Cherry expressed in insect cell and purified using TALON cobalt affinity resins. Culture medium of AtCB2Cherry producing cells was mixed with TALON cobalt resins and purified as described in chapter 2. 15µl flow through (FT), wash and elution fractions were loaded and separated on 12% SDS-PAGE and visualised using G250 coomassie blue staining. Anti-His tag western blot analysis was carried out as described in chapter 2.

Purification of AtCB3Cherry expressed in insect cell using BacMagic baculovirus expression kit

Lacking the C-terminal 6×His-tag, the purification of AtCB3Cherry produced using BacMagic baculovirus in insect cell expression system was more challenging. A combination of cation exchange chromatography and FPLC miniS chromatography resulted in the isolation of AtCB3Cherry to near homogeneity (Fig 5.18 B). As discussed previously, clipping of AtCB3Cherry during expression is due to viral cathepsins. However, further cleavage due to autocatalytic processing occurred during the purification since all buffers used were acidic (Fig 5.18).

Culture medium containing truncated AtCB3Cherry was acidified to pH 4.5 and loaded into HiTrap SP FF cation exchanger. The theoretical pI of AtCB3Cherry is predicted as 5.65 using the Isotopident programme at the ExPASy proteomic server. When acidified to pH 4.5, molecules of AtCB3Cherry will carry positive net charge and bind to the SP FF cation exchanger. In this way, some contaminants i.e. nucleic acid, lipids, sugars and vitamins from culture medium can be eliminated and the target protein can be partially purified. A stepped NaCl gradient (0.1M to 1.0M) in the elution buffer was tested. As shown in Fig 5.17, the target protein could not be eluted off at concentrations lower than 0.6M NaCl and completely eluted off in elution buffer containing 0.7M NaCl. Thus an elution buffer containing 0.7M NaCl was used for SP FF cation exchanger purification. A clearer eluate with both a contaminating virus protein (higher band) and AtCB3Cherry (lower band) were visualised in Fig 5.18 A. It seemed that during SP FF cation exchanger purification, the target protein loss was negligible but a slight activation occurred in the acidic environment used even though the purification was carried out at 4℃ and for a short period of time. The N-terminal sequence of the main AtCB3Cherry form was determined by the proteomic facility at the University of Leeds and found to be 'GIEAE'. The HiTrap elution buffer contained 700 mM NaCl. Thus the eluate from cation exchanger column had to be desalted prior to miniS FPLC chromatography. Unfortunately, the target protein was lost when desalting using dialysis, possibly because it came out of solution (data not shown).

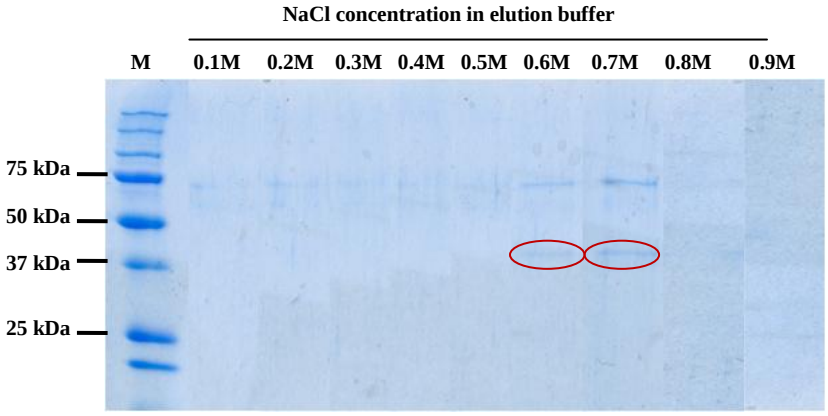

Fig 5.17 AtCB2Cherry expressed in insect cell purified from HiTrap SP FF cation exchanger with varying NaCl concentration in elution buffer. Culture medium of AtCB2Cherry was acidified to pH4.5 using HCl and purified using SP FF cation exchanger as described in chapter 2. Elution was carried out with the elution buffer containing a range of NaCl concentrations. 15µl elution fractions were separated on 15% SDS-PAGE and visualised using G250 coomassie blue staining. The lower bands circled are recombinant AtCB2Cherry.

As an alternative to dialysis, the eluate from SP FF cation exchanger was diluted twice using a 0.05M sodium phosphate buffer pH4.5, thus NaCl concentration was reduced to 0.35 M. Subsequently, the eluate was loaded onto a miniS FPLC column. During the miniS FPLC, two peaks were recorded representing the two bands visualised on the gel in Fig 5.18A. Fractions were collected and protein concentrations as well as caspase-3-like activity were analysed (data not shown). As shown in Fig 5.18B, two lower bands (AtCB3C-α and AtCB3C-β) were visualised after the FPLC purification and both were identified as AtCathB-3 (Fig 5.18C) using mass spectrometry identification. This can be explained by a rapid autocatalytic processing of AtCathB-3 when the sample was analysed in the acidic pH environment at room temperature.

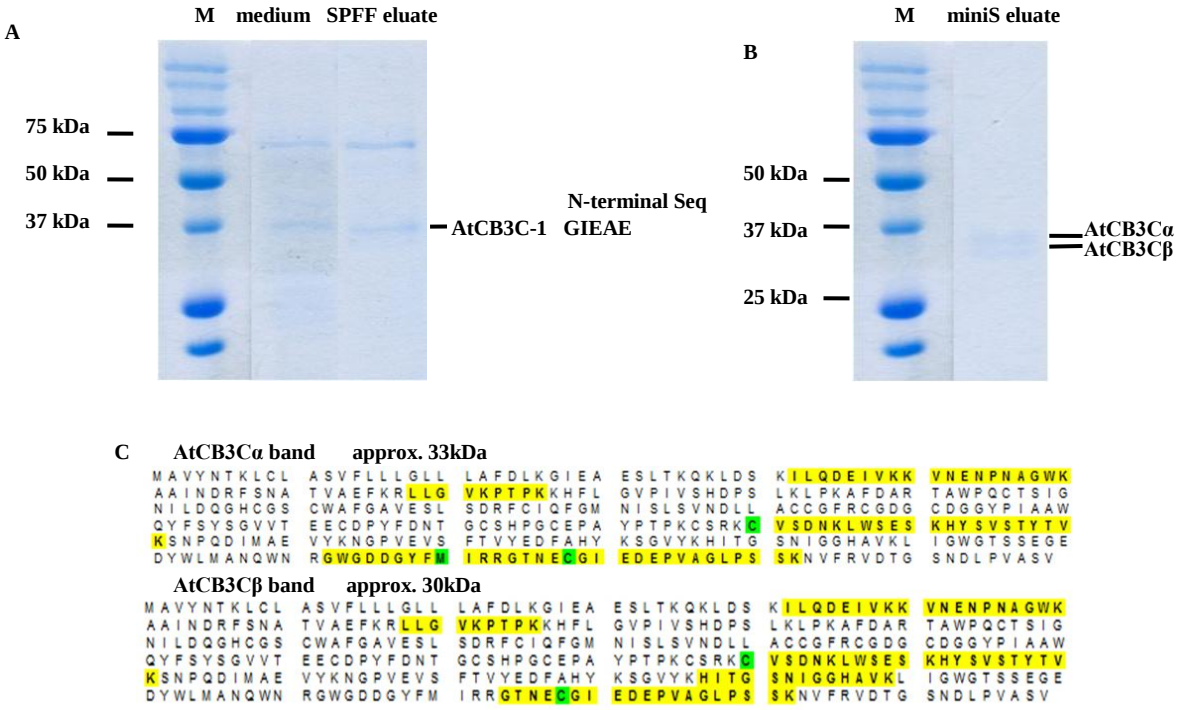

Fig 5.18 AtCB2Cherry expressed in insect cell and purified using HiTrap SP FF cation exchanger and miniS FPLC. (A) The culture medium of AtCB2Cherry was acidified to pH 4.5 using HCl and purified primarily using a SP FF cation exchanger as described in chapter 2. The N-terminal sequence of the 37kDa band was obtained; (B) The purified fraction from SP FF cation exchanger was loaded onto a miniS FPLC column and purified as described in chapter 2. 15µl of proteins from (A) and (B) were separated using 15% SDS-PAGE and visualised using G250 coomassie blue staining; (C) Band AtCB3Cα and AtCB3Cβ obtained from miniS purification were analysed using LC-MS/MS and both identified as AtCathB-3. Specific peptides of AtCathB-3 detected in LC-MS/MS are highlighted in yellow.

Autocatalytic processing analysis of AtCB2Cherry and AtCB3Cherry

In vivo, the activation of human procathepsin B is ascribed to both cathepsin D, L and some other proteases processing and to autocatalytic processing. Since endogenous inhibitors for human cathepsin B is not efficient enough, the cleaved prodomain is then involved in an intermolecular inhibitory mechanism. *In vitro*, pepsin is frequently used in procathepsin B activation by removing the prodomain. In this thesis, refolded AtCB2Cherry and AtCB3Cherry expressed from *E.coli* were also activated using a pepsin treatment while an autocatalytic processing was not observed in that expression system. AtCB2Cherry and AtCB3Cherry expressed in insect cell using cathepsins-deleted baculovirus are believed to be unprocessed in culture medium and after purification (Fig 5.14 and Fig 5.15). However, the unprocessed procathepsin B can readily be labelled by biotin-DEVD-FMK in culture medium (data not shown). It is therefore suggested that AtCathB with its full prodomain displayed caspase-3-like proteolytic activity. In addition, cathepsin B-like activity was also detectable in purified AtCB2Cherry before activation (Fig 5.19 C).

Autoproteolysis and activation of intact AtCB2Cherry was consequently studied at different pH, incubation temperature and incubation time. In neutral pH (pH 7), purified AtCB2Cherry could not perform an autocatalytic processing whatever the incubation time or temperature. At acidic pH (pH 5.5) and 20℃, purified AtCB2Cherry was degraded after 12h incubation with a complete loss of proteolytic activity (data not shown). Analysis of AtCB2Cherry autocatalytic processing was therefore carried out at pH 5.5 and at 4℃. As shown in Fig 5.19 A, AtCB2Cherry was clipped into three bands after overnight incubation. The 6×His-tag was still detectable for the three bands, indicating that the autocatalytic processing occurred at the N-terminus in this stage. After 7d at 4℃, two bands (AtCB2C-1 and AtCB2C-2) were visualised on gel but only the upper one (AtCB2C-1) was detectable by anti-His tag western blot analysis, indicating that the C-terminus was clipped in low band (AtCB2C-2). After a 100-fold concentrating, the lower band (AtCB2C-2) increased in intensity because of further autocatalytic processing during the concentration process. Although it has been reported that human procathepsin B autoproteolysis is concentration-independent (Mach *et al.*, 1994), the result here does not support this point of view. To investigate the sequence of the mature AtCathB-2, N-terminal amino acid residue sequencing and MALDI-TOF were applied on the concentrated AtCB2Cherry. Although AtCB2C-1 and AtCB2C-2 present a different size

using SDS-PAGE, the same N-terminal sequence was obtained as Gly-Ile-Ala-Ala-Glu. This suggested that between these two forms, autoproteolytic processing occurred only at the C-terminus. As indicated in Fig 5.19 C, the proteolytic activities, especially the caspase-3-like activity, increased significantly after activation.

We found that AtCB3Cherry expressed in insect cell using BacMagic kit was truncated both at the N- and C- terminus to give AtCB3C-1 (Fig 5.18A). The N-terminal sequence of AtCB3C-1 was found to be Gly-Ile-Glu-Ala-Glu, which is the same cleavage site as AtCB2Cherry after autocatalysis. This therefore implied that out prediction of the prodomain cleavage site approx. 120 amino acid residues downstream of Gly-Ile-Ala-Ala-Glu was incorrect.

In order to try to calculate the C-terminal cleavage site we used a MALDI-TOF approach on the intact protein. The rational is that if the N-terminus is known, then and accurate mass generated by MALDI-TOF should allow us to calculate the C terminus cleavage using the known full sequence. One peak was detected at 24490.250 Da possible for AtCB2C-2 and one peak at 30353.754 Da was possible for AtCB3C-1. However, such MALDI-TOF results do not agree with their Mw estimated on gel and the fixed N-terminus sequence obtained. The calculation of an accurate C-terminus was therefore impossible. Failure of the MALDI-TOF approach may be explained by possible protein degradation occurring during the sample manipulation at room temperature before analysis. Consistent with this explanation, no protein was visualised using SDS-PAGE in the unused sample returned back from mass spectrometry facility.

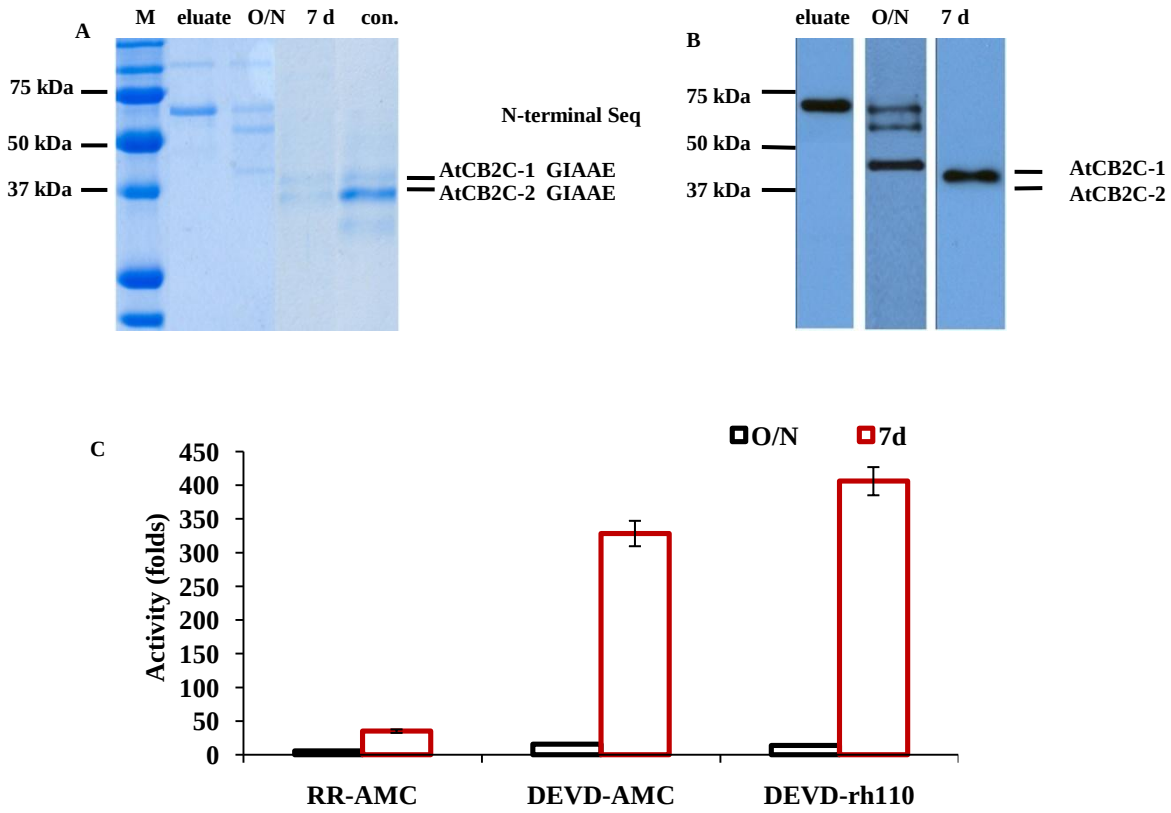

Fig 5.19 Self-processing of purified AtCB2Cherry. AtCB2Cherry expressed in insect cell was purified using TALON cobalt resins as described in chapter 2. The column eluate was acidified to pH 5.5 using HCl and incubated at 4℃ for self-processing. Overnight self-processing fraction (O/N) and 7d self-processing fraction (7d) were collected. In addition, the 7d fraction was also concentrated by 100 folds using a microcon tube. (A) 15µl unprocessed, overnight and 7d self-processing fractions were separated on 15% SDS-PAGE and visualised using G250 coomassie blue staining; (B) Anti-His tag western blot of unprocessed eluate, overnight and 7d self-processing fractions were carried out as describe in chapter 2; (C) Proteolytic activity of unprocessed eluate, overnight and 7d self-processing fractions were assayed using RR-AMC, DEVD-AMC and DEVD-rhodamine110 respectively. Activity of the unprocessed eluate before self-activation was set as 1 fold. Error bars indicate ±S.D. value for triplicates.

5.2.3.4 Proteolytic activity assay and kinetic measurements of AtCB2Cherry and AtCB3Cherry expressed in insect cell

AtCB2Cherry and AtCB3Cherry expressed in insect cell were purified to near homogeneity under native conditions as described in 5.3.2.3, therefore reliable proteolytic activity results can be obtained. High caspase-3-like and human cathepsin B-like activities as well as low caspase-1-like activity were detected while other caspase-like activities: caspase-6-like (VEIDase) and -8-like (IETDase) activities were absent in AtCB2Cherry and AtCB3Cherry expressed in insect cell. As shown in Fig 5. 20, AtCathB-2 presented a

higher proteolytic activity against RR-AMC (cathepsin B), AAN-AMC (legumain), DEVD-AMC (caspase-3), DEVD-rhodamine110 (caspase-3) substrates than AtCathB-3. It is consistent with our *in vivo* functional analysis results suggesting that AtCathB-2 plays a more important role than AtCathB-3 in PCD regulation. By contrast, AtCathB-3 possessed a higher caspase-1-like (YVADase) and papain-like (FRase) activities than AtCathB-2. Both of them displayed low papain-like (FRase), GRRase-like and legumain-like (AANase) activities, which were not detectable in refolded AtCathB expressed in *E.coli*. This result could be dependent on the function of N-glycosylation status of recombinant proteins, which is not provided in prokaryotic expression system.

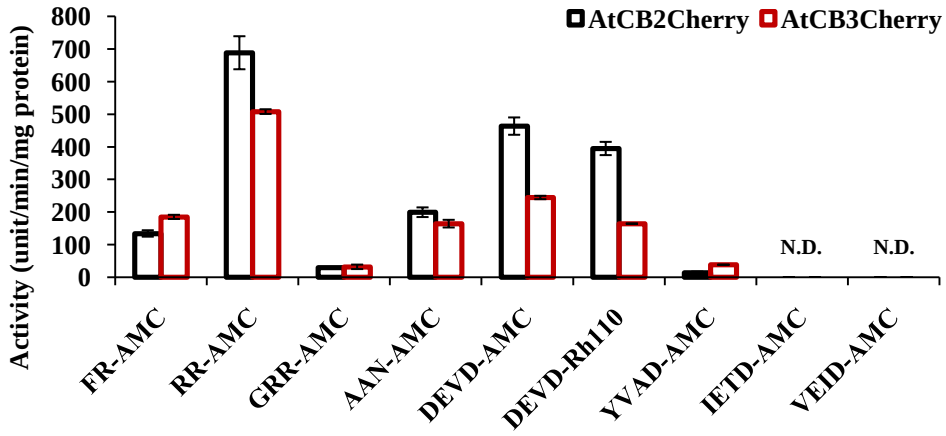

Fig 5.20 Proteolytic activity of recombinant AtCB2Cherry, AtCB3Cherry expressed in insect cell. Recombinant AtCB2Cherry and AtCB3Cherry were produced in insect cell and purified as describe in chapter 2. Proteolytic activity was assayed using RR-AMC (cathepsin B subsrate), FR-AMC (papain substrate), GRR-AMC, AAN-AMC (legumain substrate) and synthetic caspase substrates: YVAD-AMC, DEVD-AMC, DEVD-rhodamine110, IETD-AMC and VEID-AMC. Activity is given as fluorescence unit/min/mg protein. Error bars indicate ±S.D. value for triplicates. N.D. means corresponding proteolytic activity is not detected.

The inhibition profile of AtCB2Cherry and AtCB3Cherry with regards to their caspase-3-like activity against DVED-rhodamine110 is shown in table 5.2. Human cathepsin B selective inhibitors, FA-FMK, LVK-CHO and CA-074 completely suppressed caspase-3-like activity in AtCathB-2 and AtCathB-3. Inhibitors of plant and animal 20S proteasome, ac-PnLD-CHO and lactone suppressed caspase-3-like activity presented by AtCathB-2 by approx. 65% and 75% respectively. Inhibiting both cathepsin B and proteasome is probably the reason why ac-PnLD-CHO and lactone added to *Arabidopsis* protein extracts supressed caspase-3-like activity more efficiently than CA-074. As shown in Fig 5.21,

biotinylation of recombinant AtCathB using biotin-DEVD-FMK is abolished by both CA-074 and LVK-CHO pre-incubation. This is consistent with CA-074 and LVK-CHO suppression of the biotinylation profile in *Arabidopsis* protein extracts.

Table 5.2 Effect of inhibitors on AtCB2Cherry and AtCB3Cherry expressed in insect cell

Inhibitors	Concentration	Remained Activity (%)	
		AtCB2Cherry	AtCB3Cherry
Control	**N/A**	100 ±1.245	100 ±4.322
FA-FMK	**100µM**	0.216 ±0.110	0
LVK-CHO	**100µM**	0	0
CA-074	**1mM**	0	0
YVAD-CHO	**100µM**	39.897 ±1.772	43.349 ±0.630
DEVD-CHO	**100µM**	0.610 ±0.399	0.340 ±0.005
VEID-CHO	**100µM**	40.199 ±0.122	No data
Lactone	**100µM**	24.738 ±2.612	No data
PnLD-CHO	**100 µM**	35.466 ±7.812	No data

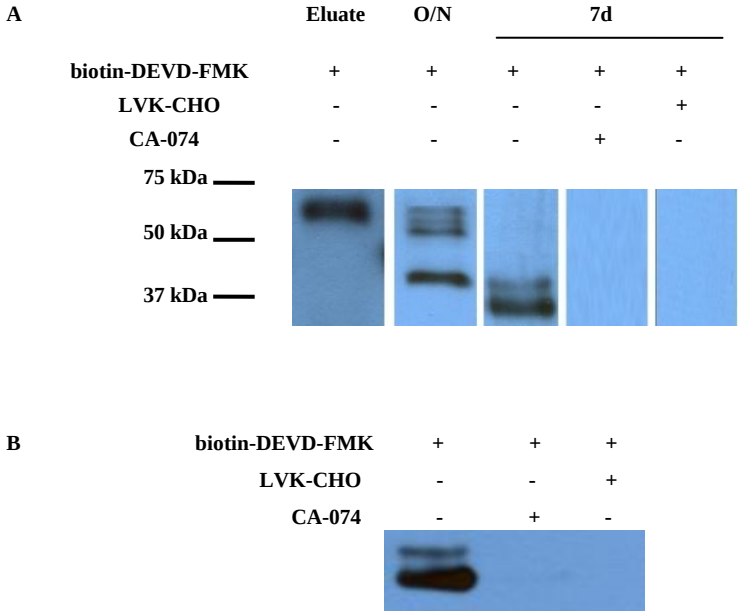

Fig 5.21 Biotinylation of AtCB2Cherry and AtCB3Cherry expressed in insect cell. Purified recombinant AtCB2Cherry and AtCB3Cherry were produced and labelled with 10 µM biotin-DEVD-FMK at 30 ℃ for 1h as described in chapter 2. DTT was added to a final concentration of 6mM. Fractions were also pre-incubated with 100 µM LVK-CHO or 1mM CA-074 at 30 ℃ for 30min before labelling. Following labelling, biotinylated proteins were separated on 15% SDS-PAGE and transferred to a membrane. After incubation with streptavidin-HRP, the biotinylated proteins were detected using a mixture of supersignal west pico chemiluminescent substrate (4/5 vol) and west femto chemiluminescent substrate (1/5 vol). (A) Biotinylation of AtCB2Cherry unprocessed fraction, overnight self-processing fraction (O/N) and 7d self-processing fraction. Effect of a pre-incubation with inhibitors LVK-CHO or CA-074 on 7d self-processing fraction labelling was also illustrated. (B) Biotinylation of AtCB3Cherry purified fraction from miniS FPLC. Effect of a pre-incubation with inhibitors LVK-CHO or CA-074 on 7d self-processing fraction labelling was also illustrated.

The Michaelis constant (Km) is defined as the substrate concentration required for 1/2 of the maximum catalytic reaction velocity, indicating the kinetic property of a specific enzyme for a specific substrate. Km and Vmax of activated recombinant AtCathB-2 was calculated using varying caspase-3 substrate (DEVD-AMC) concentrations and the software EXCEL solver as described in Fig 5.22. The Km of recombinant AtCathB-2 was 11.8 µM and Vmax was 69.1unit/min against DEVD-AMC substrate. As reported in the literature, Km of human caspase-3 against DEVD-AMC is 11 µM (Stennicke & Salvesen, 1999). This result shows that *Arabidopsis* cathepsin B share similar kinetic property and catalytic capacity against DEVD substrate as human caspase-3. Thus the association between *Arabidopsis* cathepsin B and caspase-3 like activity is finally confirmed.

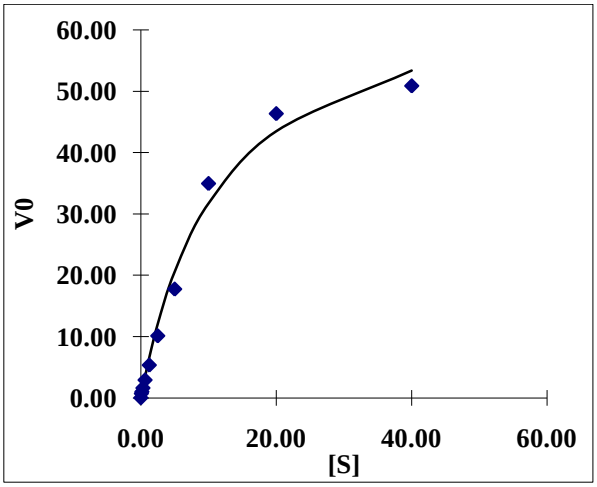

Fig 5.22 Km and Vmax of AtCB2Cherry against DEVD-AMC. Proteolytic activity assay of self-processed recombinant AtCB2Cherry expressed in insect cell was carried out using varying substrate concentrations from 0.5 µM to 100 µM. Km and Vmax were calculated using Microsoft Excel solver.

5.2.4 Preliminary characterization of *Arabidopsis* cathepsin B *in vivo* substrate

The availability of large quantities of activated recombinant AtCathB open the door to various experiments aimed at identifying *in vivo* substrates. Diagonal SDS-PAGE is a simple approach that has been applied to identify caspase substrates (Shao *et al.*, 2007). The rational is to digest whole protein extracts with a recombinant protease and identify some of the cleaved proteins by comparing migration profiles of the digested sample and of a mock sample using SDS-PAGE. The principle is described in Fig 5.23A. Total proteins extracts are separated using 2D gels where Mw is the parameter used for both dimensions. This results in the control protein samples running diagonally across the gel. If a protease is added to the gel after the first dimension, cleaved protein fragments will run below the diagonal in the second dimension. Any protein running below the diagonal can then be submitted to LC-MS/mass spectrometry analysis for identification. Putative substrates identified according to this approach need then to be confirmed with further *in vitro* and *in vivo* cleavage analysis.

This method was applied to identify *Arabidopsis* cathepsin B substrates. Total proteins extracted from wild type (Col-0) *Arabidopsis thaliana* seedlings were separated according to Mw using a first dimension SDS-PAGE (Fig 5.23 B). Two lanes containing the total protein separated on the first dimension gel were excised and incubated in 10ml

proteolytic activity assay buffer with or without 2mg active recombinant AtCathB-2 (purified AtCB2Cherry expressed in insect cell) at 30℃ overnight. After rinsing, each of the two lanes were boiled in SDS-loading buffer and placed on the second dimension gel. As shown in Fig 5.23 B and C, two protein spots were visualised by silver staining on the second dimension gel and both were excised and identified using mass spectrometry as fragment of the large chain of Ribulose-1, 5-bisphosphate carboxylase oxygenase (RuBisCO).

RuBisCO is an enzyme involved in the calvin cycle in photosynthesis and initiates inorganic carbon fixation. In plants, RuBisCO is regulated by several factors including ions, RuBisCO activase, ATP/ADP and stromal reduction/oxidation state, phosphate and CO_2 (Bowes, 1991). RuBisCO degradation is considered as a feature in senescence (Weidhase *et al.*, 1987; Ferreira & Davies, 1989). In addition, caspase-like proteases regulate RuBisCO is also reported in plant PCD (Coffeen & Wolpert, 2004). In victorin-induced cell death, proteolysis of RuBisCO large chain can be suppressed by caspase inhibitors and general cysteine protease inhibitors including cathepsin B inhibitor E64. Saspase-1 and saspase-2, serine proteases with caspase-like activity can cleave RubisCO except chloroplast-localised proteases (Coffeen & Wolpert, 2004). The results in Fig 5.23 indicates *Arabidopsis* cathepsin B can also cleave RuBisCO *in vivo* which is consistent with the proteolysis function of the first identified caspase-like protease in plants, saspase-1 and saspase-2 in victorin-induced PCD, suggesting RuBisCO degradation is involved in different types of PCD regulation pathway.

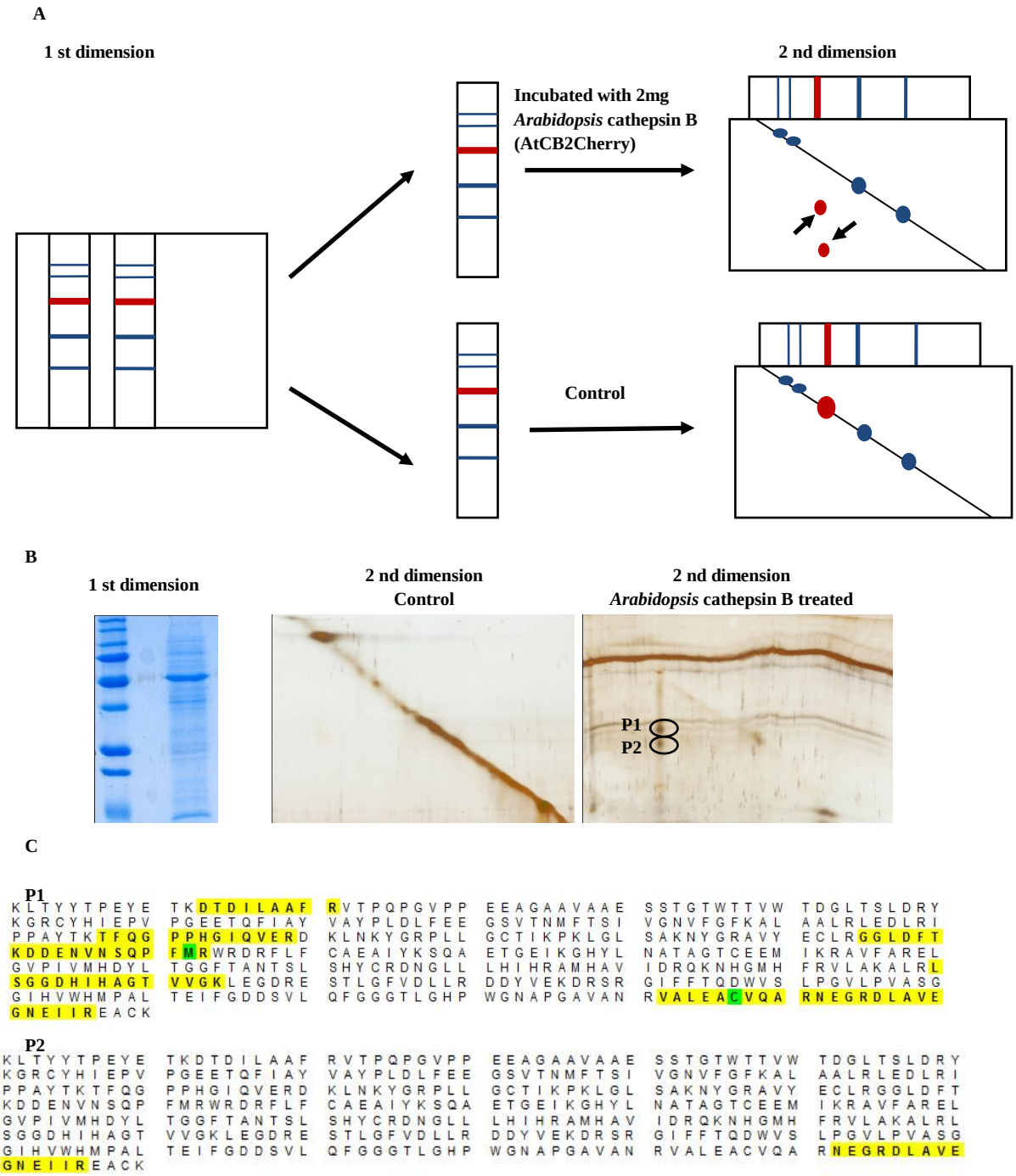

Fig 5.23 Identification of *Arabidopsis* cathepsin B *in vivo* substrate using diagonal SDS-PAGE. (A) Schematic diagram of the diagonal SDS-PAGE method. Total protein was extracted and separated on the first dimension SDS-PAGE. The lanes were excised and incubated with or without *Arabidopsis* cathepsin B at 30℃ overnight. The first dimension gel lane was then layed flat on the second dimension SDS-PAGE. The proteins cleaved by *Arabidopsis* cathepsin B are expected to drop under the diagonal and are excised for identification by LC-MS/MS. (B) Diagonal SDS-PAGE analysis for protein substrates of *Arabidopsis* cathespin B *in vivo* substrate as described in chapter 2. The first dimension gel was stained using coomassie blue and second dimension gel was stained using MS compatible silver staining. Two spots were detected under the diagonal and named as P1 and P2. (C) Marked point P1 and P2 were excised and analysed using LC-MS/MS and both identified as RuBisCO. RuBisCO peptides detected usingin LC-MS/MS are highlighted in yellow.

5.3 Discussion

Recombinant expression of human and animal cathepsin B has been reported in different systems including *E.coli*, yeast, insect cell and mammalian cell. Cathepsin B is synthesised *in vivo* as preprocathepsin B with a signal peptide and prodomains. It is known that the prodomains are essential for correct folding of recombinant cathepsin B (Muntener *et al.*, 2005). In one case the signal peptide domain was suspected to be harmful to the host cells resulting in unexpected culture cessation (Mach *et al.*, 1994). Cathepsin B expressed in prokaryotic system was found to accumulate in inclusion bodies and this made native purification approaches impossible. Human cathepsinB was however successfully renatured and found to be active by Kuhelj *et al.* (1995). An advantage of using a eukaryotic system for cathepsin B expression is the occurrence of post-translational modification. However, unglycosylated cathepsin B showed identical enzymatic activity to the glycosylated cathepsin B purified from rat liver (Hasnain *et al.*, 1992). Thus the expression of *Arabidopsis* cathepsin B in *E.coli* was not expected to lead to significant problems in the following enzymatic analysis. In this chapter, *E.coli* system and baculovirus insect cell expression system were both used to produce recombinant AtCathB-2 and AtCathB-3 using various constructs *in vitro*.

Both insoluble and soluble AtCathB-2 and AtCathB-3 with full prodomains were obtained when expressed in *E.coli*. However, native purification was impossible because the 6×His-tag was presumably buried in the protein structure. Purification using denaturing conditions with urea, followed by a careful refolding was relatively inefficient and lead to only a small amount of active AtCathB. In parallel, several variants of AtCathB-3 were expressed in insect cell to establish the most appropriate construct to obtain soluble forms. Similar to the results reported for human cathepsin B (Muntener *et al.*, 2005), the catalytic unit form of AtCathB-3 (AtCB3m) did not fold properly and remained insoluble. The results obtained with the construct AtCB3tPro indicated that the C-terminal prodomain acted as an important chaperone for proper folding. This had not been mentioned in previous studies of animal cathepsin B expression. Although the AtCB3Cherry contruct with full length prodomains led to a protein that folded and was secreted properly, an unexpected C-terminal processing probably due to baculoviral cathepsin D and L was observed. This removed the C-terminal 6×His-tag and made the affinity purification impossible. The problem was solved by using a new strain of virus with the genomic

cathepsin D and L deleted. This led to the production of soluble and full length AtCathB-2 and AtCathB-3 which were purified successfully and used for enzymatic activity studies.

Activation and maturation of procathepsin B is another important topic that we studied using recombinant expression. Two sequential processes are reported to be involved in procathepsin B maturation *in vivo*, namely proenzyme activation ascribed to other proteases i.e. cathepsin D, L, legumains etc. and autocatalysis (Turk *et al.*, 2009; Hara-Nishimura *et al.*, 2005). Refolded AtCathB-2 and AtCathB-3 produced from *E.coli* were matured using porcine pepsin before enzymatic assay. In this case, autocatalysis was not observed. By contrast, AtCathB-2 and AtCathB-3 expressed in insect cell were activated by autocatalysis in acidic pH resulting in a very significant elevation of proteolytic activity. We found that the autocatalysis started with the cleavage of the N-terminal prodomain as a first step and the C-terminal domain cleavage as a second step.

The most striking results of this chapter is the confirmation that refolded AtCathB-2 and -3 showed caspase-1-like, caspase-3-like and also human cathepsin B-like activity. Kinetic measurement confirmed similar enzymatic property between AtCathB-2 and human caspase-3 against the synthetic substrate DEVD-AMC. Both AtCathB can be labelling using a biotinylated caspase-3 inhibitor, which is consistent with cathepsin B being identified as an *Arabidopsis* caspase-3-like proteases. Similar proteolytic activity and labelling were detected in AtCathB-2 and -3 expressed in insect cells. However, some slight difference was observed in enzymatic activity and inhibition between recombinant AtCathB expressed in *E.coli* and insect cell. The simplest explanation is that the catalytic unit does not refold exactly to its native form after the denaturation by urea. Future enzymatic studies and substrate analysis should therefore be carried out using recombinant cathepsin B expressed in insect cells.

Unexpectedly, we found that *Arabidopsis* cathepsin B has both caspase-1 and caspase-3-like activity. This is contrary to the suggestion made by Hatsugai *et al.* (2004) that all caspase-1 activity in plants can be assigned to the proteases called vacuolar processing enzymes (VPE). As reviewed in chapter 1, caspase-1 plays a minor role and acts as an initiator while caspase-3 is the major executioner in caspase-dependent apoptotic pathway in animals. At this stage it is not clear which *Arabidopsis* cathepsin B activity (caspase-1-like or -3-like) is important for plant PCD regulation.

However, it cannot be concluded that cathepsin B acts as human caspase-3 in PCD regulation without the knowledge of its *in vivo* substrates. RuBisCO, the enzyme involved in photosynthesis was identified as a possible *in vivo* substrate for AtCath-3. Consistent with the reported proteolysis of RuBisCO during PCD induced by victorin (Coffeen & Wolpert, 2004), we therefore speculate that AtCathB-3 is involved in a chloroplast mediated PCD. The subcellular localisation of AtCathB-2 and -3 will be analysed in the following chapter and will contribute to a better elucidation of *Arabidopsis* cathepsin B function *in vivo*.

CHAPTER 6

SUBCELLULAR LOCALISATION OF *ARABIDOPSIS* CATHEPSIN B

6.1 Introduction

Cathepsin B in animals, as its name suggests, is a lysosomal protease. Subcellular localisation and trafficking research of cathepsin B in mouse cells revealed a transportation pathway from the ER to lysosomes through the Golgi apparatus and trans-Golgi networks. In addition, cathepsin B has been reported to be secreted in its active form into the extracellular spaces in FRTL-5 cells to contribute to the proteolysis in the thyroid (Linke *et al.*, 2002). In *Nicotiana benthamiana*, cathepsin B was found to be translocated in the apoplast and activated during the secretion but there was no evidence of vacuole localisation (Gilroy *et al.*, 2007).

Although the requirement of *Arabidopsi*s cathepsin B in PCD regulation and its caspase-3 like activity has been confirmed in chapter 4 and 5, the specific function of *Arabidopsis* cathepsin B in PCD regulatory pathways is still unknown. The knowledge of its subcellular localisation is essential for the elucidation of the function of cathepsin B in *Arabidopsis*. Using Cell eFP Browser in the BAR database (bar.utoronto.ca), AtCathB-2 was predicted to be localised in the cell wall, vacuole, chloroplast while AtCathB-3 was predicted to be localised in the cell wall, vacuole and the ER. In this chapter, the subcellular localisation of AtCathB-2 and AtCathB-3 was investigated. The full length ORF of *AtCathB-2* and *AtCathB-3* with 3' end stop codon deleted were fused to fluorescent protein genes and overexpressed in onion epidermal cells using biolistic particle bombardment. Biolistic transfection is a mechanical method that bombards subcellular-sized gold particles coated with DNA of interest into the targeted cells (O'Brien & Lummins, 2006). It was initially developed as a method to transfer foreign DNA into plants across cell walls and becoming applicable in a variety of cell and tissue types. Compared to the *Agrobacterium*-mediated *in planta* transformation method, biolistic bombardment in onion epidermal cells provides an easier method to express a gene of interest transiently for subcellular localisation research. In addition, onion epidermal cells have the advantage of enabling a better view GFP or YFP localisation under a fluorescent microscope since chloroplasts are absent.

6.2 Results

Since the deletion of the prodomain could lead to the misfolding of *Arabidopsis* cathepsin B in insect cells, the full length of *AtCathB-2* and *AtCathB-3* ORF without stop codon were amplified and introduced into pENTR1A vectors using the high-fidelity polymerase VELOCITY (Bioline, UK). After validation using DNA sequencing, *AtCathB-2* and *AtCathB-3* ORFs were fused with either the red fluorescent protein (RFP) or the yellow fluorescent protein (YFP) gene respectively using the gateway LR reactions. In the two constructs, the fused *AtCathB-2::mRFP* and *AtCathB-3::YFP* were both under the control of a 35S promoter. The two constructs were bombarded into onion epidermal cells and observed using a fluorescent microscope after 24. In order to label the cytoplasm, the construct of *AtCathB-2::mRFP* were co-expressed with same DNA amount of the vector pDH4-YFP containing expressing cytosolic YFP under the control of a 35S promoter.

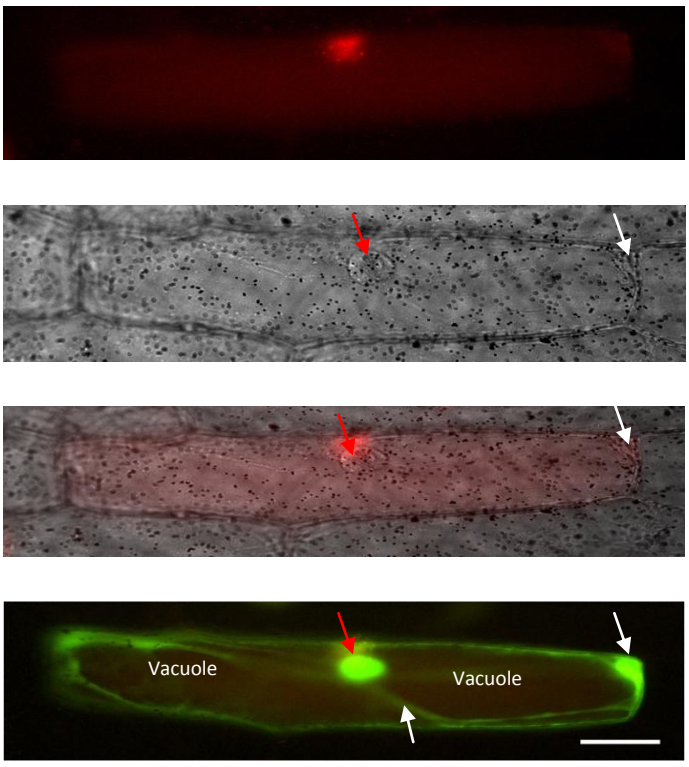

A. AtCathB-2::mRFP

B. The same onion epidermal cell under white light

C. Overlay

D. Co-expression of AtCathB-2::mRFP and cytosolic YFP

Fig 6.1 Subcellular localisation of AtCathB-2. *AtCathB-2::mRFP* and cytosolic *YFP* were co-expressed in onion epidermal cells using biolistic bombardment. Observation was carried out 24h post-bombardment under a fluorescent microscope. (A) The red fluorescence observed under the fluorescent microscopy is AtCathB-2::mRFP. (B) The same cell observed under white light. (C) Overlay of the pictures in (A) and (B). (D) Co-expression of AtCathB2::mRFP (red) and cytosolic YFP (green). Overlay in green and red channels. Nuclei are indicated by red arrows and the cytoplasm is indicated by white arrow. Vacuoles are also indicated. Scale bar is 100 μm.

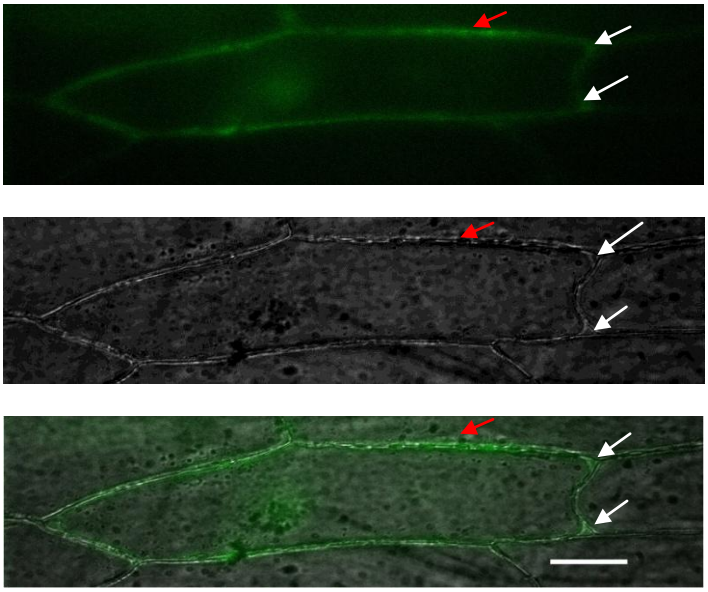

A. AtCathB-3::YFP

B. The same onion epidermal cell under white light

C. Overlay

Fig 6.2 Subcellular localisation of AtCathB-3. *AtCathB-3::YFP* was expressed in onion epidermal cells using biolistic bombardment. Observation was carried out 24h post-bombardment under a fluorescent microscope. (A) The green fluorescence observed under the fluorescent microscopy is AtCathB-3::YFP. (B) The same cell observed under white light. (C)Overlay of the pictures in (A) and (B).The cell wall is indicated by red arrow and the cytoplasm is indicated by white arrow. Scale bar is 100 μm.

As shown in Fig 6.1 (A) (B) and (C), a clear red fluorescence was observed in some of onion epidermal cells transfected with *AtCathB-2::mRFP* 24h post-bombardment. The expression of cytosolic YFP resulted in a green fluorescence localised in the cytoplasm and the nucleus. As shown in Fig 6.1 (A) (B) and (C), a clear red fluorescence was observed in some of onion epidermal cells transfected with *AtCathB-2::mRFP* 24h post-bombardment. The expression of cytosolic YFP resulted in a green fluorescence localised in the cytoplasm and the nucleus. Using the YFP fluorescence (Fig 6.1D) as a reference to define the localisation of the vacuole, we can deduce that AtCathB-2 is localised in the vacuole. In addition, the top right corner of the cell presented in Fig 6.1 corresponds to the cytoplasm only since the vacuole was retracted from the cell wall (Fig 6.1C) and the border between the cytoplasm and vacuole is clearly visible in the white light image (Fig 6.1B) .This area showed a red fluorescence, suggesting that AtCathB-2 is also localised in the cytoplasm. The strong red fluorescent point is above the cell under the observation. It does not correspond to an RFP signal in the cell. By contrast, after *AtCathB-3::YFP* transfection, a green fluorescence was observed in the cytoplasm and cell wall but was absent from the vacuole in onion epidermal cells (Fig 6.2). In Fig 6.2B, the retraction of the vacuole from the cell wall and the border between the cytoplasm and vacuole were

clearly visible. This result suggests that AtCathB-3 is localised in both the apoplast and cytoplasm but not in the vacuole.

6.3 Discussion

As published previously, human cathepsin B is localised in the lysosome and secreted into the extracellular space after activation while *Nicotiana* cathepsin B was reported only localised in the apoplast (Turk *et al.*, 2010; Gilroy *et al.*, 2007). The caspase-3-like activity in Chara cells was detected in the cytoplasm and vacuole using a fluorescent substrate Ac-DEVD-AMC micro-injection (Korthout *et al.*, 2000). However, we identified two different subcellular localisation patterns between two of the *Arabidopsis* cathepsin B paralogues.

AtCathB-3 has a higher similarity at the protein sequence level with NbCathB than AtCathB-1 and AtCathB-2 and is found to be localised in the cell wall and cytosol. It is consistent with the subcellur localisation of NbCathB (Gilroy *et al.*, 2007), suggesting that an extracellular function might be attributed to AtCathB-3. By contrast, AtCathB-2 was localised in the vacuole and cytoplasm, corresponding to the second localisation and translocation pathway as reported for animal cathepsin B. In the previous chapter, we postulated a distinct function for AtCathB-2 and AtCathB-3 in PCD regulation. The results obtained in subcellular localisation supports the postulated functional difference.

Because *Arabidopsis* cathepsin B has caspase-3-like activity and caspase-3 cleaves proteins which are important to nuclear integrity in animal apoptosis, we postulated that the proteolysis of these proteins in plants might be ascribed to cathepsin B. Furthermore, RuBisCo was identified as a possible substrate to AtCathB-2 in chapter 5. However, whether AtCathB-2 could enter and function in cell nuclei and chloroplasts is still unknown in this stage. Further investigation using specific cellular compartment fluorescent markers in *Arabidopsis* or *Nicotiana* cells with chloroplasts is essential to the final answer to these questions. It should be noted that the fluorescent protein fused to AtCathB-2 or -3 is expected to be clipped during the maturation of the C-termimal prodomain. Therefore, the final destination of AtCathB-2 and -3 during PCD could not be ascertained by the experiments carried out so far. Further constructs where the fluorescent protein remains attached during maturation need to be designed and tested.

CHAPTER 7

CONCLUSION

7.1 *Arabidopsis* cathepsin B is responsible for part of, if not all, caspase-3-like activity required for PCD regulation

The discovery of a caspase cascade as the main apoptotic pathway in animals originated from the identification of CED-3 using *C. Elegans* mutants (Yuan *et al.*, 1993). However, the search for caspase homologues in plant, alga and yeast genomes eventually confirmed their absence. Several caspase-like activities which are required for plant PCD regulation have been identified using synthetic tetrapeptide substrates and inhibitors (Rotari *et al.*, 2005; Bonneau *et al.*, 2008). Furthermore, several plant proteases i.e. saspase, phytaspase and the 20S proteasome, which are required for HR-mediated PCD, display caspase-like activity but share no homology in protein sequence or structure with animal caspases (Coffeen & Wolpert, 2004; Hatsugai *et al.*, 2009; Chichkova *et al.*, 2010). The order of His and Cys residues in the caspases catalytic dyad is unique among cysteine proteases. Plant VPEs, as published, have homologous catalytic dyads (in the order of His-Cys) with human caspase-1 in addition to their caspase-1-like activity (Nishimura *et al.*, 2005). Van der Hoorn defined the term 'plant caspase-like proteases' with two prerequisites: the specific cleavage of substrates after an Aspartic acid residue and homology in protein sequence or structure (van der Hoorn, 2008). Hence only VPEs probably qualify as plant caspase-like proteases. Nevertheless, in this thesis, the term caspase-like protease refers to proteases with a caspase-like proteolytic activity without consideration of its protein sequence and structure.

Metacaspases are annotated as ancient and distant homologues of animal caspase and were hypothesized as being functional analogues of animal caspases in plants and fungi (Watanabe & Lam, 2005; Vercammen *et al.*, 2006; He *et al.*, 2007). The involvement of metacaspases in plant PCD regulation has been reported. Surprisingly, metacaspases were found to be without caspase-like proteolytic activity. McII-Pa, a metacaspase from Norway spruce, cleaves the protein Tudor staphylococcal nuclease (TSN), a gene-expression regulator which happened to be cleaved by caspase-3 during human apoptosis, both in development and stress-induced PCD (Sundstrom *et al.*, 2009). However, whether

metacaspases qualify to be recognized as plant caspase is still hotly debated (Carmona-Gutierrez *et al.*, 2010; Enoksson & Salvesen, 2010).

Cathepsins in animals are lysosomal proteolysis proteases. The function of cathepsin B, a papain-like cysteine protease was initially limited to the turnover of exogenous harmful proteins or intracellular waste in the lysosome. Cathepsin B acts as a versatile protease with both endopeptidase activity and peptidyldipeptidase activity (Illy *et al.*, 1997). The role of lysosome and cathepsins in animal apoptosis has been unravelled in the last decade with the existence of a caspase-independent pathway. Cathepsin B has been published to be required for apoptosis in neuronal development and oncogenesis. In addition, cathepsin B is implicated in the activation of caspase-3, -11 and as such, increases of cytochrome *c* release (Turk *et al.*, 2009). Recombinant human cathepsin B was found to be inactive against caspase-3 substrates whereas caspase-3 inhibitor, ac-DEVD-FMK inhibits human cathepsin B proteolytic activity completely (Rozman-Pungercar *et al.*, 2003). Interestingly, cathepsin B purified from rat brain can cleave the caspase-3 substrate ac-DEVD-AMC *in vitro* (Yakovlev *et al.*, 2008). In plants, the involvement of *Nicotiana* cathepsin B and *Arabidopsis* cathepsin B in HR-mediated PCD has been reported (Gilroy *et al.*, 2007; McLellan *et al.*, 2009).

Our research originated at the identification of *Arabidopsis* cathepsin B as a possible caspase-3-like protease isolated from *Arabidopsis* seedlings undergoing PCD using biotinylated caspase-3 inhibitor. This lead us to show that in response to oxidative cell death stimuli, i.e. UV-C, methyl viologen or H_2O_2, *Arabidopsis* cathepsin B knockout plants displayed a reduced PCD. In addition to their involvement in oxidative stress-induced PCD, we confirmed a reduced caspase-3-like activity in *Arabidopsis* cathepsin B knockout plants using biotinylated inhibitor labelling and fluorescent enzymatic assay. Recombinant AtCathB-2 and AtCathB-3 produced in *E.coli* and insect cell displayed human cathepsin B-like activity, human caspase-3-like activity and some level of caspase-1-like activity. Collectively, these results demonstrate that *Arabidopsis* cathepsin B is responsible for at least some of caspase-3-like activity required for plant PCD. Nevertheless, it should be noted that caspase-like activity is still detectable in *Arabidopsis* cathepsin B loss-of-function plants. The remaining caspase-3-like activity which is not inhibited by cathepsin B selective inhibitors might be ascribed to the 20S proteasome, another protease with caspase-3-like activity identified by Nishimura and her co-workers (Hatsugai *et al.*, 2009).

Although we showed that the three cathepsin B paralogues were all required for PCD regulation, their individual function in the pathway might be distinct. The transcript level of *AtCathB-1* in physiological conditions is extremely low. In addition, we were able to show that in untreated seedlings or after heat shock induction, three different isoforms of aberrantly spliced *AtCathB-1*mRNA are present in cells. All of them should translate into a truncated protease without proteolytic activity unless some stop-suppression mechanisms are involved. The role of these truncated forms remains to be explained especially since knockout studies have suggested that *AtCathB-1*contributes to the overall cathepsin B activity. It is possible that the truncated forms somehow contribute to the activation of the two other cathepsin B via protein-protein interaction with cathepsin B or its inhibitors. In addition, it cannot be excluded that a correctly spliced isoform may be produced in some specific tissues or under some specific stresses. AtCathB-2 displayed the most important contribution to caspase-3-like activity and PCD regulation compared to the two other AtCathB. AtCathB-2 is localised in the vacuole while AtCathB-3 is localised in the cell wall and cytoplasm, suggesting they have distinct roles. However, functional analysis using *Arabidopsis* cathepsin B double knockout plants suggested that both AtCathB-2 and AtCathB-3 seem to cooperate for PCD induction. AtCathB-2 might be responsible for the proteolysis of RuBisCO *in vivo* but whether AtCathB-3 hydrolyses RuBisCO is still unknown. The enzyme RuBisCO participates in photosynthesis and its proteolysis by AtCathB-2 indicates the involvement of plant cathepsin B in a chloroplast mediated PCD. However, the cleavage of RuBisCO exerted by AtCathB-2 *in vitro* might not exist *in*. The identification of substrate of AtCathB-2 *in vivo* requires further experiments. The localisation of AtCathB-3 in the cell wall makes it the orthologue of the *Nicotiana* cathepsin B described to be present in the same compartment (Gilroy *et al.*, 2007). Unlike what is described for saspase, in *Nicotiana* there is no evidence that cathepsin B is imported into the cytoplasm during PCD. How AtCathB-3 can influence stress-induced PCD from its cell wall location remains to be explained.

7.2 Is cathepsin B a common and conserved PCD mediator across evolution?

In addition to the classical caspase-dependent apoptotic pathway, a caspase-independent pathway also exists in animal apoptosis (Turk *et al.*, 2002). Cathepsin B, together with other cathepsins, calpains and granzymes can either participate in the caspase cascade or trigger apoptosis independently after various apoptotic stimuli i.e. TNF receptor, p53 tumour suppressor protein, bile salt and ROS (Jaattela, 2002; Turk *et al.*, 2002; Turk *et al.*, 2009). The inhibition of cathepsin B can abolish TNF-induced apoptosis without preventing cathepsin B release from the lysosome, indicating the translocation of cathepsin B before apoptosis triggering (Foghsgaarda *et al.*, 2001).

In addition to their regulatory function in oxidative stress-induced PCD, we showed that *Arabidopsis* cathepsin B displayed human cathepsin B like activity, human caspase-1-like activity and human caspase-3-like activity, suggesting they can act as initiator (caspase-1 like) and executioner (caspase-3 like) in the protease cascade. However, human cathepsin B lacks these caspase-like activities although its proteolytic activity is inhibited by DEVD-FMK *in vitro*. It is not clear whether native human cathepsin B would display caspase-like activities *in vivo*. However, at this stage, we would like to speculate that plant cathepsin B is more versatile than its human homologue. Keeping in mind the involvement of cathepsin B in animal caspase-independent apoptotic pathways, we postulate that cathepsin B is a conserved mediator of PCD across evolution. When animal cells evolved the caspase cascade from metacaspases or paracaspases as a more efficient apoptotic pathway, the role of cathepsin B was reduced from a major PCD modulator (both initiator and executioner) to an alternative and complementary apoptotic modulator. In plants, cathepsin B would have retained its ancestral pivotal role in PCD regulation. According to this hypothesis, the caspase-independent apoptotic pathway is likely to be ‘a common way to die’ in all organisms with or without caspases.

Fig 7.1 shows a proposed caspase-like protease cascade in plant PCD regulation. However, with little knowledge of the *in vivo* substrates of these proteases and their interactions, the preparation of a convincing plant PCD pathway is difficult. In Fig 7.1, initiators are defined as ‘upstream’ proteases involved in the downstream proteases activation or death signal transduction. Executioners refer to the proteases responsible for the proteolysis of proteins which are important for cytological and nuclear events in plant PCD. The context of these proteases in this proposed PCD pathway is predicted according to their caspase-

like acitivity, possible substrates and functions. For example, phytaspase might be initiator or executioner since it has a similar cleavage site in the motif of TATD as human caspase-3 against the *Agrobacterium tumefaciens* VirD2 protein and labelled by biotin-DEVD-CHO (Chichkova *et al.*, 2004; Chichkova *et al.*, 2010). VPEs are first fixed in initiator group since they are responsible for the HR-mediated PCD initiation and the maturation of target proteins engaged in vacuolar membranes disintegration (Hatsugai *et al.*, 2006). However, the caspase-3-like activity of VPEs reported recently might enable them to function as executioners in plant PCD (Bosch *et al.*, 2010). In addition to the RuBisCO identified as a possible *in vivo* substrate of AtCathB-2, ARP DNA-(apurinic or apyrimidinic site) lyase is predicted to interact with AtCathB-2 and -3 in Arabidopsis Interactions Viewer, BAR (Popescu *et al.*, 2007; Popescu *et al.*, 2009). Type I metacaspases contain CARD/DED-like domain which are homologous to initiator caspases. MCII-Pa, a type II metacaspase from Norway spruce performs a caspase-3-like proteolysis against the nuclease TSN (Vercammen *et al.*, 2006; Sundstrom *et al.*, 2009). Thus metacaspases type I are fit in initiator group and metacaspases type II are classified as executioners.

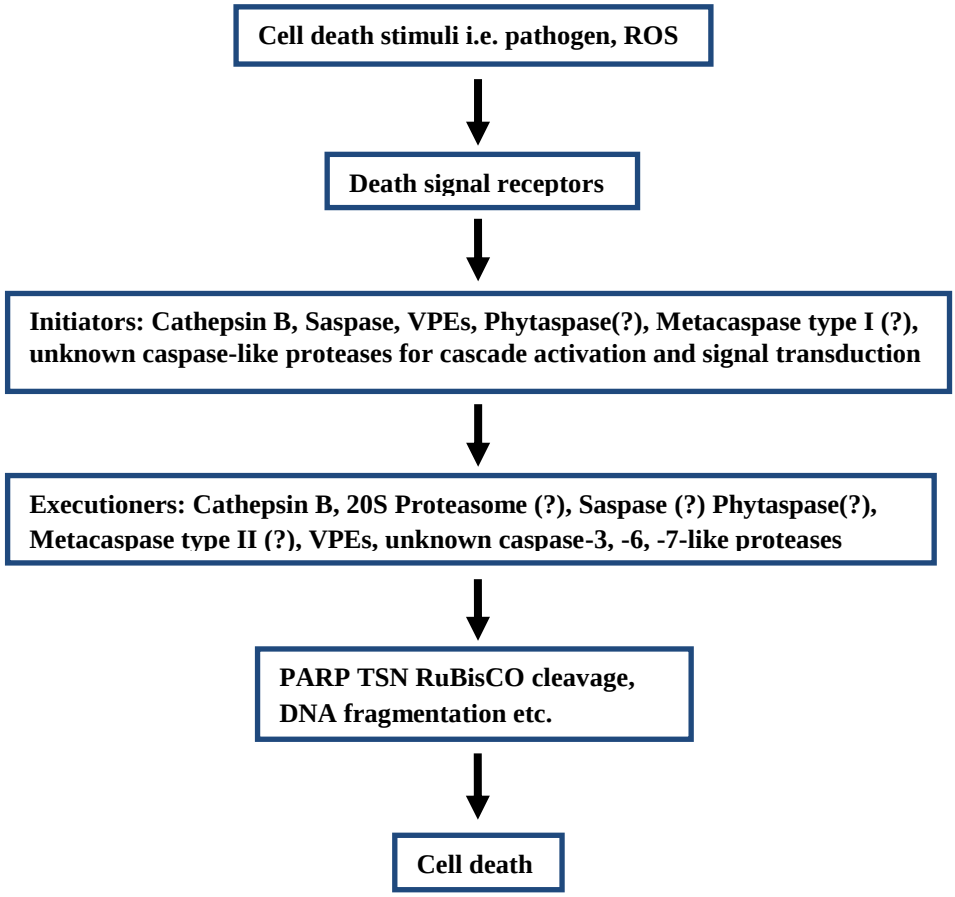

Fig 7.1 A proposed caspase-like protease cascade in plant PCD regulation. The cell death stimuli are first passed to the initiator proteases from death receptors. The initiators are responsible for the activation of their downstream execution proteases or the further transduction of the death signal. The activation of executioners triggers the proteolysis of the proteins which are important to cell integrity i.e. PARP, TSN, RuBisCO and leads to cell death eventually.

7.3 Future work

In this thesis, we confirmed the involvement of *Arabidopsis* cathepsin B in PCD regulation as well as their caspase-like activity. More work in cathepsin B and other related proteases in plants require to be completed for a better elucidation of the role of proteases in plant PCD regulation.

Further work in order to improve the understanding in *Arabidopsis* cathepsin B could be carried out in the following aspects:

We showed the existence of truncated and probable non-functional AtCathB-1 in plants. The mechanism of how AtCathB-1 function in PCD requires further investigation using recombinant AtCathB-1 to identify a possible role in activation or inhibition of AtCathB-2 and -3 enzymatic activity.

(1) The possible subcellular localisation and translocation of *Arabidopsis* cathepsin B in cells undergoing PCD is essential to the explanation of their *in vivo* function. The C-terminus of procathepsin B is processed during maturation *in vivo* therefore the C-terminal fluorescent tag (YFP/RFP) fused with procathepsin B becomes detached preventing the analysis of translocation post-maturation. However, we demonstrated the auxiliary function of N-terminal and C-terminal prodomains in cathepsin B folding as chaperones. In the next step, cleavage site in procathepsin B maturation should be revealed and new AtCathB fusions with RFP should be created where the C-terminal prodomain is abolished consequently.

(2) In this thesis, we showed the autocatalysis of *Arabidopsis* cathepsin B *in vitro* only and we postulated the existence of a reservoir of *Arabidopsis* cathepsin B activity *in vivo* composed of different partially activated variants. Antibodies against the catalytic unit of AtCathB should be produced to investigate their activation and maturation *in vivo* before and during PCD.

(3) The identification of cathepsin B *in vivo* substrates is central to the elucidation of the protease cascade in cell death. In this thesis, a possible *in vivo* substrate of *Arabidopsis* cathepsin B was identified preliminarily. This result requires to be supported with more experimental evidence. For example, the diagonal gel approach should be repeated with more proteins to attempt the identification of additional substrates. In addition, the proteolysis of RuBisCO during PCD should be confirmed *in vivo* using an antibody

against RuBisCO. The cleavage site in RuBisCO provided by *Arabidopsis* cathepsin B should be identified *in vitro* and *in vivo*. In *Arabidopsis* cathepsin B loss-of-function plants, the cathepsin B mediated RuBisCO proteolysis should be abolished. Finally, transgenic RuBisCO with the cathepsin B cleavage sites mutated should be overexpressed in plants and the phenotypes in PCD would be analysed.

(4) At this stage, only the role of individual proteases: cathepsin B, VPEs, metacaspases, saspases and phytaspases has been confirmed in plant PCD. However, the possible interactions between them are still unknown. More work needs to be carried out to built an image of the PCD protease network using transgenic plants. For example, the overexpression of *Arabidopsis* cathepsin B in VPEs knockout plants will probably help to provide their context in PCD. More research on the activation of procathepsin B in plants by other proteases will provide additional knowledge to fit cathepsin B in the PCD cascade. The activation status of procathepsin B in various protease knockout plants could be detected using anti-AtCathB antibodies.

(5) In addition, KOD, a short peptide isolated from *Arabidopsis*, is a novel PCD inducer isolated in our lab (Young & Gallois, submitted). The investigation of the function of cathepsin B in KOD-induced PCD will benefit the understanding in both cathepsin B and KOD research. Finally our hypothesis is that there is a conserved cathepsins-mediated PCD pathway in plants. The function of other *Arabidopsis* cathepsins and their interactions in PCD should be investigated using gene knockout lines for each family.

In summary, cathepsin B is a common PCD mediator in plants and animals. In addition, the regulatory function of *Arabidopsis* cathepsin B in PCD is highlighted by their caspase-3-like activity. The challenge for future is to sort out more evidences to verify the hypothesized cathepsins-mediated PCD pathway and fit *Arabidopsis* cathepsin B in the protease cascade for a better elucidation of the molecular mechanism of PCD.

REFERENCES

Ame JC, Spenlehauer C & de Murcia G (2004). The PARP superfamily. *BioEssays* **26**, 882–893.

Apel K & Hirt H (2004). Reactive oxygen species: metabolism, oxidative stress, and signal transduction. *Annual Review of Plant Biology* **55**, 373-399.

Aravind L, Walker R & Koonin EV (1999). The domains of death: evolution of the apoptosis machinery *Trends in Biochemical Sciences* **24**, 47-53

Baehrecke EH (2003). Autophagic programmed cell death in Drosophila. *Cell Death and Differentiation* **10**, 940-945.

Bais HP, Vepachedu R, Gilroy S, Callaway RM & Vivanco JM (2003). Allelopathy and exotic plant invasion: from molecules and genes to species interactions. *Science* **301**, 1377 - 1380.

Bako L, Umeda M, Tiburcio AF, Schell J & Koncz C (2003). The VirD2 pilot protein of *Agrobacterium*-transferred DNA interacts with the TATA box-binding protein and a nuclear protein kinase in plants *Proceedings of National Academy of Science, USA* **100** 10108-10113

Baneyx F & Mujacic M (2004). Recombinant protein folding and misfolding in E.coli. *Nature biotechnology* **11**, 1399-1408.

Belenghi B, Salomon M & Levine A (2004). Caspase-like activity in the seedlings of Pisum sativum eliminates weaker shoots during early vegetative development by induction of cell death. *Journal of Experimental Botany* **55**, 889-897.

Belkhadir Y, Subramaniam R & Dangl JL (2004). Plant disease resistance protein signaling: NBS–LRR proteins and their partners. *Current opinion in Plant Biology* **7**, 391-399.

Bellamy C, Malcomson R, Harrison D & Wyllie A (1995). Cell death in health and disease: the biology and regulation of apoptosis. *Seminars in Cancer Biology* **6**, 3-16.

Berardi S, Lang A, Kostoulas G, Horler D, Vilei EM & Baici A (2001). Alternative messenger RNA splicing and enzyme forms of cathepsin B in human osteoarthritic cartilage and cultured chondrocytes. *Arthritis and Rheumatism* **44**, 1819–1831.

Binns AN (2002). T-DNA of Agrobacterium tumefaciens: 25 years and counting. *Trends in Plant Science* **7**, 232-233.

Blackstone NW & Kirkwood TBL (2003). *Mitochondria and programmed cell death*. Cambridge, MA: MIT Press.

Blissard GW (1996). Baculovirus-insect cell interactions. *Cytotechnology* **20**, 73-93.

Bonneau L, Ge Y, Drury GE & Gallois P (2008). What happened to plant caspases? *Journal of Experimental Botany* **59**, 491-499.

Boren M, Hoglund AS, Bozhkov P & Jansson C (2006). Developmental regulation of a VEIDase caspase-like proteolytic activity in barley caryopsis. *Journal of Experimental Botany* **57**, 3747-3753.

Bosch M & Franklin-Tong VE (2007). Temporal and spatial activation of caspase-like enzymes induced by self-incompatibility in Papaver pollen. *Proceedings of the National Academy of Sciences, USA* **104**, 18327-18332.

Bosch M, Poulter NS, Perry RM, Wilkins KA & Franklin-Tong VE (2010). Characterization of a legumain/vacuolar processing enzyme and YVADase activity in Papaver pollen. *Plant Molecular Biology* **Epub ahead of print**.

Bowes G (1991). Growth at elevated CO2: photosynthetic responses mediated through RuBisCO. *Plant, Cell and Environment*, 795-806.

Bozhkov PV, Filonova LH, Suarez MF, Helmersson A, Smertenko AP, Zhivotovsky B & Von Arnold S (2004). VEIDase is a principal caspase-like activity involved in plant programmed cell death and essential for embryonic pattern formation. *Cell Death and Differentiation* **11**, 175-182.

Bryson K, McGuffin LJ, Marsden RL, Ward JJ, Sodhi JS & DT, J. (2005). Protein structure prediction servers at University College London. *Nucleic Acids Research* **33**, W36-W38.

Buttner S, Eisenberg T, Carmona-Gutierrez D, Ruli D, Knauer H, Ruckenstuhl H, Sigrist C & Madeo F (2007). Endonuclease g regulates budding yeast life and death *Molecular Cell* **25**, 233-246

Caglic D, Kosec G, Bojic L, Reinheckel T, Turk V & B., T. (2009). Murine and human cathepsin B exhibit similar properties: possible implications for drug discovery. *Biological Chemistry* **390**, 175-179.

Carmona-Gutierrez D, Frohlich KU, Kroemer G & Madeo F (2010). Metacaspases are caspases. Doubt no more. *Cell Death and Differentiation* **17**, 377-378.

Cerretti DP, Kozlosky CJ, Mosley B, Nelson N, van Ness K & *et al.* (1992). Molecular cloning of the interleukin-1 beta converting enzyme. *Science* **256**, 97-100.

Chen JM, Rawlings ND, Stevens R & Barrett AJ (1998). Identification of the active site of legumain links it to caspases, clostripain and gingipains in a new clan of cysteine endopeptidases *FEBS Letters* **441**, 361-365.

Chen S & Dickman MB (2004). Bcl-2 family members localize to tobacco chloroplasts and inhibit programmed cell death induced by chloroplast-targeted herbicides *Journal of Experimental Botany* **55**, 2617-2623.

Chichkova NV, Kim SH, Titova ES, Kalkum M, Morozov VS, Rubtsov YP, Kalinina NO, Taliansky ME & Vartapetian AB (2004). A plant caspase-like protease activated during the hypersensitive response. *Plant Cell* **16**, 157-171.

Chichkova NV, Shaw J, Galiullina RA, Drury GE, Tuzhikov AI, Kim SH, Kalkum M, Hong TB, Gorshkova EN, Torrance L, Vartapetian AB & Taliansky M (2010). Phytaspase, a relocalisable cell death promoting plant protease with caspase specificity. *The EMBO Journal*, 1-13.

Chwieralski CE, Welte T & Buhling F (2006). Cathepsin-regulated apoptosis. *Apoptosis* **11**, 143-149.

Coffeen WC & Wolpert TJ (2004). Purification and characterization of serine proteases that exhibit caspase-like activity and are associated with programmed cell death in *Avena sativa*. *Plant Cell* **16**, 857-873.

Cogan JD, Prince MA, Lekhakula S, Bundey S, Futrakul A, McCarthy EMS & Phillips III JA (1997). A novel mechanism of aberrant pre-mRNA splicing in humans. *Human Molecular Genetics* **6**, 909–912.

Damme PV, Vandekerckhove J & Gevaert K (2008). Disentanglement of protease substrate repertoires. *Biological Chemistry* **389**, 371–381.

Danon A, Delorme V, Mailhac N & Gallois P (2000). Plant programmed cell death: a common way to die. *Plant Physiology and Biochemistry* **38**, 647-655.

Danon A, Rotari VI, Gordon A, Mailhac N & Gallois P (2004). Ultraviolet-c overexposure induces programmed cell death in Arabidopsis, which is mediated by caspase-like activities and which can be suppressed by caspase inhibitors, p35 and defender against apoptotic death. *Journal of Biological Chemistry* **279**, 779–787.

Dat J, Vandenabeele S, Vranova E, Van Montagu M & Inze D (2000). Dual action of the active oxygen species during plant stress responses. *Cell Molecular Life Science* **57**, 779-795.

De Jong AJ, Hoeberichts FA, Yakimova ET, Maximova E & Woltering EJ (2000). Chemical-induced apoptotic cell death in tomato cells: involvement of caspase-like proteases. *Planta* **211**, 656-662.

del Pozo O & Lam E (1998). Caspases and programmed cell death in the hypersensitive response of plants to pathogens. *Current Biology* **8**, 1129-1132.

Demidchik V, Cuin TA, Svistunenko D, Smith SJ, Miller AJ, Shabala S, Sokolik A & Yurin V (2010). Arabidopsis root K+-efflux conductance activated by hydroxyl radicals: single-channel properties, genetic basis and involvement in stress-induced cell death. *Journal of Cell Science* **123**, 1468-1479.

Denault JD & Salvesen GS (2002). Caspases: keys in the ignition of cell death. *Chemistry Review* **102**, 4489-4499.

Deveraux QL & Reed JC (1999). IAP family proteins-suppressors of apoptosis. *Gene and Development* **13**, 239-252.

Doyle SM, Diamond M & McCabe PF (2010). Chloroplast and reactive oxygen species involvement in apoptotic-like programmed cell death in Arabidopsis suspension cultures. *Journal of Experimental Botany* **61**, 473 - 482.

Droga-Mazovec G, Bojic L, Petelin A, Ivanova S, Romih R, Repnik U, Salvesen GS, Stoka V, Turk V & Turk B (2008). Cysteine cathepsins trigger caspase-dependent cell death through cleavage of bid and antiapoptotic Bcl-2 homologues. *Journal of Biological Chemistry* **283**, 19140-19150.

Earnshaw WC, Martins LM & Kaufmann SH (1999). Mammalian caspase: structure, activation, substrates and functions during apoptosis. *Annual Review of Biochemistry* **68**, 383-424

Edinger AL & Thompson CB (2004). Death by design: apoptosis, necrosis and autophagy. *Current Opinion in Cell Biology* **16**, 663-669.

Eichinger A, Beisel HG, Jacob U, Huber R, Medrano FJ, Banbula A, Potempa J, Travis J & Bode W (1999). Crystal structure of gingipain R: an Arg-specific bacterial cysteine proteinase with a caspase-like fold. *The EMBO Journal* **18**, 5453 - 5462.

Elbaz M, Avni A & Weil M (2002). Constitutive caspase-like machinery executes programmed cell death in plant cells. *Cell Death and Differentiation* **9**, 726-733.

Enoksson M & Salvesen GS (2010). Metacaspases are not caspases –always doubt. *Cell Death and Differentiation* **17**, 1221.

Faisal M, Schafhausera DY, Garreisa KA, Elsayeda E & La Peyrea JF (1999). Isolation and characterization of Perkinsus marinus proteases using bacitracin–sepharose affinity chromatography *Comparative Biochemistry and Physiology Part B: Biochemistry and Molecular Biology* **123**, 417-426.

Fan TJ, Han LH, Cong RS & Liang J (2005). Caspase family proteases and apoptosis. *Acta Biochimica et Biophysica Sinica* **37**, 719-727.

Faubion WA & Gores GJ (1999). Death receptors in liver biology and pathobiology. *Hepatology* **29**, 1-4.

Faubion WA, Guicciardi ME & Miyoshi H (1999). Toxic bile salts induce rodent hepatocyte apoptosis via direct activation of Fas. *Journal of Clinic Investigation* **103**, 137-145.

Felbor U, Kessler B & Mothes W (2002). Neuronal loss and brain atrophy in mice lacking cathepsins B and L. *Proceedings of National Academy of Science, USA* **99**, 7883–7888.

Feldmann KA (1991). T-DNA insertion mutagenesis in Arabidopsis: mutational spectrum. *The Plant Journals* **1**, 71-82.

Ferre F & Clote P (2005). DiANNA: a web server for disulfide connectivity prediction. *Nucleic Acids Research* **33**, W230-W232.

Ferreira RB & Davies DD (1989). Conversion of ribulose-1,5-bisphosphate carboxylase to an acidic and catalytically inactive form by extracts of osmotically stressed Lemna minor fronds. *Planta* **179**, 448-455.

Filichkin SA, Priest HD, Givan SA, Shen R, Bryant DW, Fox SE, Wong W-K & Mockler TC (2010). Genome-wide mapping of alternative splicing in *Arabidopsis thaliana*. *Genome Research* **20**, 45-58.

Foghsgaard L, Wissinga D, Mauchb D, Lademanna U & Bastholmc L (2001). Cathepsin B acts as a dominant execution protease in tumor cell apoptosis induced by tumor necrosis factor. *Journal of Cell Biology* **153**, 999-1009.

Fuentes-Prior P & Salvesen GS (2004). The protein structures that shape caspase activity, specificity, activation and inhibition. *Biochemical Journal* **384**, 201-232.

Fujibe T, Saji H, Arakawa K, Yabe N, Takeuchi Y & Yamamoto KT (2004). A methyl viologen-resistant mutant of arabidopsis, which is allelic to ozone-sensitive rcd1, is tolerant to supplemental ultraviolet-B irradiation. *Plant Physiology* **134**, 275-285.

Fujikawa T, Yamashita T & Tsuyumu S (2006). Hypersensitive response suppression by type III effectors of plant pathogenic bacteria. *Journal of general plant pathology* **72**, 176-179.

Fukuda H (1997). Tracheary element differentiation. *Plant Cell* **9**, 1147-1156.

Fukuda H (2000). Programmed cell death of tracheary elements as a paradigm in plants. *Plant Molecular Biology* **44**, 245-253.

Gapper C & Dolan L (2006). Control of plant development by reactive oxygen species. Plant Physiol 141:341–345. *Plant physiology* **141**, 341-345.

Ge Z-Q, Yang S, Cheng J-S & Yuan Y-J (2005). Signal role for activation of caspase-3-like protease and burst of superoxide anions during Ce4+-induced apoptosis of cultured Taxus cuspidata cells. *BioMetals* **18**, 221-232.

Gechev TS & Hille J (2005). Hydrogen peroxide as a signal controlling plant programmed cell death. *Journal of Cell Biology* **168**, 17-20.

Gechev TS, Breusegem FV, Stone JM, Denev L & Laloi C (2006). Reactive oxygen species as signals that modulate plant stress responses and programmed cell death. *BioEssays* **28**, 1091-1101.

Gerner C, Frohwein U, Gotzmann J, Bayer E, Gelbmann D, Bursch W & Schulte-Hermann R (2000). The Fas-induced apoptosis analyzed by high throughput proteome analysis. *Journal of Biological Chemistry* **275**, 39018-39026.

Gilroy EM, Hein I, van der Hoorn R, Boevink PC, Venter E, McLellan H, Kaffarnik F, Hrubikova K, Shaw J, Holeva M, Borras-Hidalgo O, Pritchard L & Birch P (2007). Involvement of cathepsin B in the plant disease resistance hypersensitive response. *Plant Journal* **52**, 1-13.

Glucksmann A (1951). Cell deaths in normal vertebrate development. *Biology Review* **26**, 59-86.

Gozuacik D & Kimchi A (2004). Autophagy as a cell death and tumor suppressor mechanism. *Oncogene* **12**, 2891-2906.

Green DR & Reed JC (1998). Mitochondria and apoptosis. *Science* **281**, 1309-1312.

Guicciardi ME, Deussing J, Miyoshi H, Bronk SF & Svingen PA (2000). Cathepsin B contributes to TNF-α-mediated hepatocyte apoptosis by promoting mitochondrial release of cytochrome c. *Journal of Clinic Investigation* **106**, 1127-1137.

Gunawardena A (2008). Programmed cell death and tissue remodeling in plants. *Journal of Experimental Botany* **59**, 445-451.

Gurtu V, Kain SR & Zhang G (1997). Fluorometric and colorimetric detection of caspase activity associated with apoptosis. *Analytical Biochemistry* **251**, 98-102

Hara-Nishimura I, Inoue K & Nishimura M (1991). A unique vacuolar processing enzyme responsible for conversion of several proprotein precursors into the mature forms. *FEBS Letters* **294**, 89-93.

Hara-Nishimura I, Hatsugai N, Nakaune S, Kuroyanagi M & Nishimura M (2005). Vacuolar processing enzyme: an executor of plant cell death. *Current Opinion in Plant Biology* **8**, 404-408.

Hasnain S, Hirama T, Tam A & Mort JS (1992). Characterization of recombinant rat cathepsin B and nonglycosylated mutants expressed in yeast. *Journal of Biological Chemistry* **267**, 4713-4721.

Hatsugai N, Kuroyanagi M, Yamada K, Meshi T, Tsuda S, Kondo M, Nishimura M & Hara-Nishimura I (2004). A plant vacuolar protease, VPE, mediates virus-induced hypersensitive cell death. *Science* **305**, 855-858.

Hatsugai N, Iwasaki S, Tamura K, Kondo M, Fuji K, Ogasawara K, Nishimura M & Hara-Nishimura I (2009). A novel membrane fusion-mediated plant immunity against bacterial pathogens. *Genes and Development* **Epub ahead print**.

Hauptmann P, Riel C, Kunz-Schughart LA, Frohlich K, Madeo F & Lehle L (2006). Defects in N-glycosylation induce apoptosis in yeast. *Molecular Microbiology* **59**, 765-778.

He R, Drury GE, Rotari VI, Gordon A, Willer M, Farzaneh T, Woltering EJ & Gallois P (2007). Metacaspase-8 modulates programmed cell death induced by ultraviolet light and H2O2 in Arabidopsis. *Journal of Biological Chemistry* **283**, 774-783.

He X & Kermode AR (2003). Proteases associated with programmed cell death of megagametophyte cells after germination of white spruce (*Picea glauca*) seeds. *Plant Molecular Biology* **52**, 729-744.

Heath MC (2000). Hypersensitive response-related death. *Plant Molecular Biology* **44**, 321-334.

Hengartner MO & Horvitz HR (1994). The ins and outs of programmed cell death during C. elegans development. *Philosophical Transactions of the Royal Society B* **345**, 243-248.

Higashi K, Takasawa R, Yoshimori A, Goh T, Tanuma S & Kuchitsu K (2005). Identification of a novel gene family, paralogs of inhibitor of apoptosis proteins present in plants, fungi, and animals. *Apoptosis* **10**, 471-480.

Hitomi J, Katayama T, Eguchi Y, Kudo T, Taniguchi M & Koyama Y (2004). Involvement of caspase-4 in endoplasmic reticulum stress-induced apoptosis and Aβ-induced cell death. *Journal of Cell Biology* **165**, 347-356.

Hockney RC (1994). Recent developments in heterologous protein production in *Escherichia coli*. *Trends of Biotechnology* **12**, 456-463.

Hoeberichts FA & Woltering EJ (2002). Multiple mediators of plant programmed cell death: interplay of conserved cell death mechanisms and plant-specific regulators. *BioEssays* **25**, 47-57.

Hoeberichts FA, Have A & Woltering EJ (2003). A tomato metacaspase gene is upregulated during programmed cell death in Botrytis cinerea-infected leaves. *Planta* **217**, 517-522.

Hofius S, Schultz-Larsen T, Joensen J, Tsitsigiannis DI, Petersen NHT, Mattsson O, Jorgensen LB, Jones JDG, Mundy J & Petersen M (2009). Autophagic components contribute to hypersensitive cell death in *Arabidopsis. Cell* **137**, 773-783

Ikonomou L, Schneider J & Agathos SN (2003). Insect cell culture for industrial production of recombinant proteins. *Applied Microbiology and Biotechnology* **62**, 1-20.

Illy C, Quraishi O, Wang J, Purisima E, Vernet T & Mort JS (1997). Role of the occluding loop in cathepsin B activity. *Journal of Biological Chemistry* **272**, 1197-1202.

Irvine JW, Coombs GH & North MJ (1993). Purification of cysteine proteinases from trichomonads using bacitracin-Sepharose. *FEMS Microbiology Letters* **110**, 113-119.

Jaattela M (2002). Programmed cell death: many ways for cells to die decently. *Annals of Medicine* **34**, 480-488.

Janicke RU, Ng P, Sprengart ML & Porter AG (1998). Caspase-3 is required for α-Fodrin cleavage but dispensable for cleavage of other death substrates in apoptosis. *Journal of Biological Chemistry* **273**, 15540-15545.

Jarvis DL & Finn EE (1996). Modifying the insect cell N-glycosylation pathway with immediate early baculovirus expression vectors. *Nature Biotechnology* **14**, 1288-1292.

Jarvis DL (1997). Baculovirus expression vectors. *The Baculoviruses, Plenum Press, New York*, pp. 389–431.

Jarvis DL (2003). Developing baculovirus-insect cell expression systems for humanized recombinant glycoprotein production *Virology* **310**, 1-7.

Jones AM (2001). Programmed cell Death in development and defense. *Plant Physiology* **125**, 94-97.

Jones B, Roberts PJ, Faubion WA, Kominami E & Gores GJ (1998). Cystatin A expression reduces bile salt-induced apoptosis in a rat hepatoma cell line. *Amerian Journal of Physiology* **275**, 723-730.

Jones DT (1999). Protein secondary structure prediction based on position-specific scoring matrices. *Journal of Molecular Biology* **292**, 195-202.

Kamada S, Washida M, Hasegawa J, Kusano H, Funahashi Y & Tsujimoto Y (1997). Involvement of caspase-4(-like) protease in Fas-mediated apoptotic pathway. *Oncogene* **15**, 285-290.

Kaufmann D, Leistner W, Kruse P, Kenner O, Hoffmeyer S & Hein C (2002). Aberrant splicing in several human tumors in the tumor suppressor genes neurofibromatosis type 1, neurofibromatosis type 2, and tuberous sclerosis 2. *Caner Research* **62**, 1503–1509.

Kerr J, Wylhe A & Curne R (1972). Apoptosis: a basic biological phenomenon with wide-ranging implications in tissue kinetics. *British Journal of Cancer* **26**, 239-257.

Kim J, Hana J & Yoon Y (1999). Biochemical and morphological identification of ceramide-induced cell cycle arrest and apoptosis in cultured granulosa cells. *Tissue and Cell* **31**, 531-539.

Kim M, Ahn J-W, Jin U-H, Choi D, Paek K-H & Pai H-S (2003). Activation of the programmed cell death pathway by inhibition of proteasome function in plants. *Journal of Biological Chemistry* **278**, 19406-19415.

Kisselev AF, Garcia-Calvo M, Overkleeft HS, Peterson E, Pennington MW, Ploegh HL, Thornberry NA & Goldberg AL (2003). The caspase-like sites of proteasomes, their substrate specificity, new inhibitors and substrates, and allosteric interactions with the rypsin-like sites. *Journal of Biological Chemistry* **278**, 35869-35877.

Korthout HA, Berecki G, Bruin W, van Duijn B & Wang M (2000). The presence and subcellular localization of caspase-3-like proteinases in plant cells. *FEBS Letters* **475**, 139-144.

Kovtun Y, Chiu W, Tena G & Sheen J (2000). Functional analysis of oxidative stress-activated mitogen-activated protein kinase cascade in plants. *Proceedings of National Academy of Science, USA* **97**, 2940-2945

Kroemer G & Martin SJ (2005). Caspase-indepent cell death. *Nature Medicine* **11**, 725-730.

Krzymowska M, Konopka-Postupolska D, Sobczak M, Macioszek V, Ellis BE & Hennig J (2007). Infection of tobacco with different Pseudomonas syringae pathovars leads to distinct morphotypes of programmed cell death. *Plant Journal* **50**, 253–264.

Kuhelj R, Dolinar M, Pungercar J & Turk V (1995). The preparation of catalytically active human cathepsin B from its precursor expressed in Escherichia coli in the form of inclusion bodies. *European Journal of Biochemistry* **229**, 533-539.

Kuriyama H & Fukuda H (2002). Developmental programmed cell death in plants. *Current Opinion in Plant Biology* **5**, 568-573.

Kuroyanagi M, Yamada K, Hatsugai N, Kondo M, Nishimura M & Hara-Nishimura I (2005). Vacuolar processing enzyme is essential for mycotoxin-induced cell death in *Arabidopsis thaliana*. *Journal of Biological Chemistry* **280**, 32914-32920.

Levine B & Klionsky DJ (2004). Development by self-digestion: molecular mechanisms and biological functions of autophagy. *Development Cell* **6**, 463-477.

Linke M, Herzog V & Brix K (2002). Trafficking of lysosomal cathepsin B–green fluorescent protein to the surface of thyroid epithelial cells involves the endosomal/lysosomal compartment. *Journal of Cell Science* **115**, 4877-4889.

Liu N, Raja SM & Zazzeroni F (2003). NF-kappa B protects from the lysosomal pathway of cell death. *EMBO Journal* **53**, 5312-5322.

Lockshin RA & Beaulaton J (1974). Programmed cell death. *Life Science* **15**, 1549-1565.

Lockshin RA & Zakeri Z (2001). Programmed cell death and apoptosis: origins of the theory. *Molecular Cell Biology* **2**, 545-555.

Lorrain S, Vailleau F, Balague C & Roby D (2003). Lesion mimic mutants: keys for deciphering cell death and defense pathways in plants? *Trends in Plant Sciences* **8**, 263-271.

Luckow VL & Summers MD (1988). Trends in the development of baculovirus expression vectors. *Biotechnology* **6**, 47-55.

Mach L, Mort JS & Glossl J (1994). Maturation of human procathepsin B. *Journal of Biological Chemistry* **269**, 13030-13035.

Madeo F, Herker E, Maldener C, Wissing S, Lachelt S, Herlan M & et al. (2002). A caspase-related protease regulates apoptosis in yeast *Molecular Cell* **9**, 911-917

Madeo F, Herker E, Wissing S, Jungwirth H, Eisenberg T & Fröhlich K (2004). Apoptosis in yeast. *Current Opinion in Microbiology* **7**, 655-660.

Makrides SC (1996). Strategies for achieving high level expression of genes in Escherichia coli. *Microbiol Review* **60**, 512-538.

Mathiasen IS, Sergeev IN, Bastholm L, Elling F, Norman AW & Jaattela M (2002). Calcium and calpain as key mediators of apoptosis-like death induced by vitamin d compounds in breast cancer cells. *Journal of Biological Chemistry* **277**, 30738-30745.

Matile P (1978). Biochemistry and function of vacuoles. *Annual Review in Plant Physiology* **55**, 1678-1694

Matsui JI, Haque A, Huss D, Messana EP, Alosi JA, Roberson DW, Cotanche DA, Dickman JD & Warchol ME (2003). Caspase inhibitors promote vestibular hair cell survival and function after aminoglycoside treatment *in vivo*. *Journal of Neuroscience* **23**, 6111-6122.

McLellan H, Gilroy EM, Yun BW, Birch P & Loake GJ (2009). Functional redundancy in the Arabidopsis CathepsinB gene family contributes to basal defence, the hypersensitive response and senescence. *New Phytologist* **183**, 408-418.

Mehtani S, Gong Q, Panella J, Subbiah S, Peffley DM & Frankfater A (1998). *In vivo* expression of an alternatively spliced human tumor message that encodes a truncated form of cathepsin B. *Journal of Biological Chemistry* **273**, 13236–13244.

Mlejnek P & Prochazka S (2002). Activation of caspase-like proteases and induction of apoptosis by isopentenyladenosine tobacco BY-2 cells. *Planta* **215**, 158-166.

Moffett P, Farnham G, Peart J & Baulcombe DC (2002). Interaction between domains of a plant NBS–LRR protein in disease resistance-related cell death. *EMBO Journal* **21**, 4511-4519.

Morishima M, Nakanishi K, Takenouchi H, Shibata T & Yasuhiko Y (2002). An endoplasmic reticulum stress-specific caspase cascade in apoptosis: cytochrome c-independent activation of caspase-9 by caspase-12. *Journal of Biological Chemistry* **277**, 34287-34294.

Mort JS & Buttle DJ (1997). Molecules in focus: cathepsin B. *International Journal of Biochemstry* **29**, 715-720.

Muntener K, Willimann A, Zwicky R, Svoboda B, Mach L & Baici A (2005). Folding competence of N-terminally truncated forms of human procathepsin B. *Journal of Biological Chemistry* **280**, 11973–11980.

Muntz K & Shutov AD (2002). Legumains and their functions in plants. *Trends in Plant Science* **7**, 340-344.

Mur L, Kenton P, Lloyd AJ, Ougham H & Prats E (2008). The hypersensitive response: the centenary is upon us but how much do we know? *Journal of Experimental Botany* **59**, 501-520.

Nakaunea S, Yamada K, Kondo M, Kato T, Tabata S, Nishimura M & Hara-Nishimura I (2005). A vacuolar processing enzyme, delta-VPE, is involved in seed coat formation at the early stage of seed development. *Plant Cell* **17**, 876-887.

Navarrea DA & Wolperta TJ (1999). Victorin induction of an apoptotic/senescence–like response in oats. *Plant Cell* **11**, 237-250.

Nicholson DW, Ali A, Thornberry AA, Vaillancourt JP, Ding CK, Gallant M, Gareau Y, Griffin PR, Labelle M, Yu VL & Miller DK (1995). Identification and inhibition of the ICE/CED-3 protease necessary for mammalian apoptosis. *Nature* **376**, 37 – 43.

Obara K, Kuriyama H & Fukuda H (2001). Direct evidence of active and rapid nuclear degradation triggered by vacuole rupture during programmed cell death in zinnia. *Plant Physiology* **125**, 615-626.

O'Brien JA & Lummis S (2006). Biolistic transfection of neuronal cultures using a hand-held gene gun. *Nature Protocols* **1**, 977-981.

Ossowski S, Schwab R & Weigel D (2008). Gene silencing in plants using artificial microRNAs and other small RNAs. *Plant Journals* **53**, 674-690.

Perry DK, Smyth MJ, Stennicke HR, Salvesen GS, Duriez P, Poirier GG & Hannun YA (1997). Zinc is a potent inhibitor of the apoptotic protease, caspase-3. *Journal of Biological Chemistry* **272**, 18530–18533.

Pierce GB, Parchment RE & Lewellyn AL (1991). Hydrogen peroxide as a mediator of programmed cell death in the blastocyst. *Differentiation* **46**, 181-186.

Pinkoski MJ, Waterhouse NJ, Heibein JA, Wolf BB, Kuwana T, Goldstein JC, Newmeyer DD, Bleackley RC & Green DR (2001). Granzyme b-mediated apoptosis proceeds predominantly through a BCL-2-inhibitable mitochondrial pathway. *Journal of Biological Chemistry* **276**, 12060-12067.

Popescu SC, Popescu GV, Bachan S, Zhang Z, Seay M, Gerstein M, Snyder M & Dinesh-Kumar SP (2007). Differential binding of calmodulin-related proteins to their targets revealed through high-density Arabidopsis protein microarrays. *Proceedings of National Academy of Science, USA* **104**, 4730-4735.

Popescu SC, Popescu GV, Bachan S, Zhang Z, Gerstein M, Snyder M & Dinesh-Kumar SP (2009). MAPK target networks in *Arabidopsis thaliana* revealed using functional protein microarrays. *Genes and Devevelopment* **23**, 80-92

Reape TJ & McCabe PF (2008). Apoptotic-like programmed cell death in plants. *New Phytologist* **180**, 13-26.

Reape TJ, Molony EM & McCabe PF. (2008). Programmed cell death in plants: distinguishing between different modes. *Journal of Experimental Botany* **59**, 435-444.

Reavy B, Bagirova S, Chichkova NV, Fedoseeva SV, Kim SH, Vartapetian AB & Taliansky ME (2007). Caspase-resistant VirD2 protein provides enhanced gene delivery and expression in plants. *Plant Cell Reports* **26**, 1215-1219.

Reski R (1998). Physcomitrella and Arabidopsis: the David and Goliath of reverse genetics. *Trends Plant in Science* **3**, 209-210.

Roberts LR, Kurosawa H & Bronk SF (1997). Cathepsin B contributes to bile salt-induced apoptosis of rat hepatocytes. *Gastroenterology* **113**, 1714-1726.

Rotari VI, He R & Gallois P (2005). Death by proteases in plants: whodunit. *Physiologia Plantarum* **123**, 376-385.

Rowan AD, Mason P, Mach L & Mort JS (1992). Rat procathepsin B: proteolytic processing to the mature form *in vitro*. *Journal of Biological Chemistry* **267**, 15993-15999.

Roy N & Cardone MH (2002). *The caspases: consequential cleavage*. *Apoptosis*: Oxford University Press.

Rozman-Pungercar J, Kopitar-Jerala N, Bogyo M & other authors (2003). Inhibition of papain-like cysteine proteases and legumain by caspase-specific inhibitors: when reaction mechanism is more important than specificity. *Cell Death and Differentiation* **10**, 881-888.

Salvesen GS (2001). A lysosomal protease enters the death scene. *Journal of Clinic Investigation* **107**, 21-23.

Samadi L & Shahsavan Behboodi B (2006). Fusaric acid induces apoptosis in saffron root-tip cells: roles of caspase-like activity, cytochrome *c*, and H_2O_2. *Planta* **225**, 223-234.

Sanchez P, Zabala MT & Grant M (2000). AtBI-1, a plant homologue of Bax Inhibitor-1, suppresses Bax-induced cell death in yeast and is rapidly upregulated during wounding and pathogen challenge. *Plant Journal* **21**, 393-399.

Sanmartin M, Jaroszewski L, Raikhel NV & Rojo E (2005). Caspases. Regulating death since the origin of life. *Plant Physiology* **137**, 841-847.

Saunders JW & Fallon JS (1966). *Cell death in morphogenesis*. New York: Academic Press.

Savill J (1997). Recognition and phagocytosis of cells undergoing apoptosis *British Medical Bulletin* **53**, 491-508.

Schwab R, Ossowski S, Riester M, Warthmann N & Weigel D (2006). Highly Specific Gene Silencing by Artificial MicroRNAs in Arabidopsis. *Plant Cell* **18**, 1121-1133.

Schweichel JU & Merkel HJ (1974). The morphology of various types of cell death in prenatal tissue. *Teratology* **7**, 253-266.

Shao W, Yeretssian G, Doiron K, Hussain SN & Saleh M (2007). The caspase-1 digestome identifies the glycolysis pathway as a target during infection and septic shock. *Journal of Biological Chemistry* **282**, 36321-36329.

Shi Y (2004). Caspase activation, inhibition, and reactivation: a mechanistic view. *Protein Science* **13**, 1979–1987.

Simon HU, Haj-Yehia A & Levi-Schaffer F (2000). Role of reactive oxygen species (ROS) in apoptosis induction. *Apoptosis* **5**, 415-418.

Steed PM, Lasala D, Liebman J, Wigg A, Clark K & Knap AK (1998). Characterization of recombinant human cathepsin B expressed at high levels in baculovirus. *Prorein Science* **7**, 2033-2037.

Stennicke HR & Salvesen GS (1999). Catalytic properties of the caspases. *Cell Death and Differentiation* **6**, 1054-1059.

Stoka V, Turk B, Schendel SL, Kim T & Cirman T (2001). Lysosomal protease pathways to apoptosis. *Journal of Biological Chemistry* **276**, 3149-3157.

Stoka V, Turk V & Turk B (2007). Lysosomal cysteine cathepsins: signaling pathways in apoptosis. *Biological Chemistry* **388**, 555-560.

Suarez MF, Filonova LH, Smertenko A, Savenkov EI, Clapham DH, von Arnold S, Zhivotovsky B & Bozhkov PV (2004). Metacaspase-dependent programmed cell death is essential for plant embryogenesis. *Current Biology* **14**, R339-340.

Sun Y-L, Zhao Y, Hong X & Zhai Z-H (1999). Cytocrome c release and caspase activation during menadion-induced apoptosis in plants. *FEBS Letters* **462**, 317-321.

Sundstrom JF, Vaculova A, Smertenko AP, Savenkov EI, Golovko A & Bozhkov PV (2009). Tudor staphylococcal nuclease is an evolutionarily conserved component of the programmed cell death degradome. *Nature Cell Biology* **11**, 1347 - 1354.

Talanian RV, Quinlan C, Trautz S, Hackett MC, Mankovich JA, Banach D, Ghayur T, Brady KD & Wong WW (1997). Substrate specificity for caspase family proteases. *Journal of Biological Chemistry* **272**, 17907-17911.

Terpe K (2006). Overview of bacterial expression systems for heterologous protein production: from molecular and biochemical fundamentals to commercial systems. *Applied Microbiolology Biotechnology* **72**, 211-222.

Thomas SG & Franklin-Tong VE (2004). Self-incompatibility triggers programmed cell death in Papaver pollen. *Nature* **429**, 305-309.

Thornberry NA, Bull HG, Calaycay JR, Chapman KT, Howard AD, Kostur MJ Miller DK, Molineaux SM, Weidner JR, Mumford RA, Schmidt JA & Tocci MJ (1992). A novel heterodimeric cysteine protease is required for interleukin-1processing in monocytes. *Nature* **356**, 768 - 774

Thornberry NA, Rano TA, Peterson EP, Rasper DM, Timkey T, Garcia-Calvo M, Houtzager VM, Nordstrom PA, Roy S, Vaillancourt JP, Chapman KT & Nicholson DW (1997). A combinatorial approach defines specificities of members of the caspase family and granzyme B. *Journal of Biological Chemistry* **272**, 9677-9682.

Tian R, Zhang G, Yan C & Dai Y (2000). Involvement of poly(ADPribose) polymerase and activation of caspase-3-like protease in heat shock-induced apoptosis in tobacco suspension cells. *FEBS Letters* **474**, 11-15.

Traut TW (1994). The functions and consensus motifs of nine types of peptide segments that form different types of nucleotide-binding sites. *European Journal of Biochemistry* **222**, 9-19.

Tsuji A, Kikuchi Y, Ogawa K, Saika H, Yuasa K & Nagahama M (2008). Purification and characterization of cathepsin B-like cysteine protease from cotyledons of daikon radish, Raphanus sativus. *FEBS Journal* **275**, 5429-5443.

Turk B, Dolenc I, Zerovnik E, Turk D, Gubensek F & Turk V (1994). Human cathepsin B is a metastable enzyme stabilized by specific ionic interactions associated with the active site. *Biochemistry* **33**, 14800- 14806.

Turk B, Turk D & Turk V (2001). Lysosomal cysteine proteases: facts and opportunities. *EMBO Journal* **20**, 4629 - 4633.

Turk B, Stoka V, Rozman J, Cirman T, Droga-Mazovec G, Oresic K & Turk V (2002). Apoptotic pathways: involvement of lysosomal proteases. *Biological Chemisry* **383**, 1035-1044.

Turk D, Podobnik M, Kuhelj R, Dolinar M & Turk V (1996). Crystal structures of human procathepsin B at 3.2 and 3.3 Angstroms resolution reveal an interaction motif between a papain-like cysteine protease and its propeptide. *FEBS Letters* **384**, 211-214.

Turk V, Turk B & Turk D (2009). Lysosomes as "Suicide Bags" in cell death: myth or reality? *Journal of Biological Chemistry* **284**, 21783-21787.

Uren AG, Beilharz T, O'Connell MJ, Bugg SJ, van Driel R, Vaux DL & Lithgow T (1999). Role for yeast inhibitor of apoptosis (IAP)-like proteins in cell division. *Proceedings of National Academy of Science, USA* **96** 10170-10175

Vacca RA, Valenti D, Bobba A, Merafina RS, Passarella S & Marra E (2006). Cytochrome c is released in a reactive oxygen species-dependent manner and is degraded via caspase-like proteases in tobacco bright-yellow 2 cells en route to heat shockinduced cell death. *Plant Physiology* **141**, 208-219.

van Acker GJD, Saluja AK, Bhagat L, Singh VP, Song AM & Steer ML (2002). Cathepsin B inhibition prevents trypsinogen activation and reduces pancreatitis severity *Amerian Journal of Physiololgy- Gastrointestianl and Liver Physiology* **283**, G794-G800.

van Breusegem F, Vranova E, Dat JF & Inze D (2001). The role of active oxygen species in plant signal transduction. *Plant Science* **161**, 405-414.

van der Biezen EA & Jones JD (1998). Plant disease-resistance proteins and the gene-for-gene concept. *Trends of Biochemistry Science* **23**, 454-456.

van der Hoorn RAL & Jones JDG (2004). The plant proteolytic machinery and its role in defense. *Current Opinion in Plant Biology* **7**, 400-407.

van der Hoorn RAL (2008). Plant proteases: from phenotypes to molecular mechanisms. *Annual Review of Plant Biology* **59**, 191–223.

van Doorn WG & Woltering EJ (2005). Many ways to exit? Cell death categories in plants. *Trends in Plant Science* **10**, 117-122.

Vancompernolle K, Herreweghe FV, Pynaert G & other authors (1998). Atractyloside-induced release of cathepsin B, a protease with caspase-processing activity. *FEBS Letters* **438**, 150-158.

Vegran F, Boidot R, Oudin C, Riedinger JM, Bonnetain F & Lizard-Nacol S (2006). Overexpression of caspase-3s splice variant in locally advanced breast carcinoma is associated with poor response to neoadjuvant chemotherapy. *Clinical Cancer Research* **12**, 5794-5800.

Venables JP (2004). Aberrant and alternative splicing in cancer. *Caner Research* **64**, 7647–7654.

Vercammen D, van de Cotte B, de Jaeger G, Eeckhout D, Casteels P, Vandepoele K, Vandenberghe I, van Beeumen J, Inze D & van Breusegem F(2004). Type 2 metacaspases atmc4 and atmc9 of *Arabidopsis thaliana* cleave substrates after arginine and lysine. *Journal of Biological Chemistry* **279**, 45329-45336.

Vercammen D, Belenghi B, van de Cotte B, Beunens T, Gavigan J, Rycke RD, Brackenier A, Inze D, Harris JL & van Breusegem F (2006). Serpin1 of *Arabidopsis thaliana* is a suicide inhibitor for metacaspase-9. *Journal of Molecular Biology* **364**, 625-636.

Vercammen D, Declercq W, Vandenabeele P & Breusegem FV (2007). Are metacaspases caspases? *Journal of Cell Biology* **179**, 375-380

Vranova E, Inze D & Breusegem FV (2002). Signal transduction during oxidative stress. *Journal of Experimental Botany* **53**, 1227-1236.

Wang Z, Sting L, Morrison C, Jantsch M, Los M, Schulze-Osthoff M & Wagner EF (1997). PARP is important for genomic stability but dispensable in apoptosis. *Genes and Devevelopment* **11**, 2347-2358

Watanabe N & Lam E (2005). Two Arabidopsis metacaspases atmcp1b and atmcp2b are arginine/lysine-specific cysteine proteases and activate apoptosis-like cell death in yeast. *Journal of Biological Chemistry* **280**, 14691-14699.

Weidhase RA, Lehmann J, Kramell H, Sembdner G & Parthier B (1987). Degradation of ribulose-1,5-bisphosphate carboxylase and chlorophyll in senescing barley leaf segments triggered by jasmonic acid methyl ester, and counteraction by cytokinin. *Physiology of Plant* **69**, 161-166.

Wink M (1993). The plant vacuole: a multifunctional compartment. *Journal of Experimental Botany* **44**, 231-246.

Winter D, Vinegar B, Nahal H, Ammar R, Wilson GV & Provart NJ (2007). An "Electronic Fluorescent Pictograph"browser for exploring and analyzing large-scale biological data sets. *PLoS ONE* **2**, e718.

Wissing S, Ludovico P, Herker E, Buttner S, Engelhardt SM, Decker T, Link A, Proksch A, Rodrigues F, Corte-Real M, Frohlich K, Manns J, Cande C, Sigrist SJ, Kroemer G & Madeo F (2004). An AIF orthologue regulates apoptosis in yeast. *Journal of Cell Biology* **166**, 969-974.

Wu Q & Krainer AR (1999). AT-AC pre-mRNA splicing mechanisms and conservation of minor introns in voltage-gated ion channel genes. *Molecular and Cellular Biology* **19**, 3225-3236.

Wyllie AH (1997). Apoptosis: an overview. *British Medical Bulletin* **53**, 451-465.

Wyllie AH & Golstein P (2001). More than one way to go. *Proceedings of National Academy of Science, USA* **98**, 11-13.

Y Sun & Z-L Peng (2009). Programmed cell death and cancer. *Postgraduate Medical Journal* **85**, 134-140.

Yakovlev AA, Gorokhovatsky AY, Onufriev MV, Beletsky IP & Gulyaeva IV (2008). Brain cathepsin B cleaves a caspase substrate. *Biochemistry (Moscow)* **73**, 332-336.

Ye Z (2002). Vascular tissue differentiation and pattern formation in plants. *Annual Review in Plant Biology* **53**, 183-202.

Yuan J, Shaham S, Ledoux S, Ellis HM & Horvitz HR (1993). The *C. elegans* cell death gene ced-3 encodes a protein similar to mammalian interleukin-1b-converting enzyme. *Cell* **75**, 641-652.

Yuste VJ, Moubarak RS, Delettre C, Bras M, Sancho P, Robert N, d'Alayer J & Susin SA (2005). Cysteine protease inhibition prevents mitochondrial apoptosis-inducing factor (AIF) release. *Cell Death and Differentiation* **12**, 1445–1448.